Endothelial and smooth muscle cell-to-cell communication within rat small mesenteric arteries

Winter, Polly

Award date:
2007

Awarding institution:
University of Bath

Endothelial and smooth muscle cell-to-cell communication within rat small mesenteric arteries

Polly Winter

A thesis submitted for the degree of Doctor of Philosophy

University of Bath

Department of Pharmacy and Pharmacology

March 2007

ProQuest LLC
789 East Eisenhower Parkway
P.O. Box 1346
Ann Arbor, MI 48106-1346

Abstract

1. Endothelium-derived hyperpolarizing factor (EDHF)-mediated vasodilatation responses are facilitated by the radial (endothelium to smooth muscle) and longitudinal (inter-endothelial cell or inter-smooth muscle cell) cell-to-cell transfer of hyperpolarization. Experiments were designed to investigate the contribution of gap junctions to both communication pathways.
2. Morphological studies demonstrated that connexin 40 and the small (S-) conductance calcium-activated potassium (K_{Ca}) channels were localized to endothelial cell borders and areas aligned with holes in the internal elastic lamina (IEL), whereas intermediate (I-) K_{Ca} channels were restricted to areas aligned with holes in the IEL.
3. In contrast to the non-selective gap junction uncoupler carbenoxolone, combinations of connexin-specific gap peptides did not affect the radial EDHF response to acetylcholine (ACh). A new technique based on pinocytic loading of cell-impermeant molecules was therefore established to selectively load the endothelium with anti-connexin antibodies. Connexin 40 antibody was shown to mimic the effects of carbenoxolone.
4. Focal, abluminal application of acetylcholine (ACh) and levcromakalim (LVK) evoked robust longitudinally-conducted vasodilatation responses, which were attenuated by carbenoxolone but unaffected following selective pinocytic loading of anti-connexin antibodies.
5. Luminal perfusion of the nucleotides ATP, ADPβS, and UTP each evoked an EDHF-type dilatation response that was sensitive to blockade of SK_{Ca} and IK_{Ca} channels with apamin and TRAM-34, respectively. Inhibition of PKC with bisindolylmaleimide I (BIS I) enhanced the nucleotide-evoked dilatation response, but had no effect on dilatation to ACh.
6. Focal, abluminal application of ADPβS evoked a robust spreading dilatation response, however dilatation responses to ATP and UTP were complicated by robust vasoconstriction when applied abluminally. In contrast, using a novel triple cannulation technique, dilatation responses to luminal perfusion of the three agonists were seen to spread longitudinally upstream into the parent artery.

7. These data highlight the difficulty in selectively inhibiting gap junctions, and provide new approaches that may be used to investigate the role of endothelium-dependent agonists in controlling arterial diameter.

Acknowledgments

Firstly I would like to thank everyone who has helped make it possible for me to complete this thesis including the British Heart Foundation who funded this work. Without your help and support it would not have been possible.

I particularly owe a huge thank you to Dr. Kim Dora. The positive encouragement, advice and guidance over the last few years have been fantastic and I could not have asked for better supervision. I would also like to thank both Kim and Professor Chris Garland for the opportunities given to me to present my work at both UK and international meetings, as they were generously given and are much appreciated. I also have to thank everyone in the laboratory past and present for their advice, support and the happy memories I take with me.

Parts of this thesis were done in conjunction with others. Therefore I would like to thank Dr. Simon Mather for his guidance on the pinocytic loading technique and his contributions to the work presented herein, Dr. Kim Dora and Miss Hannah Norris for their contributions to the nucleotide work and Dr. Shaun Sandow for the electron microscopy work within this thesis. I also have to thank Professor Chris Garland, Dr. Amanda MacKenzie and Dr. Richard Rivers for their advice, which has proved to be a valuable contribution to the work described in the present study.

There are numerous friends and family to whom I owe a big thank you. I particularly have to thank Alex as he has supported and encouraged me through the tough patches and helped share the happiest times of my PhD.

Published work arising from this thesis

ATP and UTP stimulate spreading dilatation responses in rat isolated small mesenteric arteries. Winter, P. & Dora, K.A. 2006 (presented at the 75th Anniversary Meeting of the British Pharmacological Society, University of Oxford, Oxford UK).

Contribution of PKC to the desensitisation of the relaxation response of small rat mesenteric arteries to luminally-perfused purinoceptor agonists. Winter, P. & Dora, K.A. *Purinergic Signalling* 2006; 2: 157 (presented at the 8th International Symposium on Adenosine and Adenine Nucleotides, University of Ferrara, Italy).

Differential role of K_{Ca} in dilatation evoked by luminally-perfused purinoceptor agonists in rat small mesenteric arteries. Winter, P. & Dora, K.A. 2005. Please see http://www.pa2online.org/abstracts/Vol3Issue4abst039.pdf (presented at the Winter 2005 Meeting of the British Pharmacological Society, Institute of Education, London UK and Experimental Biology 2006, San Francisco, USA).

Rapid endothelial cell-selective loading of connexin 40 antibody blocks endothelium-derived hyperpolarizing factor dilation in rat small mesenteric arteries. Mather, S., Dora, K.A., Sandow, S.L., Winter, P. & Garland, C.J. *Circulation Research* 2005; 97: 399-407.

Specificity and viability of a pinocytotic method for loading endothelial cells in intact arteries. Winter, P., Sandow, S.L., Mather, S., Garland, C.J. & Dora, K.A. *Journal of Vascular Research* 2004; 41 (suppl. 2): 1-68, PEF 5 (presented at the 23rd Conference for Microcirculation of the European Society, Lisbon, Portugal).

Table of Contents

List of Figures

List of Tables

List of Abbreviations

ACh, acetylcholine; ADP, adenosine 5'-diphosphate; ADPβS, adenosine 5'[β-thio]diphosphate; AKAP, A-kinase anchoring protein; anandamide, *N*-arachidonyl ethanolamide; 2-APB, 2-aminoethoxydiphenyl borate; ATP, adenosine 5'-triphosphate; ATPγS, adenosine 5'-(3-thiotriphosphate); B, large conductance; BIS I, bisindolylmaleimide I; BSA, bovine serum albumin; C, carboxy; CaMKII, calmodulin-dependent protein kinase II; cAMP, 3'-5'-cyclic adenosine monophosphate; cGMP, 3'-5'-cyclic guanosine monophosphate; CGRP, calcitonin gene-related peptide; Cl^-, chloride; Cl^-_{Ca}, Ca^{2+}-activated Cl^- channel; CNP, C-type natriuretic peptide; CYP, cytochrome P450 monooxygenases; DAG, diacylglycerol; DMSO, dimethylsulfoxide; e, endothelial; EC, endothelial cell; EDHF, endothelium-derived hyperpolarizing factor; EDRF, endothelium-derived relaxing factor; EETs, epoxyeicosatrienoic acids; eNOS, endothelial nitric oxide synthase; ER, endoplasmic reticulum; ETYA, eicosatetraeinoic acid; GDP, guanosine diphosphate; GIRK, G protein-gated inwardly-rectifying K^+ channel; GPCR, G protein-coupled receptor; GTP, guanosine triphosphate; H_2O_2, hydrogen peroxide; H_2S, hydrogen sulphide; i, inducible; I, intermediate conductance; IEL, internal elastic lamina; IP_3, inositol 1,4,5-trisphosphate; IP_3R, inositol 1,4,5-trisphosphate receptor; K^+, potassium; K_{ATP}, ATP-sensitive K^+ channel; K_{Ca}, Ca^{2+}-activated K^+ channel; K_{ir}, inwardly rectifying K^+ channel; K_v, voltage-dependent K^+ channel; L-NAME, N^{ω}-Nitro-L-arginine methyl ester; L-NNA, nitro-L-arginine; LVK, levcromakalim; MEGJ, myoendothelial gap junction; MLC, myosin light chain; MLCK, MLC kinase; MOPS, 3-[N-morpholino]propanesulfonic acid; mOsm, milliosmolar; MRS2179, 2'deoxy-*N*6-methyladenosine 3'5' diphosphate; N, amino; n, neuronal; Na^+, sodium; Na_v, voltage-dependent Na^+ channels; NO, nitric oxide; NOS, nitric oxide synthase; NPR, natriuretic peptide receptor; NSCC, non-selective cation channels; OAG, 1-oleoyl-2-acetyl-*sn*-glycerol; 17-ODYA, 17-octadecynoic acid; PBS, phosphate-buffered saline; pD_2, negative logarithm to base 10 of the EC_{50}; PE, phenylephrine; PECAM-1, platelet-endothelial cell adhesion molecule-1; PEG, polyethylene glycol; PI, phosphoinositide; PIP_2, phosphatidylinositol-bisphosphate; PKA, cAMP-dependent protein kinase; PKC, protein kinase C; PKG, cGMP-sensitive protein kinase; PLC, phospholipase C; ROCC, receptor-operated cation channel; RyR, ryanodine receptor; S, small conductance; siRNA, small interfering RNA; SKF 96365, 1-[β-[3-(4-methoxyphenyl)propoxy]-4-methoxyphenethyl]-1*H*-imidazole hydrochloride; SMC,

smooth muscle cell; SOC, store-operated channel; SOCE, store-operated Ca^{2+} entry, SR, sarcoplasmic reticulum; STIC, spontaneous transient inward current; STOC, spontaneous transient outward current; TPEN, N,N,N',N'-tetrakis (2-pyridylmethyl) ethylenediamine; TRAM-34, 1-[(2-chlorophenyl)diphenylmethyl]-1H-pyrazole; TRP transient receptor potential channel TRPC, canonical TRP; TRPM, melastatin TRP; TRPV, vanilloid TRP; U-73122, 1-(6-((17β-3-methoxyestra-1.3.5(10)-trien-17-yl)amino)hexyl)-1H-pyrrole-2,5-dione; UTP, uridine triphosphate; VDCC, voltage-dependent Ca^{2+} channels.

1. Introduction

1.1. Arterial function and morphology

1.1.1. Function of resistance arteries

Resistance arteries are defined as small pre-capillary arteries and arterioles of diameter less than 500μm that may facilitate, under physiological control, a large drop in blood pressure as blood flows from the large conduit vessels to the capillaries (Fenger-Gron *et al.*, 1997; Mulvany & Aalkjaer, 1990). As blood moves through the vascular system the pressure gradient and the resistance to flow will influence blood flow. This can be expressed using an adaptation of Ohm's Law where blood flow is equivalent to the current, and the pressure gradient to the electromotive force (Levy, 1979):

$$\text{Blood flow} = \frac{\text{Pressure gradient}}{\text{Resistance}} \tag{1.1}$$

Resistance to blood flow is determined by the friction exerted on the vessel wall by the flowing blood and the resistance between the circulating cells and constituents of the blood (Lipowsky, 2005). Therefore the dimensions of a blood vessel and the blood viscosity are key determinants of vascular resistance. Assuming for simplicity that blood is Newtonian, i.e. the viscosity of blood does not change, the relationship between the flow of blood through a vessel may be described by the Hagen-Poiseuille equation (Ganong, 1999):

$$\text{Blood flow} = \frac{\text{Hydrostatic pressure} \times \pi \times \text{Vessel radius}^4}{8 \times \text{Viscosity} \times \text{Length}} \tag{1.2}$$

Using equation 1.1 the Hagen-Poiseuille equation may be substituted such that,

$$\text{Resistance} = \frac{8 \times \text{Viscosity} \times \text{Length}}{\pi \times \text{Vessel radius}^4} \tag{1.3}$$

From equation 1.3 it is possible to see that resistance varies inversely with the fourth power of the radius. As such changes in vessel radius have the most significant effect on

Figure 1.1 Mesenteric segmental, fractional blood pressure drops taken from Fenger-Gron *et al.* (1995)
The figure shows the mean fractional blood pressure drops over the sections of the mesenteric vasculature indicated. Given systemic blood pressure was 121±2mmHg, blood pressure at the superior mesenteric artery may be calculated to be ~115mmHg, ~77mmHg in the arcade arteries and ~16mmHg in the intramural vessels.

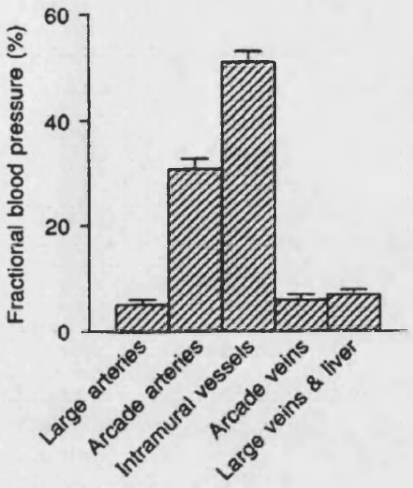

resistance to blood flow. Vessels such as the resistance arteries, which can exert marked changes in diameter in response to physiological stimuli therefore have an important role in the regulation of blood flow and can facilitate the drop in blood pressure that is required as blood flows from larger arteries to the capillaries (Fenger-Gron *et al.*, 1997; Fenger-Gron *et al.*, 1995; Mulvany & Aalkjaer, 1990). Given that cardiac output and total peripheral resistance determine blood pressure (Equation 1.4; Levy, 1979), the regulation of blood flow by the resistance arteries contributes significantly to the control of systemic blood pressure.

$$\text{Blood pressure} = \text{Cardiac output} \times \text{Total peripheral resistance} \tag{1.4}$$

1.1.2. Anatomy of rat mesenteric arteries

Within this thesis vasomotor responses to isolated third order branches of the rat superior mesenteric artery were studied. The contribution of these small arteries to the maintenance of vascular resistance in the mesenteric bed was demonstrated functionally by Fenger-Gron and colleagues (1997; 1995) who measured the blood pressure in freely moving rats at the aorta and at four points in the mesenteric circulation. The small mesenteric arteries were shown to be one of two key sites contributing to mesenteric resistance, the second being the smaller arterioles of the intramural circulation (Figure 1.1). These functional data correlate with anatomical observations that put their small size in the range of resistance arteries (Mulvany & Aalkjaer, 1990).

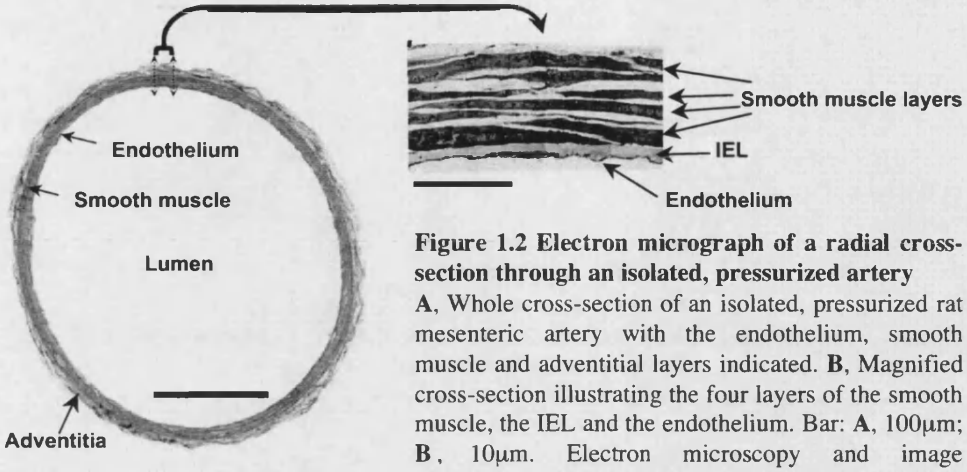

Figure 1.2 Electron micrograph of a radial cross-section through an isolated, pressurized artery
A, Whole cross-section of an isolated, pressurized rat mesenteric artery with the endothelium, smooth muscle and adventitial layers indicated. **B**, Magnified cross-section illustrating the four layers of the smooth muscle, the IEL and the endothelium. Bar: **A**, 100μm; **B**, 10μm. Electron microscopy and image construction performed by Dr. Shaun Sandow.

The structure of the rat small mesenteric artery (Figure 1.2) is similar to other resistance arteries: An outer layer, the tunica adventitia, consisting of connective tissue, nerve cells, macrophages, mast cells and fibroblasts, surrounding approximately four layers of smooth muscle cells (the tunica media), which are separated from the innermost, single layer of endothelial cells (the tunica intima) by the internal elastic lamina (Mulvany & Aalkjaer, 1990). Endothelial cells may project through holes in the IEL to contact the smooth muscle layer (Sandow & Hill, 2000).

The superior mesenteric artery supplies blood to the duodenum and transverse colon. Frequent branches in the artery form an arcade that allows perfusion of the gut via multiple routes and minimises tissue ischemia during instances where blood flow may be compromised. The level of blood flow differs markedly between fasting and feeding states and is largely regulated by the vasomotor responses of the small resistance arteries as described (third, fourth and fifth order branches of the superior mesenteric artery; section 1.1.1). Mesenteric arteries respond to metabolites released from the perfused tissue (active hyperaemia) and humoral, hormonal and neuronal (sympathetic) influences (Mulvany & Aalkjaer, 1990) and so constitute good models for resistance artery function. Given the rat small mesenteric artery is frequently used in the study of vasomotor responses experimental procedures for its use are also well reported.

1.2. Vasoconstrictor mechanisms

1.2.1. Smooth muscle constriction

The contraction mechanism within smooth muscle is thought to principally rely on the global levels of cytosolic calcium (Ca^{2+}) and the degree of myosin phosphorylation (for review see Somlyo & Somlyo, 1994). A rise in cytosolic Ca^{2+} concentration enhances the binding of Ca^{2+} to calmodulin and subsequently the association of this complex with the myosin light chain kinase (MLCK) catalytic subunit (Figure 1.3; Kamm & Stull, 1985; Somlyo & Himpens, 1989). This activates the enzyme permitting phosphorylation of the 20kDa regulatory myosin light chain (MLC_{20}) of myosin II on a serine residue at position 19 (Kamm & Stull, 1985; Sweeney *et al.*, 1994). Phosphorylation of the MLC_{20} at serine 19 causes a net reduction in charge at the amino (N)-terminus, which facilitates a conformational change of the myosin ATPase allowing activation by actin (Sweeney *et al.*, 1994). This allows the hydrolysis of adenosine 5'-triphosphate (ATP) and the formation of cross-bridges between the actin and myosin filaments resulting in generation of contractile force.

The extent of contractile force is attributed to the number of active cross bridges generating force additively, which is determined by acto-myosin ATPase activity (Figure 1.3; Kamm & Stull, 1985). As there is a correlation between phosphorylation of MLC and myosin ATPase activity in many smooth muscle preparations it is clear that the extent of MLC phosphorylation is crucial in determining the degree of contractile force in response to a given stimulus (Butler & Siegman, 1998; Buus *et al.*, 1998; Chacko & Rosenfeld, 1982). In the rat small mesenteric artery preparation it has been demonstrated that a threshold of approximately 25% of the MLC needs to be phosphorylated to elicit even small increases in contractile force (Rembold & Murphy, 1988). Whilst this mechanism of contraction is universal amongst all smooth muscle tissues the source of Ca^{2+} and the ion channels through which it passes, as well as the degree and mechanism of myosin phosphorylation varies between different preparations (McFadzean & Gibson, 2002). Additionally the coupling of these processes to receptor activation by excitatory stimuli may also vary widely depending on the agonist used to evoke contraction.

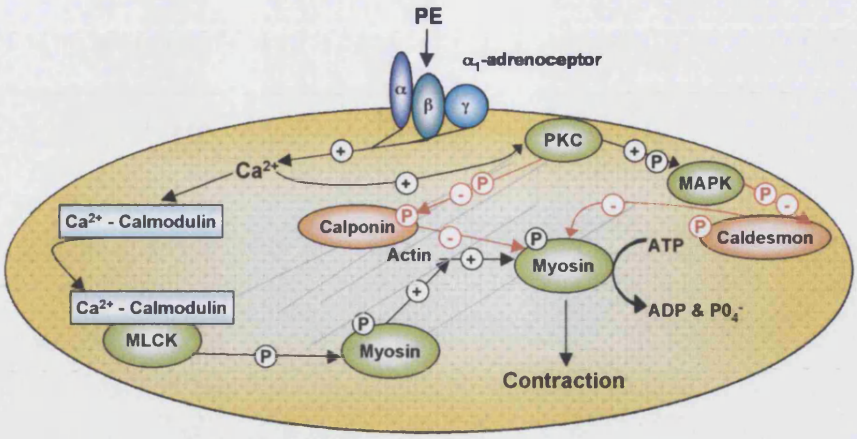

Figure 1.3 Smooth muscle contraction
Cartoon illustrating the mechanism of contraction in smooth muscle downstream of a rise in intracellular Ca^{2+} stimulated by α_1-adrenoceptor stimulation with PE. + and - represent stimulation and inhibition. P represents phosphorylation.

Two key mechanisms couple excitatory stimuli to the generation of contractile force: Electromechanical coupling and pharmacomechanical coupling (Somlyo & Himpens, 1989; Somlyo & Somlyo, 1994; Somlyo & Somlyo, 1968). Electromechanical coupling refers to the effects of changes in membrane potential on cytosolic Ca^{2+} and the subsequent contractile response. Pharmacomechanical coupling refers to smooth muscle contraction evoked as a consequence of multiple cellular signalling mechanisms independently of a change in membrane potential (although changes may occur) (Somlyo & Somlyo, 1994). The relative importance of these two coupling mechanisms varies depending on the smooth muscle under study. In phasic smooth muscle tissues such as the smooth muscle layer within rat small mesenteric arteries it is thought that electromechanical mechanisms predominate (McFadzean & Gibson, 2002). The agonist used to evoke contraction can also dictate the coupling mechanisms involved, which are not always distinct. This is the case for PE-evoked smooth muscle contraction where both coupling mechanisms are employed.

1.2.2. Phenylephrine-evoked vasoconstriction

PE is frequently used in studies of vascular function as α_1-adrenoceptor activation contributes to, but does not wholly facilitate the effects of sympathetic nerve stimulation and the stress response in the rat circulation (Angus *et al.*, 1988; Mulvany & Aalkjaer, 1990; Wier & Morgan, 2003). In isolated rat small mesenteric arteries PE acts on α_1- adrenoceptors on the smooth muscle cell surface membrane (for review see

Docherty, 1998). Controversy surrounds the α_1-adrenoceptor-subtype that facilitates the functional response to PE. Studies supporting both the involvement of the α_{1A} subtype (Marti *et al.*, 2005) and the α_{1D} subtype in PE-evoked vasoconstriction have been reported (Hussain & Marshall, 1997) with some investigators proposing a more heterogenic population of receptors in the vasoconstriction response to PE (Hussain & Marshall, 1997). Further definition of the receptor subtypes with regards to their affinity for prazosin has led to increased complexity with regards to α_1-adrenoceptor classification that may reflect different receptor states of the same receptor genotype (Ford *et al.*, 1997) or may represent a completely different sub set of receptors as suggested by Van der Graaf and colleagues (Stam *et al.*, 1999; 1996). For the purpose of this thesis PE-evoked constriction mechanisms will therefore be discussed in terms of the consequences of α_1-adrenoceptor-stimulation, ignoring subtype specificity.

1.2.3. Pharmacomechanical coupling downstream of the α_1-adrenoceptor

1.2.3.1. $G_{q/11}$ G protein-coupled responses

Each of the α_1-adrenoceptor subtypes is a heterotrimeric $G_{q/11}$ G-protein coupled receptor (GPCR; Docherty, 1998) and so is associated with the activation of phospholipase C (PLC) β1 and Ca^{2+}-sensitization pathways (Figure 1.3; for review see Berridge, 1993; Somlyo & Somlyo, 1994; Somlyo & Somlyo, 2000). Classically, the $G_{\beta\gamma}$ subunits of the G-protein trimer coupled to the receptor are thought to facilitate agonist binding with the associated receptor by stabilizing the interaction of the G_α subunit with guanosine diphosphate (GDP) whilst the G_α subunit mediates activation of downstream signalling pathways.

G_α subunit functionality firstly requires its dissociation from the other trimer composite proteins (Clapham & Neer, 1997). In brief, agonist binding elicits a conformational change in the receptor, which catalyzes the dissociation of GDP and association of guanosine triphosphate (GTP) with the subunits G_α and $G_{\beta\gamma}$ and subsequently dissociation of the component G-proteins and the receptor (Clapham & Neer, 1997). Once dissociated, the $G_{\alpha q}$ subunits activate PLC β1, facilitating the hydrolysis of the membrane-bound phospholipid, phosphatidylinositol-bisphosphate (PIP_2) into

diacylglycerol (DAG) and inositol 1,4,5-trisphosphate (IP_3) (Berridge & Irvine, 1989; Lee *et al.*, 1992; Wu *et al.*, 1992).

1.2.3.2. IP_3 and intracellular Ca^{2+} stores

Within rat mesenteric arteries, IP_3 receptor 1 (IP_3R1)-activated Ca^{2+} channels on the sarcoplasmic reticulum (SR) bind IP_3, which in a concentration-dependent manner, opens the channel allowing the quantal movement of Ca^{2+} into the cytosol (Berridge, 1993; Grayson *et al.*, 2004; Iino & Endo, 1992). A positive feedback mechanism then occurs whereby increasing intracellular Ca^{2+} concentrations further stimulate the release of Ca^{2+} through the IP_3R1 causing a propagating 'all or nothing' Ca^{2+} wave, the magnitude of which is independent of PE concentration: The increased probability of an individual cell responding to PE linked to increasing PE concentrations (Mauban *et al.*, 2001; Zang *et al.*, 2001). The Ca^{2+} wave may subsequently extend throughout the cell and, together with other Ca^{2+} sensitizing mechanisms, influx of extracellular Ca^{2+} and modulation of the contractile apparatus, serve to maintain the vasoconstriction to PE. Further increases in intracellular Ca^{2+} then inhibit IP_3R Ca^{2+} flux (Please see section 1.2.2.3; Berridge, 1993; Iino & Endo, 1992; Wier & Morgan, 2003).

The initial synchronous Ca^{2+} release from the SR following IP_3R activation is sufficient to evoke a transient contraction. However, the limited Ca^{2+} in the SR, the extrusion of Ca^{2+} from the cell by active exchange and pumping mechanisms and the negative feedback pathways associated with high intracellular Ca^{2+} concentrations preclude a rise in intracellular Ca^{2+} sufficient to evoke a maintained response from depletion of intracellular stores alone (Lamont & Wier, 2004; Mauban *et al.*, 2001; Nilsson *et al.*, 1998; Wier & Morgan, 2003; Zang *et al.*, 2001). This is supported by experimental evidence whereby removal of extracellular Ca^{2+} was shown to abolish the maintained contraction response to PE in isolated rat small mesenteric arteries (Lagaud *et al.*, 1999; Lamont & Wier, 2004; Mauban *et al.*, 2001).

1.2.3.3. Ryanodine receptors and intracellular Ca^{2+} stores

Ryanodine receptor Ca^{2+} channels (RyR) on the SR membrane may also enable Ca^{2+} influx from the SR into the cytosol. Of the three subtypes of RyR, all are present in rat small mesenteric artery smooth muscle (Neylon *et al.*, 1995). Opening of these channels

may be stimulated by a number of different mechanisms, although within vascular smooth muscle activation of these channels by the influx of Ca^{2+} through voltage-dependent Ca^{2+} channels is thought to predominate (Neylon *et al.*, 1995; Thorneloe & Nelson, 2005). In contrast to the IP_3R, the primary role of the RyR in vascular smooth muscle contraction is one of negative feedback, whereby Ca^{2+} released from this channel as Ca^{2+} sparks activates plasmalemmal K_{Ca} channels situated in close proximity to the SR causing hyperpolarization and relaxation of the smooth muscle (please see section 1.2.2.4; Jaggar *et al.*, 1998; Lamont & Wier, 2004; Nelson *et al.*, 1995; Perez *et al.*, 1999; Thorneloe & Nelson, 2005; Wellman & Nelson, 2003).

1.2.3.4. Influx of extracellular Ca^{2+} and store-operated Ca^{2+} channels

As described previously, influx of extracellular Ca^{2+} is crucial to maintain PE-evoked constriction in rat mesenteric arteries, but it is also required to replenish Ca^{2+} stores following IP_3R activation as Ca^{2+} released into the cytosol may be actively pumped out of the cell (Lagaud *et al.*, 1999; Wier & Morgan, 2003). It has been proposed that the primary role of store depletion by activation of the IP_3R is to stimulate the opening of Ca^{2+}-permeable store-operated channels (SOC) on the plasma membrane, a phenomenon termed store-operated Ca^{2+} entry (SOCE) or capacitative Ca^{2+} entry (Putney, 1986). A role for SOCE in PE-evoked contraction in isolated rat mesenteric arteries is supported by a number of studies. Lamont and Wier (2004) reported a block of the contractile response to PE in a denuded rat mesenteric artery preparation by 2-aminoethoxydiphenyl borate (2-APB). Although originally described as an IP_3R antagonist, 2-APB has also been shown to mediate other effects including potentiation of SOCE currents at concentrations of 1 to 5μM and inhibition of SOCE currents at concentrations greater than 10μM (Prakriya & Lewis, 2001; Smyth *et al.*, 2006). Inhibition of maintained contractions of isolated rat mesenteric small arteries to PE was also reported following treatment with the putative SOCE blocker Mg^{2+}. Furthermore, in the same study, a contraction was elicited following replacement of extracellular Ca^{2+} after depletion of intracellular stores by the Ca^{2+} chelator N,N,N',N'-tetrakis (2-pyridylmethyl) ethylenediamine (TPEN), indicative of SOCE channel activity (Zhang *et al.*, 2002).

Transient receptor potential channels

The molecular identity of the SOC and the mechanisms associated with its activation have, however, remained elusive. Multiple currents may be evoked by store depletion of which the cation, relative selectivity and current size may vary (Smyth *et al.*, 2006). The most discussed identity of the voltage-independent channel mediating the SOCE current first proposed by Putney (Putney, 1986) has, until recently been that of the canonical transient receptor potential channel (TRPC), a Ca^{2+}-permeable cation channel, predominantly activated downstream of PLC activation. Numerous over-expression studies increasing SOC Ca^{2+} entry and knock down studies reducing SOC Ca^{2+} entry supported this hypothesis, particularly highlighting a role for TRPC1 and TRPC4 (Brueggemann *et al.*, 2006; Clapham, 2003; McFadzean & Gibson, 2002; Smyth *et al.*, 2006). Indeed, in rat small mesenteric arteries TRPC1, TRPC4 and TRPC6 have all been detected in the smooth muscle (Brueggemann *et al.*, 2006; Hill *et al.*, 2006). However, none of the TRPC channels are able to fully mimic the native SOCE current. Therefore, although these channels may contribute to a different store-operated inward current, or even comprise the receptor-operated cation channel (ROCC; see below) it seemed unlikely that they alone constitute the SOCE channel (Clapham, 2003; McFadzean & Gibson, 2002; Smyth *et al.*, 2006).

STIM1

Two recent studies screening *Drosophilia* S2 cells for possible SOCE channels by studying the effects of small interfering RNA (siRNA) on SOCE currents in mammalian cells identified the *Stim* gene, and its mammalian protein counterpart STIM1 as a key component of the SOCE pathway (Liou *et al.*, 2005; Roos *et al.*, 2005). Knock down of *Stim* in S2 cells or suppression of its homologue STIM1 in HEK293 and SH-SY5 cell lines was found to abolish SOCE currents without modification of intracellular Ca^{2+} concentration, SR Ca^{2+} release or modification of voltage-dependent Ca^{2+} influx (Roos *et al.*, 2005). In HeLa cells siRNAs directed against STIM1 and STIM2 also abrogated the plateau phase of thapsigargin and histamine-evoked increases in intracellular Ca^{2+} concentration and inhibited Ca^{2+} influx upon replacement of extracellular Ca^{2+} (Liou *et al.*, 2005). However, the single transmembrane domain structure of the protein and the relatively small enhancement of the SOC current by STIM1 overexpression made it unlikely that this protein was the channel mediating the SOCE current

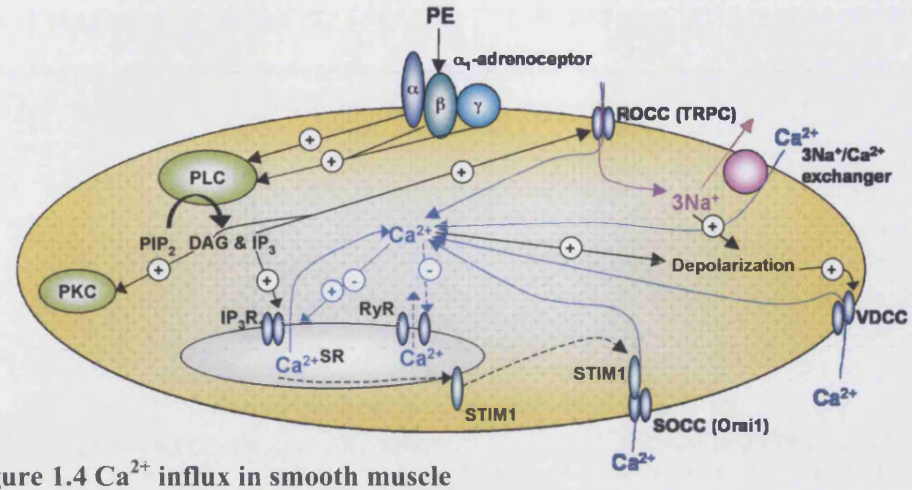

Figure 1.4 Ca^{2+} influx in smooth muscle
Cartoon illustrating the mechanisms associated with Ca^{2+} influx upstream of contraction in smooth muscle following stimulation of α_1-adrenoceptors with PE. + and – represent stimulation and inhibition respectively. P represent phosphorylation.

(Roos *et al.*, 2005). Instead it was proposed that STIM1 acts as the Ca^{2+} sensing component of the SOCE mechanism, translocating to regions of the endoplasmic reticulum (ER) adjacent to the plasma membrane to convey the store depletion of Ca^{2+} (Baba *et al.*, 2006; Liou *et al.*, 2005; Zhang *et al.*, 2005).

Shortly after the identification of STIM1 the four transmembrane domain protein Orai1 was identified as a second essential component of the SOCE in two reports: One group describing a mutation in Orai1 that leads to malfunction of SOCE and subsequently non-functional nuclear transcription in T-cells resulting in severe combined immunodeficiency (Vig *et al.*, 2006), the other identifying the same protein, termed as Ca^{2+} release activated Ca^{2+} modulator 1 (CRACM1) following a RNA interference screen of *Drosophilia* (Feske *et al.*, 2006). Expression of Orai1 was found to restore SOCE currents in SCID T cells (Feske *et al.*, 2006) whilst co-overexpression of Orai1 with STIM1 resulted in a larger IP_3 and BAPTA-evoked SOCE current in HEK293 (60-fold) and Jurkat (10-fold) cells, that was potentiated and inhibited by 2-APB in a manner similar to that of native SOC currents (Peinelt *et al.*, 2006; Soboloff *et al.*, 2006). Subsequent point mutations of conserved transmembrane regions of Orai1 resulted in modulation of the ion selectivity of the Orai1 current supporting a role for Orai1 as the pore of the SOC channel (Prakriya *et al.*, 2006; Yeromin *et al.*, 2006).

Whether the SOC current evoked by Ca^{2+} depletion of the SR in the smooth muscle of rat small mesenteric arteries is mediated by STIM-1/Orai1 activation is unknown. Although this channel has been found to be important in airway smooth muscle-mediated contractions (Peel *et al.*, 2006) no studies in isolated rat mesenteric arteries, or indeed any vascular smooth muscle preparations have yet been reported. Furthermore, although a contribution of STIM1 and Orai1 may be key to the SOCE current, smaller Ba^{2+} and Sr^{2+} currents in STIM-1/Orai-1 overexpressed cells versus native SOCE currents have been reported suggesting that other proteins may contribute to the complete channel structure further modulating the channel pore and its ion permeability (Peinelt *et al.*, 2006; Smyth *et al.*, 2006).

1.2.3.5. Receptor-operated Ca^{2+} channels

In addition to SOCE, influx of Ca^{2+} downstream of the α_1-adrenoceptor may be mediated by activation of ROCCs with the subsequent cation influx leading to membrane depolarization and activation of voltage-dependent Ca^{2+} channels (VDCCs) and the $3Na^+/Ca^{2+}$ exchanger in rat small mesenteric artery and other vascular preparations (Albert & Large, 2003; Hill *et al.*, 2006; Inoue *et al.*, 2001; Lagaud *et al.*, 1999; Thorneloe & Nelson, 2005). Indeed blockade of $3Na^+/Ca^{2+}$ exchangers with amiloride and 1,3-dimethyl-2-thiourea (DMTU) was shown to reduce both increases in intracellular Ca^{2+} and tension in response to noradrenaline following depletion of intracellular Ca^{2+} stores. Whilst blockade of VDCC and ROCC by nitrendipine and 1-[β-[3-(4-methoxyphenylpropoxy]-4-mehoxyphenethyl]-1H-imidazole hydrochloride (SKF 96365) respectively, was also shown to reduce noradrenaline-evoked increases in extracellular Ca^{2+} following intracellular store depletion in the same study (Lagaud *et al.*, 1999). Like the SOCE current the ROCC current may have multiple identities, and is only clearly distinguished from the SOCE current by its activation occurring independently of store depletion and subsequent to agonist stimulation (Albert & Large, 2003; McFadzean & Gibson, 2002; Thorneloe & Nelson, 2005). The most reported molecular identity of the ROCC is a composite of members of the TRPC family of channel proteins. However, in contrast to the rather mixed evidence available for the SOCE current, evidence in support of a role for TRPC channels in mediating the ROCC is more consistent between reports and more akin to native ROCC currents (Clapham, 2003; Thorneloe & Nelson, 2005).

Within rat small mesenteric arteries three TRPC subtypes have been identified of which TRPC1, TRPC4 (Brueggemann *et al.*, 2006 only) and TRPC6 are localized to the smooth muscle whilst TRPC3 is found in the endothelium (Hill *et al.*, 2006). Hill and colleagues (2006) demonstrated that the cell permeant analogue of DAG, 1-oleoyl-2-acetyl-*sn*-glycerol (OAG), was capable of activating a TRPC6-like non-selective cation channel current independently of protein kinase C (PKC) and potentiated by PKC inhibition. This is consistent with previous reports describing a PKC-independent role for DAG in activation of ROCC currents in rabbit portal vein myocytes and a more inhibitory action of PKC on TRPC-like currents in rabbit ear arteries (Albert & Large, 2004; Helliwell & Large, 1997; Inoue *et al.*, 2001). In the same study, it was demonstrated that PE when compared to OAG-evoked currents augmented the ROCC current. Given previous reports describing a synergistic action of inositol phosphates and DAG on native TRPC6 currents in rabbit portal vein myocytes in the presence of the Ca^{2+} chelator BAPTA (Albert & Large, 2003) it is likely that both second messengers contribute to activation of the TRPC6-like ROCC current downstream of α_1-adrenoceptor activation by PE (Albert & Large, 2003; Hill *et al.*, 2006).

Although these data clearly support a TRPC6 component in the ROCC channel the heterogeneity of the ROCC current between various vascular beds and the heteromeric structure typical of many TRPC channels suggests that other TRPC proteins, particularly TRPC1, may play an important role in the ROCC in rat mesenteric artery smooth muscle contraction (Hill *et al.*, 2006). Furthermore, the activation of the ROCC current likely goes beyond the actions of DAG and IP_3 alone as modulation of ROCC by intracellular Ca^{2+} and numerous kinases has been reported in a range of preparations (McFadzean & Gibson, 2002; Please see the following for review and references therein; Thorneloe & Nelson, 2005).

1.2.3.6. Protein kinase C

The rise in intracellular Ca^{2+} following the activation of IP_3R on the sarcoplasmic reticulum, in addition to direct initiation of the contractile process, may also stimulate translocation of PKC to the membrane and its subsequent activation by increasing the strength and specificity of PKC interactions with phosphatidylserine (Morgan &

Leinweber, 1998). PKC translocation may also independently of Ca^{2+} be initiated by binding of DAG. This facilitates the incorporation of PKC into the cell membrane and thus reduces its requirement for Ca^{2+} (Kishimoto *et al.*, 1980; Minneman, 1988; Morgan & Leinweber, 1998; Ohanian *et al.*, 1996). The subsequent role for PKC in the contractile response is then controversial but may include direct phosphorylation, and thus inactivation of calponin, and indirectly (via phosphorylation and activation of mitogen activated protein kinase (MAPK)), the phosphorylation of caldesmon. Both calponin and caldesmon are actin-binding thin filament proteins which when unphosphorylated may inhibit myosin ATPase activity. Consequently, inhibition of these proteins by PKC would enhance contractile force (see Morgan & Leinweber, 1998 for review). Such a role for PKC would be consistent with reports that prolonged treatment of isolated small rat mesenteric arteries with the phorbol ester phorbol 12,13-dibutyrate resulted in downregulation of the α and δ isoforms of PKC with a parallel reduction in the contractile response to the phorbol ester and the force of contractions elicited by noradrenaline at submaximal concentrations (Ohanian *et al.*, 1996). One function of PKC activation that is also consistent with such experiments, particularly within isolated rat small mesenteric arteries is the contribution of PKC to Ca^{2+}-sensitization and the subsequent maintenance of contractile force (Budzyn *et al.*, 2006; Buus *et al.*, 1998).

1.2.3.7. Ca^{2+}-sensitization

Ca^{2+} concentration is clearly a key component of the contractile mechanism. However, based on the force of contraction evoked by depolarization-induced rises in Ca^{2+}, the level of contraction to GPCR agonist stimulation is often higher than expected (Somlyo & Somlyo, 1994). This suggests that a secondary Ca^{2+}-sensitizing mechanism may be elicited upon GPCR activation. The dependence of contractile force on the degree of myosin phosphorylation implicates dynamic modulation of MLCK and myosin phosphatase in its regulation. This may arise from a number of second messenger or cell signalling pathways the nature of which depends on the tissue and the agonist used to evoke GPCR stimulation. (for review please see Fukata *et al.*, 2001; Morgan & Leinweber, 1998; Somlyo & Somlyo, 1998; Somlyo & Somlyo, 1994; Somlyo & Somlyo, 2000).

PKC and Ca^{2+}-sensitization

PKC activation has been shown to facilitate Ca^{2+}-sensitization in response to PE and noradrenaline in isolated rat mesenteric artery preparations (Budzyn *et al.*, 2006; Buus *et al.*, 1998). This is achieved by direct phosphorylation and inhibition of myosin phosphatase (Itoh *et al.*, 1993) and by the phosphorylation and subsequent activation of the myosin phosphatase inhibitor CPI-17 (Figure 1.3; Kitazawa *et al.*, 2000). Both mechanisms allow increased phosphorylation of the myosin light chain thereby facilitating an increase in contractile force. Conflicting studies have been published with regards to the importance of PKC-mediated pathways in α_1-adrenoceptor-mediated contractions in rat small mesenteric arteries (Buyukafsar *et al.*, 2004; Ward *et al.*, 2002). Furthermore the selectivity of PKC inhibitors such as Ro 318220 and the physiological, rather than pathological, relevance of PKC-mediated Ca^{2+}-sensitization has come under question (Davies *et al.*, 2000; Somlyo & Somlyo, 1998). However, it would seem PKC at least partly contributes to Ca^{2+}-sensitization in this preparation.

Rho kinase and Ca^{2+}-sensitization

CPI-17 may also be activated downstream of the Rho-Rho kinase pathway (Kitazawa *et al.*, 2000; Koyama *et al.*, 2000). In brief (for details and review please see Fukata *et al.*, 2001 and references therein), the Rho kinase pathway begins downstream of the dissociation of the G-protein α subunit from the agonist receptor. In addition to binding with PLC, activated α subunits downstream of G_{12} and G_{13}-proteins can bind to the guanine nucleotide exchange factor p115 Rho GEF, which can catalyze the exchange of GDP-Rho to GTP-Rho (Somlyo & Somlyo, 2000). Rho is a small GTPase and a member of the Rho subfamily of Ras GTPases, which can bind to and activate Rho kinase. Downstream of Rho kinase the Zip-like kinase, M110 then mediates phosphorylation of both the myosin-binding subunit of myosin phosphatase and the inhibitory phosphoprotein CPI-17 (Kitazawa *et al.*, 2000; Koyama *et al.*, 2000; MacDonald *et al.*, 2001a; MacDonald *et al.*, 2001b; Somlyo & Somlyo, 2000). Phosphorylation of myosin phosphatase inhibits the enzyme, so combined with the effects of CPI-17, increased MLC_{20} phosphorylation is facilitated and consequently there is a greater contractile force for a given Ca^{2+} concentration (Figure 1.5).

Although p115 Rho GEF was previously only thought to couple to receptors of the G_{12}

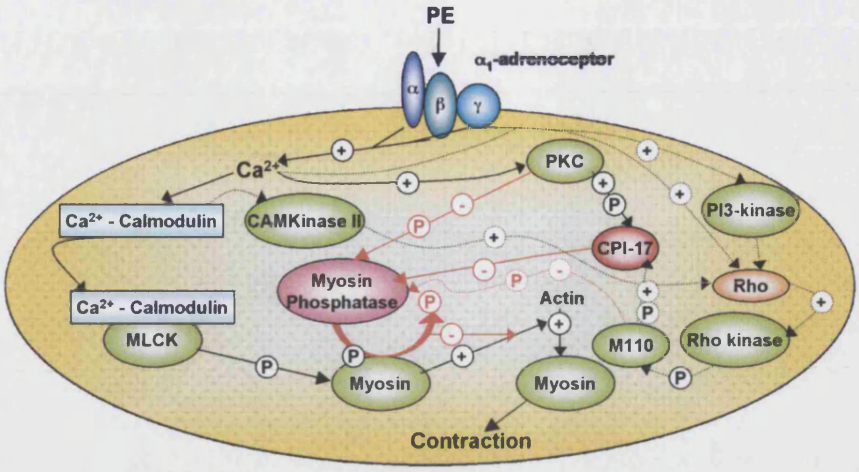

Figure 1.5 Ca^{2+}-sensitization in rat small mesenteric artery smooth muscle
Cartoon illustrating the mechanisms associated with Ca^{2+} sensitization following stimulation of α_1-adrenoceptors with PE. Dotted lines indicate mechanisms not wholly defined or established in the rat mesenteric artery preparation. + and – represent stimulation and inhibition respectively. P represents phosphorylation.

and G_{13} subtype, evidence from Gohla (2000) and later Chikumi and colleagues (2002) in cell culture systems suggests that $G_{q/11}$ G-protein-coupled receptors may also activate this and other guanine nucleotide exchange factors. More recent evidence in rabbit aortic vascular smooth muscle preparations has subsequently coupled activation of the Rho kinase pathway to noradrenaline-induced $G_{q/11}$ activation by calcium-dependent activation of class II phosphoinositide (PI)-3 kinases and possibly Ca^{2+}-dependent activation of calmodulin-dependent protein kinase II (CaMKII; Sakurada *et al.*, 2003; Wang *et al.*, 2006). Whether this data translates to downstream signalling pathways in isolated mesenteric resistance arteries is as yet unknown.

In support of a role for Rho-kinase-mediated Ca^{2+} sensitization in the rat mesenteric artery VanBavel and colleagues (2001) have reported a significant inhibition of PE-evoked constriction and pressure-induced tone in isolated rat mesenteric arteries following treatment with the selective Rho kinase inhibitor Y-27632. Additionally, in the perfused mesenteric bed a concentration-dependent inhibition of PE-evoked contraction by Y-27632 has been demonstrated (Buyukafsar *et al.*, 2004). However, these findings are contrary to studies reporting a lack of Rho kinase activity downstream of PE-evoked contraction in isolated rat small mesenteric arteries (Asano & Nomura, 2003; Budzyn *et al.*, 2006; Shaw *et al.*, 2004).

1.2.4. Electromechanical coupling

Ion	Extracellular free ion concentration (mM)	Intracellular free ion concentration (mM)	Equilibrium potential (mV)
Na^+	150	10 - 20	+50
Cl^-	140	40 - 70	-20
K^+	3 - 5	130 - 160	-90
Ca^{2+}	2	0.001 – 0.00001 *	+150

Table 1.1 Typical ionic concentrations for smooth muscle cells in a physiological salt solution and the associated equilibrium potentials as calculated using the Nernst equation. Table assimilated from values take from Hirst and Edwards (1989). *Free intracellular Ca^{2+} concentration.

A second component of α_1-adrenoceptor-mediated contraction is facilitated by electromechanical coupling mechanisms, which principally rely on the effect of changes in membrane potential on cytosolic Ca^{2+} (Nilsson, 1998; Somlyo & Somlyo, 1994). The membrane potential and electrical excitability of most smooth muscle cells are principally governed by the concentration differences of free sodium (Na^+), potassium (K^+), Ca^{2+} and chloride (Cl^-) ions between the inside and outside of the cell and their equilibrium potential as estimated using the Nernst equation (summarized in Table 1.1) (Mulvany *et al.*, 1982). Within vascular smooth muscle cells passive movement of K^+ out of the cell is likely to be the largest contributory factor to resting membrane potential (Hirst & Edwards, 1989; Nelson & Quayle, 1995). This is supported by experimental *in vitro* values for the resting membrane potential of rat small mesenteric arteries of approximately -60mV, a value relatively near the equilibrium potential for K^+ in this tissue, and the observed depolarization and subsequent contraction of arteries placed in high K^+ solutions (Garland & McPherson, 1992; Mulvany *et al.*, 1982).

1.2.4.1. Maintenance of smooth muscle resting membrane potential

Within isolated rat small mesenteric artery smooth muscle the delayed rectifier subtype of voltage-dependent (K_v) channels contributes most significantly to the maintenance of resting membrane potential, as it is the dominant repolarizing current. A heteromeric assembly of the K_v subunits $K_v1.2$, $K_v1.3$, $K_v1.5$ and $K_v2.1$ most likely comprises the K_v channel that facilitates this major outward current (Xu *et al.*, 1999).

ATP-sensitive K^+ channel (K_{ATP}) currents also contribute to the maintenance of basal tone. Treatment with the K_{ATP} channel antagonists glibenclamide and tetraphenylphosphonium increased tone in the absence of a K_{ATP} channel opener and depolarized rat mesenteric artery smooth muscle preparations (Gardiner *et al.*, 1996; Jackson, 2005; McPherson & Angus, 1991; Tang *et al.*, 2005; Zhang *et al.*, 1998). These channels are thought to be of a distinct small conductance subtype (~35pS; also referred to as K_{NDP}), activated by products of metabolism including the cytosolic nucleoside diphosphates uridine diphosphate and guanidine diphosphate (Cole & Clement-Chomienne, 2003; Zhang & Bolton, 1995). However, the role for other K_{ATP} subtypes cannot be excluded as multiple K_{ATP} subtypes have been shown to be expressed in other vascular preparations (please see Cole & Clement-Chomienne, 2003 for review). Electrophysiological data, *in situ* hybridization and analysis of recombinant K_{ATP} channels expressed in other cell types supports a heteromeric complex consisting of four pore-forming $K_{ir}6.1$ channels and four modulatory sulfonylurea (SUR)2B subunits (Cole & Clement-Chomienne, 2003; Isomoto *et al.*, 1996; Wang *et al.*, 2003; Yamada *et al.*, 1997). In contrast to the classical K_{ATP} channels found in cardiac and pancreatic cells the small conductance K_{ATP} channels are inhibited by a lack of ATP and high concentrations of ATP. Maximal activity is seen in the range of 0.1 and 1mM ATP, facilitating their open state and contribution to membrane potential under resting conditions (Cole & Clement-Chomienne, 2003; Zhang & Bolton, 1995). Indeed the contribution of K_{ATP} to the resting membrane potential in rat mesenteric arteries is thought to be facilitated by steady-state activation of 3'-5'-cyclic adenosine monophosphate (cAMP)-dependent protein kinase (PKA) and subsequent association of A-kinase anchoring protein (AKAP) with the K_{ATP} channel complex in a nucleotide dependent manner (Cole & Clement-Chomienne, 2003; Hayabuchi *et al.*, 2001).

A small depolarization of rat small mesenteric arteries under resting conditions may be evoked by treatment with the inwardly rectifying K^+ channel (K_{ir}) inhibitor barium. However, an outward current through K_{ir} has only been measured in the endothelium of this preparation so electrical conductance through myoendothelial gap junctions (MEGJ) would have to facilitate the transfer of this voltage change to the smooth muscle layer (Please see section 1.4; Crane *et al.*, 2003b; Doughty *et al.*, 2001; Goto *et al.*, 2004).

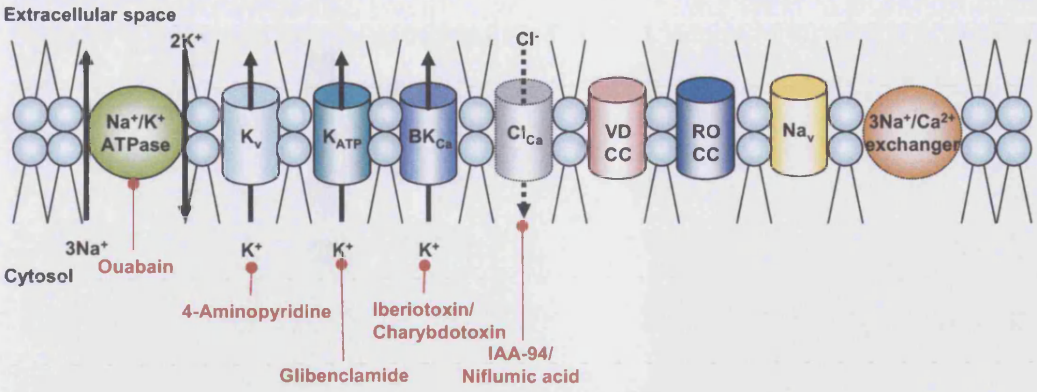

Figure 1.6 Ion channels in the smooth muscle plasma membrane contributing to maintenance of smooth muscle membrane potential
Cartoon illustrating the ion channels, exchangers and active pumping mechanisms contributing to the maintenance of the smooth muscle resting membrane potential at approximately -60mV. Arrows indicate the direction of ion flux across the plasma membrane. The absence of an arrow indicates channel closure. Dotted lines represent currents that are not yet clearly recognised in rat mesenteric artery smooth muscle tissue but that could contribute to the maintenance of resting membrane potential. The red lines and text indicate the commonly used inhibitors for each channel.

Furthermore, at the commonly reported resting membrane potential of approximately –60mV, although the K_{ir} would likely be active (Crane *et al.*, 2003b) whether or not this channel would contribute significantly to resting membrane potential in these arteries is contentious (Doughty *et al.*, 2001; Hirst & Edwards, 1989).

A more significant contribution to resting membrane potential is made by the large conductance calcium-activated K^+ (BK_{Ca}) channel. This channel is though to be located in plasmalemmal regions adjacent to the sarcoplasmic reticulum (SR) and is frequently activated in a transient nature by the small, single RyR channel release of Ca^{2+} sparks from the SR that may occur even when the artery is in the resting state (Jaggar *et al.*, 1998; Perez *et al.*, 1999; Wellman & Nelson, 2003). Such activation of the BK_{Ca} channel elicits a transient outward K^+ current (described as a spontaneous transient outward current (STOC) by Benham and Bolton (1986)) by shifting the basal activation and voltage sensitivity of this channel to the range of resting membrane potential (Perez *et al.*, 2001). As such it is thought to contribute to the reversal of pressure-induced tone and myogenic tone within numerous vascular preparations, including the rat mesenteric artery (Dora *et al.*, 2002; Jaggar *et al.*, 1998; Nelson *et al.*, 1995; Wellman & Nelson, 2003; Wesselman *et al.*, 1997).

The ~20mV difference between the equilibrium potential for K^+ and resting membrane potential implies the involvement of a small inward current at resting tone. In rat mesenteric artery preparations a smooth muscle, volume sensitive, outward chloride (Cl^-) conductance could contribute to a more positive resting membrane potential as the more positive equilibrium potential of Cl^- (Table 1.1) would encourage an outward movement of the ion following channel activation (Doughty *et al.*, 2001; Hirst & Edwards, 1989). Spontaneous transient inward currents (STICs) have been detected in a number of smooth muscle tissues, and like BK_{Ca}, the channels mediating this current are thought to be activated under resting conditions by Ca^{2+} sparks released from the SR. Indeed the sensitivity of STICs to Cl^- channel inhibitors suggests that STICs may reflect the activation of Ca^{2+}-dependent Cl^- (Cl^-_{Ca}) channels (Wellman & Nelson, 2003). At resting membrane potential the activation of both Cl^- channel STICs or BK_{Ca} channel STOCs by Ca^{2+} sparks has been observed and treatment with the Cl^- channel inhibitors IAA-94 and niflumic acid resulted in hyperpolarization of ~20mV in rat mesenteric arteries mounted under isometric tension supporting this proposal (Nilsson *et al.*, 1998).

Recent evidence suggests that two types of Cl^-_{Ca} channels may exist in rat small mesenteric smooth muscle preparations, those that are dependent on 3'5'-cyclic guanosine monophosphate (cGMP) and those that are not (Matchkov *et al.*, 2004a; Piper & Large, 2004). However it was proposed that neither would greatly contribute to resting membrane potential in this tissue as alteration of the transmembrane gradient for Cl^- had only a small (~+7mV) effect on membrane potential (Matchkov *et al.*, 2004a; Nilsson *et al.*, 1998). Instead, expanding on previous reports it was proposed that Cl^-_{Ca} channels likely to contribute to the maintenance of voltage-dependent calcium entry following depolarization and that cGMP-dependent Cl^-_{Ca} channels in particular contribute to the oscillations in membrane potential seen following α-adrenoceptor stimulation (Doughty *et al.*, 2001; Matchkov *et al.*, 2004a; Peng *et al.*, 2001; Piper & Large, 2004; Thorneloe & Nelson, 2005).

A small influence on smooth muscle resting membrane potential is attributed to the $3Na^+/2K^+$-ATPase which exchanges three Na^+ to the extracellular solution in exchange for two K^+ and in so doing evokes a small hyperpolarization of the smooth muscle cell

(~3-5mV) (Nilsson, 1998). Although Na^+ conductance is seen as relatively small and so would likely be reflected by a low $3Na^+/2K^+$ ATPase pump activity, treatment of isolated rat small mesenteric arteries with ouabain evoked a small depolarization and increase in vessel tension (Aalkjaer & Mulvany, 1985; Crane *et al.*, 2003b; Hirst & Edwards, 1989; Mulvany *et al.*, 1984). An inward Na^+ current through non-selective cation channels (NSCC) or voltage-dependent Na^+ channels (Na_v) does not contribute to resting membrane potential as raising extracellular Na^+ had little effect on the inward current observed in isolated rat mesenteric artery myocytes. Furthermore, it is unlikely that at the resting membrane potential Na_v are open (Berra-Romani *et al.*, 2005; Matchkov *et al.*, 2004a; Thorneloe & Nelson, 2005).

1.2.4.2. α-Adrenoceptor-evoked smooth muscle cell depolarization

Early experiments performing simultaneous measurements of membrane potential and smooth muscle tension coupled an increase in tension in response to noradrenaline to a concomitant depolarization of rat mesenteric artery smooth muscle cells to approximately -34mV (Mulvany *et al.*, 1982). However, the authors described only a 38% increase in tension following treatment with K^+ at concentrations able to elicit depolarization over the membrane potential range of noradrenaline-evoked contractions. Electromechanical coupling is therefore only thought to partially contribute to noradrenaline-evoked responses in this preparation, the remainder of the contractile response attributable to pharmacomechanical coupling mechanisms (please see section1.2.3 for review). However, within rat mesenteric artery preparations at least, depolarization is crucial for initiation of the response as blockade of VDCC with nifedipine or felodipine inhibited the initial peak constriction and rise in Ca^{2+} in response to PE in the majority of arteries tested. Indeed Ca^{2+} entry through VDCC contributes significantly to the initial peak and maintenance of PE-evoked contraction (Nelson *et al.*, 1988; Nilsson *et al.*, 1994; Thorneloe & Nelson, 2005; Zhang *et al.*, 2002).

Within rat small mesenteric artery smooth muscle cells depolarization is achieved by the influx of K^+, Na^+ and Ca^{2+} whilst Cl- efflux is associated with oscillations in tone and the maintenance of resting membrane potential as previously described

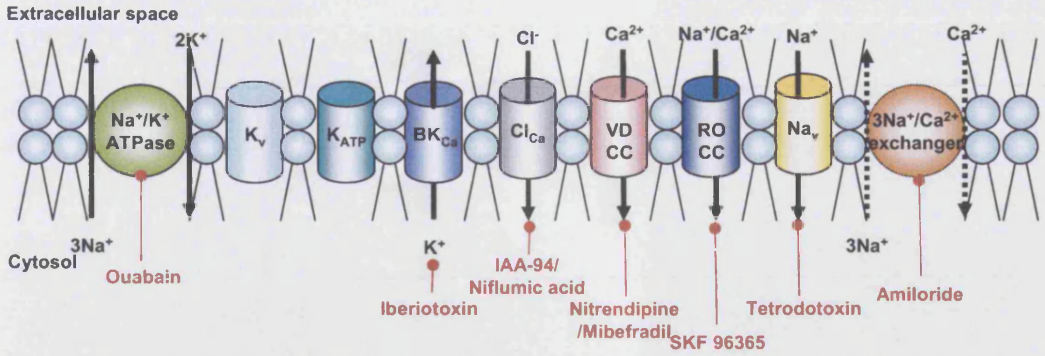

Figure 1.7 Ion channels in the smooth muscle plasma membrane contributing to α-adrenoceptor-evoked depolarization
Cartoon illustrating the ion channels, exchangers and active pumping mechanisms contributing to the depolarization evoked by smooth muscle α-adrenoceptor activation. Arrows indicate the direction of ion flux across the plasma membrane. The absence of an arrow indicates channel closure. Broken lines represent currents that are not yet clearly recognised in rat mesenteric artery smooth muscle tissue but that could contribute to α-adrenoceptor-evoked smooth muscle cell depolarization. The red lines and text indicate the commonly used inhibitors for each channel.

(Aalkjaer & Mulvany, 1985; Doughty *et al.*, 2000; Matchkov *et al.*, 2004a; Mulvany *et al.*, 1984; Nilsson, 1998; Nilsson *et al.*, 1998; Peng *et al.*, 2001; Piper & Large, 2004). Although a rise in intracellular Ca^{2+} is essential to the contractile mechanism and contributes significantly to depolarization, a reduced depolarization response (~50% of control) has been evoked in rat mesenteric small arteries following removal of extracellular Ca^{2+} and emptying of intracellular stores suggesting that influx of Na^+ and K^+ contribute substantially to the initial α-adrenoceptor-evoked decrease in membrane potential (Nilsson *et al.*, 1998).

Influx of Na^+, K^+ and Ca^{2+} may be mediated by the activation of ROCC downstream of α-adrenoceptor activation as has previously been described (please see section 1.2.3). However closure of the various K^+ channels thought to contribute to the outward K^+ current key to the maintenance of resting membrane potential may also contribute to PE-evoked depolarization (please see section 1.2.4.1). Elevated intracellular Ca^{2+} and activation of PKC are thought to close both K_v and K_{ATP} channels contributing to a rise in intracellular K^+ and membrane depolarization in various arterial preparations including the rat mesenteric artery (Bonev & Nelson, 1996; Cole & Clement-Chomienne, 2003; Cole *et al.*, 2000; Jackson, 2000; Jackson, 2005; Kubo *et al.*, 1997; Wilson *et al.*, 2000). Within rat aortic smooth muscle cells protein phosphatase-2B

activation has been shown to play a role in the Ca^{2+}-sensitivity of the K_{ATP} channel, with its activation in response to raised Ca^{2+} leading to channel closure (Wilson *et al.*, 2000). The details of this mechanism and whether it applies to the low conductance K_{ATP} channels of the rat small mesenteric artery remain to be determined.

Importantly, upon depolarization to ~-30mV K_v channels may be opened activating a negative feedback mechanism that may also contribute to the regulation of vascular tone (Jackson, 2000). Similar negative feedback mechanisms are achieved by activation of BK_{Ca}. Although Ca^{2+} sparks may be inhibited with increasing concentrations of PE (Mauban *et al.*, 2001) BK_{Ca} may be activated by membrane depolarization and the raised intracellular Ca^{2+} caused following receptor stimulation (Jackson, 2000). Indeed, a role for BK_{Ca} in regulation of tone within rat mesenteric artery preparations is supported by the observation of an iberiotoxin-sensitive smooth muscle cell current following PE stimulation (Crane *et al.*, 2003b).

In contrast to the maintenance of resting membrane potential Na^+ plays a key role in the initiation and maintenance of depolarization. Upon ROCC activation the potential for Na^+ to move into the cell is far higher than Ca^{2+} such that Na^+ is likely to be the predominating inward current (Nilsson, 1998). In addition, Na^+ influx may be mediated by the opening of Na_v, a channel recently identified in rat smooth muscle cells that may open as a consequence of the membrane depolarization evoked by other inward currents (Berra-Romani *et al.*, 2005; Matchkov *et al.*, 2004a; Thorneloe & Nelson, 2005). These observations are supported by experimental evidence whereby a decrease in the extracellular Na^+ concentration reduced noradrenaline-evoked depolarization in rat mesenteric small arteries (Mulvany *et al.*, 1984). To a lesser extent, a reversal of $3Na^+/Ca^{2+}$-exchange mechanisms may also be initiated by the influx of Na^+ further contributing to an increase in cytosolic Ca^{2+} and contraction, however the contribution of this mechanism to depolarization in rat mesenteric arteries is unclear (Berra-Romani *et al.*, 2005; Nilsson, 1998). As with K^+, negative feedback mechanisms may also exist for the Na^+ inward current in the form of the Na^+/K^+ ATPase, which may be activated at high intracellular Na^+ concentrations following Na^+ influx, and following K^+ efflux via smooth muscle BK_{Ca} and K_{ir} on the endothelium (Dora & Garland, 2001; Nilsson, 1998; Richards *et al.*, 2001; Weston *et al.*, 2002).

Both high voltage-activated L-type Ca^{2+} channels and low voltage-activated T-type Ca^{2+} channels have been shown to contribute to VDCC currents in various vascular smooth muscle cell tissues, with L-type channels contributing to the initial peak influx of Ca^{2+} whilst T-type channels mediate the maintained influx of Ca^{2+} (Cribbs, 2006). The dihydropyridine sensitivity of the PE and noradrenaline-evoked currents in rat mesenteric arteries and the expression of the mRNA encoding the pore-forming subunits of these arteries in the resistance-sized vessels supports a role for the L-type VDCC (Gustafsson *et al.*, 2001; Lagaud *et al.*, 1999; Nilsson, 1998; Nilsson *et al.*, 1994; Thorneloe & Nelson, 2005). The pore-forming subunit ($Ca_v3.1$) of the T-type channel has also been identified at the mRNA level in rat mesenteric arteriole and resistance artery smooth muscle (Gustafsson *et al.*, 2001; Jensen *et al.*, 2004). Indeed these authors demonstrated a role for this mibefradil-sensitive channel in contraction evoked by raised extracellular K^+ in the small arterioles of this vascular bed. However, the same laboratory have also reported an absence of the pore forming subunits of the L-type Ca^{2+} channel ($Ca_v1.2$) in the same preparation (Gustafsson *et al.*, 2001). Therefore, it may be that as with numerous other aspects of vascular pharmacology the importance of the L-type and T-type Ca^{2+} channels varies with vessel size and as such further functional studies would be required to confirm a role for the T-type channel in PE-evoked contractions of rat mesenteric resistance arteries.

1.2.5. KCl-evoked vasoconstriction

For many years the contractions evoked by raising extracellular K^+ have been attributed to Ca^{2+} influx through L-type VDCC following a change in the potential for K^+ to move out of the cell (Bolton, 1979; Nelson *et al.*, 1988). This was supported by observations in isolated rat small mesenteric arteries that the depolarization evoked by KCl preceded contraction whilst upon removal of K^+, repolarization exactly paralleled the decrease in wall tension (Mulvany *et al.*, 1982). However, more recently it has become apparent in some vascular beds that the Ca^{2+}-sensitizing and intracellular release mechanisms associated with G protein-coupled receptor evoked contraction are also activated downstream of a rise in extracellular K^+ (for review please see Ratz and colleagues 2005). One clear pathway for activation of Ca^{2+} sensitization is the activation of CaMKII (please see section 1.2.3.7). Whether this kinase is activated in rat small

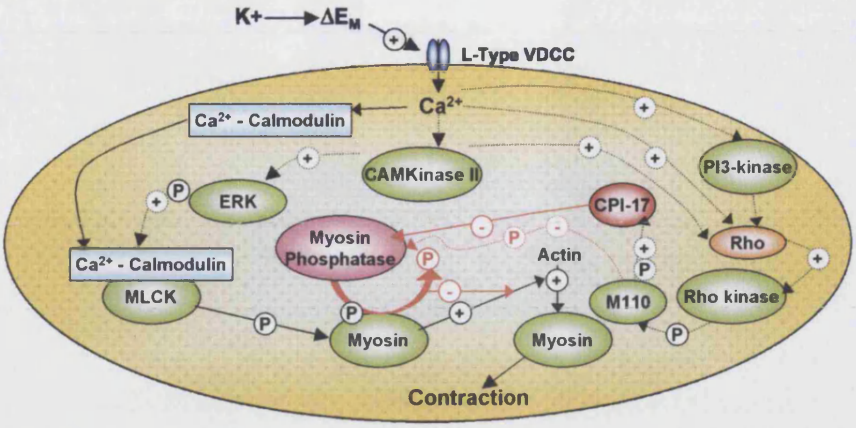

Figure 1.8 KCl-evoked contraction mechanisms.
Cartoon illustrating the possible mechanisms associated with contraction in response to depolarization evoked by KCl. Dotted arrows represent pathways not clearly defined in rat mesenteric artery smooth muscle tissue, but reported in other vascular smooth muscle preparations. ΔE_M corresponds to the change in membrane potential evoked by K^+. + and – represent stimulation and inhibition respectively. P represents phosphorylation.

mesenteric arteries remains to be established. Although, activation of Rho can occur downstream of CaMKII (Ratz *et al.*, 2005; Sakurada *et al.*, 2003) and Rho Kinase has been implicated in KCl-evoked contraction of rat mesenteric artery smooth muscle (Asano & Nomura, 2003). How depolarization by KCl evokes Rho Kinase activation ina mode independent of G-protein activation is currently unknown (Ratz *et al.*, 2005). In rabbit aortic smooth muscle the Class II PI-3 Kinase α-isoform may be activated by raised Ca^{2+} and could subsequently activate Rho (Wang *et al.*, 2006), however, such reports are not yet available for the rat small mesenteric artery.

1.3. Mechanisms of vasodilatation

The balance between contractile and relaxant stimuli acting on vascular smooth muscle regulates the level of vascular tone. Vasodilatation may therefore be evoked either by removal of the contractile stimuli (passive dilatation) or by activation of dilatation mechanisms that reverse the contraction (active dilatation). Active vasodilatation is principally achieved by two mechanisms: A reduction in smooth muscle Ca^{2+} or a reduction in myosin phosphorylation (Woodrum & Brophy, 2001). Both mechanisms

may be achieved as a result of direct action of agonists on the smooth muscle or by endothelium-dependent pathways.

1.3.1. Endothelium-independent vasodilatation

Numerous physiological molecules are able to evoke a vasodilatation response at least partly by their actions on the smooth muscle. In the rat mesenteric artery these include *N*-arachidonyl ethanolamide (anandamide; Ho & Hiley, 2003) adenosine (Mian & Marshall, 1995), adrenomedullin (Ross & Yallampalli, 2006), calcitonin gene-related peptide (cGRP; Champion *et al.*, 2001; Zygmunt *et al.*, 1995), vasoactive intestinal peptide (Ganz *et al.*, 1986), nitric oxide (NO; Ignarro *et al.*, 1987; MacLeod *et al.*, 1987; Palmer *et al.*, 1987) and endothelium derived hyperpolarizing factor(s) (EDHF(s)) (Busse *et al.*, 2002; Feletou & Vanhoutte, 2006; Fleming & Busse, 2006; Griffith, 2004; McGuire *et al.*, 2001; Sandow & Tare, 2007). The latter two, released from the endothelium in response to other vasoactive agonists are regarded as mediators of endothelium-dependent vasodilatation and so will be discussed in section 1.3.2. However all of the dilators listed evoke a dilatation response by one or more of the following mechanisms; increasing cyclic nucleotide concentration, decreasing intracellular Ca^{2+}, opening smooth muscle K^+ channels and reducing Ca^{2+}-sensitivity and myosin phosphorylation (Brain & Grant, 2004; Brayden, 2002; Kleppisch & Nelson, 1995; MacLeod *et al.*, 1987; McGuire *et al.*, 2001; Mistry & Garland, 1998; Plane *et al.*, 1996; Ross & Yallampalli, 2006; Sandow & Tare, 2007; Standen *et al.*, 1989; Tanaka *et al.*, 1999). For the purpose of this study the modes of action of LVK, a synthetic K_{ATP} channel opener and adenosine will be discussed. Comprehensive reviews for the other agonists may be found elsewhere (Brain & Grant, 2004; Brayden, 2002).

1.3.1.1. Levcromakalim

LVK, the more potent enantiomer of cromakalim (Quast & Villhauer, 1993) is a member of the benzopyran group of K^+ channel openers and can directly facilitate relaxation by opening K_{ATP} channels on the smooth muscle (Cole & Clement-Chomienne, 2003; Criddle *et al.*, 1994; Standen *et al.*, 1989). Helices 12 to 17 of transmembrane domain 2 of the SUR2B subunit of the K_{ATP} channel (please see section 1.2.4.1) are thought to modulate the binding and activity of LVK with LVK acting as a substrate for the SUR subunit of the channel. At least for the SUR-K_{ir}6.2 complex it is

then proposed that the conformational changes evoked by LVK acting upon SUR are transmitted to the closely associated K_{ir} domain, causing distortion of the channel, transforming the channel into the open state (Moreau *et al.*, 2005). Opening the K_{ATP} channel enables K^+ efflux and hyperpolarization of the smooth muscle cell (Standen *et al.*, 1989; Takano *et al.*, 2004; Weston & Abbott, 1987; White & Hiley, 2000). This leads to closure of VDCC and inhibition of IP_3 synthesis by PLC causing a reduction in intracellular Ca^{2+} and as a result a gradual reduction in excitation-contraction coupling and smooth muscle relaxation (Figure 1.9; please also see section 1.2.1 and 1.2.4.2; Cook, 1988; Criddle *et al.*, 1994; Ito *et al.*, 1991; Quast & Baumlin, 1991).

Cromakalim and its derivatives have also been found to cause stimulation of endothelial cell hyperpolarization in the perfused mesenteric bed and rat isolated mesenteric artery preparations (Feleder & Adler-Graschinsky, 1997; White & Hiley, 1997b). White and Hiley (1997b) demonstrated a distinct rightward shift in the concentration-response curve to LVK following removal of the endothelium and inhibition of cannabinoid receptors on the smooth muscle, indicative of a role for anandamide (although please see section 1.3.2.6 for further details), whilst in other reports inhibition of the endothelial NO synthase (eNOS; please see section 1.3.2.5) with N^{ω}-nitro-L-arginine methyl ester (L-NAME) attenuated LVK-evoked responses (Feleder & Adler-Graschinsky, 1997).

More recent data suggests that rather than acting directly upon endothelial cell K_{ATP} channels, hyperpolarization of the endothelium is evoked by the gap junction-mediated transfer of hyperpolarization from the smooth muscle to the endothelium. Indeed, treatment with the putative gap junction blockers 18-α glycyrrhetinic acid and 18-β glycyrrhetinic acid blocked endothelial cell hyperpolarizations to LVK in both rat and rabbit mesenteric arteries (Beny & Pacicca, 1994; Murai *et al.*, 1999; White & Hiley, 2000; Yamamoto *et al.*, 1998), whilst LVK had no effect on the resting membrane potential of isolated rat mesenteric endothelial cells (Takano *et al.*, 2004). Endothelial cell hyperpolarization could subsequently initiate other endothelium-dependent mechanisms of vasodilatation such as the synthesis and release of NO and EDHF by increasing the electrochemical gradient for Ca^{2+} (White & Hiley, 1997b). Given previous reports describing such hyperpolarization-driven influxes of Ca^{2+} into

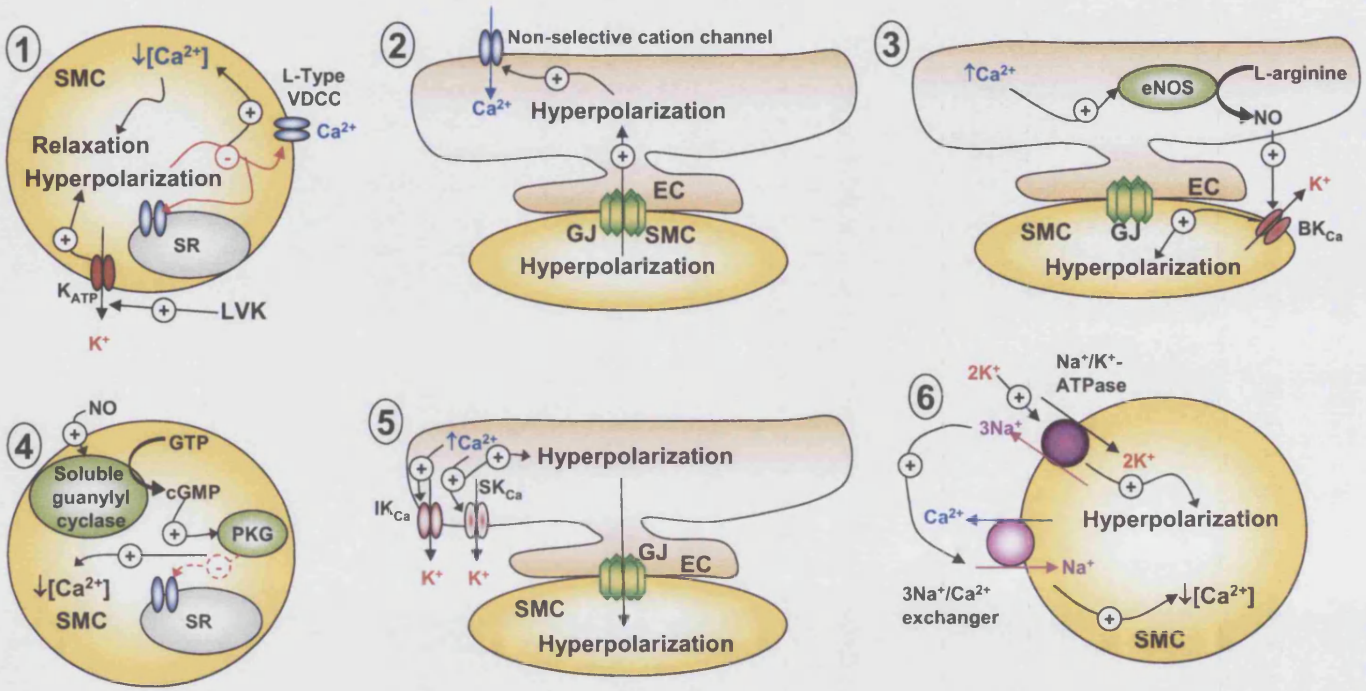

Figure 1.9A

Figure 1.9 Mechanisms of LVK-evoked vasodilatation Cartoons illustrating the different mechanisms possibly associated with LVK-evoked vasodilatation in rat mesenteric arteries. **A**, Each numbered panel depicts a different aspect of the vasodilatation mechanism that are brought together in **B** (next page). **1,** Direct hyperpolarization of the smooth muscle by the action of LVK on smooth muscle cell (SMC) K_{ATP} channels leads to closure of VDCC and SMC relaxation. **2,** The hyperpolarization may be transferrred to the endothelium via gap junctions (GJ) stimulating endothelial cell (EC) Ca^{2+} influx. **3**, The rise in Ca^{2+} can stimulate NO release which can subsequently act directly on SMC BK_{Ca} channels to cause SMC hyperpolarization, again causing relaxation as in 1. **4**, NO may also evoke SMC cGMP synthesis resulting in activation of PKG and possible (dashed line) inhibition of intracellular Ca^{2+} release from the SR promoting relaxation. **5**, A rise in EC Ca^{2+} may also activate IK_{Ca} and SK_{Ca} channels causing EC hyperpolarization which may be transferred to the SMC via GJ. **6**, Additionally the K^+ effluxed through the K_{Ca} channels may act upon SMC $3Na^+/2K^+$-ATPase leading to hyperpolarization and a decrease in SMC Ca^{2+}, both contributing to SMC relaxation. +, stimulation; -, inhibition.

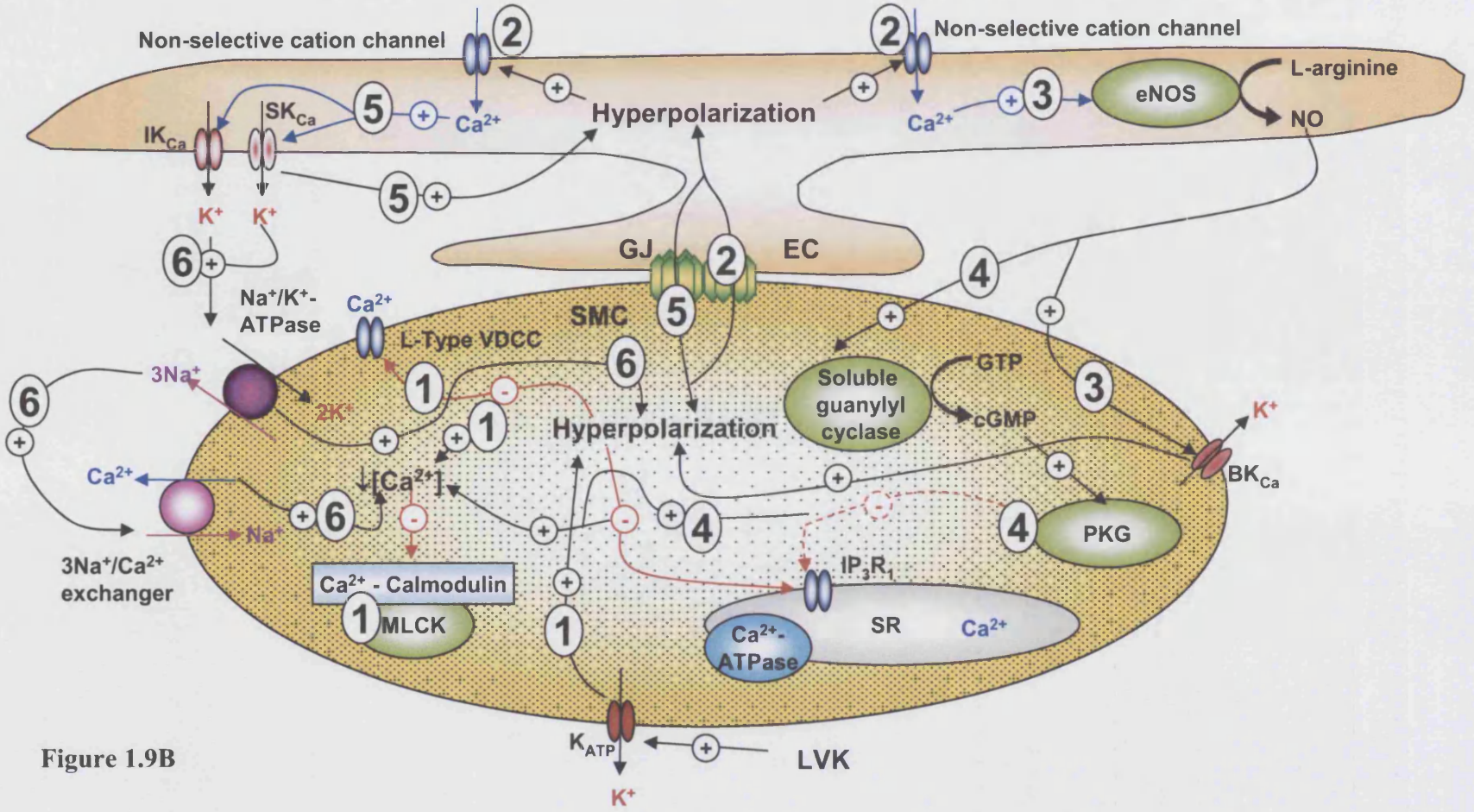
Non-selective cation channel
Non-selective cation channel
L-arginine
eNOS
NO
Hyperpolarization
IK$_{Ca}$
SK$_{Ca}$
Ca^{2+}
K$^+$
GJ
EC
SMC
Na$^+$/K$^+$-ATPase
L-Type VDCC
3Na$^+$
2K$^+$
Soluble guanylyl cyclase
GTP
cGMP
PKG
BK$_{Ca}$
↓[Ca^{2+}]
3Na$^+$/Ca^{2+} exchanger
Ca^{2+} - Calmodulin
MLCK
IP$_3$R$_1$
Ca^{2+}-ATPase
SR
K$_{ATP}$
LVK

Figure 1.9B

endothelial cells such a hypothesis is entirely plausible (Campbell *et al.*, 1991; Groschner *et al.*, 1994; Luckhoff & Busse, 1990a; Luckhoff & Busse, 1990b).

More recent reports investigating the ability of LVK to evoke conducted vasodilatation responses (please see chapter 5) in rat isolated and pressurized mesenteric arteries documented that the LVK-evoked spread of hyperpolarization and depolarization was endothelium-dependent, but that neither the local or remote responses to LVK were accompanied by a rise in endothelial cell Ca^{2+} (Takano *et al.*, 2004). Within this preparation therefore it would seem an increase in endothelial cell membrane potential does not necessarily always drive Ca^{2+} into the cell. Indeed a report investigating endothelial cell Ca^{2+} influx in response to ACh in the rat mesenteric artery also showed that the maintained phase of the Ca^{2+} response, that associated with Ca^{2+} influx from the extracellular space (please see section 1.3.2.2), was unaffected following inhibition of endothelial cell hyperpolarization, implying that each process can occur independently (McSherry *et al.*, 2005). Crucially, however, the image resolution and magnification in the experiments of Takano *et al.* (2004) and McSherry *et al.* (2005) would not have allowed visualization of any transient and localized rises in endothelial cell Ca^{2+}, for example in the microdomains associated with eNOS (Fleming & Busse, 2003; Frank *et al.*, 2003). Therefore, NO, or given recent observations (please see chapters 3 and 6; Sandow *et al.*, 2006) EDHF may still have a role in the LVK-evoked response described by White & Hiley (1997b).

The production of NO, stimulation of smooth muscle adenylyl cyclases (please see section 1.3.1.2) or activation of an EDHF would be expected to augment the dilatation response in intact arteries when compared to denuded arteries. However, experimentally this is not always the case. Within the perfused rat mesentery and small mesenteric arteries it was demonstrated that basal release of NO from the endothelium or addition of S-nitroso-N-acetylpenicillamine (SNAP) reduced the dilatation response to LVK (McCulloch & Randall, 1996; White & Hiley, 1998b). Additionally, LVK and another structurally distinct K_{ATP} channel opener pinacidil inhibited carbachol-induced EDHF-type dilatations, leaving NO-mediated responses intact (White & Hiley, 1998a). This interaction could arise as a result of a change in the relative K^+ concentrations inside and outside of the cell following each of the modes of smooth muscle cell and

endothelial cell stimulation (please see sections 1.3.2.6 and 1.3.2.9; White & Hiley, 1998b).

In the absence of any other modulators of tone or membrane potential, stimulation of K_{ATP} will allow movement of K^+ out of the smooth muscle cells. This will increase the K^+ concentration outside of the cell bringing both the endothelial and smooth muscle cell membrane potentials nearer the equilibrium potential for K^+. As a result efflux of K^+ through the endothelial cell K_{Ca} following agonist stimulation will be limited so endothelial cell hyperpolarization and the drive for Ca^{2+} influx will be diminished (please see section 1.2.4). Activation of SK_{Ca} and IK_{Ca} by stimulation of the endothelium with agonists such as carbachol (White & Hiley, 1998a), or indeed activation of smooth muscle BK_{Ca} by NO (Mistry & Garland, 1998; Plane *et al.*, 2001) would similarly prevent efflux of K^+ from smooth muscle K_{ATP}, thus attenuating LVK-evoked dilatation responses (McCulloch & Randall, 1996).

The differential LVK-evoked activation and inhibition of EDHF and NO pathways in the same preparation is difficult to reconcile solely by this mechanism. However, other factors, beyond the efflux of K^+ clearly overlap between these pathways. Both cGMP and cAMP are implicated in NO and EDHF-mediated dilatation pathways (Griffith *et al.*, 2004; Griffith *et al.*, 2002; MacLeod *et al.*, 1987). Given that K_{ATP} channels are also regulated by these nucleotides (please see below) and feedback pathways exist to regulate their accumulation, the production of cAMP and cGMP could have a significant effect on LVK-evoked responses in the intact preparation (McCulloch & Randall, 1996; Omar *et al.*, 2000; Plane *et al.*, 1996; Plane *et al.*, 2001; White & Hiley, 1998b). Indeed, within the rat mesenteric artery exogenous NO-evoked dilatation was inhibited by the presence of the endothelium in a cGMP-dependent manner (Plane *et al.*, 2001) whilst in the superior mesenteric artery removal of basal NO or the endothelium was shown to augment LVK-evoked responses in a manner that could be reversed by addition of 8-bromo cGMP (McCulloch & Randall, 1996).

cAMP, PKA and K_{ATP}

Activation of K_{ATP} by LVK partly reflects the actions of endogenous mediators such as adenosine and CGRP, which have been shown to activate K_{ATP} in various vascular

preparations including the rat mesenteric artery (Cheng *et al.*, 2004; Cole & Clement-Chomienne, 2003; Dart & Standen, 1993; Garland & McPherson, 1992; Jackson, 2005; Standen *et al.*, 1989; Tang *et al.*, 2005; Weidelt *et al.*, 1997; Wellman *et al.*, 1998). To evoke vasodilatation adenosine and CGRP act respectively on A_2 and CGRP1 receptors on the smooth muscle (Brain & Grant, 2004; Hiley *et al.*, 1995; Prentice *et al.*, 1997; Rubino *et al.*, 1995). Both receptors are seven transmembrane domain G_s-coupled GPCR that upon activation undergo a conformational change to allow dissociation of the $G_{\alpha S}$ subunit from the inhibitory $G_{\beta\gamma}$ subunits. The $G_{\alpha S}$ subunit subsequently interacts with adenylyl cyclase to activate the enzyme and initiate the transformation of ATP to cAMP (Kamenetsky *et al.*, 2006). In addition to other effector proteins such as the cyclic nucleotide gated ion channels, cAMP may bind to cAMP-dependent protein kinase (PKA), promoting dissociation of the catalytic subunit from the inhibitory subunit and activation of the serine-threonine kinase (Kamenetsky *et al.*, 2006). Association of PKA with AKAP localizes the enzyme to specific microdomains near the plasma membrane enabling the serine-threonine kinase to phosphorylate and activate, amongst other proteins, the K_{ATP} channel (Figure 1.10; Cole & Clement-Chomienne, 2003; Hayabuchi *et al.*, 2001; Michel & Scott, 2002).

cGMP, PKG and K_{ATP}

In contrast to CGRP and adenosine, NO activates K_{ATP} independently of cAMP. NO may be released from the endothelium or perivascular nerves (Boric *et al.*, 1999; Ferrer *et al.*, 2000) and diffuse to the smooth muscle where it may bind to a prosthetic heme group in the soluble guanylate cyclase complex activating the enzyme (Carvajal *et al.*, 2000). Like adenylate cyclase, guanylate cyclase catalyzes a cyclization reaction: the formation of cGMP from guanosine-5'-triphosphate. cGMP then activates a range of effector proteins including ion channels, cGMP-sensitive phosphodiesterases and soluble cGMP-sensitive protein kinase G (PKG) (Carvajal *et al.*, 2000). Activation of PKG stimulates translocation of the protein from the cytosol to the plasma membrane where in addition to other cellular targets it may phosphorylate K_{ATP} leading to its activation as described for PKA (please see section 1.3.2.5 for details of further NO-mediated dilatation pathways).

Physiological activation of K_{ATP} in the rat mesenteric artery

As described several physiological agonists including CGRP, adenosine, hydrogen sulphide (H_2S) and NO activate the K_{ATP} channel. However the importance of K_{ATP} to smooth muscle cell hyperpolarization and dilatation varies depending on the agonist used to evoke K_{ATP} channel activation and the vascular bed under study (Cole & Clement-Chomienne, 2003; Dart & Standen, 1993; Jackson, 2005; Standen *et al.*, 1989; Wellman *et al.*, 1998). CGRP-evoked a hyperpolarization response in rat small mesenteric artery smooth muscle cells and porcine coronary artery smooth muscle cells that was completely blocked by application of the SUR blocker glibenclamide (Hayabuchi *et al.*, 2001; Wellman *et al.*, 1998). Similarly H_2S-evoked endothelium-independent dilatation responses are abolished by glibenclamide (Cheng *et al.*, 2004). Attenuation of an adenosine-evoked hyperpolarizing current with glibenclamide in rabbit mesenteric artery and pig coronary artery smooth muscle cells has also been described (Dart & Standen, 1993; Kleppisch & Nelson, 1995). However, despite numerous reports of a vasodilatation response to adenosine in rat mesenteric artery preparations the relaxation response was not found to be sensitive to K_{ATP} channel blockers (Hiley *et al.*, 1995; Mian & Marshall, 1995; Prentice *et al.*, 1997; Rubino *et al.*, 1995). This may reflect the multi-faceted mechanism by which adenosine evokes a dilatation response, with other mechanisms compensating for the loss of K_{ATP}-evoked hyperpolarization (please see section 1.3.1.2). Alternatively it may reflect the observation that within rat isolated mesenteric arteries activation of K_{ATP} does not necessarily correlate with a vasodilatation response. K_{ATP} is reportedly activated by NO in rat mesenteric arteries and has been shown to contribute to NO-evoked smooth muscle hyperpolarization in this preparation in the absence of tone (Garland & McPherson, 1992). However, in arteries depolarized with noradrenaline, K_{ATP}-evoked hyperpolarization or vasodilatation was not observed in response to NO (Garland & McPherson, 1992; White & Hiley, 1998b).

Despite the inconsistencies observed with physiological activation of the K_{ATP} channel the demonstration of robust hyperpolarization and dilatation responses in isolated mesenteric arteries in response to LVK supports the presence of these channels in this preparation and their significant influence on membrane potential and vascular tone (Omar *et al.*, 2000; Takano *et al.*, 2004; White & Hiley, 1997b; White & Hiley, 2000;

White & Hiley, 1998b). Indeed, the sensitivity of the channel to intracellular nucleotide concentrations, CO_2 and pH supports a key role for K_{ATP} in regulation of vascular tone under various metabolic and hypoxic conditions (Brayden, 2002; Dart & Standen, 1993; Kleppisch & Nelson, 1995; Mian & Marshall, 1995; Wang *et al.*, 2003). Therefore the use of LVK as an agonist to evoke dilatation responses in the rat isolated mesenteric artery, although not wholly reflecting physiological events, may at least partly mimic the effects of endogenous mediators such as adenosine (please see section 1.3.1.2) and CGRP, which have been shown to be present and effective in this vascular bed.

1.3.1.2. Adenosine

Adenosine is a purine nucleoside that can be released into the circulation from a number of sources. Under conditions of acute and chronic hypoxia adenosine may be released from the endothelium of rat mesenteric arteries and skeletal muscle arterioles (Bryan & Marshall, 1999b; Mian & Marshall, 1995; Skinner & Marshall, 1996). In skeletal muscle preparations adenosine may also be released into the circulation as a product of metabolism following increased muscle contraction. However it is the endothelium-derived adenosine that is thought to mediate the local and spreading dilatation responses (please see chapter 5) required to improve tissue blood flow (Bryan & Marshall, 1999b; Duza & Sarelius, 2003; Murrant & Sarelius, 2002; Skinner & Marshall, 1996). Adenosine may also be produced (Figure 1.10) either as a result of the gradual breakdown of ATP by various intracellular and extracellular nucleotidases or as a result of the hydrolysis of *S*-adenosylhomocysteine by *S*-adenosylhomocysteine hydrolase (Gorlach, 2005). Given that ATP may be released into the circulation from circulating cells, nerve terminals and the vascular wall itself there is a strong likelihood that endogenous adenosine would be present in a number of vascular beds, if not all (Burnstock, 2006; Burnstock, 1999; Gonzalez-Alonso *et al.*, 2002; Pearce *et al.*, 1996; Rosenmeier *et al.*, 2004).

The classical pathway by which adenosine mediates vasodilatation is by a direct action on vascular smooth muscle cells as has previously been described (Figure 1.11). Adenosine acts upon smooth muscle $A_{2A/B}$ G protein-coupled receptors to stimulate adenylyl cyclase and the production of cAMP (Rubino *et al.*, 1995) . However, in addition to the activation of K_{ATP} observed in some vascular beds (please see section

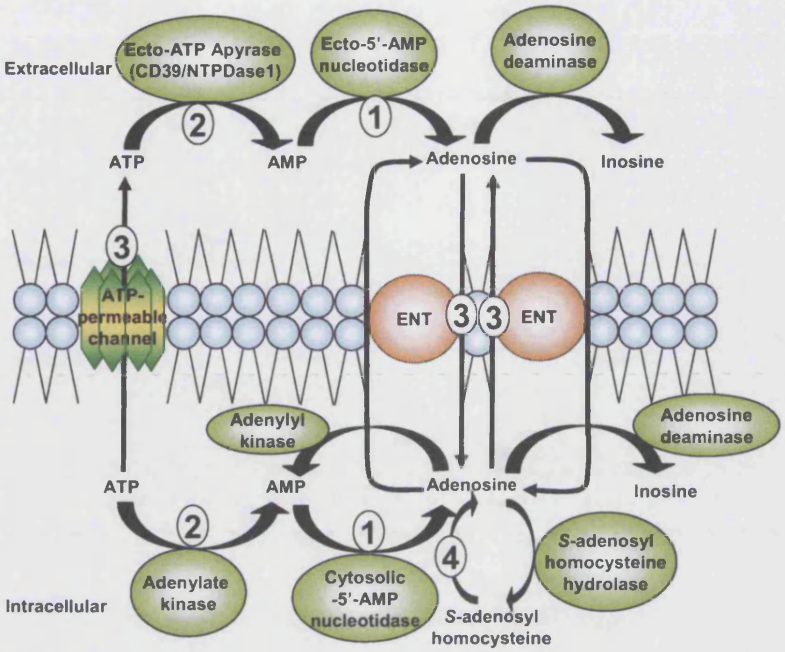

Figure 1.10

Adenosine production in the endothelium (adapted from Görlach *et al.*, 2005)
Cartoon illustrating the adenosine synthesis and degradation pathways both within the endothelium and on its external surface. **1**, Cytosolic 5'- and membrane-bound ecto-5'-AMP nucleotidases produce adenosine from AMP. **2**, AMP may be formed intracellularly by the breakdown of ATP by adenylate kinase or extracellularly by the breakdown of ATP by ecto-Apyrase enzymes. **3**, Adenosine may also be transferred across the membrane by the equilibrative nucleoside transporter (ENT) or via ATP-permeable channels. **4**, Alternatively, adenosine may be produced intracellularly from S-adenosyl homocysteine.

1.3.1.1), cAMP may also regulate a number of other effector proteins to mediate relaxation of vascular smooth muscle (Figure 1.11).

cAMP and smooth muscle relaxation

cAMP-evoked smooth muscle relaxation is associated with a decrease in the cytosolic Ca^{2+} concentration and a reduction in myosin phosphorylation. Within rat isolated mesenteric artery preparations this was shown to be a two-stage process initially dependent on a reduction in cytosolic Ca^{2+}, but at later stages requiring recruitment of Ca^{2+}-independent mechanisms (Taylor *et al.*, 1999).

A reduction in cytosolic Ca^{2+} may be mediated by VDCC closure as a result of the hyperpolarization caused by activation of K_{ATP} channels by cAMP as has been

described (please see section 1.3.1.1). Additionally activation of vascular smooth muscle K_{Ca} channels downstream of cAMP and PKA activation may also contribute to smooth muscle hyperpolarization and VDCC closure in the rat mesenteric artery (Ross & Yallampalli, 2006). Further reductions in cytosolic Ca^{2+} are achieved by cAMP-mediated activation of the SR Ca^{2+}-ATPase and through enhanced Ca^{2+} extrusion as a consequence of cAMP-facilitated activation of the $3Na^{+}/2K^{+}$ ATPase and subsequent $3Na^{+}/Ca^{2+}$ exchanger activation by cAMP (Nishimura, 2006). Furthermore, release of Ca^{2+} from intracellular stores by activation of IP_3R may be inhibited by PKA-dependent acceleration of $G_{\alpha q}$ sequestration (please see section 1.2.3.1; Abdel-Latif, 2001).

Nishimura and van Breemen (Nishimura & van Breemen, 1989) demonstrated that cAMP could also mediate a decrease in tension independently of the cytosolic Ca^{2+} concentration. Pre-treatment with cAMP was shown to abolish phorbol 12,13 dibutyrate (PDBu)-induced contractions indicating a cAMP-mediated Ca^{2+}-desensitization of the contractile apparatus. Based on earlier proposals it was suggested that cAMP would induce smooth muscle cell relaxation by activation of PKA and subsequent phosphorylation and inactivation of MLCK (please see section 1.2.1; Adelstein *et al.*, 1978; Nishimura & van Breemen, 1989). More recently, in non-vascular smooth muscle preparations PKA has also been shown to mediate both direct and indirect (via Rho) recruitment and activation of myosin phosphatase (please see section 1.2.3.7; Abdel-Latif, 2001; Murthy *et al.*, 2003; Taylor *et al.*, 1999). Interestingly the cAMP-mediated decrease in Ca^{2+}-sensitivity in branches of the rat superior mesenteric artery and in the perfused anterior mesenteric artery has also been demonstrated to be dependent on activation of PKG (Kawada *et al.*, 1997; Northover & Northover, 1997). Removal of vascular smooth muscle cell PKG was shown to result in an increase in cytosolic Ca^{2+} in response to forskolin treatment of rat aortic smooth muscle cells, possibly reflecting the increased open probability of VDCC documented in the presence of cAMP and (Kawada *et al.*, 1997; Lincoln *et al.*, 1990; Taguchi *et al.*, 1997). Indeed in rat aortic smooth muscle cells exogenous PKA was shown to be far less effective than PKG at activating the smooth muscle Ca^{2+}-ATPase (Rashatwar *et al.*, 1987) and PKG was found to mediate the cAMP-induced inhibition of Ca^{2+} release from intracellular stores by phosphorylation of the IP_3R (Komalavilas & Lincoln, 1996). Cross talk between PKA and PKG through cAMP and cGMP could feasibly occur, as both PKG and PKA

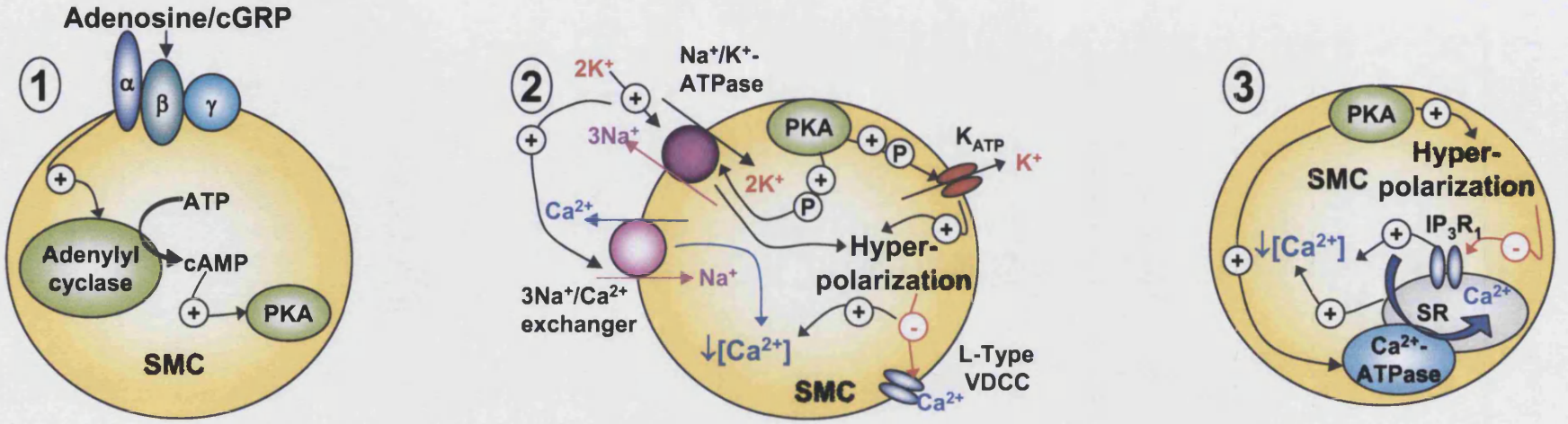

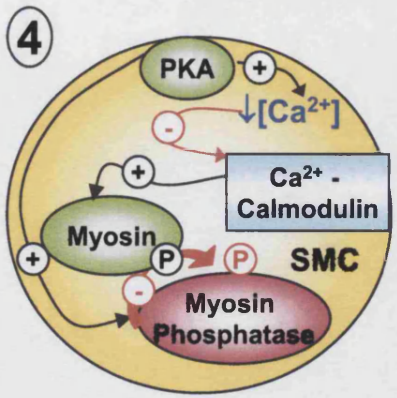

Figure 1.11A

Figure 1.11 Mechanisms of adenosine-evoked vasodilatation

Cartoons illustrating the different mechanisms possibly associated with adenosine or CGRP-evoked vasodilatation in rat mesenteric arteries. **A**, Each numbered panel depicts a different aspect of the vasodilatation mechanism that are brought together in **B** (next page) with the endothelium-dependent mechanisms described previously in Figure 1.9 panel A (numbers 2-6) arising from the transfer of hyperpolarization from the smooth muscle cell (SMC) to the endothelium. **1,** Activation of $G_{\alpha s}$ G protein-coupled receptors by adenosine or CGRP results in activation of adenylyl cyclase and production of cAMP, subsequently leading to PKA activation. 2, PKA may then phosphorylate ((P)) various proteins leading to their activation. These include the K_{ATP} channel and the $3Na^+/2K^+$-ATPase, which may both result in SMC hyperpolarization and closure of VDCC, causing a reduction in SMC Ca^{2+}. 3, Additionally PKA may phosphorylate and activate the SR Ca^{2+}-ATPase, leading to Ca^{2+} sequestration within the intracellular stores, again causing a decrease in SMC Ca^{2+}. 4, The reduction in SMC Ca^{2+} prevents the association of Ca^{2+} with calmodulin and hence MLCK activation. PKA itself may also limit myosin phosphorylation by activating myosin phosphatase. +, activated; -, inhibited.

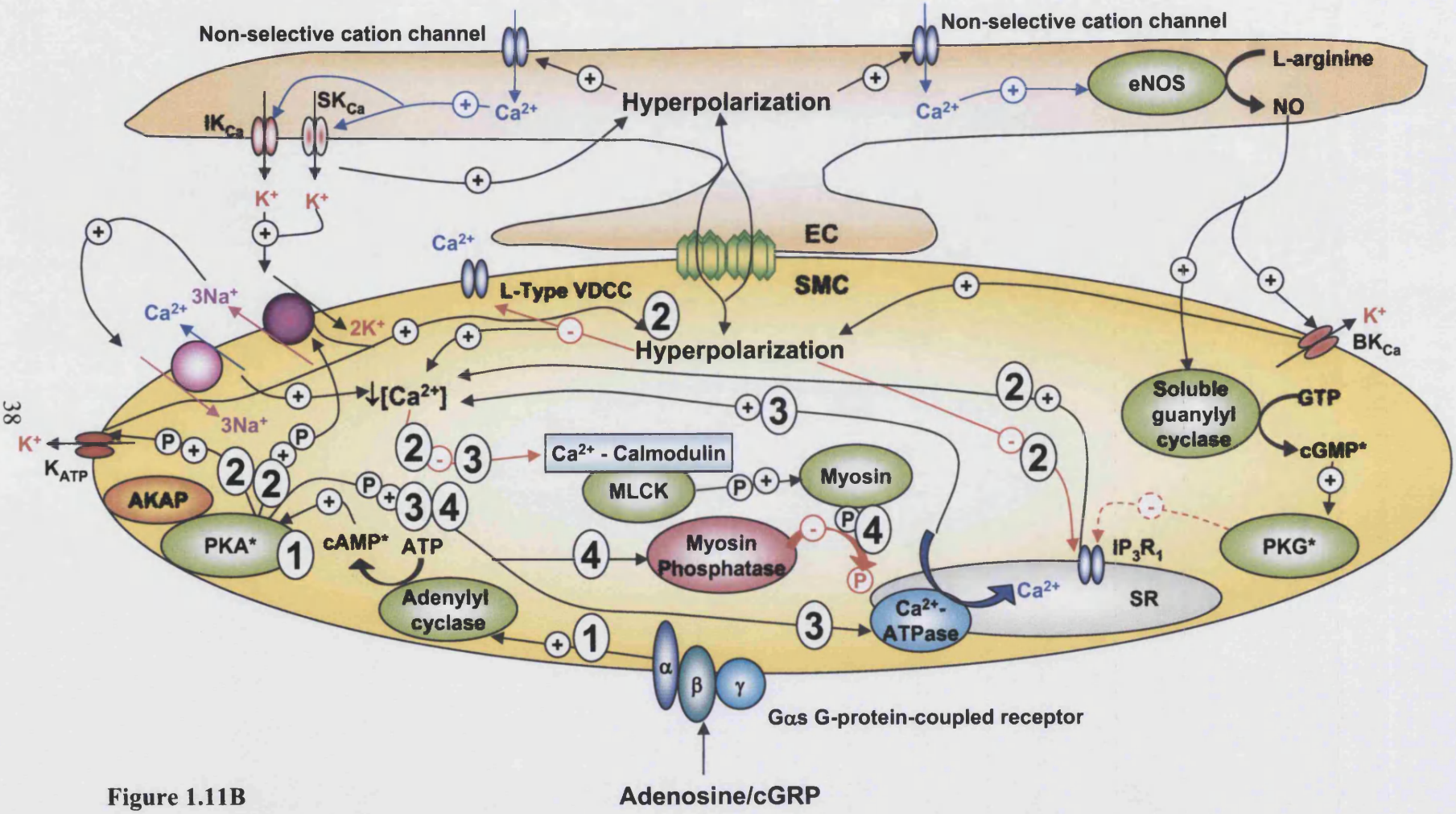
Non-selective cation channel
Non-selective cation channel
Hyperpolarization
eNOS
L-arginine
NO
IK_{Ca}
SK_{Ca}
Ca^{2+}
K^+
EC
SMC
L-Type VDCC
$3Na^+$
$2K^+$
Hyperpolarization
$\downarrow[Ca^{2+}]$
BK_{Ca}
Soluble guanylyl cyclase
GTP
cGMP*
K_{ATP}
AKAP
PKA*
cAMP*
ATP
Ca^{2+} - Calmodulin
MLCK
Myosin
Myosin Phosphatase
PKG*
IP_3R_1
SR
Ca^{2+}-ATPase
Adenylyl cyclase
α
β
γ
Gαs G-protein-coupled receptor
Adenosine/cGRP

Figure 1.11B

are sensitive to cAMP and cGMP (Figure 1.11). Furthermore the differing sensitivities of the serine-threonine kinases can be modulated by autophosphorylation enhancing their sensitivity for the opposite nucleotide (Lincoln *et al.*, 1990; Northover & Northover, 1997).

More recently adenosine has also been reported to have endothelium-dependent effects in some vascular beds including the rat superior mesenteric arterial bed (Bryan & Marshall, 1999b; Ray & Marshall, 2005; Rubino *et al.*, 1995). Within skeletal muscle vascular beds and aortic preparations a nitric oxide-dependent vasodilatation component downstream of A_1 and $A2_A$ receptor activation has been documented that was associated with endothelial cell K_{ATP} channel activation, hyperpolarization, Ca^{2+} influx and prostacyclin production (Bryan & Marshall, 1999a; Bryan & Marshall, 1999b; Ray *et al.*, 2002; Ray & Marshall, 2005; Ray & Marshall, 2006; Skinner & Marshall, 1996). Within rat small mesenteric arteries an endothelium-dependent component for adenosine-evoked dilatation responses has not been reported indeed K_{ATP} channels are not thought to be localized to the endothelium (Takano *et al.*, 2004; White & Hiley, 2000). However, given the recent report describing the transfer of hyperpolarization from the smooth muscle to the endothelium in response to LVK and the subsequent release of NO from the endothelium it is highly likely that such a mechanism could exist in response to A_{2A} activation (White & Hiley, 2000).

1.3.2. Endothelium-dependent vasodilatation.

The role of the endothelium in regulating subjacent smooth muscle cells and thus agonist-induced vasodilatation and smooth muscle hyperpolarization has long been established (Furchgott & Zawadzki, 1980). Numerous chemical and mechanical stimuli such as ACh, bradykinin, ATP, UTP, substance P and shear stress evoke vasodilatation by endothelium-dependent mechanisms (Buvinic *et al.*, 2002; Edwards *et al.*, 2000; Furchgott, 1983; Furchgott & Zawadzki, 1980; Malmsjo *et al.*, 2002; Malmsjo *et al.*, 1998; Pohl *et al.*, 1986; Thorsgaard *et al.*, 2003). The factors produced by the endothelium to mediate these dilatation responses include the endothelium-derived relaxing factor NO (Ignarro *et al.*, 1987; Palmer *et al.*, 1987), prostacyclin (Moncada & Vane, 1978) and the non-NO, non-prostanoid EDHF(s) (Chen *et al.*, 1988; Feletou & Vanhoutte, 1988; Taylor *et al.*, 1988; Taylor & Weston, 1988). The nature and

importance of these endothelium-derived mediators of relaxation varies according to the size and species of the vessel (Shimokawa *et al.*, 1996); NO being the main mediator of relaxation in the larger vessels of the arterial tree whilst having no obligatory role in smaller vessels where EDHF is thought to predominate (Garland & McPherson, 1992; Hill *et al.*, 2001; Shimokawa *et al.*, 1996; Urakami-Harasawa *et al.*, 1997).

Within this thesis dilatation responses to the endothelium-dependent GPCR agonists ACh, ATP, UTP, ADPβS and ATPγS were studied (Furchgott & Zawadzki, 1980; Malmsjo *et al.*, 2002; Malmsjo *et al.*, 1998; Mistry *et al.*, 2003). Within the mesenteric circulation ACh is regarded as an agonist for the endothelial cell muscarinic $(M)_3$ receptor, a $G_{q/11}$ GPCR (Blin *et al.*, 1995; Fujimoto & Matsuda, 1991; Wu *et al.*, 1997). Within the rat mesenteric artery preparation ATP, UTP, ADPβS and ATPγS also all evoke endothelium-dependent vasodilatation responses, predominantly by their actions on the P2Y family of GPCRs; more specifically the $P2Y_1$, $P2Y_2$, $P2Y_4$ and $P2Y_6$ $G_{q/11}$ G protein-coupled receptors (Buvinic *et al.*, 2002; Malmsjo *et al.*, 2000a; Malmsjo *et al.*, 2002; Malmsjo *et al.*, 1999; Mistry *et al.*, 2003). Therefore, for the purposes of this thesis only the mechanisms associated with endothelium-dependent dilatation responses to $G_{q/11}$ GPCR activation will be discussed with reference to section 1.2.3. For a detailed discussion of dilatation responses to physical stimuli such as shear stress and the downstream signalling processes associated with P2Y receptor activation readers are directed to the following reviews (Busse & Fleming, 2003; Ralevic & Burnstock, 1998).

1.3.2.1. Endothelial cell $G_{q/11}$ G protein-coupled receptor activation

As described previously (please see section 1.2.3.1), agonist binding to $G_{q/11}$ GPCRs activates PLCβ1, catalyzing the synthesis of IP_3 and DAG from PIP_2 (Berridge, 1993; Lee *et al.*, 1992; Newby & Henderson, 1990; Pirotton *et al.*, 1987; Wu *et al.*, 1992). As IP_3R1, IP_3R2 and IP_3R3 are all expressed on the endothelium of the rat small mesenteric artery, IP_3 could theoretically activate each of these receptors to stimulate Ca^{2+} release from the ER (Grayson *et al.*, 2004). However, given the differing IP_3 sensitivities of the receptors it is likely that the subtype of IP_3R activated depends upon the type of vasoactive stimuli and the level of that stimulus. Whichever IP_3R is activated the subsequent rapid rise in endothelial cell Ca^{2+} (Figure 1.13) is then key to the initiation

of the stimulus-secretion/hyperpolarization response (Berridge, 1993; Freay *et al.*, 1989; Fukao *et al.*, 1997b; Muller *et al.*, 1999).

1.3.2.2. Endothelial cell sources of Ca^{2+}

In the isolated, pressurized rat small mesenteric artery the endothelial cell Ca^{2+} response is characterized by an increase in Ca^{2+} that is maintained for the duration of the period of stimulation (Figure 1.12; McSherry *et al.*, 2005). However, the endothelial cell Ca^{2+} response actually comprises two phases that may be distinguished pharmacologically: a rapid increase in cytosolic Ca^{2+} that is dependent on the release of Ca^{2+} from intracellular stores and a second sustained rise that is dependent on the influx of extracellular Ca^{2+} (Cannell & Sage, 1989; Hallam & Pearson, 1986; McSherry *et al.*, 2006; McSherry *et al.*, 2005).

When Hallam & Pearson (1986) observed that the ATP-evoked increase in intracellular Ca^{2+} became transient following removal of extracellular Ca^{2+}, although the importance of extracellular Ca^{2+} to the response was highlighted (see below), it was also recognised that an intracellular Ca^{2+} source must exist to enable this transient Ca^{2+} response. Studies applying IP_3 to isolated endothelial cells subsequently demonstrated that this intracellular Ca^{2+} release likely reflected the IP_3-dependent quantal release of Ca^{2+} from ER stores (please see section 1.2.3.2; Freay *et al.*, 1989; Huser *et al.*, 1999). Reports to the contrary have demonstrated that in rabbit aortic endothelial cells the ACh-evoked rise in endothelial cell Ca^{2+} may be dependent on the release of Ca^{2+} from a ryanodine- and caffeine-sensitive store (please see section 1.2.3.3; Wang *et al.*, 1995). However, within the rat mesenteric artery, the ACh-evoked Ca^{2+} response would appear to be dependent on IP_3-stimulated intracellular Ca^{2+} stores as ryanodine was shown to have no effect on the ACh-evoked, Ca^{2+}-dependent hyperpolarization response, whilst both thapsigargin and CPA significantly attenuated ACh-evoked smooth muscle cell hyperpolarization and dilatation responses (please see section 1.3.2.7; Fukao *et al.*, 1997b; McSherry *et al.*, 2005).

As described, a role for extracellular Ca^{2+} is clear. Indeed, early experiments performed to characterise the endothelium-dependent response to ACh in the rat aortic ring preparation demonstrated a marked attenuation of the dilatation response following

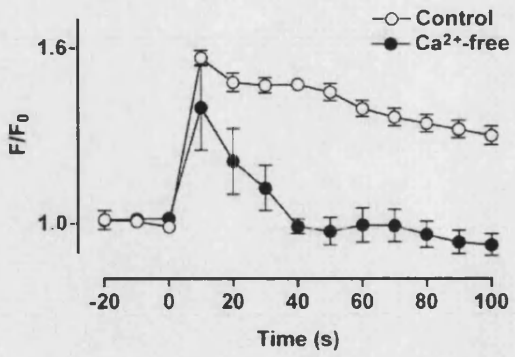

Figure 1.12 Average endothelial cell Ca^{2+} response to ACh in the rat isolated and pressurized mesenteric artery modified from McSherry *et al.*, 2005
The figure demonstrates the change in relative fluorescence (F/F_0) of the Ca^{2+}-sensitive dye fluo-4 AM averaged from 16 endothelial cells of an intact rat isolated, pressurized mesenteric artery in response to application of ACh (0.3μM) in the presence of extracellular Ca^{2+} (control) and in Ca^{2+}-free solution.

removal of extracellular Ca^{2+} (Long & Stone, 1985; Singer & Peach, 1982; Winquist *et al.*, 1985). More recent studies performed in a number of preparations including the rat mesenteric artery expand these observations to demonstrate that removal of extracellular Ca^{2+} or treatment with the NSCC antagonists SKF-96365 and mefenamic acid attenuated agonist-evoked endothelial cell Ca^{2+}, hyperpolarization and dilatation responses such that only transient increases in each were observed (Fukao *et al.*, 1997b; Fukao *et al.*, 2001; McSherry *et al.*, 2005).

The poor sensitivity of the agonist-evoked endothelial cell Ca^{2+} response to dihydropyridine treatment and the absence of a depolarization-induced increase in endothelial cell Ca^{2+} preclude a role for L-type VDCC in the response (Cannell & Sage, 1989; Colden-Stanfield *et al.*, 1987). Indeed, the pathway for influx of Ca^{2+} was initially attributed to the movement of Ca^{2+} down its electrochemical gradient following endothelial cell hyperpolarization (please see section 1.3.2.7; Campbell *et al.*, 1991; Groschner *et al.*, 1994; Luckhoff & Busse, 1990b). Within intact rat small mesenteric artery preparations however, recent evidence demonstrating that the frequency of Ca^{2+} oscillations and the time course of the Ca^{2+} response to ACh was unchanged following inhibition of the endothelial cell hyperpolarization response suggest that the influx of Ca^{2+} can occur independently of any changes in endothelial cell membrane potential (McSherry *et al.*, 2005), although small changes in intracellular Ca^{2+} downstream of

endothelial cell hyperpolarization cannot be ruled out by this study (please see section 1.3.1.1). Reports detailing thapsigargin and CPA evoked hyperpolarization responses of ~12mV (Fukao *et al.*, 1997b) and the previously described blockade of the endothelium-dependent Ca^{2+}, hyperpolarization and dilatation responses with SKF-96365 or the PLC inhibitor 1-(6-((17β-3-methoxyestra-1,3,5(10)-trien-17-yl)amino)hexyl)-1H-pyrrole-2,5-dione (U-73122) support Ca^{2+} influx via SOCE and ROCC in the rat mesenteric artery following $G_{q/11}$ GPCR stimulation (Fukao *et al.*, 1997b; McSherry *et al.*, 2005).

1.3.2.3. The identity of the endothelial cell Ca^{2+} influx channel

Both SOCE and ROCC currents in the vascular endothelium are characterized by a NSCC current (Freichel *et al.*, 2001; Groschner *et al.*, 1998; Leung *et al.*, 2006; Nilius *et al.*, 2003), possibly facilitating an influx of Ca^{2+} (Figure 1.13) via activation of the reverse phase of the $3Na^{+}/Ca^{2+}$ exchanger (Bondarenko, 2004; Sedova & Blatter, 1999; Teubl *et al.*, 1999; Winquist *et al.*, 1985). As such both currents could be associated with activation of the TRP family of ion channels (please see sections 1.2.3.4 and 1.2.3.5; Freichel *et al.*, 2001; Groschner *et al.*, 1998; Leung *et al.*, 2006; McFadzean & Gibson, 2002; Nilius *et al.*, 2003; Yao & Garland, 2005).

Members of each of the three TRP channel subfamilies, canonical (TRPC), vanilloid (TRPV) and melastatin (TRPM) have been documented within the vascular endothelium, the most widely expressed channels being members of the TRPC and TRPV subfamilies (please see Nilius *et al.*, 2003; Yao & Garland, 2005 for review). The ability of these channels to form heteromultimers within the limits of each subfamily has led to difficulties associated with the identification of each TRP channel and its relationship to endogenous Ca^{2+} entry pathways (Nilius *et al.*, 2003; Yao & Garland, 2005). However, a role for TRPC3 either as a ROCC or SOCE channel has been proposed within a number of cell culture preparations. Indeed, within human umbilical vein endothelial cells many of the characteristics of the TRPC3 current mimic those of the endogenous NSCC current (Nilius *et al.*, 2003), whilst the endogenous IP_3-evoked SOCE current can be inhibited by expression of the dominant-negative N-terminal fragment of TRPC3 (Groschner *et al.*, 1998). However, within the rat mesenteric artery, where TRPC3 is well expressed in the endothelium (Hill *et al.*, 2006)

acute knock down of TRPC3 had only small effects on bradykinin-evoked dilatation responses and absolutely none on those to ATP, CPA and histamine suggesting that at least within this preparation other TRP channel subtypes or indeed channel proteins (please see section 1.2.3.4) contribute to the vasodilatation response (Liu *et al.*, 2006b).

In support of this hypothesis robust rises in endothelial cell Ca^{2+} have been observed downstream of the activation of both TRPV1 and TRPV4 channel subtypes. (Kotlikoff, 2005; Marrelli *et al.*, 2006; Nilius *et al.*, 2003; Vriens *et al.*, 2005; Watanabe *et al.*, 2003; Yao & Garland, 2005). Furthermore, targeted endothelial cell knock out of TRPC4 markedly reduced ATP- and ACh-induced endothelial cell Ca^{2+} influx and attenuated the ACh-evoked dilatation response in mouse aortic and pulmonary arteries (Freichel *et al.*, 2001). Indeed, other channel proteins and signalling molecules distinct from the TRP family for example the STIM1/Orai1 pathway could also contribute to the influx of Ca^{2+} in response to store depletion (please see section 1.2.3.4).

1.3.2.4. Prostacyclin

Prostacyclin is a product of the metabolism of arachidonic acid by cyclooxygenase (COX) enzymes expressed within the endothelium and as such is ultimately dependent on the activation of the enzyme PLA_2, which produces arachidonic acid from membrane phospholipids (Busse & Fleming, 2003; Moncada & Vane, 1978; Parkington *et al.*, 2004). PLA_2 may be activated by both an increase in intracellular Ca^{2+} and by Ca^{2+}-independent mechanisms (Busse & Fleming, 2003). Once produced, prostacyclin is able to diffuse to the smooth muscle where it may activate the IP-prostanoid receptors stimulating the production of cAMP (Alexander *et al.*, 2006; Breyer *et al.*, 2001; Parkington *et al.*, 2004), which by mechanisms described previously including smooth muscle cell hyperpolarization (please see sections 1.2.3.7 and 1.3.1.2), may decrease smooth muscle cell Ca^{2+} and the Ca^{2+} sensitivity of the contractile machinery (Parkington *et al.*, 2004). However, within the rat mesenteric artery endogenous prostacyclin release is not thought to contribute significantly to the endothelium-dependent vasodilatation or hyperpolarization response (Chen & Cheung, 1997; Garland & McPherson, 1992; Hansen & Olesen, 1997; Waldron & Garland, 1994; Wu *et al.*, 1994).

1.3.2.5. Nitric oxide

In contrast a role for NO in the endothelium-dependent dilatation response of the rat mesenteric artery is well established (Garland & McPherson, 1992). Indeed some of the earliest experiments documenting the endothelium-dependent dilatation responses to agonists such as ACh and bradykinin detailed the release of the endothelium-dependent relaxing factor (EDRF) NO (Ignarro *et al.*, 1987; Palmer *et al.*, 1987) and showed it to be dependent on the influx of extracellular Ca^{2+} (Adams *et al.*, 1989; Furchgott, 1983; Luckhoff *et al.*, 1988). Soon after its identification, NO was shown to be generated from the precursor L-arginine (Palmer, 1988) thus enabling the production of various inhibitory analogues and the subsequent identification of the synthetic enzyme, nitric oxide synthase (NOS) (Vane, 1994). Three subtypes of NOS have since been identified: neuronal (n-) NOS (NOS I), inducible (i-) NOS (NOS II) and the constitutively active subtype endothelial (e-) NOS (NOS III), the latter of which is regarded as the enzyme largely responsible for the production of endothelium-derived NO under normal conditions (Busse & Fleming, 2003; Vane, 1994). eNOS activity was shown to be dependent on the presence of raised intracellular Ca^{2+}, which binds to calmodulin and with the activation of various kinases and phosphatases facilitates activation of the enzyme (Bredt & Snyder, 1990; Vane, 1994). However, the production of NO when activated by endothelial cell surface shear stress may be maintained after the Ca^{2+} response has ceased as eNOS can be activated following phosphorylation by the serine/threonine kinases Akt (PKB) and PKA in the presence of basal levels of Ca^{2+} (Boo & Jo, 2003; Busse & Fleming, 2003; Corson *et al.*, 1996; Dimmeler *et al.*, 1999; Fleming & Busse, 2003; Fleming *et al.*, 2005; Muller *et al.*, 1999; Tarbell & Pahakis, 2006). Multiple mechanisms mediate the transduction of the shear-induced signal to the activation of eNOS. These include the recruitment of caveolae to the plasma membrane and the subsequent association of signalling molecules with eNOS in these plasmalemmal domains, including platelet-endothelial cell adhesion moleule-1 (PECAM-1), heparan sulphate proteoglycans and PKC (Boo & Jo, 2003; Dusserre *et al.*, 2004; Fleming *et al.*, 2005; Frank *et al.*, 2003; Rizzo *et al.*, 1998; Tarbell & Pahakis, 2006). For review please see Tarbell & Pahakis (2006) and Busse *et al.* (2003)

Following its synthesis in the endothelium, NO subsequently diffuses to the smooth muscle where it may bind to soluble guanylate cyclase, stimulating cGMP formation,

and subsequently activating PKG (Figure 1.13) (Andriantsitohaina *et al.*, 1995; MacLeod *et al.*, 1987; Martin *et al.*, 1985; Rapoport & Murad, 1983). In addition to the stimulation of smooth muscle K_{ATP} channels (please see section 1.3.1.1) PKG mediates a decrease in smooth muscle cytosolic Ca^{2+} and hyperpolarization by a number of direct and indirect mechanisms (Figure 1.13). These include stimulating the sarcoplasmic Ca^{2+}-ATPase, thus promoting Ca^{2+} uptake into the intracellular stores, direct reduction of the open probability of the VDCC, phosphorylation of PLCβ (please see section 1.2.3.2), phosphorylation and inactivation of the IP_3R and acceleration of the sequestration of the $G_{\alpha q}$ subunit (please see section 1.2.3.1; Abdel-Latif, 2001; Andriantsitohaina *et al.*, 1995; Carvajal *et al.*, 2000; Komalavilas & Lincoln, 1996; Murthy *et al.*, 2003; Rashatwar *et al.*, 1987; Taguchi *et al.*, 1997; Twort & van Breemen, 1988). Like PKA-facilitated smooth muscle relaxation the PKG-evoked response also has a second Ca^{2+}-desensitization phase (Taylor *et al.*, 1999). PKG may reverse the Rho-mediated inhibition of myosin phosphatase and it may activate thin filaments such as calponin (Figure 1.13), both of which inhibit phosphorylation of the MLC_{20} (please see section 1.2.3.7; Murphy & Walker, 1998; Murthy *et al.*, 2003; Nishimura & van Breemen, 1989).

Although the activation of K_{ATP} by NO was reported not to contribute to smooth muscle cell hyperpolarization in noradrenaline-constricted rat mesenteric arteries (please see section 1.3.1.1; Garland & McPherson, 1992) higher concentrations of exogenous NO can evoke a hyperpolarization response in this artery and a range of other vascular preparations via activation of BK_{Ca}, and to a lesser extent K_v channels (Plane *et al.*, 2001). In some blood vessels this occurs via cGMP (Archer *et al.*, 1994; Robertson *et al.*, 1993) but in rat mesenteric arteries the hyperpolarizing action of NO appears to occur by a direct action of NO on the K^+ channels (Bolotina *et al.*, 1994; Mistry & Garland, 1998; Plane *et al.*, 1996; Plane *et al.*, 2001).

NO may also be released basally from the endothelium as demonstrated by the ability of NOS inhibitors to augment vasoconstrictor-evoked responses and reduce basal smooth muscle cGMP (Dora *et al.*, 1997; Dora *et al.*, 2000b; Fukuda *et al.*, 1992; Tuttle & Falcone, 2001). Indeed, the basal release of NO is reported to have an important modulatory role on the ability of exogenous NO or indeed other dilator agonists to

evoke hyperpolarization and relaxation. This could be a result of extracellular accumulation of K^+ and the reversal of the electrochemical gradient or, alternatively, the activation of negative feedback pathways associated with cGMP accumulation (please see section 1.3.1.1; Plane *et al.*, 1996; Plane *et al.*, 2001). TRPV4, which is widely expressed in the endothelium and may contribute to the agonist-induced Ca^{2+} influx (please see section 1.3.2.3) may be constitutively activated at body temperature (Nilius *et al.*, 2003) and thus could enable basal NO production. Alternatively the production of NO in the absence of endothelial cell stimulation may reflect the activation of eNOS following diffusion of Ca^{2+} from the smooth muscle to the endothelium through MEGJ(please see section 1.3.2.9) following, for example α-adrenoceptor stimulation (Dora *et al.*, 1997; Dora *et al.*, 2000b; Oishi *et al.*, 2001; Schuster *et al.*, 2001; Yashiro & Duling, 2000).

1.3.2.6. EDHF

A third endothelium-derived relaxing factor, EDHF, may also be released from the endothelium following agonist or mechanical stimulation (Chen *et al.*, 1988; Feletou & Vanhoutte, 1988). The EDHF-facilitated dilatation response is characterized by the transfer of endothelial cell hyperpolarization to the smooth muscle resulting in closure of VDCC and a reduction in smooth muscle intracellular Ca^{2+} (Busse *et al.*, 2002; Busse & Fleming, 2003; McGuire *et al.*, 2001; Sandow & Tare, 2007). Thus endothelial cell membrane potential is key to the regulation of the EDHF-type dilatation response. Experimental values for the resting membrane potential of isolated endothelial cells range from –80mV to 0mV under differing experimental conditions (Nilius & Droogmans, 2001), although recent evidence in the rat small mesenteric artery suggests endothelial cell resting membrane potential to be ~-50mV (McSherry *et al.*, 2005; Sandow *et al.*, 2002; White & Hiley, 2000).

1.3.2.7. Regulation of endothelial cell resting membrane potential

Endothelial cells are not considered to be electrically excitable, as they do not have VDCC (Cannell & Sage, 1989; Colden-Stanfield *et al.*, 1987; Nilius & Droogmans, 2001). The setting of endothelial cell membrane potential (if regarded independently of the subjacent smooth muscle layer) is instead facilitated mainly by the regulation of K^+ conductance, specifically through K_{Ca}, K_{ir} and possibly also K_v channels, although an

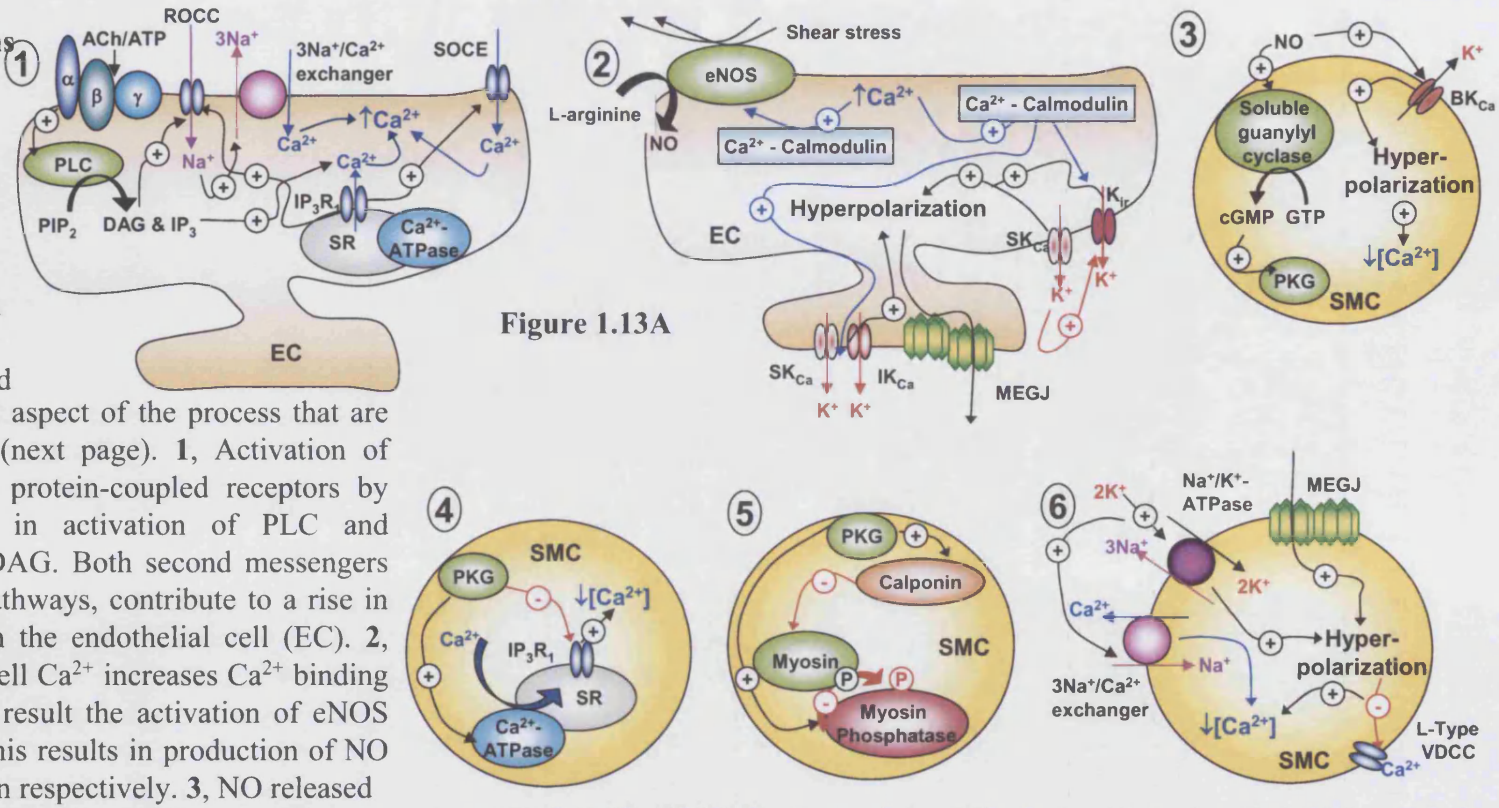

Figure 1.13A

Figure 1.13 Mechanisms of endothelium-dependent vasodilatation

Cartoons illustrating the mechanisms associated with endothelium-dependent vasodilatation in the rat mesenteric artery. A, Each numbered panel depicts a different aspect of the process that are brought together in B (next page). **1**, Activation of endothelial cell $G_{\alpha q}$ G protein-coupled receptors by ACh or ATP results in activation of PLC and production of IP_3 and DAG. Both second messengers may then, by distinct pathways, contribute to a rise in intracellular Ca^{2+} within the endothelial cell (EC). **2**, The rise in endothelial cell Ca^{2+} increases Ca^{2+} binding to calmodulin and as a result the activation of eNOS and EC K_{Ca} channels. This results in production of NO and EC hyperpolarization respectively. **3**, NO released from the endothelium may activate BK_{Ca} on subjacent smooth muscle cells (SMC) leading to hyperpolarization and relaxation of the smooth muscle as has been described previously. NO may also stimulate cGMP production leading to activation of PKG, **4,** sequestration of SMC Ca^{2+} and direct inhibition of **5**, myosin ATPase activity. **6**, The hyperpolarization initiated in the endothelium (2) may be transferred to the smooth muscle via myoendothelial gap junctions (MEGJ). Alternatively the K^+ effluxed from the endothelium through the K_{Ca} channels may stimulate SMC hyperpolarization and a reduction in intracellular Ca^{2+} but activation of the $3Na^+/2K^+$-ATPase. +, stimulation; -, inhibition.

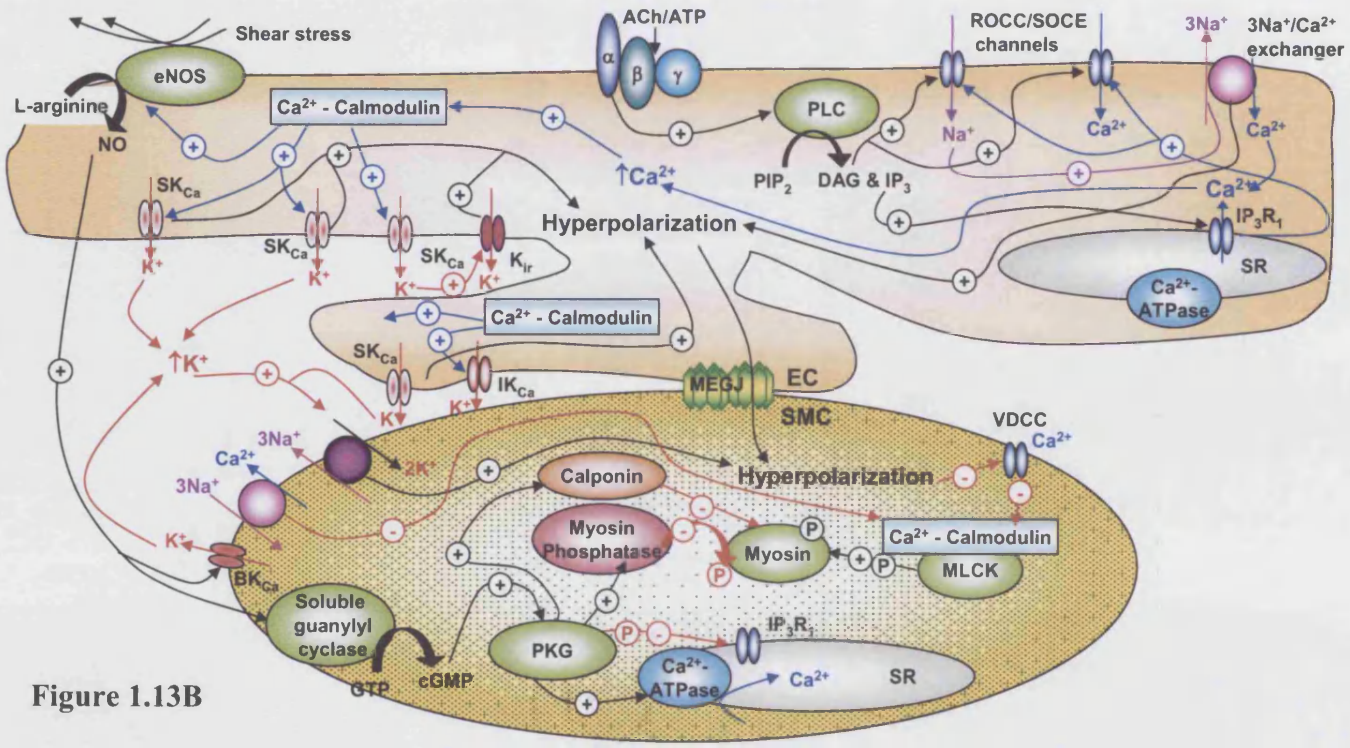
Shear stress
eNOS
L-arginine
NO
ACh/ATP
α
β
γ
Ca2+ - Calmodulin
PLC
PIP2
DAG & IP3
ROCC/SOCE channels
Na+
Ca2+
3Na+
3Na+/Ca2+ exchanger
↑Ca2+
SKCa
KIr
Hyperpolarization
IP3R1
SR
Ca2+-ATPase
↑K+
IKCa
MEGJ
EC
SMC
VDCC
2K+
Calponin
Myosin Phosphatase
Myosin
MLCK
BKCa
Soluble guanylyl cyclase
GTP
cGMP
PKG

Figure 1.13B

additional depolarizing Cl^- current has also been proposed (Nilius & Droogmans, 2001). To date, only K_{ir} channels have been shown to contribute to the regulation of endothelial cell resting membrane potential (Doughty *et al.*, 2001; Nilius & Droogmans, 2001), the open K_{ir} channel enabling an outward K^+ current leading to hyperpolarization of the endothelial cell as has previously been described (please see section 1.2.4.1) (Crane *et al.*, 2003b; Doughty *et al.*, 2001; Nilius & Droogmans, 2001). The other endothelial cell ion channels are only activated upon agonist or mechanical stimulation (Gao *et al.*, 2003; Nilius & Droogmans, 2001). Indeed the dominant regulatory component of the endothelial cell resting membrane potential is actually thought to be he underlying smooth muscle, partly accounting for the variation in the membrane potential of isolated endothelial cells.

In contrast to the endothelial cell membrane potential in intact arterial preparations, the resting membrane potential of isolated rat mesenteric endothelial cells was ~-19mV suggesting that the underlying smooth muscle layer likely plays a key role in the regulation of the endothelial cell membrane potential, possibly via the transfer of current through MEGJ (please see sections 1.2.4.1 and 1.3.3; McSherry *et al.*, 2005; White & Hiley, 2000). Indeed results comparing the incidence of MEGJ and hyperpolarization responses in the rat femoral and mesenteric arteries demonstrated that the large difference in the resting membrane potential of femoral artery endothelial (~-26mV) and smooth muscle (~-58mV) cells correlated with the absence of MEGJs in this preparation. Whereas in the intact rat mesenteric artery, where the endothelium and smooth muscle are well coupled electrically, the resting membrane potential for the endothelial (~-54mV) and smooth muscle (~-57mV) cells were more aligned (Sandow *et al.*, 2002). Indeed, blockade of gap junctions in this preparation with 18-α glycyrrhetinic acid evoked a large depolarisation of the resting membrane potential of the endothelium (from ~–51mV to ~–28mV) (White & Hiley, 2000) supporting the influence of the smooth muscle on the endothelial cell resting membrane potential.

1.3.2.8. Direct endothelial cell hyperpolarization

Within rat mesenteric arteries hyperpolarization following endothelial cell $G_{q/11}$ GPCR stimulation has been shown to be dependent on an increase in endothelial cell Ca^{2+} and has been shown to last for the duration of the Ca^{2+} response (please see section 1.3.2.2)

(Fukao *et al.*, 1997b; McSherry *et al.*, 2005). Early reports documenting the sensitivity of the hyperpolarization response to raised K^+, endothelial cell ^{86}Rb efflux and K^+ currents in response to ACh implied an important role for K^+ channels (Busse *et al.*, 1988; Olesen *et al.*, 1988; Taylor *et al.*, 1988; Taylor & Weston, 1988; Waldron & Garland, 1994). Within the rat mesenteric artery both K_{ATP} channels and BK_{Ca} channels are thought to be restricted to the smooth muscle layer as LVK and the BK_{Ca} channel activator, NS1619, had no direct effects on endothelial cell conductance (Takano *et al.*, 2004; Walker *et al.*, 2001; White & Hiley, 2000). Evidence in support of a role for K_v channels in regulation of the endothelial cell membrane potential is currently unavailable. However, within a range of arteries combined blockade of IK_{Ca} (with charybdotoxin, maurotoxin, TRAM-34 or TRAM-39) and SK_{Ca} channels (with apamin) completely blocked agonist-evoked endothelial cell hyperpolarization (Edwards *et al.*, 1998; Edwards *et al.*, 2000; Eichler *et al.*, 2003; Gluais *et al.*, 2005; Hinton & Langton, 2003) and subsequently smooth muscle hyperpolarization and relaxation supporting the suggestion that these two channels comprise the endothelial cell agonist-evoked outward K^+ current (Figure 1.13) that is an essential component of the EDHF response (Chataigneau *et al.*, 1998; Chen & Cheung, 1997; Crane *et al.*, 2003a; Doughty *et al.*, 1999; Edwards *et al.*, 1998; Edwards *et al.*, 2000; Eichler *et al.*, 2003; Hinton & Langton, 2003; McSherry *et al.*, 2005; Petersson *et al.*, 1997; Ungvari *et al.*, 2002; Zygmunt & Hogestatt, 1996). Recent experiments within rat aortic endothelial cells also support a role for the reverse mode of the electrogenic $3Na^+/Ca^{2+}$-exchanger in the ACh-evoked hyperpolarization response (Bondarenko, 2004). Such a hypothesis is consistent with the influx of Ca^{2+} required to evoke the response and the activation of an inward Na^+ current following store-depletion as has been described previously (please see section 1.3.2.2; Figure 1.13). However, the relevance of this observation to the rat mesenteric artery preparation has yet to be ascertained.

Although agonist stimulation of the endothelium clearly evokes a hyperpolarization response, following blockade of endothelial cell K^+ channels ACh has also been shown to evoke a small depolarization (Marchenko & Sage, 1993; McSherry *et al.*, 2005). This depolarization response has been attributed to the activation of the volume-regulated anion channel (VRAC) and Cl^- transporters activated by the ion fluxes caused by agonist stimulation of the endothelium (Doughty *et al.*, 2001; Marchenko & Sage, 1993;

McSherry *et al.*, 2005; Nilius & Droogmans, 2001; Ohashi *et al.*, 1999). Interestingly however, unlike the hyperpolarization response within the rat mesenteric artery preparation, the depolarization is not conducted to the underlying smooth muscle (McSherry *et al.*, 2005). Furthermore, the basal activation of the volume-sensitive current in both isolated rat mesenteric arteries and calf pulmonary artery endothelial cells has been shown to be highly variable, possibly contributing to the variable resting membrane potential described previously (Doughty *et al.*, 2001; Nilius & Droogmans, 2001; Voets *et al.*, 1996).

1.3.2.9. Candidates for the identity of EDHF

Mechanisms associated with the generation of hyperpolarization within the endothelium are well established. However the identity of the EDHF, and whether the transfer of hyperpolarization from the endothelium to the smooth muscle is in fact a contact-mediated cell-to-cell transfer of hyperpolarization (please see section 1.3.3) rather than the transfer of a diffusible factor (EDHF) is still unclear. Indeed, some investigators have proposed that the response is mediated by multiple EDHFs thus further complicating their identification and characterization (Busse *et al.*, 2002; Dora & Garland, 2001; Edwards *et al.*, 1998; Edwards *et al.*, 2000; Mather *et al.*, 2005; McGuire *et al.*, 2001; Sandow & Tare, 2007; Triggle & Ding, 2002). Whichever identity the transfer of hyperpolarization takes one universally accepted characteristic is that its generation must be abolished by blockade of endothelial IK_{Ca} and/or SK_{Ca} channels (Busse *et al.*, 2002; Dora & Garland, 2001; Fleming, 2004; Garland & Plane, 1996; Sandow & Tare, 2007).

Potential candidates for the classically, non-prostacyclin, non-NO EDHF response include diffusible factors such as K^+ efflux from the endothelium (Edwards *et al.*, 1998), the products of arachidonic acid metabolism by cytochrome P450-dependent monooxygenases (CYP), the epoxyeicosatrienoic acids (EETs)(Campbell *et al.*, 1996; Popp *et al.*, 1996), endogenous cannabinoids (Randall *et al.*, 1996), C-type natriuretic peptide (CNP; Chauhan *et al.*, 2003b) and hydrogen peroxide (H_2O_2; Matoba *et al.*, 2000). For excellent reviews of the EDHF response and potential candidates for its identity please see McGuire *et al.* (2001) and Félétou & Vanhoutte (2006).

K^+

A K^+ identity for EDHF was proposed when Edwards *et al.* (1998) detailed the charybdotoxin- and apamin-sensitive release of K^+ into the myoendothelial space and the dilatation of rat mesenteric and hepatic arteries to increasing concentrations of K^+ (Edwards *et al.*, 1998). The authors documented that both EDHF-type responses, that to K^+ and that to ACh, were sensitive to the $3Na^+/2K^+$-ATPase and K_{ir} inhibitors ouabain and barium, proposing that agonist stimulation evoked release of K^+ from the endothelium, which stimulated the $3Na^+/2K^+$ATPase and K_{ir} on the smooth muscle to facilitate smooth muscle hyperpolarization, relaxation and subsequently vasodilatation (Figure 1.13; please see section 1.2.4; Edwards *et al* (1998)). However, subsequent studies also using the rat mesenteric artery reported contrary observations (Doughty *et al.*, 2000; Lacy *et al.*, 2000). Firstly, reports from a number of groups documented that the barium-sensitive component of the dilatation response to exogenous K^+ was removed upon denudation of the artery. This indicated that the K_{ir} channels were restricted to the endothelium and thus did not *directly* contribute to the K^+-evoked hyperpolarization of the smooth muscle, but instead likely augmented endothelial cell hyperpolarization (Doughty *et al.*, 2000; Lacy *et al.*, 2000). Indeed, the endothelial cell location of the K_{ir} was later confirmed in both intact rat mesenteric artery and isolated cell preparations (Crane *et al.*, 2003b; Dora & Garland, 2001).

Perhaps of most relevance to this thesis however (please see chapter 4), are the observations detailed by Doughty *et al.* (2000) and Lacy *et al.* (2000) that exogenous K^+ was unable to evoke consistent EDHF-type dilatation responses in either pressurized or wire-mounted rat mesenteric arteries of the same profile or magnitude as that seen in response to ACh. Indeed within both preparations only 30-40% of arteries evoked any kind of dilatation response to exogenous K^+ (Doughty *et al.*, 2000; Lacy *et al.*, 2000). Richards *et al.* (2001) then demonstrated that the degree of smooth muscle depolarization influenced the K^+-evoked hyperpolarization response: Robust, endothelium-dependent hyperpolarization responses to 5mM KCl, consistent with those observed by Edwards *et al.* (1998) were observed in the absence of PE-evoked depolarization, however following depolarization of the smooth muscle in response to 1μM PE and subsequently 10μM PE, K^+-evoked hyperpolarization responses were attenuated in a concentration-dependent manner.

Richards *et al.* (2001; Weston *et al.*, 2002) subsequently demonstrated that this effect of PE could be reversed by treatment with iberiotoxin, a BK_{Ca} channel blocker. This observation was consistent with the activation of BK_{Ca} channels following smooth muscle depolarization (Dora *et al.*, 2000b; Jackson, 2000) (please see section 1.2.4.2). Thus, it was proposed that following high levels of smooth muscle cell stimulation, K^+ effluxed from the smooth muscle through BK_{Ca} channels formed a 'K^+ cloud' in the interstitial space. Hence upon activation of the smooth muscle maximal stimulation of the $3Na^+/2K^+$-ATPase could occur, preventing further activation by exogenous K^+ (Richards *et al.*, 2001; Weston *et al.*, 2002). Indeed, these observations were consistent with reports from Dora *et al.* (2001; 2002) demonstrating that K^+ evoked dilatation and hyperpolarization responses could be achieved under conditions of submaximal PE-evoked contraction that were not possible under conditions of increased PE-evoked tone. Furthermore these observations were extended to show that activation of endothelial cell K_{Ca}, likely as a result of diffusion of Ca^{2+} from the smooth muscle to the endothelium though MEGJ (Dora *et al.*, 1997; Dora *et al.*, 2000b; Oishi *et al.*, 2001; Schuster *et al.*, 2001; Yashiro & Duling, 2000) also contributed to the 'K^+ cloud' within isometric preparations (Dora *et al.*, 2002). Importantly, however, each of these studies demonstrated that even in the presence of barium and ouabain an endothelium-dependent dilatation and hyperpolarization response to ACh could still be evoked, indicative of a second candidate for EDHF within the rat mesenteric artery (Dora & Garland, 2001; Doughty *et al.*, 2000; Edwards *et al.*, 1998; Lacy *et al.*, 2000).

EETS

EETs are the products of arachidonic acid metabolism by CYP 2C epoxygenases so their synthesis depends on endothelial cell Ca^{2+} influx and the subsequent formation of arachidonic acid by PLA_2 (Figure 1.14). The increased arachidonic acid then initiates the CYP 2C –mediated generation of 5,6-, 8,9-, 11,12-, 14,15- EETs (Busse & Fleming, 2003; Campbell *et al.*, 1996; Fisslthaler *et al.*, 1999; Fleming, 2004). The EETs were classed as mediators of the EDHF-type vasodilator response as agonist-evoked dilatation responses sensitive to charybdotoxin and the non-selective K_{Ca} inhibitor, TEA, were also sensitive to selective inhibition of CYP 2C8/34 (Campbell *et al.*, 1996; Fisslthaler *et al.*, 1999; Popp *et al.*, 1996). Furthermore when applied exogenously, or

their production upregulated following chemical or physical stimulation of the endothelium, EETs facilitated smooth muscle cell hyperpolarization (Busse & Fleming, 2003; Campbell *et al.*, 1996; Fisslthaler *et al.*, 1999; Huang *et al.*, 2005; Popp *et al.*, 1996); either by increasing Ca^{2+} spark frequency and thus BK_{Ca} channel activity via activation of smooth muscle TRPV4 channels (Earley *et al.*, 2005) or by activating smooth muscle cell BK_{Ca} (Li & Campbell, 1997).

It has been proposed, however that the lipophilic nature of the EETs would limit their diffusion to the smooth muscle implying that EETs could not be an EDHF but would rather act to amplify the endothelial cell hyperpolarization response (Fleming, 2004). EETs have been reported to regulate gap junctional communication (Popp *et al.*, 2002) and activate endothelial cell TRPV4 channels, the latter increasing endothelial cell Ca^{2+} and hyperpolarization (Nilius *et al.*, 2003; Vriens *et al.*, 2005; Watanabe *et al.*, 2003) so such a hypothesis is entirely feasible. Indeed, it is perhaps more likely in arteries such as the rat mesenteric where firstly, iberiotoxin is not an effective inhibitor of the EDHF response (Doughty *et al.*, 1999; Vanheel & Van de Voorde, 1997), secondly, arachidonic acid was unable to evoke a smooth muscle hyperpolarization or dilatation response (Fukao *et al.*, 1997a; White & Hiley, 1998c) and thirdly, the suicide substrate inhibitors of the CYP enzymes, 17-octadecynoic acid (17-ODYA) and eicostetraeinoic acid (ETYA), also did not affect ACh-evoked rat mesenteric smooth muscle cell hyperpolarization (Fukao *et al.*, 1997a; Vanheel & Van de Voorde, 1997). Although this latter point could perhaps preclude even a modulatory role for the EETs both 17-ODYA and ETYA are non-selective for the CYP isoforms. Therefore their lack of efficacy could reflect the dual inhibition of arachidonic acid metabolite-evoked hyperpolarization and depolarization responses (the latter mediated by the ω-terminal hydroxyeicosatetraenoic acids (HETEs), arachidonic acid metabolites of the CYP 4A ω-hydroxylase enzymes) (Fleming, 2004; McGuire *et al.*, 2001). Indeed, Wang *et al.* (2001) recently detailed a contribution of 20-HETE to constrictor responses within hypertensive rat mesenteric resistance arteries, whilst Earley *et al.* (2003) described the upregulation of CYP 2C, an elevation in endothelial cell 11, 12-EETs and attenuated smooth muscle reactivity in rat small mesenteric arteries following chronic hypoxia.

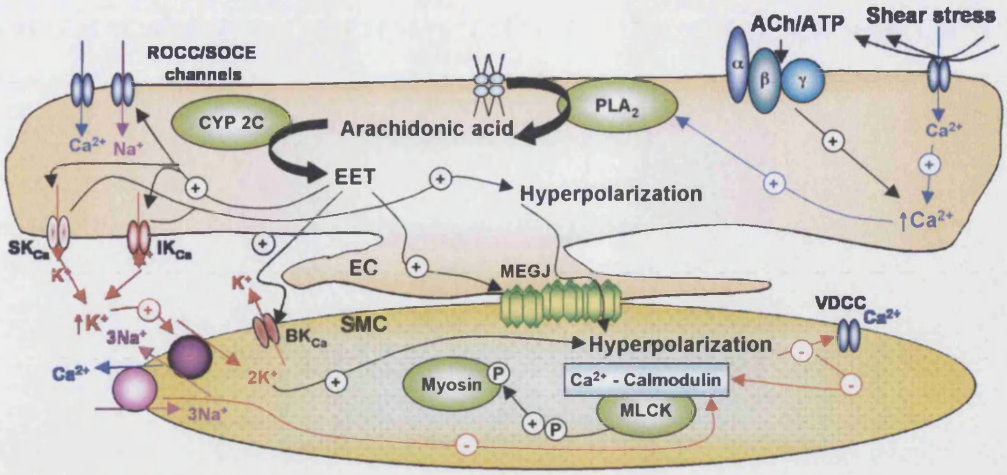

Figure 1.14 EET synthesis and mechanism of action
Cartoon illustrating the mechanisms associated with endothelial cell EET synthesis and the EET-evoked smooth muscle cell hyperpolarization. EC, endothelial cell; SMC, smooth muscle cell. + and – represent stimulation and inhibition. P represent phosphorylation.

Endogenous cannabinoids

The identification of the novel chemical mediator *N*-arachidonyl ethanolamide (anandamide), also a metabolite of arachidonic acid and an endogenous cannabinoid, prompted Randall *et al.* (1996) to investigate its potential as an EDHF in the rat mesenteric arterial bed. The authors demonstrated a severe attenuation of the anandamide response in the presence of raised K^+ and a partial blockade following removal of the endothelium. This combined with the observation of an arachidonic acid metabolite from the perfusate following carbachol stimulation led the authors to speculate that an endothelium-derived cannabinoid could act as an EDHF in this vascular bed (Randall *et al.*, 1996). Subsequent studies in the rat isolated small mesenteric artery demonstrated that although anandamide could evoke a substantial high K^+-sensitive repolarization and dilatation response, the sensitivity of the dilatation response to K^+ channel antagonists was not consistent with a role for the cannabinoid as an EDHF (Plane *et al.*, 1997; White & Hiley, 1997a). Later reports subsequently demonstrated that anandamide-evoked vasodilatation of the mesenteric bed was associated with activation of sensory perivascular nerve TRPV1 receptors and the stimulation of CGRP production (Harris *et al.*, 2002; Ho & Hiley, 2003a; White *et al.*, 2001; Zygmunt *et al.*, 1999) and to a lesser extent the direct endothelium-independent

stimulation of a smooth muscle (Randall *et al.*, 1996; White & Hiley, 1997a) abnormal-cannabidol (abn-cbd) receptor, distinct from the classical CB1 and CB2 receptors (Harris *et al.*, 2002; Ho & Hiley, 2003a). Although the cannabinoid derivatives are not candidates for EDHF more recent studies have demonstrated that in addition to actions involving stimulation of sensory nerves and direct smooth muscle relaxation, compounds such as virodhamine, N-arachidonyl dopamine and oleamide can evoke an endothelium-dependent vasodilatation response by their actions on the abn-cbd receptor and other as yet unidentified receptors. Furthermore the vasodilatation responses are dependent on the activation of IK_{Ca} and SK_{Ca} channels, characteristic of an EDHF-type response (Ho & Hiley, 2003b; Ho & Hiley, 2004; Hoi & Hiley, 2006; O'Sullivan *et al.*, 2004).

CNP

CNP is a member of the natriuretic peptide family and is stored as a pro-hormone prior to conversion to the active peptide by a mechanism not yet fully clarified, although the production of CNP has been demonstrated downstream of a range of inflammatory mediators (Ahluwalia & Hobbs, 2005; Stingo *et al.*, 1992). CNP would appear an ideal candidate for EDHF as it is present in high concentrations within the endothelium (Stingo *et al.*, 1992), the receptors for CNP (natriuretic peptide receptor (NPR)-B and NPR-C) are highly expressed in vascular smooth muscle (Chen & Burnett, 1998) and crucially, CNP is able to stimulate vasodilatation by hyperpolarization of the vascular smooth muscle (Honing *et al.*, 2001). Indeed, recent experiments performed in rat mesenteric arteries imply that CNP is a candidate for EDHF (Chauhan *et al.*, 2003b). Ahluwalia and Hobbs (Ahluwalia *et al.*, 2005; Chauhan *et al.*, 2003b) demonstrated that CNP could be released from the endothelium in response to ACh and that both endogenous EDHF and CNP-evoked dilatation responses could evoke endothelium-independent vasodilatation and hyperpolarization responses that were sensitive to pertussis toxin and the NPR C receptor antagonist M372049. Both ACh- and CNP-evoked hyperpolarization responses were also identical in their amplitude and sensitivity to barium and ouabain and indeed the dilatation response to both ACh and CNP were both attenuated by the combination of barium and ouabain or by raising extracellular K^+ (Chauhan *et al.*, 2003b).

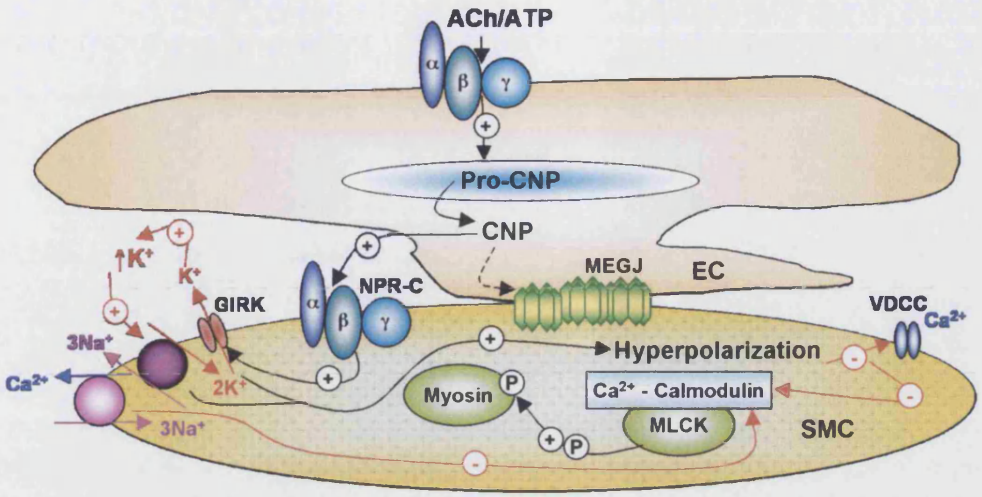

Figure 1.15 CNP mechanism of action
Cartoon illustrating the mechanisms associated with endothelial cell CNP-evoked smooth muscle cell hyperpolarization. EC, endothelial cell; SMC, smooth muscle cell. + and – represent stimulation and inhibition. P represent phosphorylation.

Based on the inhibitory effects of tertiapin, a G protein-gated inwardly rectifying K^+ (GIRK) channel inhibitor, it was proposed that the NPR-C receptor on the smooth muscle was coupled to activation of smooth muscle GIRK channels, thereby facilitating K^+ efflux and smooth muscle hyperpolarization upon CNP binding (Figure 1.15; Chauhan *et al.*, 2003). Although a role for MEGJ coupling was proposed based on the inhibitory effects of the gap junction uncoupler 18α-glycyrrhetinic acid (please see sections 1.3.3 and 4.1), the non-selective nature of this class of compounds mean such an interpretation requires further investigation (Chaytor *et al.*, 2000; Matchkov *et al.*, 2004b; Sandow & Tare, 2007; Tare *et al.*, 2002). Indeed, although the capability of CNP to act as an endothelium-derived hyperpolarizing and relaxing factor has been demonstrated, the inhibition of CNP release following blockade of IK_{Ca} and SK_{Ca} channels has not been reported precluding the identification of EDHF as CNP (Garland & Plane, 1996; Sandow & Tare, 2007).

H_2O_2

A role for H_2O_2 in the regulation of vascular tone has been recognised for over 20 years (Rubanyi & Vanhoutte, 1986). However, the concept of H_2O_2 as an EDHF was only advanced when Matoba *et al* (2000) documented ACh evoked H_2O_2 synthesis in the endothelium of mice small mesenteric arteries and the attenuation of ACh-evoked

vasodilatation and smooth muscle hyperpolarization with catalase. H_2O_2 may be synthesized from superoxide anion (O_2^-), which is produced by a number of enzymes including eNOS, CYP, and COX (Ellis & Triggle, 2003; Feletou & Vanhoutte, 2004; McGuire *et al.*, 2001; Shimokawa & Matoba, 2004). Most reports suggest that the vascular smooth muscle hyperpolarization to H_2O_2 occurs via activation of smooth muscle K_{Ca} channels although K_{ATP} and K_v channels may also be modulated by H_2O_2 (Barlow & White, 1998; Gao *et al.*, 2003; Matoba *et al.*, 2000; Shimokawa & Matoba, 2004) and additional mechanisms associated with the activation of endothelial cell K_{Ca} have been proposed (Bychkov *et al.*, 1999).

Within rat mesenteric arteries ATP- and flow-evoked dilatation responses have been associated with a catalase-sensitive dilatation and hyperpolarization response that was sensitive to raised K^+ (Liu *et al.*, 2006a). However, a number of studies, albeit some using far higher concentrations of H_2O_2, document a limited hyperpolarization response to H_2O_2 (Chaytor *et al.*, 2003; Ellis *et al.*, 2003) and a range of indirect and in some cases toxic side effects of the metabolite (Ellis & Triggle, 2003; Iesaki *et al.*, 1996; Mian & Martin, 1997) lending caution to the appreciation of this report (for a detailed an balanced review please see Ellis & Triggle (2003)). Furthermore, although the possibility of a physiological mechanism of dilatation cannot be ruled out the observation by Liu *et al.* (2006a) that the flow-evoked dilatation responses were insensitive to a combination of charybdotoxin and apamin means that by the definitions documented previously (please see section 1.3.2.9) H_2O_2 cannot be defined as an EDHF.

NO

As described, EDHF vasodilatation responses are classically characterized as non-NO and non-prostacyclin, endothelium dependent dilatation and smooth muscle hyperpolarization responses. However, in some vascular beds, including the superior mesenteric artery, treatment with L-NAME or nitro-L-arginine (L-NNA) is not sufficient to block endothelial cell NO release, the residual NO arising from NO stores resistant to blockade of eNOS (Chauhan *et al.*, 2003a; Cohen *et al.*, 1997; Kemp & Cocks, 1997; Stankevicius *et al.*, 2006). As NO is able to evoke hyperpolarization of the smooth muscle (please see section 1.3.2.5) it is possible that responses deemed

dependent on an EDHF distinct from NO or prostacyclin may in fact be the result of NO-evoked hyperpolarization. Within the rat small mesenteric artery the importance of residual NO to the ACh response is somewhat unclear. Some reports have shown that ACh-evoked hyperpolarization and dilatation responses are unchanged in the presence of oxyhaemoglobin whilst NO-evoked hyperpolarization and dilatation is blocked (Garland & McPherson, 1992; Hwa *et al.*, 1994). However, more recently the combined use of L-NAME and oxyhaemoglobin was shown to attenuate the EDHF-type hyperpolarization and dilatation response in this preparation (Chauhan *et al.*, 2003a). The differences between the studies are unclear. The concentrations of oxyhaemoglobin used by Chauhan *et al.* (2003a) although greater than Garland & MacPherson (1992) are the same as those used by Hwa *et al.* (1994). However, Chauhan *et al.* (2003a) do describe a second application of oxyhaemoglobin prior to ACh that is not detailed in the earlier experiments (Garland & McPherson, 1992; Hwa *et al.*, 1994). Whether in the absence of this second application of oxyhaemoglobin eNOS activity would be sufficient to overwhelm the concentrations of oxyhaemoglobin in the bath solution would require further study. Crucially, however, the blockade of agonist-evoked NO release by inhibitors of IK_{Ca} and SK_{Ca} is still required to demonstrate a role for NO as an EDHF in this preparation.

In contrast within conduit arteries there is a general agreement over a role for stored NO as an EDHF (Stankevicius *et al.*, 2006). Indeed in a recent report using the superior mesenteric artery ACh evoked the endothelial cell release of NO that was sensitive to charybdotoxin and apamin or raised K^+ (Stankevicius *et al.*, 2006). Furthermore, complete removal of NO by combined inhibition of eNOS and the use of a NO scavenger completely abolished ACh-evoked vasodilatation. In the rat small mesenteric artery an EDHF-type response was still evoked under these conditions (Chauhan *et al.*, 2003a) indicating that additional EDHF mechanisms, are present within this preparation that either wholly account for the EDHF response (Garland & McPherson, 1992; Hwa *et al.*, 1994) or with NO contribute to the EDHF response (Chauhan *et al.*, 2003a).

1.3.3. Direct cell-to-cell transfer of hyperpolarization through gap junctions

Gap junctions are aqueous channels that exist within dynamic plaques in the plasma membrane (Gaietta *et al.*, 2002; Lauf *et al.*, 2002). By allowing the transfer of small

molecules (<1000Da) and current across the lipid bilayer they enable cell-to-cell communication and the coordination of multicellular responses within tissues (Evans & Martin, 2002; Unger *et al.*, 1999). Within a range of isolated cell preparations the extracellular release of signalling molecules such as ATP from connexons or hemichannels has also been documented and is proposed to contribute to the coordination of responses between adjacent cells (Evans *et al.*, 2006; Goodenough & Paul, 2003).

1.3.3.1. Gap junction structure

Functional gap junctions can exist singularly or in plaques formed from the union of pentilaminar aggregates of connexons originating from adjacent cells (Bukauskas *et al.*, 2000; Christ *et al.*, 1996; Figueroa *et al.*, 2006). In order to make the close contact required for union of the connexons, MEGJ are commonly located on endothelial cell projections that pass through the basal lamina to the underlying smooth muscle membrane (Figure 4.7; Mather *et al.*, 2005; Sandow & Hill, 2000). Gap junctions are formed by the docking of two hemichannels or connexons, one from each of the adjacent cells (Figure 1.16; Christ *et al.*, 1996). The nature of the connexon docking (Figure 1.16) reflects a 30° rotation and interdigitation of the six connexins that constitute the hexameric hemichannel structure (Harris, 2001).

Approximately twenty connexin subtypes have been identified in the human and mouse genomes, differing mainly in the length of their carboxy (C)-terminal domain (Herve, 2005). Of those identified, four have been reported to exist in the vasculature, connexins 37, 40, 43 and 45 (Figueroa *et al.*, 2006), of which at least connexins 37, 40 and 43 are present in rat mesenteric arteries (Gustafsson *et al.*, 2003; Kansui *et al.*, 2004; Matchkov *et al.*, 2006; Sandow *et al.*, 2006). The distribution of the connexins between the endothelium and smooth muscle varies between species and tissue preparations.

Within the rat mesenteric artery connexins 37 and 40 are consistently found within the endothelium (Gustafsson *et al.*, 2003; Kansui *et al.*, 2004; Matchkov *et al.*, 2006; Sandow *et al.*, 2006). However, the presence of connexin 43 is much more variable between reports, the endothelial cell expression of connexin 43 possibly increasing with artery diameter

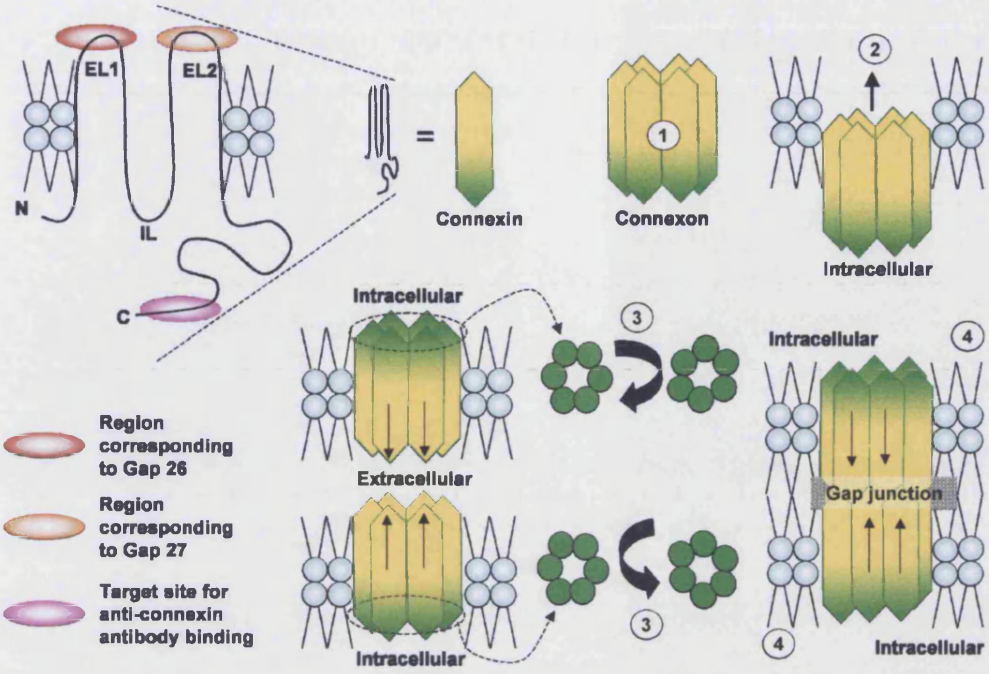

Figure 1.16 Structure of the gap junction and inhibitor binding sites

The cartoon illustrates the structure of a gap junction (4), the formation of a gap junction from its constituent connexins (1 to 4) and the connexin structure. The connexins contain four transmembrane segments with the N-terminus, intracellular loop (IL) and C-terminus located intracellularly. Gap peptides homologous to the two extracellular loops (EL) have been designed as selective inhibitors of the gap junctions. Within this thesis antibodies directed against the intracellular C-terminus were also used to modulate gap junctional communication. 1) The connexon or hemichannel comprises six connexins. 2) Connexons are inserted into the membrane before gap junction formation occurs between two adjacent cells. Gap junctions are formed by the docking of two connexons facilitated by 3) a 30° rotation of the hemichannels and 4) an interdigitation of the connexin subunits. Cartoon modified from Harris (2001) and Saez *et al* (2003).

(Gustafsson *et al.*, 2003; Hong & Hill, 1998; Kansui *et al.*, 2004; Matchkov *et al.*, 2006). Smooth muscle cell connexin expression is much more scarce and even absent in some cases (Gustafsson *et al.*, 2003) although where reported, low levels of connexins 37 and 43 have been documented within the medial layers of the rat mesenteric artery (Kansui *et al.*, 2004; Matchkov *et al.*, 2006).

1.3.3.2. Evidence for the direct cell-to-cell transfer of hyperpolarization via MEGJ

The direct, radial electrotonic transfer of hyperpolarization from the endothelium to the smooth muscle via MEGJ was one of the first mechanisms suggested for the hyperpolarization-driven dilatation response (Chaytor *et al.*, 1998; Garland &

McPherson, 1992; Segal & Duling, 1986b). Reports documenting a correlation between smooth muscle and endothelial cell membrane potential have since been detailed supporting such a proposal (Coleman *et al.*, 2001; Emerson & Segal, 2000a; Haddock *et al.*, 2006; Sandow *et al.*, 2002; Takano *et al.*, 2004; Yamamoto *et al.*, 1998). Perhaps key are the observations of Emerson & Segal (2000a) who using intact hamster feed arterioles simultaneously measured endothelial cell and smooth muscle cell membrane potentials in response to a range of stimuli including current injection and application of ACh, demonstrating synchronous changes in membrane potential thoughout the experiment. Crucially, the incidence of MEGJ (demonstrated morphologically using electron microscopy) has also been shown to correlate with the extent to which endothelium-derived hyperpolarization contributes to the dilatation response, providing further evidence for a direct cell-to-cell pathway for the transfer of hyperpolarization (please also see section 1.3.2.7). In the femoral artery, where endothelial cell-derived hyperpolarization of the smooth muscle is absent no MEGJs were reported (Sandow *et al.*, 2002). In contrast in the rat mesenteric artery, where endothelial cell hyperpolarization was efficiently transferred to the smooth muscle (endothelial cell hyperpolarization response, 22mV; smooth muscle cell hyperpolarization response, 18mV) approximately 7 MEGJ were documented per 5μm endothelial cell length (Sandow *et al.*, 2002). Similarly, in the juvenile rat saphenous artery where MEGJ are prevalent (11 MEGJs per 5μm endothelial cell length), a robust endothelium-derived smooth muscle hyperpolarization response could be measured (~14mV) that was severely attenuated in adult arteries (~5mV) where the incidence of MEGJ was reduced (1 MEGJ per 5μm endothelial cell length) (Sandow *et al.*, 2004).

In addition to the accumulating physiological evidence for the importance of the MEGJ communication in the endothelium-dependent dilatation response in a range of vascular preparations, a number of reports have also documented the attenuation of endothelium-dependent smooth muscle cell hyperpolarization and dilatation following treatment with the gap junction uncouplers the gap peptides (please see Figure 1.16) (Chaytor *et al.*, 2005; Chaytor *et al.*, 1998; Chaytor *et al.*, 2001; Dora *et al.*, 1999; Edwards *et al.*, 1999; Griffith *et al.*, 2002; Matchkov *et al.*, 2006; Sandow *et al.*, 2002) and the less specific glycyrrhetinic acid derivatives (please see section 4.1) (Dora *et al.*, 2003a; Edwards *et al.*, 1999; Goto *et al.*, 2002; Hill *et al.*, 2000; Taylor *et al.*, 1998; Yamamoto *et al.*,

1998). Indeed the dye coupling that is often apparent in electrically-coupled cells (Dora *et al.*, 2003a; Emerson & Segal, 2000a; Sandow *et al.*, 2002; Takano *et al.*, 2004; Yamamoto *et al.*, 2001) is attenuated following treatment with the gap peptides (Dora *et al.*, 1999; Martin *et al.*, 2005) consistent with the increased input resistance observed in electrically-coupled smooth muscle cell preparations following treatment with the gap peptides (Matchkov *et al.*, 2006). Thus it would seem that a role for MEGJ in the transfer of hyperpolarization from the endothelium to the smooth muscle is key in a range of vascular preparations including the rat mesenteric artery (please also see chapter 4).

1.4. Research aims

The experiments documented within this thesis were designed to investigate radial (endothelium to smooth muscle) and longitudinal (inter-endothelial cell or inter-smooth muscle cell) cell-to-cell communication pathways that contribute to vasodilatation within resistance arteries (Figure 1.1.7). Accordingly, this thesis had the following aims:

1. To evaluate how arterial structure can potentially facilitate the radial and longitudinal cell-to-cell conduction of hyperpolarization using immunohistochemical and cell labelling techniques.
2. To establish the contribution of gap junctions to both the radial EDHF-type dilatation and the longitudinal conduction of the dilatation response by evaluating the effects of gap junction uncouplers on ACh- and LVK-evoked dilatation responses.
3. To evaluate the individual contribution of the SK_{Ca} and IK_{Ca} channels to the EDHF-type response evoked by the physiological agonists ATP and UTP (Dubyak & el-Moatassim, 1993; Malmsjo *et al.*, 1999; Ralevic & Burnstock, 1998) and subsequently to investigate how these dilatation responses may be modulated by desensitization mechanisms involving PKC (Chen & Lin, 1999; Hardy *et al.*, 2005).
4. To evaluate the ability of the nucleotides to evoke a spreading dilatation response in resistance-sized arteries, particularly comparing conducted dilatation responses following abluminal *versus* luminal application of the nucleotides.

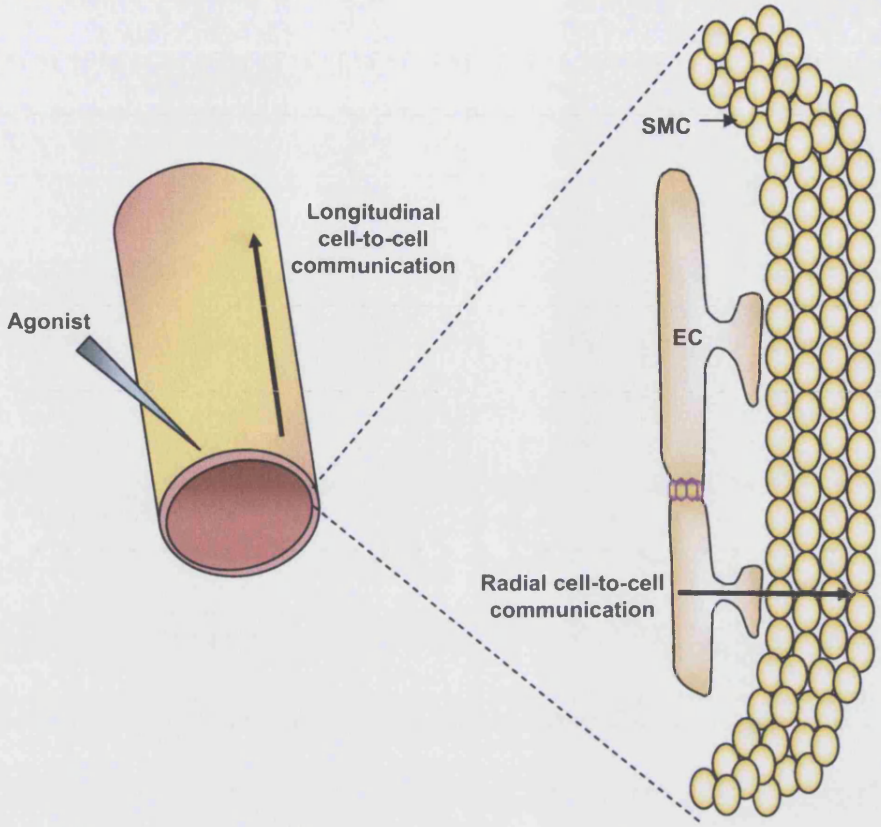

Figure 1.17 Arterial radial and longitudinal cell-to-cell communication pathways

Cartoon illustrating the longitudinal and radial directions of cell-to-cell communication within the arterial wall. EC, endothelial cell; SMC, smooth muscle cell.

2. Methods

2.1. Rat mesenteric artery isolation and cannulation

Rat mesenteric arteries were used in all studies described within this thesis. Tissue isolation was performed as follows: Male Wistar rats (200-250g) were killed by cervical dislocation and exsanguinations according to requirements detailed under Schedule 1 of the Animals (Scientific Procedure) Act 1986 (UK) and monitored by the Home Office (UK). The mesentery was removed and placed in ice-cold 3-[N-morpholino]propanesulfonic acid (MOPS) buffer (for composition see section 2.7.2). Third-order branches of the superior mesenteric artery were isolated and dissected free of adherent tissue to give a final length of approximately 2mm (>2mm where possible for conducted response experiments) with a mean diameter 349.6 ± 2.6μm (n=196; 248.8 – 469.0μm) with no visible side branches.

2.2. Pressure myography

Pressure myography (Figure 2.1) was used throughout this thesis for both functional and imaging studies. Initially performed by cannulation of one end of a rabbit cerebral or mesenteric resistance artery (50 - 250μm) (Uchida *et al.*, 1967), but later developed into a method whereby both ends of an arteriole (12-112μm) were cannulated (Duling *et al.*, 1981) the method allows evaluation of the responses of isolated, small resistance arteries by measurement of diameter under near-physiological conditions without disruption of the vessel wall (Shaw *et al.*, 2004). Furthermore the technique allows the luminal solution to be changed independently of the surrounding bath solution, which can (depending on the capacity of the solute to cross the IEL) result in minimal treatment of the smooth muscle layer.

Isolated rat mesenteric arteries (section 2.1) were cannulated at each end with small pipettes (200μm), which were either fixed into a static pressure myograph bath (10ml) (120CP; Danish Myo Technology, Denmark; Figure 2.1) or mounted onto stands and positioned independently of the microscope into a custom-made perspex bath (0.5 - 1ml) using micromanipulators (Figure 2.2 and Figure 2.3a). The custom-made bath was seated in a heated stage insert (PH-5, Warner Instruments, CT, USA; Figure 2.3a). Arteries in both set-ups were then pressurized to 50mmHg and allowed to equilibrate un-stretched for 20min at 37°C in MOPS. Subsequently, each artery was pressurized to 80mmHg,

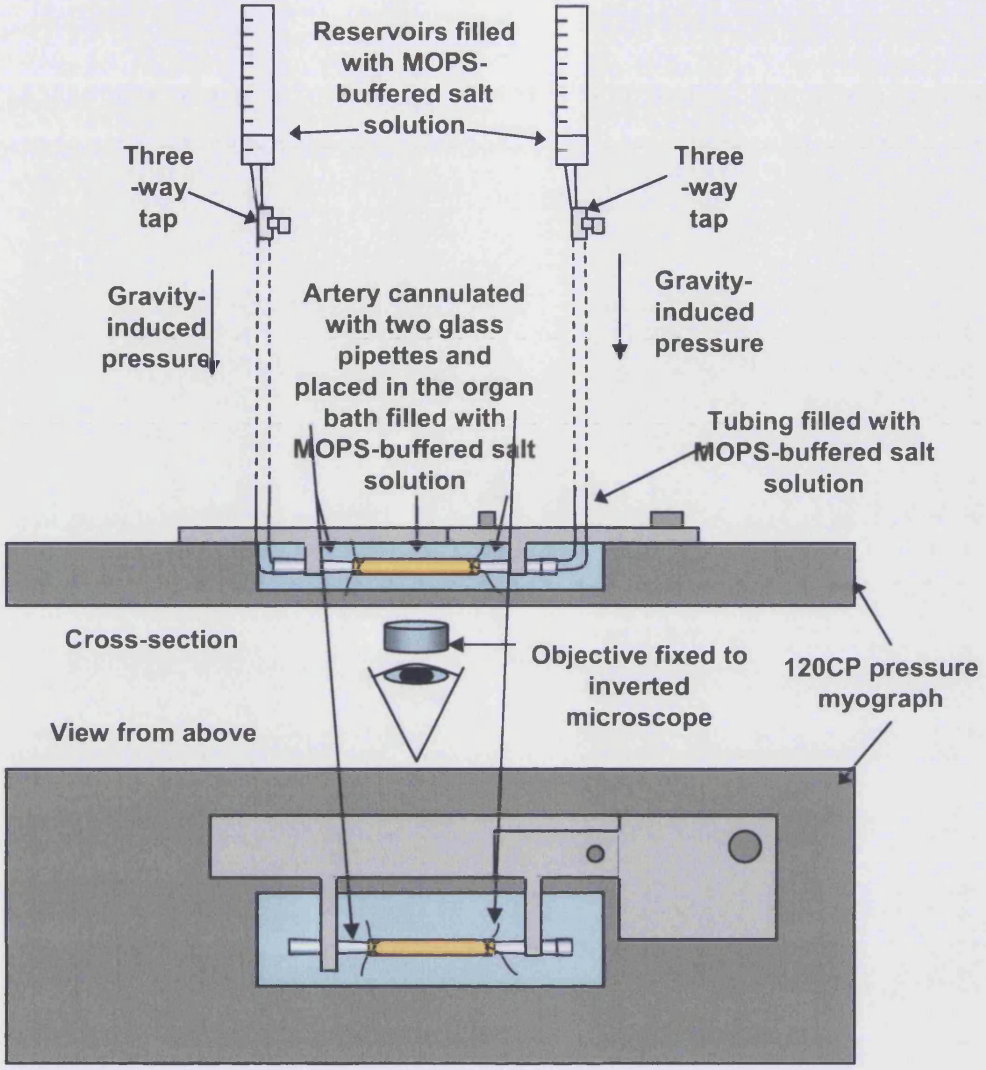

Figure 2.1 The 120CP pressure myograph set-up.
The figure shows a diagrammatic representation of an artery mounted onto two cannulation pipettes within a small organ bath chamber filled with MOPS-buffered salt solution fitted within the 120CP pressure myograph (Danish Myotechonology, Denmark). Each pipette is connected to gravity-fed tubing filled with MOPS-buffered salt solution from a reservoir so that changing the height of the reservoirs changes the pressure applied to the artery. Luminal flow may be instigated if the two reservoirs are at different heights or if tubing attached to a small peristaltic or syringe pump is attached to one cannulation pipette.

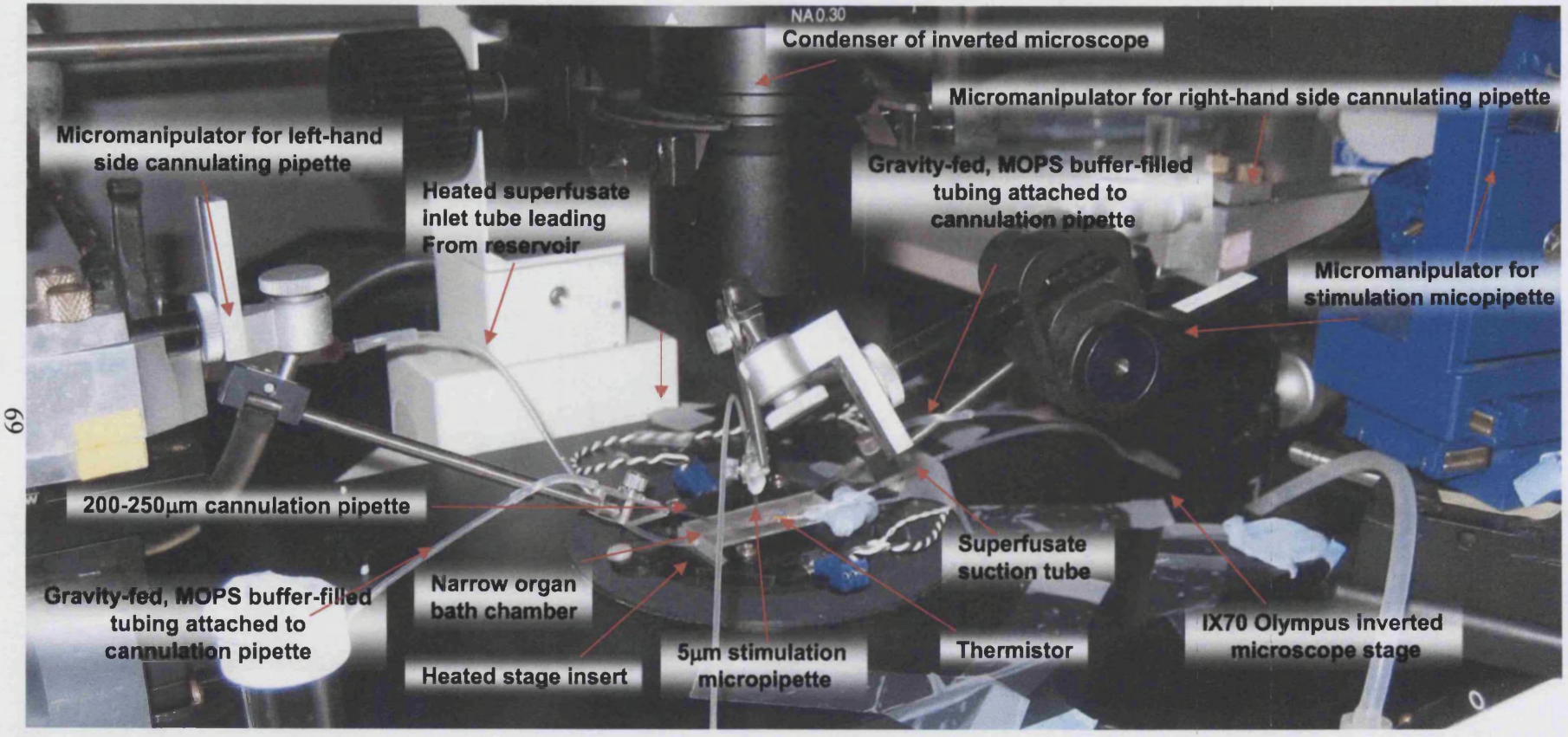

Figure 2.2 The set-up used for spreading response experiments.

The figure shows a photograph illustrating the experimental set-up used for spreading response experiments. As with the 120CP pressure set-up arteries are mounted onto two pipettes and luminally-perfused with gravity-fed MOPS-buffered salt solution from reservoirs raised to exert 50mmHg pressure on the artery. Luminal flow is achieved as previously stated (Figure 2.1).

longitudinally straightened and stretched a further 10% of the artery length to optimise responses to PE (Coats & Hillier, 1999). The pressure was then decreased to 50mmHg and maintained at that level for the duration of experiments unless otherwise stated. Endothelium viability was assessed as a >90% control relaxation to ACh (1μM) following pre-constriction with PE (1-3μM).

2.3. Focal stimulation of pressurized arteries

Focal stimulation is frequently used to observe conducted vasomotor responses within isolated arteries (Dietrich *et al.*, 1996; Dora *et al.*, 2003b; Emerson *et al.*, 2002; Emerson & Segal, 2001; Emerson & Segal, 2000b; Rivers *et al.*, 2001; Takano *et al.*, 2004; Walker & Segal, 1998; Xia & Duling, 1995; Yashiro & Duling, 2003). Within this thesis, conducted vasomotor responses were studied in isolated rat mesenteric arteries mounted on pipettes held in a custom-made narrow bath as described (Sections 2.1 and 2.2; Figure 2.2 and Figure 2.3a). This set-up was used to optimise uni-directional flow and preclude direct stimulation of cells upstream from the local site as has been demonstrated previously (Takano *et al.*, 2004). Flow direction was monitored by inclusion of small beads (5μm diameter microspheres; Molecular Probes Invitrogen, Paisley, UK) in the superfusate solution. Agonists were applied using a bevelled borosilicate glass micropipette (5μm tip; World Precision Instruments, Stevenage, UK) positioned at least 200μm from the downstream end of the artery using a micromanipulator (Scientifica, Uckfield, UK). A pneumatic pico pump (10psi, PV 820, World Precision Instruments, Stevenage, UK) was used to eject the agonist from the pipette. Superfusion was maintained at ~2ml min^{-1} throughout spreading response experiments. Maximum diameter was assessed at the end of each experiment using papaverine (150μm).

2.4. The pinocytic loading method for selective endothelial cell loading of cell impermeant molecules

A novel method for introducing molecules into endothelial cells within intact arteries has recently been reported (Mather *et al.*, 2005; Vequaud & Thorin, 2001). This technique is based on a pinocytic loading method originally developed for cell culture systems by Okada & Rechsteiner (1982). The method utilizes the physiological

A

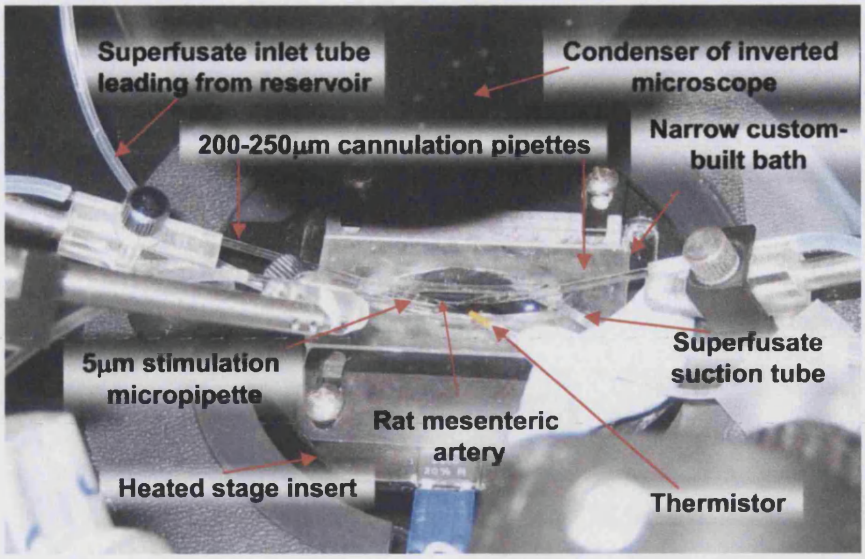

B

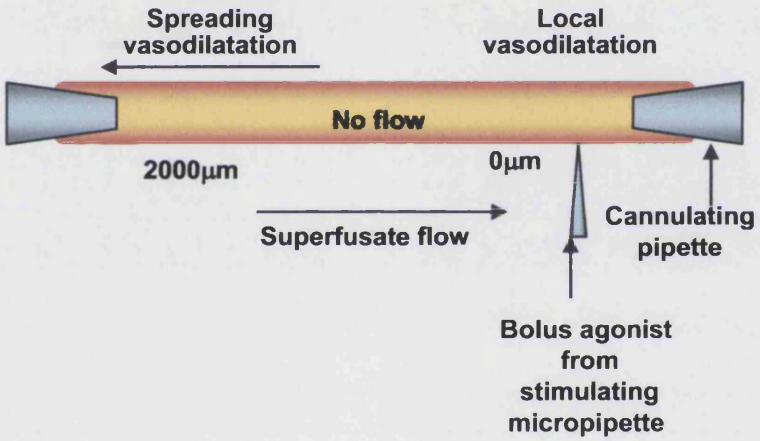

Figure 2.3 The downstream position of the stimulating micropipette in spreading response experiments.

A, B, The micropipette is positioned downstream of the superfusate flow such that only the downstream end of the artery is stimulated by the short bolus doses of agonist which are released from the stimulating micropipette by pressure ejection. **B,** Any response seen upstream is a spreading response and occurs indpendently of direct agonist stimulation.

mechanisms whereby cells may internalize macromolecules by fluid-phase endocytosis (pinocytosis; Conner & Schmid, 2003). In contrast to receptor-mediated endocytosis (phagocytosis), which only a small number of specialized cell types such as macrophages and neutrophils carry out extensively, some form of pinocytosis is available to most cell types including endothelial cells (Conner & Schmid, 2003). The method of Okada & Rechsteiner (1982) is based on the observation that it was possible to increase vesicle formation and pinocytosis in L929 cells by increasing the osmolarity and tonicity of the medium surrounding the cells. This observation is consistent with the hypothesis that endothelial cell uptake of macromolecules may be governed by the relative tonicity, osmotic pressure and concentration gradients that may act on both sides of the endothelium (Simionescu & Simionescu, 1984). Importantly Okada & Rechsteiner (1982) observed that if a substrate (for example, horseradish peroxidase) was included in the medium, that substrate would be taken up into the vesicles. The vesicles could then be ruptured and the substrate released uniformly into the cell cytoplasm by lowering the osmolarity and tonicity of the culture medium (Figure 2.4).

Using a commercially available pinocytic reagent, Véquad & Thorin (2001) described selective internalization of FITC-labelled IgG into the endothelium of intact pressurized arteries. Incorporation of antibodies directed against the G-protein coupled-receptor $\alpha_{q/11}$-subunits into the endothelium using this technique was shown to inhibit vasodilatation responses to the muscarinic (M) receptor agonist ACh (thought to be acting on the M_3 subtype) whilst leaving responses to oxymetazoline, (thought to be acting via the α_2-adrenoceptor) unaffected (Vequaud & Thorin, 2001).

Experiments conducted within this laboratory found the commercial reagent to irreversibly block functional responses in isolated arteries (Mather *et al.*, 2005). Therefore an adaptation of the approach developed by Okada & Rechsteiner (1982) was employed (Figure 2.4; Mather *et al.*, 2005). In brief, luminal pressure of isolated, pressurized arteries was reduced to ~4mmHg. A microperistaltic pump (LKB, Bromma; ~100μl min^{-1}) was used to luminally perfuse hypertonic solution (100μl; 800milliosmolar (mosM); please see section 2.7.3 for solution compositions), with which the arteries were incubated for 10min. Arteries were then flushed with hypotonic solution (200μl; 180mosM; ~100μl min^{-1}) which remained in the arteries for a further

Step 1 **The luminal pressure of an isolated, pressurized artery is decreased to ~4mmHg.**

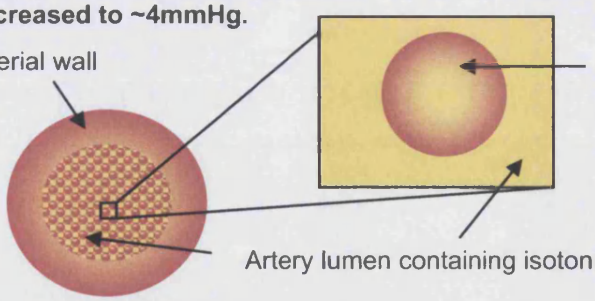

Step 2 **Hypertonic solution containing the substrate to be loaded into the endothelium is perfused into the artery lumen and incubated (10min).**

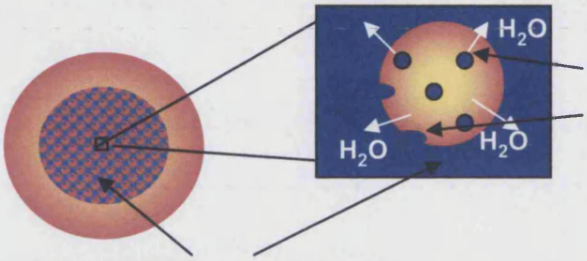

Artery lumen containing hypertonic solution with substrate

In an effort to balance the tonic and osmotic difference between the inside (300mosM) and outside (800mosM) of the cell water moves out of the cell whilst vesicles form within the endothelial cell. These vesicles contain the hypertonic solution and substrate to be loaded.

Step 3 **Hypotonic solution is perfused into the artery lumen and incubated (2min).**

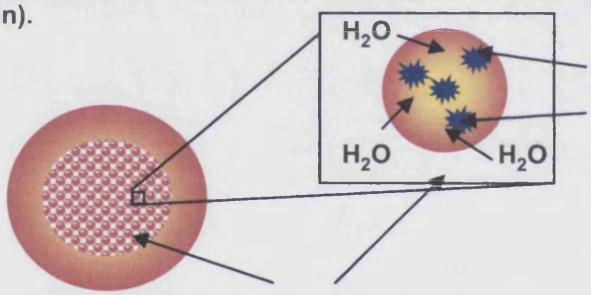

Artery lumen containing hypotonic solution

Due to the change in osmotic pressure (180mosM) and tonicity outside of the cell water moves into the cell causing the vesicles to burst releasing substrate into the cytoplasm.

Step 4 **The artery is perfused with luminal isotonic MOPS solution and then luminal pressure increased to 50mmHg**

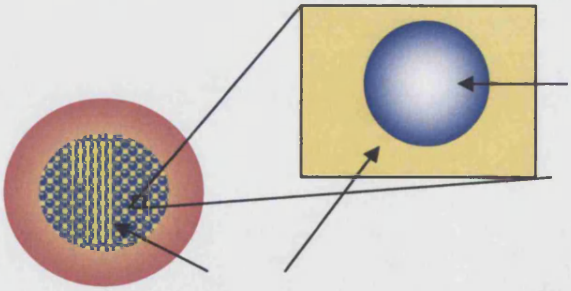

Artery lumen containing isotonic MOPS buffer

The substrate has been loaded into the cytosolic compartment of the endothelial cell in the lumen of the artery.

Figure 2.4 The pinocytic loading protocol.
Cartoon illustrating the steps taken to selectively load cell-impermeant macromolecules into arterial endothelium using the pinocytic loading protocol.

2min before luminally perfusing isotonic MOPS (250µl; 300mosM; ~100µl min^{-1}). At this stage, superfusion of the artery with isotonic MOPS was also carried out. After 2 - 5min, arteries were re-equilibrated to 50mmHg and functional or visual studies performed.

2.5. Artery diameter measurement and recording

2.5.1. Diameter measurement for single site analysis

Arteries were visualized using an inverted microscope (IX70, Olympus, Japan) with either, a 4x/0.13 numerical aperture (NA; UplanFl, Olympus, Japan) or a 10x/0.30NA objective (UplanFl, Olympus, Japan). Artery diameter was recorded using a variety of methods depending on equipment availability and the restraints of other aspects of the experiment. Typically, when measuring changes in artery diameter at a single site (for example when agents were added to the bath) a CCD video camera (Nikon, Japan) was attached to the inverted microscope and images stored to videotape. Diamtrak software (T. O. Neild, Flinders University, Adelaide, Australia) was used to measure outer diameter online at 2Hz. This set-up was also used to record concentration-response curves to ACh during spreading response protocols unless otherwise stated (please see section 2.5.2). When diameter measurement studies were carried out in conjunction with fluorescence imaging techniques brightfield images were captured with a laser scanning confocal microscope (FV500-SU, Olympus, Japan; 10x/0.30NA objective) connected to an inverted microscope and recorded at 1Hz (Tiempo software; Olympus Japan). Recordings were then stored to disc and outer diameter measurement performed offline using motion analysis software (Metamorph, Universal Imaging, USA).

2.5.2. Diameter measurement for conducted vasodilatation responses

Segments of arteries (where possible >2mm in length) were visualized using an inverted microscope (IX70, Olympus, Japan) with a 4x/0.13 NA objective (UplanFl, Olympus, Japan) to enable the visualization of >2mm of artery length, and therefore the simultaneous measurement of diameter at multiple sites on the artery (giving a resolution of 5µm being equivalent to one pixel). In these experiments the frequency of diameter measurement was increased to 12Hz to enable rates of spread of dilatation to be analyzed. Arteries were visualized using either a CCD video camera (Nikon, Japan) with which images were displayed online using Diamtrak software (T. O. Neild,

Flinders University, Adelaide Australia) and stored to videotape or an Andor Ixon digital camera (Gilden Photonics, Coventry, UK) with which images were displayed online and stored to disk using photometric software (Andor iQ1.3, Gilden Photonics, Coventry, UK). Videotaped images were digitized using iMovie software for the Mac OS X (Apple Computer, Inc USA) prior to offline diameter measurement. Motion analysis software (Metamorph, Universal Imaging USA) was used to simultaneously measure artery outer diameter at multiple sites at calibrated distances from the site of focal stimulation (Figure 2.5).

2.6. Solutions, drugs and cell markers

2.6.1. Solutions

2.6.1.1. MOPS physiological buffer and isotonic high K^+ solution

All experiments were carried out in a MOPS buffer of composition (mM): NaCl 145.0, KCl 4.7, $CaCl_2.2H_2O$ 2.0, $MgSO_4.7H_2O$ 1.17, MOPS 2.0, $NaH_2PO_4.H_2O$ 1.20, glucose 5.0, pyruvate 2.0, EDTA 0.02 NaOH 2.75 adjusted to pH 7.40±0.02 . Isotonic high K^+ (150mM) solution comprised (mM): KCl 150.0, $CaCl_2.2H_2O$ 2.0, $MgSO_4.7H_2O$ 1.17, MOPS 2.0, $NaH_2PO_4.H_2O$ 1.20, glucose 5.0, pyruvate 2.0, EDTA 0.02 NaOH 2.75 adjusted to pH 7.40 ± 0.02.

2.6.1.2. Solutions for pinocytic loading

Hypertonic solution for loading a 10µl volume of cell impermeant macromolecule comprised polyethylene glycol (PEG) 1000 (10% vv^{-1}) and sucrose (0.49M) in MOPS. Hypotonic solution comprised a dilution of MOPS (60%vv^{-1}) in MilliQ water.

2.6.2. Drugs

All drugs were purchased from Sigma Chemical Company (Poole, UK) with the exception of apamin (Latoxan, France), BIS I, PEG 1000 (Calbiochem) ^{Cx43}Gap 26 (sequence VCYDKSFPISHVR), ^{Cx37,Cx43}Gap 27 (sequence SRPTEKTIFII) and ^{Cx40}Gap27 (sequence SRPTEKNVFIV) (Severn Biotech Ltd., UK), FITC-conjugated dextran (3000Da) (Molecular Probes Invitrogen, Paisley, UK), levcromakalim (a generous gift from GlaxoSmithKline) and TRAM-34 which was a generous gift from Dr. H. Wulff (University of California, Irvine, CA USA). All drug concentrations are expressed as final organ bath concentrations. Stock solutions were prepared in MilliQ

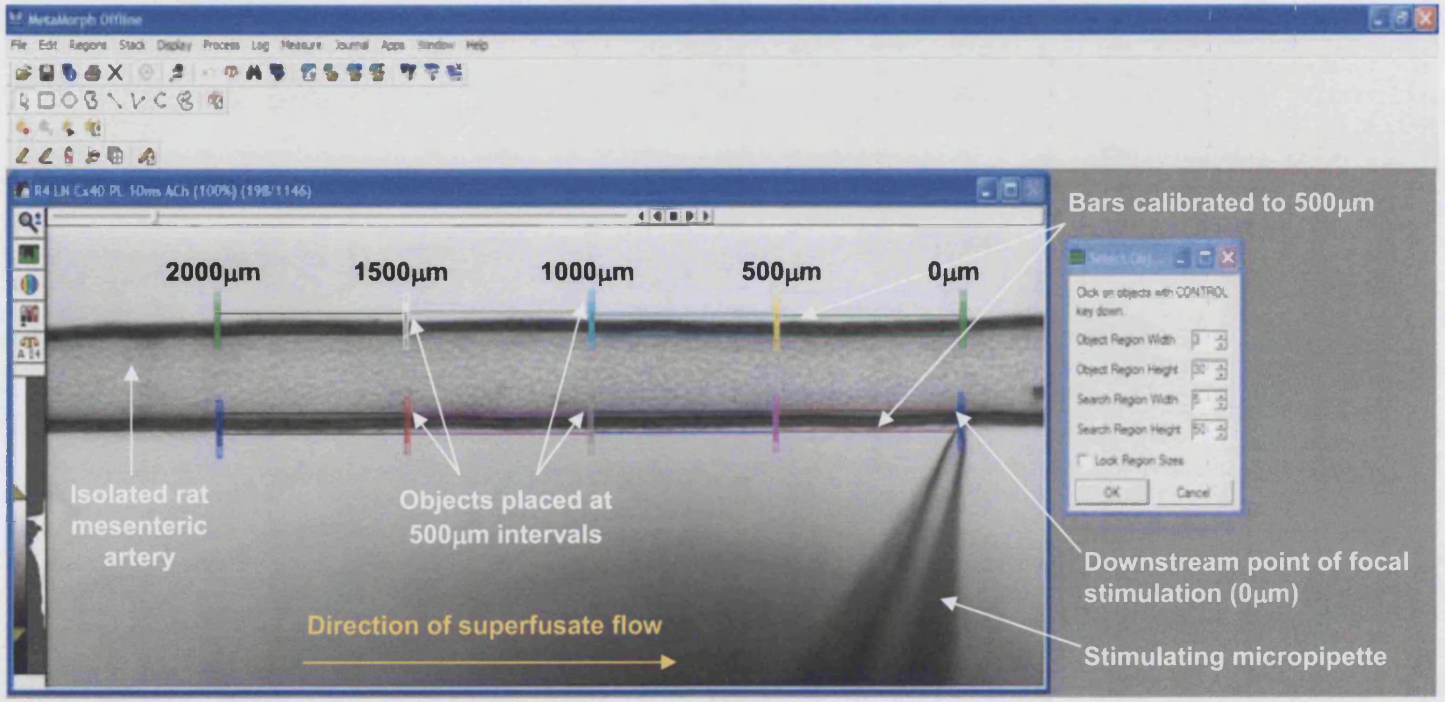

Figure 2.5 The motion analysis software used for diameter measurement.

The figure shows an annotated frame of the motion analysis software program Metamorph (Universal Imaging, USA) used for simultaneous diameter measurement of multiple sites at calibrated distances (500µm, illustrated by the length of the large coloured rectangles) from the focal point of stimulation, as used when analysing spreading response experiments. The objects (small rectangular coloured boxes) placed at 500µm intervals follow the external dark edges of the artery wall relative to the light of the bath solution to trace changes in artery diameter. These values are given as different pixel values, which are later calibrated and plotted as outer diamter values using Excel (Microsoft, USA) software. For the analysis of bath-applied agonist concentration-response curves a single site towards the centre of the artery would be chosen with objects placed on each external edge of the artery.

water (10mM) with the exception of ADPβS (50mM), ATPγS, adenosine (100mM), BIS 1 (100μM) and TRAM-34 (100μM in dimethylsulfoxide (DMSO)). All drugs were diluted in physiological buffer prior to use in experiments. The gap peptides were prepared daily directly into MOPS buffer from the anhydrous peptide to give a concentration of 300μM. The triple gap peptide solution pH was adjusted from a mean of 6.50±0.07 to 7.41±0.00. The gap peptide solutions were used to directly replace the organ bath and luminal solutions. All inhibitors were incubated in the bath and lumen of arteries for a minimum of 20min prior to obtaining responses except for 2'deoxy-*N*6-methyladenosine 3' 5' diphosphate diammonium salt (MRS2179; 5min), apamin (1h) and the gap peptides (bath solutions changed every 40min for 2h).

2.7. Data analysis

Results are summarized as means ± s.e.means of *n* arteries where $n = 1$ is equivalent to one animal. Statistical comparisons of parametric data were made using one-way ANOVA followed by Bonferroni's post-test and paired t-tests as indicated. Statistical comparisons of non-parametric data were made using the Kruskal-Wallis test followed by Dunn's multiple comparison post-test. In all cases $P<0.05$ was considered significant. The relaxation evoked by each agonist was calculated as the % maximum dilatation of PE-contracted arteries: 100% being the maximum diameter seen for each experiment. Similarly, the constriction evoked by each agonist was calculated as the % maximum constriction: 100% being the minimum diameter seen for each experiment (evoked with 10μM PE). Values for artery diameter were obtained from traces plotted for each experiment using Excel software (Microsoft, USA) following calibrations appropriate for the camera, objectives and imaging software used. Concentration-response curves and histograms were prepared using Prism version4.0 software (GraphPad Software, USA). Sigmoidal concentration-response curves were fitted where possible and were drawn using the variable plot function in Prism (equation 2.1). Agonist potency was expressed as the negative logarithm to base 10 of the EC_{50} value provided for each curve by the Prism software (pD_2).

$$y = \frac{\text{Bottom+(Top-Bottom)}}{\text{(1+10\^{}((LogEC50-x)*Hill slope))}} \qquad \text{(equation 2.1)}$$

Where; x = the logarithm of concentration, y = the response

3. The use of fluorescent markers to resolve arterial structure

3.1. Introduction

Molecular, electrophysiological and functional assays may all be used to clarify the presence and function of ion channels, receptors or signalling molecules within a cell or tissue. However, often it is difficult to fully appreciate the interactions between lipid and protein moieties without being able to visualize their positions relative to each other and to the structural components of the cell and tissue. Advances in fluorescent labelling technologies and the development of laser scanning confocal and two-photon microscopes have enabled accurate, quantitative visualization of both dynamic processes and structural localization within live cells and tissues such that in recent years the use of fluorescent markers has accelerated substantially (Lichtman & Conchello, 2005).

Within studies of vascular function in rat mesenteric arteries, fluorescent imaging has been widely used for the study of Ca^{2+} signalling within the arterial wall (Lagaud *et al.*, 1999; Lamont & Wier, 2004; Matchkov *et al.*, 2004b; Mauban & Wier, 2004; McSherry *et al.*, 2005; Nilsson *et al.*, 1994; Nilsson *et al.*, 1998; Oishi *et al.*, 2001; Shaw *et al.*, 2004; Shaw *et al.*, 2006; Takano *et al.*, 2004; VanBavel *et al.*, 2001; Zang *et al.*, 2001; Zhang *et al.*, 2002) and for the study of immunohistochemical and fluorescent localization of various receptors and proteins key to arterial function. Indeed, fluorescence immunohistochemistry is now a well-established method of cellular protein detection and localization.

The most common fixation methods used for detection of arterial proteins require either whole animal perfusion prior to tissue isolation or incubation of isolated arteries with fixative prior to membrane permeabilization and antibody incubation (Briones *et al.*, 2003; Gardener *et al.*, 2004; Gonzalez *et al.*, 2005; Grayson *et al.*, 2004; Gustafsson *et al.*, 2003; Hill *et al.*, 2006; Mather *et al.*, 2005; Sandow *et al.*, 2006; Weston *et al.*, 2005; Weston *et al.*, 2002). The whole animal perfusion method is advantageous as it allows an approximation of protein localization under physiological conditions *in vivo*. However, as many studies are carried out *in vitro* fixation by this method may not accurately capture protein expression under conditions of tissue isolation. Functional differences reported in studies of spreading dilatation responses support such a proposal (Budel *et al.*, 2003).

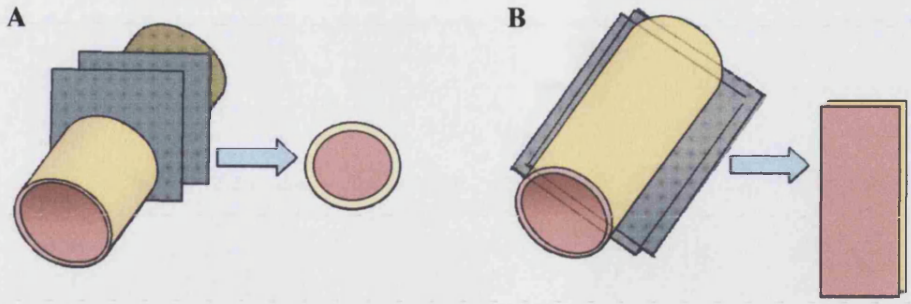

Figure 3.1

Commonly used arterial cross-sections for immunohistochemical studies

Cartoon illustrating **A,** vertical and **B,** horizontal cross-sections through the arterial wall made possible by **A,** serial sectioning, **B**, longitudinal dissection or **A,B**, by using a confocal microscope.

Studies using mesenteric arteries isolated prior to fixation have been frequently reported (Gardener *et al.*, 2004; Gustafsson *et al.*, 2003; Hill *et al.*, 2006; Weston *et al.*, 2005; Weston *et al.*, 2002). However for the tissue to be visualized arteries were either embedded or frozen whilst pinned out then sectioned or further cut longitudinally such that the tissue may be laid flat on a coverslip. Both methods are technically difficult (Sandow *et al.*, 2006). However the first allows the experimenter to obtain excellent vertical cross-sectional images of the whole artery (Figure 3.1a), enabling simultaneous estimation of protein localization in each of the layers of the artery wall, albeit with limited quantitative knowledge (Gardener *et al.*, 2004; Gustafsson *et al.*, 2003; Hill *et al.*, 2006; Weston *et al.*, 2005; Weston *et al.*, 2002). In contrast, the method of longitudinal dissection enables visualization of the vascular wall on one focal plane (Figure 3.1b). If a number of sequential sections are studies using confocal fluorescence microscopy it is possible to render and re-construct the images enabling an estimation of protein distribution throughout the wall of the artery (Grayson *et al.*, 2004; Mather *et al.*, 2005; Murphy *et al.*, 2001).

Within this thesis a modified immunohistochemical method for localization of proteins in isolated, pressurized arteries that is based upon the protocol of Murphy and colleagues (2001) was used. Whilst investigating the effects of intravascular pressure on tyrosine phosphorylation within the smooth muscle layer of isolated rat cremaster arterioles the investigators fixed arteries when pressurized and maximally dilated.

Subsequently the arteries were permeabilized and treated with antibodies using conventional protocols applied to the mounted and pressurized artery. Upon completion of the procedure the artery was dismounted and placed on a coverslip for visualization. By subsequently measuring differences in fluorescence intensity they were able to demonstrate quantitative differences in protein phosphorylation following fixation at different levels of transmural pressure, or following incubation with pervanadate, tyrphostin A47, angiotensin II, Ca^{2+}-free solution, verapamil and forskolin (Murphy *et al.*, 2001).

Using a further modification of this technique we visualized arteries whilst still mounted to enable minimal disruption of tissue integrity. We subsequently carried out preliminary studies of von Willebrand factor and α-smooth muscle actin staining before evaluating the localization of three ion channels fundamental to the mechanism of EDHF in rat mesenteric arteries: Connexin 40, SK_{Ca} and IK_{Ca} (Chen & Cheung, 1997; Crane *et al.*, 2003a; Doughty *et al.*, 1999; Hinton & Langton, 2003; Mather *et al.*, 2005; Walker *et al.*, 2001). Using well-established cell membrane and vesicular dyes preliminary experiments were also performed to evaluate other methods that may be used, either alone or in conjunction with immunohistochemical methods, to evaluate arterial structure and function.

3.2. Methods

3.2.1. Rat mesenteric artery isolation and cannulation

Please see section 2.1 for methods of artery isolation.

3.2.2. Pressure myography

Arteries were mounted in both custom-built organ baths (0.5 – 1ml; Figure 2.2) and a commercially available pressure myograph (10ml; 120CP, Danish Myo Technology, Denmark; Figure 2.1) for visualization of arterial structure. For cannulation and equilibration methods please see section 2.2. Endothelial cell viability was assessed as a >90% control dilatation to ACh (1μM) following pre-constriction with PE (1 - 3μM). Arteries were maintained at 50mmHg and 37°C unless otherwise stated.

3.2.3. Visualization of endothelial and smooth muscle cell layers using di-8-ANEPPS

Endothelial cells were loaded by luminal perfusion (2min; 100μl min^{-1}) and then incubation (38min) with the membrane potential sensitive dye di-8-ANEPPS (1μM) following a decrease in luminal pressure to ~7mmHg. Smooth muscle cell loading was achieved by addition of di-8-ANEPPS (1μM; 19min) to the bath solution. Prior to imaging arteries were washed with MOPS-buffered salt solution and the intraluminal pressure increased to 50mmHg.

3.2.4. Quinacrine and Alexa Fluor® 633 staining of rat mesenteric arteries

Quinacrine (1μM; 2h) or wheat germ agglutinin conjugated to Alexa Fluor® 633 (100μg ml^{-1}; 50min) was incubated abluminally. Arteries were washed with MOPS-buffered salt solution prior to imaging.

3.2.5. Pinocytic loading of fluorescent molecules to visualize artery layers

The pinocytic loading method described in section 2.4 was used to load the endothelium, IEL and perivascular nerves with carboxyfluorescein (~1mg ml^{-1}) or the cell impermeant dye lucifer yellow (saturated solution). Fluorescent dyes were dissolved into the hypertonic sucrose solution and filtered (0.22μm syringe filter unit) prior to the addition of PEG.

3.2.6. Immunohistochemistry

Pressurized (50mmHg) arteries were incubated with papaverine (150μM) to maintain artery diameter during fixation. Arteries were then fixed in a 2%wv^{-1} paraformaldehyde solution (10min; 37°C; please see section 3.2.8 for solution compositions). The pressure was then reduced (~7mmHg) and arteries washed and luminally-perfused (90μl min^{-1}; 1min) with phosphate-buffered saline (PBS) three times over 5min intervals. This was followed by luminal and abluminal incubation with blocking buffer (1h; 37°C; ~7mmHg; section 2.7.4) containing propidium iodide (0.05%wv^{-1}) as indicated. Arteries were then incubated overnight (4°C; ~4mmHg) with primary antibody (please see section 3.2.9) diluted (1:100) in blocking buffer applied both abluminally and luminally. Tissues were then allowed to warm to room temperature (30min) before washing with PBS as described. Secondary detection was performed with either Alexa Fluor®633 or Alexa Fluor®488 goat anti-rabbit IgG (H+L; Highly cross-adsorbed) in a modified blocking buffer (1:100) for 2h abluminally and 1h luminally (90μl min^{-1}; 2min) at room temperature. Subsequently arteries were washed as described, pressurized to 50mmHg and visualized. For higher resolution images, arteries were removed from the cannulae and placed on a coverslip in an anti fade-buffered glycerol.

3.2.7. Confocal microscopy

Images were taken using an inverted microscope (IX71, Olympus UK) attached to a laser scanning confocal microscope (FV500-SU, Olympus UK) and processed using photometric software (Tiempo software, Olympus UK). The argon-ion laser with a primary excitation peak at 488nm was used for excitation of Di-8-ANEPPS, quinacrine, carboxyfluorescein, lucifer yellow, Alexa Fluor®488-conjugated secondary antibodies and IEL autofluorescence. Green and red helium-neon lasers with respective primary excitation peaks at 543nm and 633nm were used for excitation of propidium iodide and Alexa Fluor®633-conjugated proteins respectively. To enable comparison of protein expression, settings for the red helium-neon laser for visualization of IK_{Ca} and SK_{Ca} were maintained throughout both sets of experiments (laser intensity, 50%; confocal aperture, 130μm; photomultiplier tube 635-647V).

3.2.8. Dyes and solutions

A 10mM stock solution of Di-8-ANEPPS was prepared by dissolving the anhydrous solid in DMSO to give a 10mM stock solution. A 10mM stock solution of quinacrine was prepared daily in MilliQ water. Alexa Fluor® 633 conjugated wheat germ agglutinin was prepared daily by dissolving into MOPS-buffered salt solution (please see section 2.6.1.1 for composition) to give a final stock concentration of 1mg ml^{-1}. Propidium iodide was prepared as a 1%wv^{-1} stock solution in MilliQ water. Di-8-ANEPPS stock (10mM) was diluted in a solution comprising 0.25%vv^{-1} pluronic acid dissolved in MOPS buffered solution immediately before loading and incubation. All other dyes were dissolved directly into the luminal or bath solutions unless otherwise stated.

Fixative for immunohistochemistry contained 2%wv^{-1} paraformaldehyde in phosphate-buffered saline (PBS) of composition (mM): NaCl 119.8, $Na_2HPO_4.2H_2O$ 7.0 and $NaH_2PO_4.H_2O$ 2.6, containing NaOH (3mM) adjusted to pH 7.38±0.03. Blocking buffer was of composition: bovine serum albumin (BSA; 1%wv^{-1}) and Tween 20 (0.1%vv^{-1}) in PBS. Secondary antibody buffer comprised BSA (1%wv^{-1}) and Tween 20 (0.01%vv^{-1}) in PBS. Anti fade-buffered glycerol comprised a 5%wv^{-1} solution of p-phenylenediamine made up with $NaHCO_3$ (500mM) in MilliQ water that had been adjusted to pH 8.6 with Na_2CO_3 (500mM). Glycerol was then added to the final solution (66.6%vv^{-1}).

All chemicals and dyes were purchased from Sigma (Poole, UK) with the exception of Di-8-ANEPPS and Alexa Fluor®633 conjugated wheat germ agglutinin (Molecular Probes Invitrogen, Paisley, UK).

3.2.9. Antibodies

Anti-von Willebrand factor antibody was raised in rabbits against human von Willebrand factor (SIGMA, Poole, UK). Anti-smooth muscle α-actin antibody was raised against the N-terminal synthetic decapeptide of α-smooth muscle actin in mouse clone 1 A4 (SIGMA, Poole, UK). Antibodies targeted against the K_{Ca} channels were raised in rabbits against either the N-terminus of human $K_{Ca}2.3$ ($SK_{Ca}3$; DTSGHFHDSGVGDLDEDPKC) (Alomone, Jerusalem, Israel) or the C-terminus of

$K_{Ca}3.1$ (IKCa4; RQVRLKHRKLEQV(C)) (Alomone, Jerusalem, Israel). The connexin 40 antibody was raised in rabbits and targeted against a 19 amino acid peptide sequence within the C-terminal cytoplasmic domain of mouse connexin 40 (Chemicon, CA, USA). This peptide sequence is conserved in rat connexin 40. The secondary Alexa Fluor®633 and Alexa Fluor®488 goat anti-rabbit IgG (H+L; Highly cross-adsorbed) antibodies were purchased from Molecular Probes (Invitrogen, Paisley, UK). Each of the antibodies have been previously characterised either in HEK 293, Rin or Cos-7 cell culture systems or, epithelial, neuronal and endothelial cells within gastrointestinal tract and arterial tissues (Fujita *et al.*, 2001; Gustafsson *et al.*, 2003; Sandow *et al.*, 2003b; Sandow *et al.*, 2006; Taylor *et al.*, 2003).

3.3. Results

3.3.1. Identification of smooth muscle and endothelial cell layers of a rat mesenteric artery with propidium iodide and di-8-ANEPPS

By permeabilizing pressurized rat isolated small mesenteric arteries (n = 12) with blocking buffer (1h) containing the cell membrane impermeant nuclear stain propidium iodide (0.05%wv^{-1}) it was possible to clearly stain both endothelial cell (horizontally aligned cells; Figure 3.2A) and smooth muscle cell nuclei (vertically aligned cells; Figure 3.2A). This highlighted the perpendicular orientation of the two cell types enabling differentiation between the two layers of the artery wall. The alignment of cell type seen in Figure 3.2A is used throughout this thesis. Luminal and abluminal incubation of isolated, pressurized rat mesenteric arteries with the membrane potential sensitive dye di-8-ANEPPS (1μM) resulted in clear endothelial cell (Figure 3.2B; 38min) and smooth muscle cell (Figure 3.2C; 19min) membrane staining.

3.3.2. Quinacrine and Alexa Fluor® 633 staining of the endothelium, smooth muscle and adventitia of isolated arteries

Using the dye quinacrine, which has been reported to show high affinity for ATP (Bodin & Burnstock, 2001; Irvin & Irvin, 1954; Mitchell *et al.*, 1998) the localization of ATP within each layer of the artery wall was investigated (n = 2). Abluminal incubation of rat isolated and pressurized small mesenteric arteries with quinacrine resulted in cell nuclei staining within all layers of the vascular wall (Figures 3.3A, B and C) and granular staining within the smooth muscle cells (Figure 3.3B) and perivascular nerves (Figure 3.3C). To further investigate arterial wall organelle structures we evaluated the effect of abluminal incubation of a rat isolated small mesenteric artery (n = 1) with the Alexa Fluor® 633-conjugated wheat germ agglutinin (Yang & Loscalzo, 2005). Figure 3.3D illustrates the extensive linear and fibrous staining of the external layers of the artery with the fluorescent wheat germ agglutinin. Due to damage caused to the artery by imaging (results not shown) this methodology was not further explored.

A. Propidium iodide nuclear staining

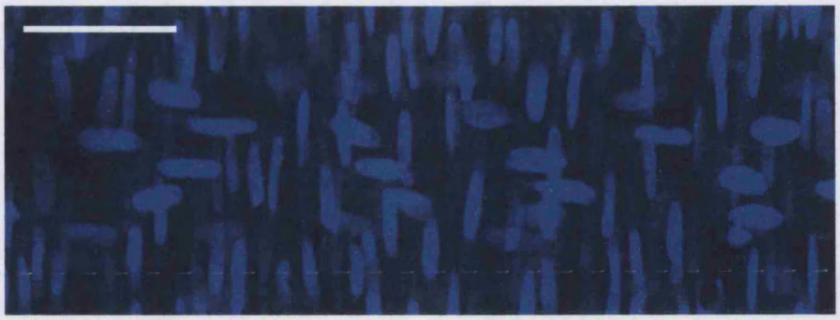

B. Di-8-ANEPPS staining of the endothelium

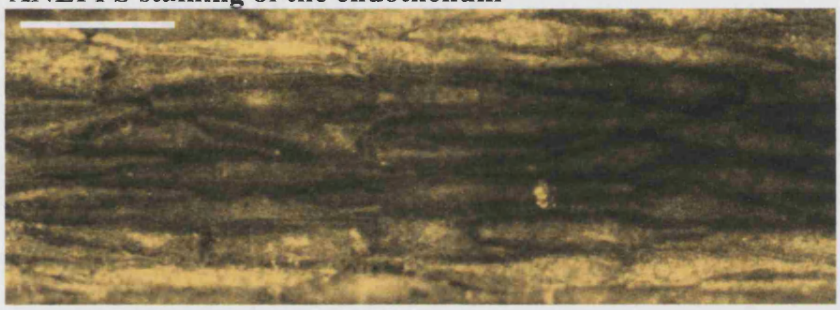

C. Di-8-ANEPPS staining of the smooth muscle

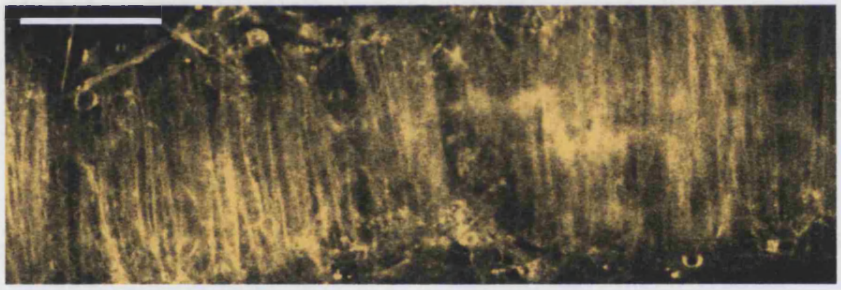

Figure 3.2 Staining of isolated, pressurized rat mesenteric arteries with fluorescent dyes to identify cell layers

A, B, C, Single plane images of the **A, B**, endothelium (horizontally aligned cells), and **A, C,** smooth muscle (vertcally alighned cells) of isolated rat small mesenteric arteries following **A**, permeabilization with blocking buffer and incubation with the nuclear stain propidium iodide ($0.05\%wv^{-1}$) o , **B** luminal and **C,** abluminal incubation with the potential sensitive membrane dye Di-8-ANEPPS (1μM). All images were captured at 50mmHg with a 40x water immersion objective. The smooth muscle cell and endothelial cell alignment illustrated in **A** is used throughout this thesis. Bar = 50μm

A. Quinacrine staining for ATP vesicles in the endothelium

B. Quinacrine staining for ATP vesicles in the smooth muscle

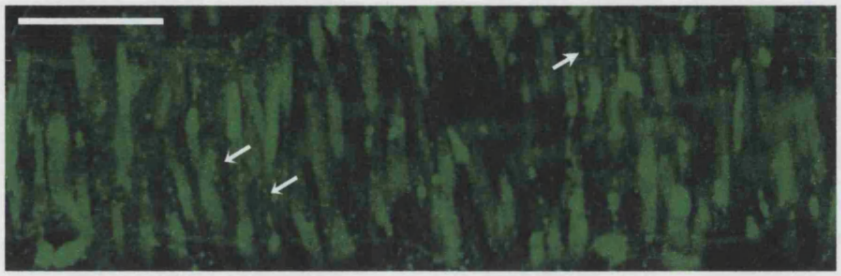

C. Quinacrine staining for ATP vesicles in the adventitia

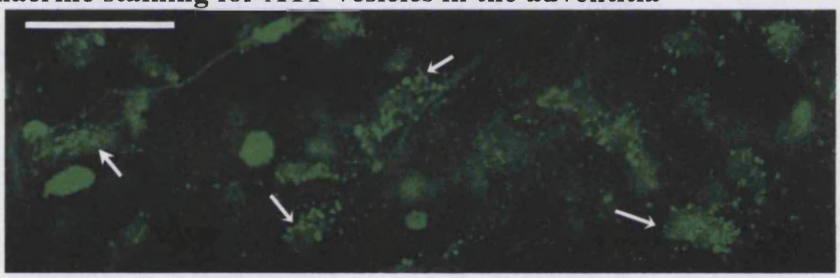

D. Wheat germ agglutinin-conjugated Alexa Fluor® 633 staining of the adventitia

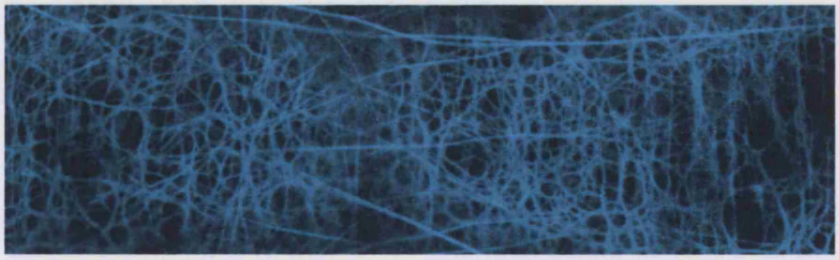

Figure 3.3. Quinacrine and Alexa Fluor® 633 staining of isolated, pressurized rat small mesenteric arteries

Single plane images of isolated pressurized rat mesenteric arteries following abluminal staining with **A, B, C,** quinacrine (1μM; green) and **D,** wheat germ agglutinin conjugated to Alexa Fluor® 633 (100μg ml^{-1}). These techniques allow visualization of **A**, the endothelium, **B**, the smooth muscle and **C, D**, the adventitia of the arteries. **B, C,** Arrows indicate possible sites of ATP vesicles. All images were captured with a x40 water immersion objective. Bar = 50μm.

3.3.3. Pinocytic loading of fluorescent molecules into rat isolated mesenteric arteries to identify cell layers

In experiments carried out to evaluate the efficacy of the pinocytic loading protocol (Figure 2.4) as a method of selectively loading macromolecules into different layers of the arterial wall the fluorescent dyes carboxyfluorescein (~1mg ml; n = 3) and lucifer yellow (saturated solution; n = 3) were included in the hypertonic solution. The extent and location of fluorescence emitted from the artery was subsequently observed. Following inclusion of carboxyfluorescein into the luminally-applied hypertonic solution extensive endothelial cell loading could be observed with only a few smooth muscle cells seen to contain carboxyfluorescein (Figure 3.4A). In contrast when lucifer yellow was added to the luminally-applied hypertonic solution only the edges of the endothelial cells could be clearly seen, but lucifer yellow did also appear to bind uniformly to the IEL (Figure 3.4B). Inclusion of carboxyfluorescein in abluminally-applied hypertonic solution resulted in staining of the perivascular nerves with some smooth muscle cell staining also apparent (Figure 3.4C).

3.3.4. Immunohistochemical localization of endothelial and smooth muscle cell markers in isolated pressurized arteries.

Rat isolated pressurized mesenteric arteries that have been fixed and stained for von Willebrand factor and smooth muscle α-actin using the protocol of Murphy and colleagues (2001) were visualized whilst still cannulated and pressurized. Von Willebrand factor was observed as small punctate spots throughout the cytosol of endothelial cells (Figure 3.5A; n = 1). Punctate smooth muscle α-actin staining was observed in both the cytosol and on the edge of the outer layer of smooth muscle cells (Figure 3.5B; n = 1).

3.3.5. Distribution of endothelial connexin 40, SK_{Ca} and IK_{Ca}

Having established the efficacy of the methods of Murphy and colleagues the distributions of connexin 40 (n = 2), SK_{Ca} (n = 1) and IK_{Ca} (n = 1) within the endothelium were determined. Using the nuclear stain propidium iodide as both a marker of cell permeability and alignment (Figures 3.6A and C) punctate staining of connexin 40 was localized to the periphery of the endothelial cells, highlighting the borders between adjacent endothelial cells (Figure 3.6B and D).

A. Endothelial cell loading with carboxyfluorescein

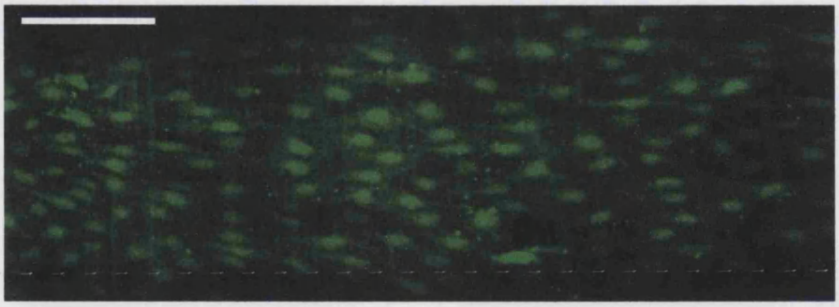

B. Lucifer yellow staining of the IEL

C. Nerve cell loading with carboxyfluorescein

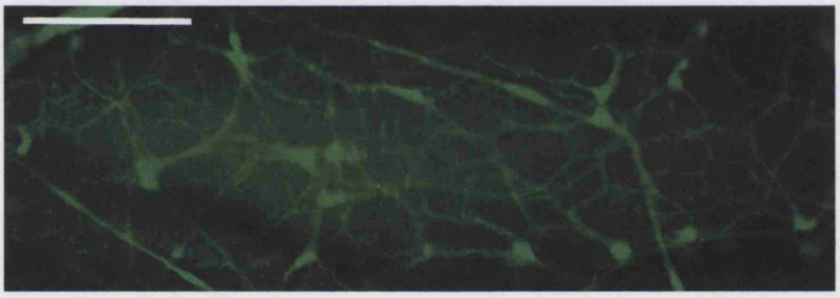

Figure 3.4 Pinocytic loading of fluorescent molecules into isolated rat mesenteric arteries to identify cell layers

A, B, Merged and **C,** single plane images of the **A,** endothelium **B,** IEL and **C,** perivascular nerve cells of isolated rat small mesenteric arteries following **A, B,** luminal and **C,** abluminal application of the pinocytic loading protocol with **A, C,** carboxyfluorescein (~1mg ml) and **B,** lucifer yellow (saturated solution) included in the hypertonic solution. All images were captured at 50mmHg with a 20x water immersion objective. Bar = 100μm

A. Von Willebrand factor localization in the endothelium

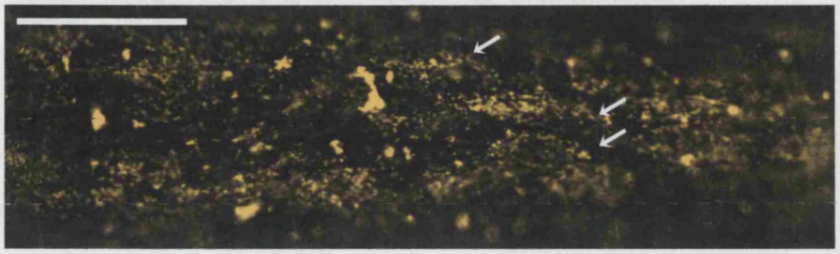

B. Smooth muscle α-actin localization

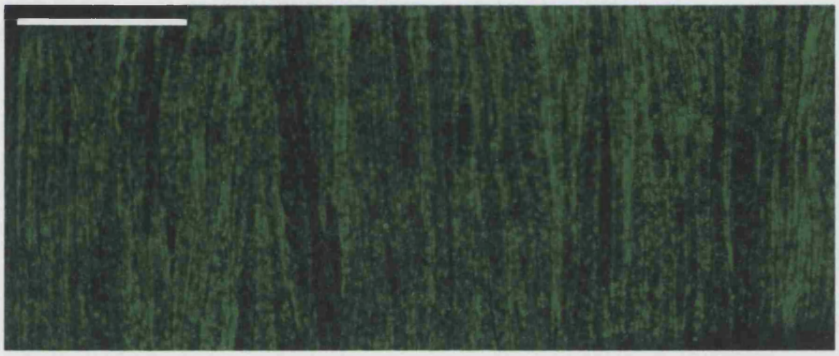

Figure 3.5 Immumohistochemical localization of endothelial and smooth muscle cell markers in isolated pressurized arteries
A, Single plane image and **B,** montaged stack images of **A,** the endothelium and **B,** smooth muscle layers following cell permeabilization with blocking buffer and subsequent staining with **A,** anti-von Willebrand factor antibody (1:100) with an Alexa fluor® 488 secondary antibody (1:100). and **B,** smooth muscle α-actin primary antibody (1:100) with an Alexa fluor® 488 goat anti-mouse secondary antibody (1:100). The images were taken at 50mmHg using a 40x water-immersion objective. Arrows indicate endothelial cells. Bar = 50μm.

A. Propidium iodide nuclear staining

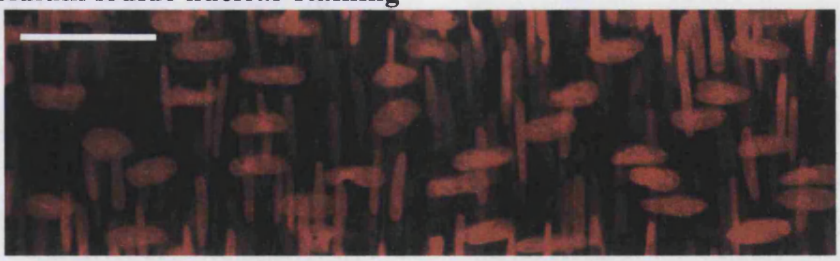

B. Connexin 40 localization

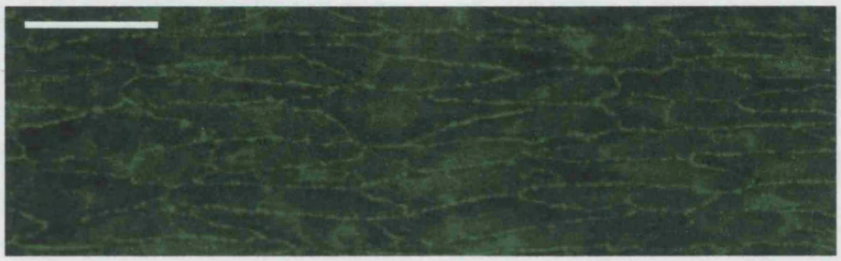

C. Connexin 40 localization and propidium iodide nuclear staining

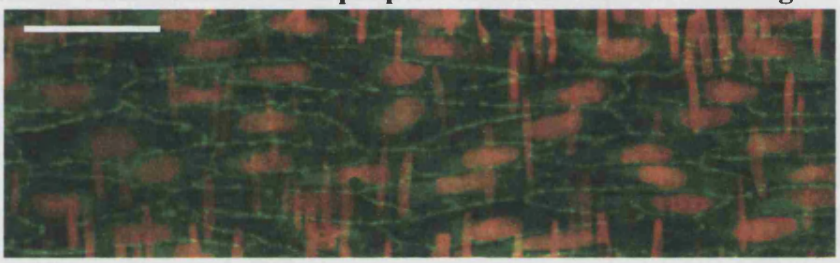

D. IEL autofluorecence **E. Connexin 40** **F. IEL & connexin 40**

Figure 3.6 Immunohistochemical localization of endothelial cell connexin 40

A, **B, D**, **E,** Single plane and **C, F** merged images of the endothelial cell layer of isolated pressurized arteries following cell permeabilization with blocking buffer **A**, **B, C,** containing propidium iodide (0.05%wv^{-1}), and subsequently stained with **B, C, E and F,** anti-connexin 40 (1:100), **A, B, C**, with an Alexa fluor® 488 goat anti-mouse secondary antibody (1:100), or **D, E, F,** with an Alexa fluor® 633 goat anti-mouse secondary antibody (1:100). **D, F,** The IEL is made visible by autofluorescence. All images were taken at 50mmHg using a 40x water-immersion objective. Arrows indicate examples of sites where holes in the IEL align with punctate Cx40 antibody staining. **A, B, C,** Bar = 50μm, **D, E, F,** bar = 10μm.

A. IEL autofluorescence

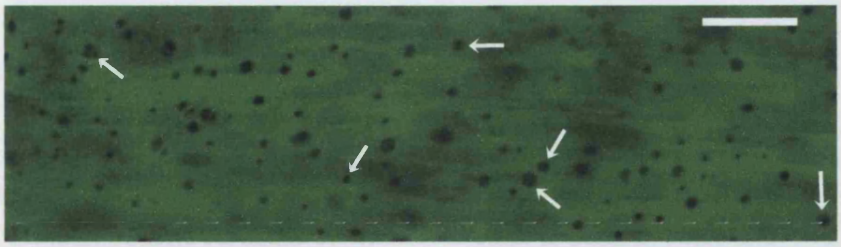

B. Connexin 40 localization

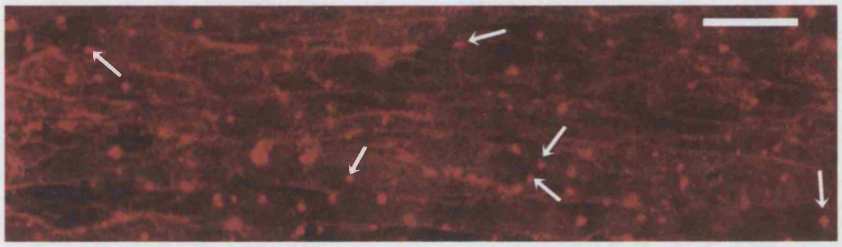

C. Connexin 40 localization and IEL autofluorescence

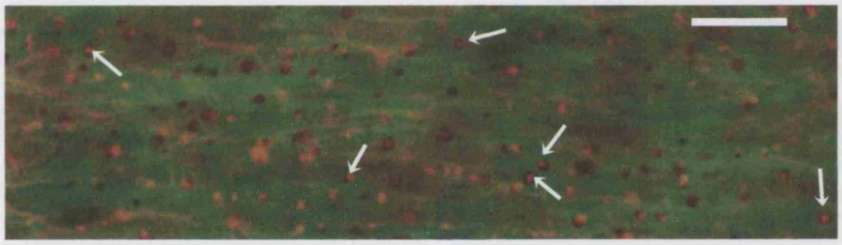

Figure 3.7 Increased resolution images of endothelial cell connexin 40 Arteries were dismounted, placed on a coverslip and visualized using a 60x oil-immersion objective to increase the available resolution. **A**, **B,** Single plane and **C,** merged images of the endothelium and IEL of an isolated pressurized artery following cell permeabilization with blocking buffer and subsequent staining with **B, C** anti-connexin 40 (1:100) with an Alexa fluor® 633 goat anti-mouse secondary antibody (1:100). **A, C,** The IEL is made visible by autofluorescence. Arrows indicate examples of sites where holes in the IEL align with punctate Cx40 antibody staining. Bar = 50μm.

In separate experiments this punctate staining was also shown to correlate with holes in the IEL, as viewed by autofluorescence at ~488nm (Figures 3.6, D, E and F). Higher resolution images obtained by removal of the artery from the cannulae, subsequent longitudinal dissection and then observation with a x60 oil immersion objective illustrated the frequency with which the holes in the IEL correlated with the punctate staining of connexin 40 (Figure 3.7). Punctate staining for SK_{Ca} was also found at the endothelial cell borders. Furthermore, SK_{Ca} localization also correlated with holes in the IEL. However, in contrast to connexin 40, SK_{Ca} could also be localized toward the centre of the cell (Figure 3.8). Punctate staining of IK_{Ca} was restricted to holes in the IEL, with no endothelial cell border staining observed (Figure 3.9).

A. IEL autofluorescence

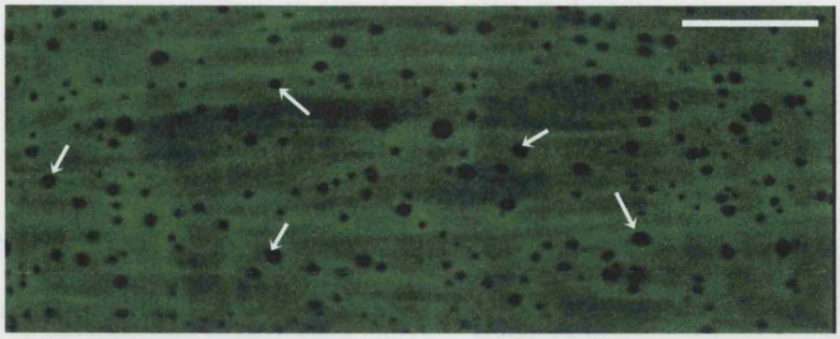

B. SK_{Ca} localization

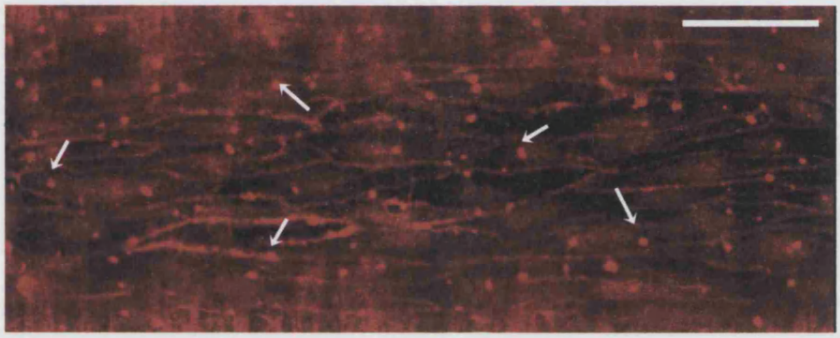

C. SK_{Ca} localization and IEL autofluorescence

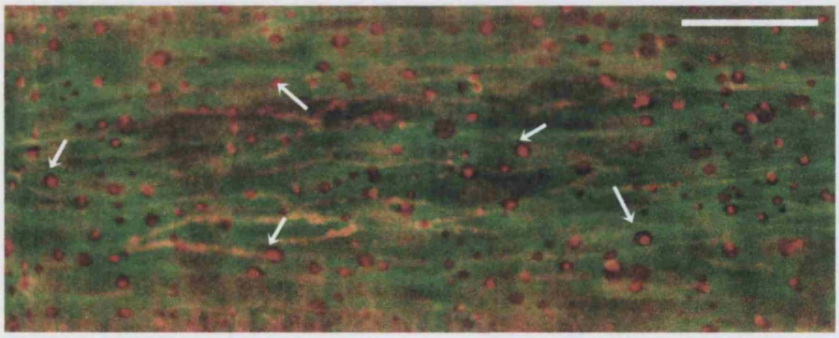

Figure 3.8 Immunohistochemical localization of endothelial cell SK_{Ca}
A, **B,** Single plane and **C,** merged images of the endothelium and IEL of an isolated pressurized artery following cell permeabilization with blocking buffer and subsequent staining with **B, C,** anti-SK_{Ca} (SK3; 1:100) with an Alexa fluor® 633 goat anti-mouse secondary antibody (1:100). **A, C,** The IEL is made visible by autofluorescence. All images were taken at 50mmHg using a 40x water-immersion objective. Arrows indicate examples of sites where holes in the IEL align with punctate SK_{Ca} antibody staining. Bar = 50μm.

A. IEL autofluorescence

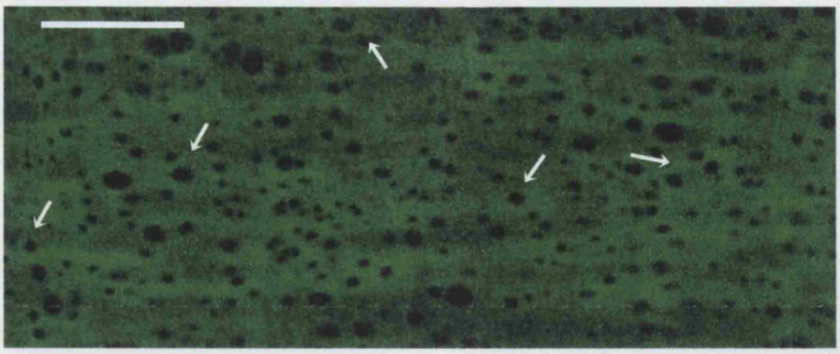

B. IK_{Ca} localization

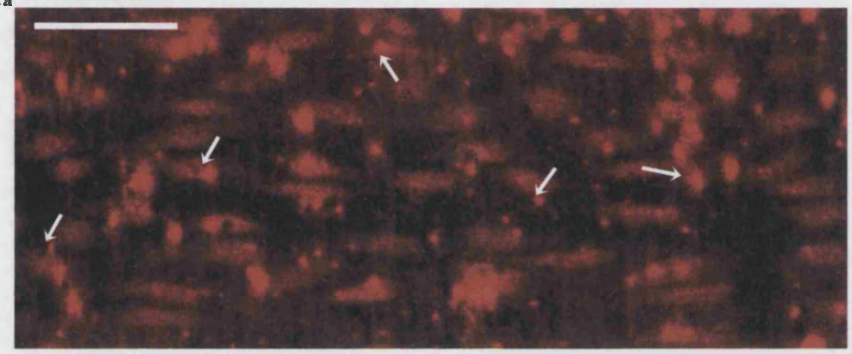

C. IK_{Ca} localization and IEL autofluorescence

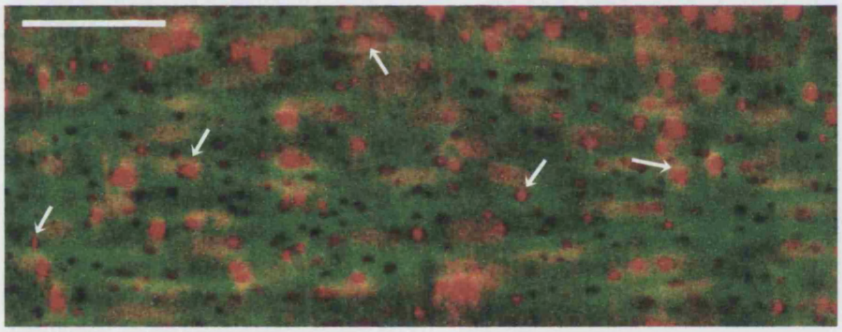

Figure 3.9 Immunohistochemical localization of endothelial cell IK_{Ca}
A, B, Single plane and **C,** merged images of the endothelium and IEL of an isolated pressurized artery following cell permeabilization with blocking buffer and subsequent staining with **B, C,** anti-IK_{Ca} (1:100) with an Alexa fluor® 633 goat anti-mouse secondary antibody (1:100). **A, C,** The IEL is made visible by autofluorescence. All images were taken at 50mmHg using a 40x water-immersion objective. Arrows indicate examples of sites where holes in the IEL align with punctate IK_{Ca} antibody staining. Bar = 50μm.

3.4. Discussion

Recent advances in imaging technology and the improved quality of fluorescent probes has led to a rapid increase in the number of reports utilising fluorescence-based imaging to evaluate tissue structure and function (Lichtman & Conchello, 2005). Of perhaps the greatest importance to whole tissue physiology experiments is the improved capacity to visualize deep into tissues using either confocal microscopy, or more recently two-photon microscopy (Lichtman & Conchello, 2005; Yuste, 2005). Given the large number of *in vitro* studies on vasomotor function we felt that it was important to evaluate different methods of arterial structure determination and subsequently protein localization *in vitro.* Within the present study a range of fluorescent dyes and loading methods were applied to rat isolated and pressurized small mesenteric arteries. The results were then visualized using confocal microscopy to determine the efficacy of each dye as a marker of arterial structure *in vitro.* Subsequently, immunohistochemical staining of pressurized small mesenteric artery preparations was performed to investigate the *in vitro* localization of ion channels fundamental to the mechanism of EDHF and to evaluate the efficacy of this method of protein detection.

3.4.1. Arterial staining with di-8-ANEPPS

The photometric dye di-8-ANEPPS has been used in studies of vascular function to enable the measurement of membrane potential without impalement of the cell (Beach *et al.*, 1998; Beach *et al.*, 1996; Chen & Rivers, 2001; Cohen & Jackson, 2005; Dora & Duling, 1998; Marrelli *et al.*, 2003; McGahren *et al.*, 1998). When in aqueous solution di-8-ANEPPS does not fluoresce. Fluorescence is activated following binding to phospholipids whereupon the absorption and emission peaks are at 467nm and 631nm respectively (Invitrogen, 2006). Given the membrane-bound nature of di-8-ANEPPS we investigated its use as a cell marker for delineation of the different cell types comprising the artery wall. In support of previous studies luminal application of di-8-ANEPPS selectively loaded the endothelium to produce extensive staining of endothelial cell plasma membranes (Dora & Duling, 1998). Endothelial cell morphology could be determined and was consistent with previous reports showing elongated cells (~100μm) aligned with the longitudinal axis of the artery (Dora & Duling, 1998; Sandow *et al.*, 2002; Takano *et al.*, 2004). Subsequent abluminal application of the photometric dye resulted in similar extensive membrane staining of the outer layer of smooth muscle

cells that consistently with previous reports demonstrated their circumferential arrangement (Dora & Duling, 1998; Sandow *et al.*, 2002; Takano *et al.*, 2004). From the presented data it is estimated that ~12 smooth muscle cells may be spanned by one endothelial cell. Although further work is needed to confirm this, such a finding supports previous reports proposing an endothelial cell pathway for conduction of spreading dilatation responses in rat mesenteric arteries and hamster cheek pouch arterioles (please see sections 1.5.2 and 3.4.7; Haas & Duling, 1997; Takano *et al.*, 2004).

3.4.2. ATP localization with quinacrine

ATP may be released from various components of the arterial wall (Bodin *et al.*, 1991; Burnstock, 2006; Burnstock, 1999; Pearson, 1979; Yamamoto *et al.*, 2003) and can evoke EDHF-type dilatation responses in rat isolated small mesenteric arteries (Liu *et al.*, 2006a; Malmsjo *et al.*, 1999; Mistry *et al.*, 2003). Therefore we investigated the localization of ATP within the adventitia, smooth muscle and endothelium of the isolated rat mesenteric artery using the high affinity ATP dye quinacrine (Bodin & Burnstock, 2001; Irvin & Irvin, 1954; Mitchell *et al.*, 1998).

Consistent with previous reports describing quinacrine staining in various cells in culture, granular staining patterns were observed in both the perivascular cells and smooth muscle cells of isolated arteries (Bodin & Burnstock, 2001; Mitchell *et al.*, 1998; Romanello *et al.*, 2005; Yegutkin *et al.*, 2006). In contrast to previous studies granular staining of the endothelium was not observed (Bodin & Burnstock, 2001). This may reflect the release of ATP by mechanical stress on the endothelium during tissue isolation and preparation (Bodin & Burnstock, 2001; Pearson, 1979). Quinacrine did however stain the nuclei of endothelial cell, smooth muscle cell and perivascular nerve cell types, reflecting the intercalation of quinacrine with nuclear DNA (Aslanoglu & Ayne, 2004; Baldini *et al.*, 1981; Stuhlmeier, 2000). The absence of nuclear staining in the reports studying cells in culture (Bodin & Burnstock, 2001; Mitchell *et al.*, 1998; Romanello *et al.*, 2005; Yegutkin *et al.*, 2006) may reflect their position in the cell cycle (Duivenvoorden *et al.*, 1995; Moser *et al.*, 1981) or the frequency of guanosine-cytosine base pairs in the nucleic acid strands (Baldini *et al.*, 1981). More simply, differences in the concentrations of quinacrine used or the methodological approaches may explain the

conflicting observations. Given the preliminary nature of these findings ($n = 2$) it would be interesting to repeat the studies reported here and also investigate the results of luminal quinacine application following treatment with *N*-ethylmaleimide, an inhibitor of vesicle fusion with the plasma membrane (Bodin & Burnstock, 2001), to ascertain if ATP vesicles may be found in the endothelium of the isolated artery preparation.

3.4.3. Alexa Fluor ® 633-conjugated wheat germ agglutinin

In an effort to further evaluate sub cellular structures within *in vitro* vascular preparations Alexa Fluor® 633-conjugated wheat germ agglutinin was used to study the localization of the Golgi apparatus (Yang & Loscalzo, 2005). In contrast to the granular staining observed by Yang and Loscalzo (Yang & Loscalzo, 2005) in cultured endothelial cells, intersecting linear lines of fluorescence were observed that likely corresponded to staining of adventitial collagen fibres (Soderstrom, 1987). Damage to the artery caused by photo bleaching limited any further use of this compound. However, it is possible that by using faster acquisition rates over a smaller region of interest luminal application of this fluorescent agent may reveal the sub cellular structures previously reported (Stephens & Allan, 2003; Yang & Loscalzo, 2005).

3.4.4. Pinocytic loading of fluorescent dyes

In experiments carried out to evaluate the efficacy and viability of the pinocytic loading method (please see section 2.4) extensive endothelial cell staining was observed following luminal pinocytic loading of carboxyfluorescein. These results were consistent with previous reports from this laboratory (Mather *et al.*, 2005) and illustrate the longitudinal orientation of the endothelial cells. The transient nature of the endothelial cell staining with carboxyfluorescein, most likely due to active transport of the dye out of the cell (Mather *et al.*, 2005; Rychlik *et al.*, 2003), limits the use of this dye as an endothelial cell marker. However, given that similar, maintained staining with fluorescent dextran (3000Da) has also been achieved and the viability of the endothelium is maintained following the pinocytic loading protocol (please see section 4.3.6; Mather *et al.*, 2005) the method in combination with other dyes may prove useful for endothelial cell visualization in future studies.

Abluminal pinocytic loading of rat isolated small mesenteric arteries with carboxyfluorescein showed clear visualization of the perivascular nerves to reveal staining patterns analogous to those previously reported in the same preparation following staining for calcitonin gene related peptide (Mupanomunda *et al.*, 1998) and α and β-adrenoceptors (Briones *et al.*, 2005). However, as would be expected, the relatively selective loading of the endothelium observed following luminal application of the pinocytic loading protocol was not replicated following abluminal application. This could largely be due to the inconsistent external surface of the vascular wall allowing rapid uptake of the dye into the sub-adventitial, smooth muscle layers as has previously been described (Mather *et al.*, 2005).

Given the success of the luminal pinocytic loading method for the transfer of carboxyfluorescein and dextran into the endothelium, the effects of inclusion of the cell impermeant dye lucifer yellow into the luminally-applied hypertonic solution were studied. In contrast to the results seen with carboxyfluorescein and FITC-labelled dextran, loading with lucifer yellow resulted in extensive staining of the IEL. Previous studies using microelectrodes to inject lucifer yellow into endothelial cells of intact rat isolated mesenteric arteries (Takano *et al.*, 2004), hamster cheek pouch arterioles (Little *et al.*, 1995; Welsh & Segal, 1998), porcine ciliary artery (Beny *et al.*, 1997) and sheets of calf aortic endothelial cells (Larson & Sheridan, 1982) showed extensive spread of the dye into adjacent cells from the site of injection. Furthermore the nature of the staining was very similar to that observed in the present study following pinocytic loading of carboxyfluorescein. The staining of the IEL by lucifer yellow reported herein could reflect a sensitivity of the pinocytic loading process to molecular charge or compound structure as the pinocytic process can be modulated by the molecule carried (Conner & Schmid, 2003; Davies *et al.*, 1981; Simionescu & Simionescu, 1984). Further research on the processes involved would need to be undertaken to fully understand the mechanism of this loading protocol. However, the excellent staining of the IEL and the illumination of endothelial cell borders by the pinocytic loading of lucifer yellow may prove a useful tool in the localization of proteins and their contribution to cell-to-cell communication within the vascular wall (please see sections 3.4.7 and 3.4.8).

3.4.5. Identification of endothelial cell and smooth muscle cell markers with immunofluorescence

Using a method of immunofluorescence for intact arteries (Murphy *et al.*, 2001) we investigated endothelial cell and smooth muscle cell staining with von Willebrand factor and smooth muscle α-actin respectively. These preliminary studies showed punctate cytosolic staining of the endothelium and smooth muscle with the two cell markers as is consistent with previous reports, supporting the use of this immunohistochemical method in future studies of arterial protein localization *in vitro.* Only abluminal staining for the smooth muscle layers and luminal staining for the endothelium were investigated so further positive and negative controls to confirm antibody specificity would be required in addition to those previously reported (Aznar-Salatti *et al.*, 1990; Bryan *et al.*, 2006; Del Pup *et al.*, 2002; Reidy *et al.*, 1989; Sandow *et al.*, 2006; Simard *et al.*, 2006; Slaninova *et al.*, 1999; Stromer *et al.*, 2002). The different staining methods employed for these two antibodies and the lack of staining of the other layers of the artery wall highlight the tissue selectivity that may be employed by using this method of cannulated artery immunohistochemistry. Furthermore, for visualization of endothelial cell protein expression the antibody volume and therefore experimental cost may be minimised by use of luminal application only. In contrast if antibodies are applied both luminally and abluminally the intact artery may provide its own positive or negative controls for analysing antibody specificity.

3.4.6. Propidium iodide as a nuclear stain and marker for cell permeabilization

Propidium iodide is well established as a cell-impermeant nuclear stain that will fluoresce when intercalated with DNA or RNA. In addition to its use as a nuclear stain it is also used in flow cytometry and studies of vascular function as a test of cell viability (Mather *et al.*, 2005; Sasaki *et al.*, 1987). The dependence of this dye on cell permeability in order to fluoresce makes it an ideal marker of cell permeability (Hill *et al.*, unpublished observations). In the present study propidium iodide was included in the blocking buffer solution during the permeabilization stage of the immunohistochemistry protocol. This made it possible to evaluate when all layers of the artery were sufficiently permeabilized by the number of cells stained. Consistent with previous studies using propidium iodide in cultured cells and arterial tissue, propidium iodide staining appeared restricted to cell nuclei (Coats *et al.*, 2003; Jones & Kniss,

1987; Kansui *et al.*, 2004; Mather *et al.*, 2005; Takano *et al.*, 2004). Based on the specific orientation of the nuclear staining it was clear that propidium iodide could also be used to determine cell type as endothelial cell nuclei could be clearly located along the longitudinal axis of the artery whilst smooth muscle cell nuclei were arranged circumferentially (Coats & Hillier, 1999; Dora & Duling, 1998).

The shift between the absorbance maximum of propidium iodide at 535nm and its emission maximum at 617nm makes it a suitable cell marker and nuclear stain during immunofluorescence studies using fluorescein-conjugated antibodies (Jones & Kniss, 1987; Kansui *et al.*, 2004; Virgintino *et al.*, 2002). Therefore within the present study we used propidium iodide as a cell marker in conjunction with endothelial staining for connexin 40.

3.4.7. Immunofluorescent staining of connexin 40

Connexin 40 is a member of the connexin family of gap-junction proteins that has been shown to be a central component of both radial and conducted dilatation responses (please see section 1.3.3 for review; (de Wit *et al.*, 2000; Figueroa *et al.*, 2003; Mather *et al.*, 2005). Connexin 40 together with connexins 37 and 43 comprise the only gap junction proteins detected in rat mesenteric arteries to date (Goto *et al.*, 2004; Gustafsson *et al.*, 2003; Hong & Hill, 1998; Kansui *et al.*, 2004; Mather *et al.*, 2005). The punctate staining of endothelial cell borders by antibodies targeted against connexin 40 observed in the present study is consistent with previous reports in preparations of rat isolated mesenteric arteries (Goto *et al.*, 2004; Kansui *et al.*, 2004; Mather *et al.*, 2005; Sandow *et al.*, 2006). Gap junction coupling between endothelial cells is thought to mediate the spread of hyperpolarization that is fundamental to conducted dilatation responses as the longitudinal orientation and low resistance of these cells would provide a far quicker conduction pathway than the circumferentially orientated smooth muscle cells (please see sections 3.4.1 and 5.1; Haas & Duling, 1997; Yamamoto *et al.*, 2001). Indeed, the abolition of ACh and LVK-evoked conducted responses following removal of the endothelium in rat isolated mesenteric arteries supports such a theory (Takano *et al.*, 2004). The extensive staining for connexin 40 observed at endothelial cell borders within this study and others (Goto *et al.*, 2004; Kansui *et al.*, 2004; Mather *et al.*, 2005;

Sandow *et al.*, 2006) therefore supports a possible role for connexin 40 in conducted dilatation responses in this preparation.

In the present study connexin 40 staining was also imaged following secondary detection with antibodies conjugated to Alexa Fluor® 633. Detection of connexin 40 at this wavelength allowed for visualization of the IEL as elastin autofluoresces in the 488 - 515nm range (Briones *et al.*, 2003; Gonzalez *et al.*, 2005).

The results presented herein together with those of previous studies (Haddock *et al.*, 2006; Sandow *et al.*, 2003a; Sandow *et al.*, 2006; Sandow *et al.*, 2002) support an important structural role for the IEL in endothelial and smooth muscle cell-to-cell communication. In addition to the endothelial cell border staining of connexin 40 just described, staining of this gap junction protein with co-visualization of the IEL revealed the co-localization of connexin 40 with holes in the IEL. These results are consistent with previous observations that connexin 40 contributes to MEGJ structure within this preparation and that holes within the IEL of various preparations may be the sites where endothelial cells can project to the smooth muscle to form MEGJ plaques (Mather *et al.*, 2005; Sandow *et al.*, 2003a; Sandow *et al.*, 2004; Sandow *et al.*, 2006; Sandow *et al.*, 2002).

3.4.8. Immunohistochemical staining of SK_{Ca} and IK_{Ca}

In the present study both IK_{Ca} and SK_{Ca} channels that are fundamental to the initiation of EDHF in contracted rat isolated small mesenteric arteries (please see chapter 4 for review), have also been found to co-localize with holes in the IEL. Staining of endothelial cell borders was not observed for IK_{Ca}, however, consistent with previous reports, SKCa was found at these sites (Sandow *et al.*, 2006). The restriction of punctate IK_{Ca} staining to holes in the IEL is consistent with a recently published report (Sandow *et al.*, 2006) within which the different spatial localization of the two K_{Ca} channels and connexins 37 and 40 was related to the functional distinction between the two K^+ channels as reported by Crane and colleagues (2003b).

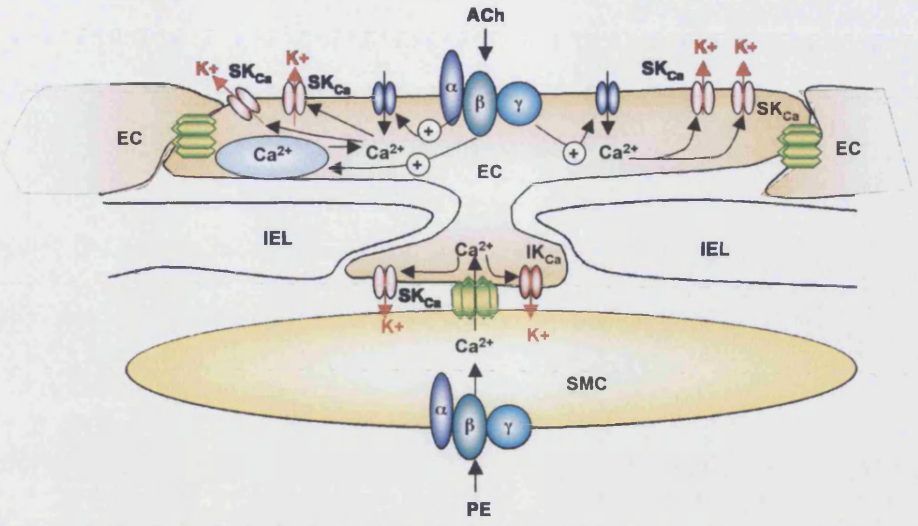

Figure 3.10 Activation of IK_{Ca} and SK_{Ca} in the absence and presence of PE-evoked smooth muscle stimulation

Cartoon illustrating a summary of the current hypothesis for the differential activation of IK_{Ca} and SK_{Ca} following ACh stimulation of rat isolated small mesenteric arteries in the presence and absence of PE. PE stimulation would stimulate a rise in Ca^{2+} that may be transferred to the EC via gap junctions (green). In the absence of PE stimulation ACh would evoke a rise in EC Ca^{2+} only in areas away from IK_{Ca} localization. EC, endothelial cell; SMC, smooth muscle cell. + represents stimulation.

Crane and co-workers (2003) demonstrated that under basal conditions in the presence of L-NAME, application of ACh evoked a hyperpolarization response in isolated rat mesenteric arteries that was fully blocked by the SK_{Ca} channel inhibitor apamin. Although the response could be replicated with CPA it could not be achieved with the IK_{Ca} channel opener 1-EBIO. Stimulation with ACh subsequent to pre-contraction and depolarization with PE evoked a similar increase in membrane potential with a concomitant dilatation response. However, in contrast to the response evoked under basal conditions the repolarization evoked by ACh could only be blocked with a combination of the IK_{Ca} channel blocker TRAM-34 and apamin. The authors proposed that IK_{Ca} and SK_{Ca} contribute to distinct components of the EDHF response dependent on the Ca^{2+} concentration within the signalling domains associated with each K_{Ca} channel and the characteristics of the hyperpolarization response evoked by each K_{Ca} channel. Our observation of SK_{Ca} co-localization with the IEL in addition to that of connexin 40 and IK_{Ca} as previously described (Mather *et al.*, 2005; Sandow *et al.*, 2006) supports such a hypothesis.

Under resting conditions endothelial cell Ca^{2+} in response to ACh will arise solely from endothelial cell Ca^{2+} stores and endothelial cell influx of Ca^{2+} and therefore may be restricted to sites of Ca^{2+} influx or Ca^{2+} store release (McSherry *et al.*, 2005; Oishi *et al.*, 2001). Therefore, the high frequency of SK_{Ca} localization around the edge of the endothelial cells would increase the likelihood of their activation (Figure 3.10). In contrast the predominant localization of IK_{Ca} to the myoendothelial compartments would restrict their activation to times at which the Ca^{2+} concentration at the projection is sufficiently raised. This may occur following stimulation with PE whereupon it has been demonstrated in rat mesenteric artery preparations that an increase in smooth muscle cell Ca^{2+} may be transferred to the endothelium (Figure 3.10; Crane *et al.*, 2003b; Oishi *et al.*, 2001), possibly via direct transfer of Ca^{2+}, or via transfer of IP_3 via gap junctions (Crane *et al.*, 2003a; Dora *et al.*, 1997; Martin *et al.*, 2005; Schuster *et al.*, 2001). The additional localization of SK_{Ca} to this site possibly reflects the dual IK_{Ca} and SK_{Ca} components of the EDHF response that may be activated under high tone. Indeed following PE-evoked contraction it has been demonstrated that EDHF may be released from the endothelium in the absence of direct endothelial cell stimulation by acetylcholine and independently of any direct effects of PE on the endothelium (Dora *et al.*, 2000b).

Importantly it should be noted that both within this report and others (Mather *et al.*, 2005; Sandow *et al.*, 2003b; Sandow *et al.*, 2006) the incidence of holes in the IEL does not correlate with the incidence of MEGJ, or in our case connexin 40 localization. This has been proposed to either reflect a dynamic localization of MEGJ (Sandow & Hill, 2000; Sandow *et al.*, 2003b) or the provision of a pathway with a short diffusion distance that is suitable for the conduction of various EDHF candidates including K^+ (Dora & Garland, 2001; Edwards *et al.*, 1998; Edwards & Weston, 2004; Sandow *et al.*, 2006).

To summarize, the present preliminary report demonstrates the value of immunofluorescence and staining of isolated arteries to visualize arterial structure. As would be expected the structure of the arterial wall, by the nature of its function as a selective barrier to various molecules within the blood limits the passage of some fluorescent stains and antibodies using the techniques described. However, this facet of

arterial structure may be used to ones advantage to independently stain different components of the artery wall. The use of dyes such as di-8-ANEPPS, propidium iodide and lucifer yellow may be combined in future studies using immunofluorescence to assist in the localization of cell proteins as described here for propidium iodide. The localization of IK_{Ca}, SK_{Ca} and connexin 40 seen within this study is consistent with previous studies *in vivo* and supports the hypothesis that myoendothelial projections may be the site of a signalling compartment or microdomain that functions to produce signals to initiate smooth muscle relaxation in periods of high smooth muscle tone (Sandow *et al.*, 2006). Such a signalling domain would be key to artery function and thus any disturbances in its structure may be associated with an increased incidence of vascular disease or hypertension. Indeed a decrease in connexins 37 and 40, both of which may be expressed at the MEGJ, has been observed in hypertensive rats (Goto *et al.*, 2004; Kansui *et al.*, 2004; Sandow *et al.*, 2006). Conversely, such changes in vascular tone as in cases of hypertension, may also increase the incidence of MEGJ to compensate for the decreased efficacy of other vasodilator mechanisms as observed in the caudal artery of the rat (Sandow *et al.*, 2003a). It is therefore proposed that further immunohistochemical studies investigating the relative localization of both smooth muscle and endothelial cell intracellular Ca^{2+} stores to the IEL, SK_{Ca} and IK_{Ca} channels be investigated to elucidate the nature of the differential activation of these channels under different levels of smooth muscle stimulation. Furthermore, given the excellent staining of the IEL that may be achieved using lucifer yellow, Ca^{2+} imaging experiments employing the use of the Rhod Ca^{2+} indicators (Molecular Probes Invitrogen, Paisley, UK) visible in the 580 to 602nm range may allow elucidation of the Ca^{2+} signalling mechanisms associated with the differential activation of IK_{Ca} and SK_{Ca} and their association with the IEL.

3.5. Acknowledgements

I would like to thank Dr. Amanda Mackenzie and Dr. Shaun Sandow for their advice during the development of the immunohistochemical protocol and on the choice of antibodies used within this study.

4. The role of connexins 37, 40 and 43 in radial cell-to-cell communication

4.1. Introduction

Hyperpolarization of endothelial cells following electrical, chemical or physical stimulation may be transferred radially (Figure 1.17) to the subjacent smooth muscle leading to vasodilatation. The transfer of hyperpolarization is facilitated by an EDHF (section 1.3.2.5), which may comprise the release of a diffusible messenger(s) from the endothelium and/or the direct passage of hyperpolarization from the endothelium to the smooth muscle through MEGJs (please see section 1.3.2.5 and references therein).

EDHF-mediated dilatation of the rat mesenteric artery has been found to comprise multiple components depending on the level of PE-evoked tone (Dora & Garland, 2001; Richards *et al.*, 2001). Of the potential candidates for EDHF (section 1.3.2.5) K^+ and MEGJ transfer of hyperpolarization have been suggested to facilitate vasodilatation to ACh but only under conditions of low to moderate PE-evoked tone (Dora & Garland, 2001; Dora *et al.*, 2002; Edwards *et al.*, 1998; Edwards *et al.*, 1999; Mather *et al.*, 2005; Richards *et al.*, 2001). Under conditions of high PE-evoked tone the K^+ component of EDHF is inhibited as maximal activation of the smooth muscle Na^+/K^+ ATPase by K^+ released from smooth muscle BK_{Ca} prevents further activation by K^+ released from the endothelium. As a result an unidentified EDHF component, possibly MEGJ-facilitated transfer of hyperpolarization, is thought to predominate (please see section 1.2.4.2; Dora & Garland, 2001; Dora *et al.*, 2000b; Dora *et al.*, 2002; Doughty *et al.*, 2000; Mather *et al.*, 2005; Richards *et al.*, 2001; Weston *et al.*, 2002).

Evidence for a gap junction-mediated pathway for transfer of hyperpolarization within rat mesenteric arteries has been demonstrated both morphologically using electron microscopy to show the existence of homocellular and heterocellular gap junctions (Gustafsson *et al.*, 2003; Hill *et al.*, 2002; Mather *et al.*, 2005; Sandow & Hill, 2000; Sandow *et al.*, 2006; Sandow *et al.*, 2002) and with dye coupling techniques (Takano *et al.*, 2004). The study of Takano *et al.* (2004) demonstrated a clear passage of propidium iodide both radially and longitudinally (Figure 1.17) supporting a gap junction-mediated pathway for EDHF-type responses and electrotonic conduction of vasodilatation (please see chapter 5; Emerson & Segal, 2001; Emerson & Segal, 2000b; Little *et al.*, 1995). However, the incidence of dye and current transfer (particularly with lucifer yellow) has not always been shown to correlate precluding definitive conclusions as to the nature of

the cell to cell coupling (Little *et al.*, 1995; Tare *et al.*, 2002). Crucially, with regards to the clarification of a role for gap junctions in the radial EDHF-mediated response, it has also not been possible to selectively block MEGJ with pharmacological agents.

Attenuation of EDHF-mediated smooth muscle cell hyperpolarization and relaxation within isolated rat mesenteric arteries by the putative gap junction uncouplers, the glycyrrhetinic acid derivatives and the gap peptides, has been documented (Edwards *et al.*, 1999; Goto *et al.*, 2002; Hill *et al.*, 2000; Sandow *et al.*, 2002). Glycyrrhetinic acid derivatives such as carbenoxolone have been shown to increase input resistance and reduce Ca^{2+} synchronization between rat mesenteric artery smooth muscle cells, supporting a gap junction uncoupler mode of action (Matchkov *et al.*, 2006; Tare *et al.*, 2002). However this class of compounds, particularly those of the β subtype, have also been shown to directly reduce rat mesenteric artery and guinea-pig coronary artery endothelial cell hyperpolarization whilst also having additional effects on smooth muscle cell Ca^{2+} and tension. As such their inhibition of EDHF-type responses cannot be solely construed as an inhibition of gap junction communication and their reliability must be questioned (Chaytor *et al.*, 2000; Matchkov *et al.*, 2006; Tare *et al.*, 2002).

The small synthetic gap peptides are reported to be specific to the first (Gap 26) and second (Gap 27) extracellular loop of individual connexin structures, and as such are more selective to inhibition of gap junctional communication (Evans & Boitano, 2001; Griffith, 2004; Martin *et al.*, 2005; Matchkov *et al.*, 2006; Warner *et al.*, 1995). However, the possible heterogeneity of most gap junction channels means they still cannot be used to definitively target either myoendothelial or homocellular gap junction subtypes. This leads to speculation, particularly in larger calibre arteries, as to whether the gap peptides have blocked the direct transfer of hyperpolarization from the endothelium to the smooth muscle via MEGJ (i.e. EDHF) or whether they have blocked the relay of hyperpolarization throughout the smooth muscle or endothelial cell layers (Chaytor *et al.*, 2005; Chaytor *et al.*, 1997; Edwards *et al.*, 2000; Yamazaki & Kitamura, 2003). Furthermore, although without non-junctional effects (Matchkov *et al.*, 2006), the exact molecular mechanism of action of the gap peptides is unclear. It does appear to be independent of the formation of *de novo* gap junctions and plaques, indeed mechanisms associated with the modulation of channel gating have been

proposed (Berman *et al.*, 2002; Griffith, 2004; Martin *et al.*, 2005). However, definitive molecular and crystallographic data regarding channel modulation by the gap peptides is lacking.

The purpose of this study was to therefore assess whether targeting *endothelial cell* connexins with antibodies selective for the known vascular connexins (37, 40, 43; (Gustafsson *et al.*, 2003; Kansui *et al.*, 2004; Matchkov *et al.*, 2006) could block EDHF-mediated dilatations under conditions of high PE-evoked tone, thus minimising non-specific effects on smooth muscle gap junctions and the involvement of K^+. Given the importance of gap junction communication to spreading dilatation in other vascular beds (de Wit *et al.*, 2006a; de Wit *et al.*, 2000; de Wit *et al.*, 2006b; Figueroa *et al.*, 2003), the results from this study would also act as a preliminary assessment of gap junction inhibitors for the study of gap junctions in spreading dilatation responses in rat intact mesenteric artery preparations (please see chapter 5).

Initial studies were performed to evaluate the effects of increased PE-evoked tone on EDHF-type responses and to confirm that the response in question was an EDHF-type response. Subsequently, the efficacy of the established gap junction uncouplers carbenoxolone and the gap peptides as inhibitors of EDHF-type responses in rat isolated and pressurized mesenteric arteries were investigated. Finally the pinocytic loading technique (please see section 2.4; Figure 2.4) was validated and employed to luminally-load anti-connexin antibodies into the endothelium in an effort to inhibit EDHF-mediated dilatation responses by selective blockade of *endothelial cell* connexins.

Parts of this work have been reported elsewhere (Mather *et al.*, 2005; Winter *et al.*, 2004).

4.2. Methods

4.2.1. Rat mesenteric artery isolation and cannulation

Please see section 2.1 for methods of artery isolation.

4.2.2. Pressure myography

Arteries were mounted in both custom-built organ baths (0.5 – 1ml; Figure 2.2) and a commercially available pressure myograph (10ml; 120CP, Danish Myo Technology, Denmark; Figure 2.1). For cannulation and equilibration methods please see section 2.2. Endothelial cell viability was assessed as a >90% control dilatation to ACh (1μM) following pre-constriction with PE (1 - 3μM). Arteries were maintained at 50mmHg and 37°C unless otherwise stated.

4.2.3. Cumulative concentration-response curves

Experiments were performed in the presence of L-NAME (100μM, 20min) where indicated. Inhibition of cyclooxygenase was not required as indomethacin (10μM) has been shown to have no effect on ACh-evoked hyperpolarization and dilatation responses within the rat mesenteric artery (please see section 1.3.2.4). Cumulative concentration-response curves to ACh (1nM-3μM) were performed following submaximal (~70%; low tone) and maximal (~90%; high tone) constriction to PE as indicated. Additional concentration-response curves to ACh were performed in the presence of high K^+ (35mM with supplementary PE to obtain maximal constriction if required).

4.2.4. Pinocytic loading of cell impermeant molecules

The efficacy of the pinocytic loading method described in section 2.4 was tested by inclusion of carboxyfluorescein (~1mg ml^{-1}) or FITC-conjugated 3000Da dextran (~6mg ml^{-1}) in the hypertonic sucrose solution prior to filtration (0.22μm syringe filter unit) and addition of PEG. For endothelial cell loading anti-connexin antibodies and Alexa Fluor® 633-conjugated IgG were diluted (1:10) with complete hypertonic solution to give final luminal concentrations of 0.1mg ml^{-1} and 0.2mg ml^{-1} respectively. Endothelial cell viability was subsequently assessed by inclusion of propidium iodide in the bath solution (0.01% wv^{-1}).

4.2.5. Fluorescent confocal microscopy

Propidium iodide, carboxyfluorescein and Alexa Fluor® 633-conjugated IgG were visualized as described (please see section 3.2.7). FITC-conjugated 3000Da dextran loading was visualized using the confocal settings established for carboxyfluorescein.

4.2.6. Electron microscopy

Arteries were fixed using a solution comprising (mM) betaine 10.0, sucrose 150.0, $CaCl_2$ 0.2 glutaraldehyde (3%wv^{-1}), paraformaldehyde (1%wv^{-1}), in sodium cacodylate 100.0 buffer, adjusted to pH 7.35-7.40. Vessels were subsequently stained and embedded for electron microscopy using conventional methods (Sandow *et al.*, 2002). From a section cut perpendicular to the longitudinal axis of each preparation, each of four 15μm long regions of endothelium 90° apart were photographed at x20 000 and vesicle (50-200nm diameter) counts (excluding surface caveolae) made from prints. Dr. Shaun Sandow performed all methods, image construction and analysis.

4.2.7. Drugs and solutions

All drugs and solutions were prepared as detailed previously (please see section 2.6).

4.2.8. Antibodies

Antibodies targeted against connexins 37, 40 and 43 were raised in rabbits against a 19 amino acid peptide sequence within the C-terminal cytoplasmic domain of rat connexin 37 (Alpha Diagnostics, TX USA), mouse connexin 40 or mouse connexin 43 (Chemicon, CA, USA). The antigen peptide sequences for mouse connexins 40 and 43 are conserved in rats. These antibodies were chosen as they have been well characterised in both transfected Rin and HeLa cells and arterial tissue (Gustafsson *et al.*, 2003; Sandow *et al.*, 2003b) whilst the C-terminal cytoplasmic domain has also been associated with the regulation of connexin channel gating and may influence gap junction assembly and trafficking (Bastide *et al.*, 1996; Burt & Steele, 2003; Contreras *et al.*, 2003; Lampe & Lau, 2000; Stergiopoulos *et al.*, 1999).

4.2.9. Data analysis

Data were collected and analysed as described previously (please see sections 2.5.1 and 2.7).

4.3. Results

4.3.1. Dilatation responses to ACh at low and high levels of PE-evoked tone

Concentration-dependent dilatation responses to ACh (1nM - 3μM) were evaluated following submaximal (0.3-3μM; Figure 4.1A) and maximal (3-10μM; Figure 4.1B) levels of PE-evoked constriction. A significant rightward shift of the concentration-response curve and a small, but significant decrease in the maximum dilatation response to ACh (Figure 4.1C) were observed with increased PE-evoked tone. Extracellular K^+ (4.7 – 19.8mM; $n = 4$) was unable to evoke a dilatation response when tested on arteries with high levels of PE-evoked tone or low levels of PE-evoked tone in the presence of ouabain.

4.3.2. Effect of inhibition of K^+ channels on dilatation responses to ACh

Following maximal pre-constriction with PE (1 - 5μM) concentration-dependent dilatation responses to ACh ($n = 4$) were largely unaffected by incubation with the selective inhibitor of eNOS, L-NAME (100μM, 20min; $n = 6$; Table 4.1; Figure 4.2A). In contrast, combined selective blockade of IK_{Ca} and SK_{Ca} channels with TRAM-34 (1μM, 20min) and apamin (50nM, 1h) resulted in a significant rightward shift in the concentration-dependent dilatation response to ACh (n = 4; Table 4.1; Figure 4.2B). Subsequent incubation with L-NAME (100μM, 20min) in the presence of TRAM-34 and apamin resulted in a further, significant attenuation of the dilatation responses to ACh with all but responses to the highest concentrations of ACh (3μM) abolished ($n = 4$; Figures 4.2A and B). Constriction with high K^+ (35 – 40mM) in the presence of L-NAME completely abolished all dilatation responses to ACh (Figure 4.2B; $n = 6$).

4.3.3. Effect of gap junction uncouplers on dilatation responses to ACh

The non-selective water-soluble β-glycyrrhetinic acid derivative carbenoxolone (100μM; 30min) had no significant effect on EDHF-type dilatation responses to ACh in arteries maximally contracted with PE (5 – 10μM; Figure 4.3B; Table 4.2; $n = 4 - 8$). However, a marked reduction in the maximum dilatation that could be evoked by 3μM ACh was observed in five of the eight arteries tested (Figure 4.3A). In paired experiments with submaximally contracted arteries ($n = 4$; 1 - 5μM PE) carbenoxolone had no effect on dilatation responses to ACh (Table 4.2).

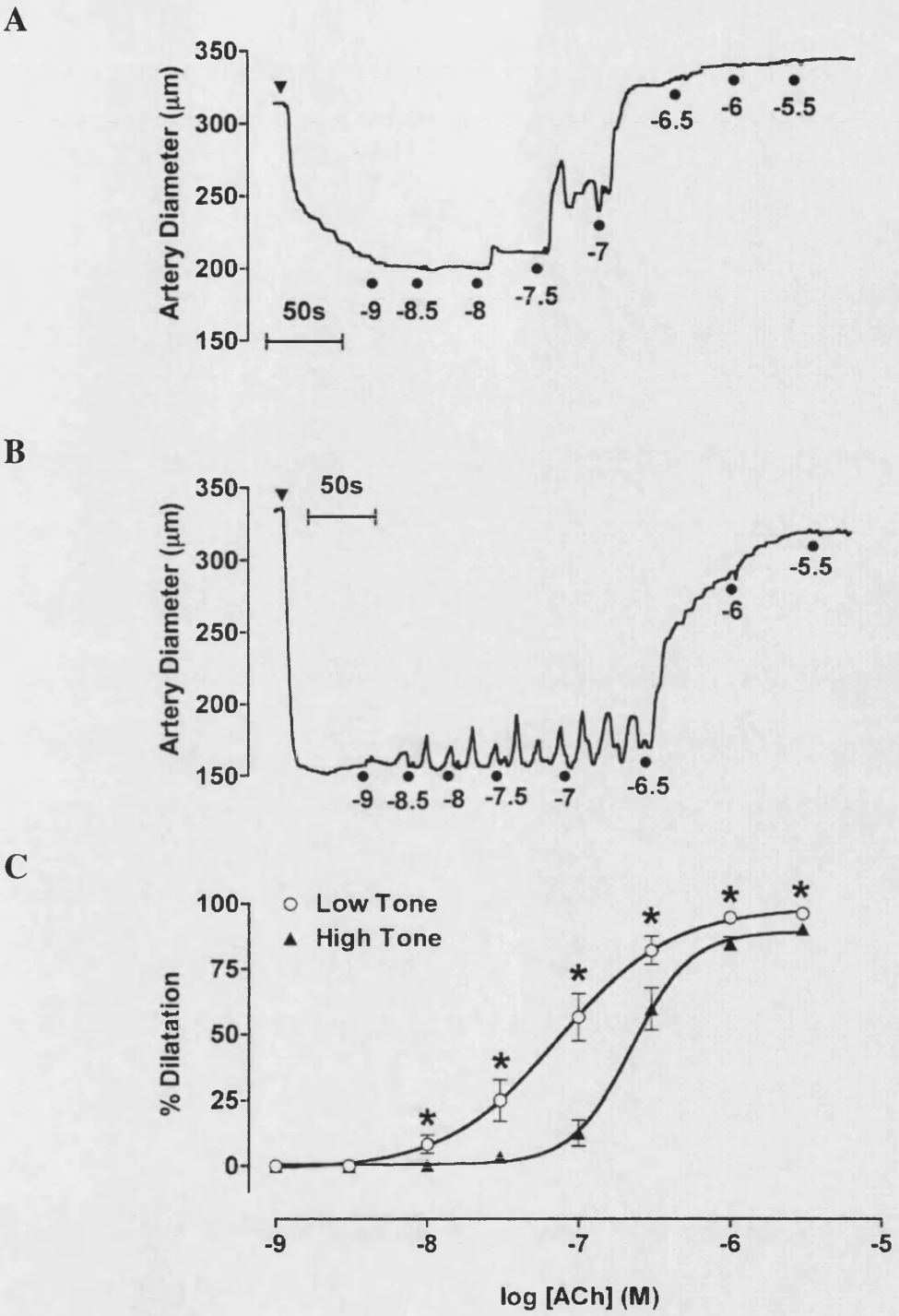

Figure 4.1 Dilatation to ACh at high and low levels of PE-evoked tone
A, B, Paired representative traces and **C**, meaned data (n=12) illustrating concentration-dependent responses of isolated rat small mesenteric arteries to ACh following **A, C**, submaximal (0.3-3μM; low tone) and **B, C**, maximal (6-10μM; high tone) PE-evoked constriction. **A, B**, The triangles indicate addition of PE. * Significantly different to low tone following a student's paired t-test. L-NAME (100μM) present in all experiments.

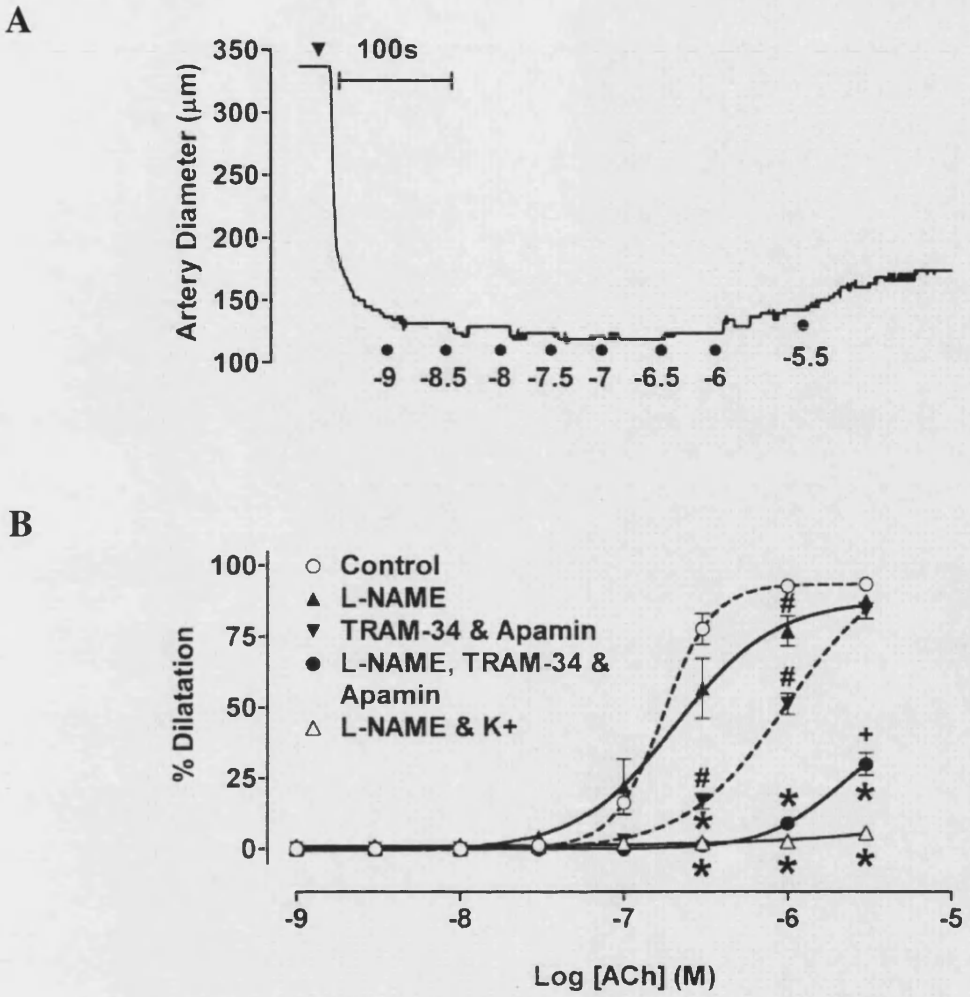

Figure 4.2 Effects of inhibition of K^+ channels on dilatation responses to ACh

A, Representative trace and **B**, meaned data (n=4-6 unpaired responses) illustrating concentration-dependent responses to ACh following K^+ channel blockade with **A**, **B,** a combination treatment of or **B,** individual treatment with TRAM-34 (1μM, 20min) and apamin (50nM, 1h) or **B,** by raising extracellular K^+ (35-45mM). Broken lines indicate experiments performed in the absence of L –NAME (100μM), which was present in all other experiments. Filled triangle indicates addition of PE (1μM). #, Significantly different to control, *significantly different to L-NAME, + significantly different to TRAM-34 and apamin following a one-way ANOVA with a Bonferroni post-test (P<0.05).

A

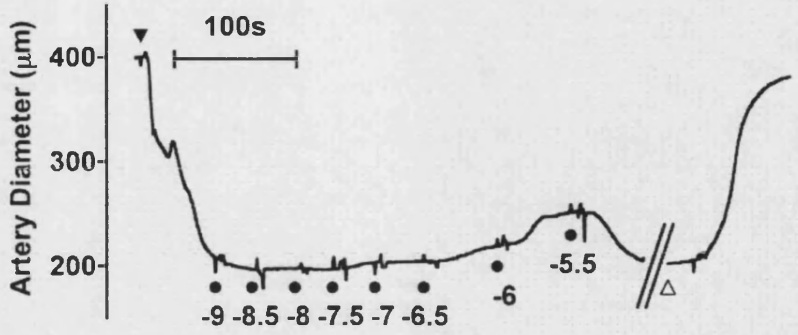

B

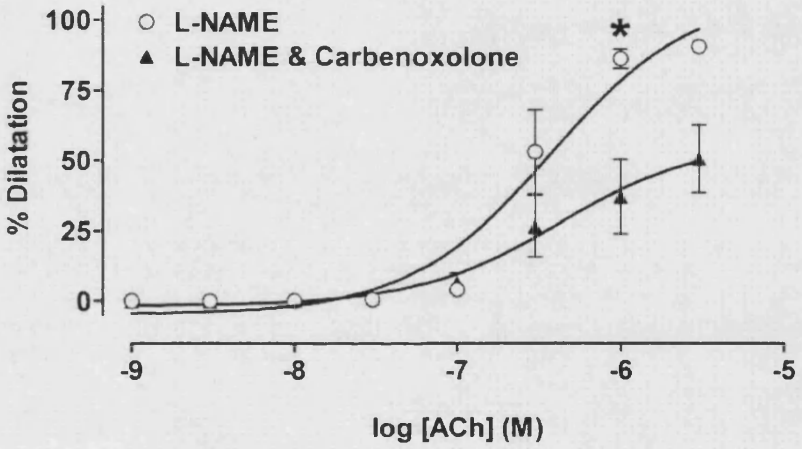

Figure 4.3 Effects of carbenoxolone treatment on dilatation responses to ACh

A, Representative trace (of *n*=5 of 8 arteries) and **B**, meaned data (*n*=3-8) illustrating concentration-dependent responses to ACh following treatment with carbenoxolone (100μM, 30min). All experiments in the presence of L-NAME (100μM). Filled triangle indicates addition of PE (10μM). Open triangle indicates addition of LVK (3μM). * Significantly different to L-NAME following an unpaired t-test ($P<0.05$).

4.3.4. Effect of incubation time on ACh-evoked dilatation responses

To serve as a time control ACh-stimulated dilatation responses during maximal contraction evoked by PE (5 - 15μM) were investigated over a 120min period in control conditions (L-NAME, 100μM). Dilatation responses to ACh were found to be unaffected by incubation time (n = 6; Figure 4.4A; Table 4.3).

4.3.5. Effect of the gap peptides on dilatation responses to ACh

In the presence of L-NAME (100μM) the effect of the inhibitory connexin mimetic peptide ^{Cx37,Cx43}Gap 27 on ACh-mediated dilatation responses following maximal PE-evoked constriction (3-10μM) was determined. Incubation with ^{Cx37,Cx43}Gap 27 (300μM, 120min) had no significant effect on concentration-dependent dilatation to ACh (Figure 4.4A; Table 4.3; n = 2 - 5) despite one artery showing marked attenuation of ACh-evoked responses (Figure 4.4B). The effects of a triple combination of gap peptides ^{Cx43}Gap 26, ^{Cx37,Cx43}Gap 27 and ^{Cx40}Gap27 (300μM each giving a total peptide concentration of 900μM, 120min) targeting all known endothelial cell connexins were subsequently evaluated. Remarkably, incubation with the triple combination of connexin-mimetic peptides had no effect on ACh-evoked dilatation responses (Figure 4.4C; Table 4.3; n = 3).

4.3.6. Efficacy of the pinocytic loading protocol

The lack of effect with the connexin-specific gap peptides forced us to develop a new technique to inhibit, selectively, *endothelial cell* gap junctions. Therefore we employed the ability of antibodies to selectively target and inhibit connexins together with selective loading into endothelial cells using the pinocytic loading protocol (please see section 2.4; Figure 2.4).

The efficacy of the pinocytic loading protocol as a method of selectively loading molecules into the endothelium of intact arteries was established by including carboxyfluorescein (1mg ml^{-1}) in the luminally-applied hypertonic solution. The extent and location of fluorescence emitted from the artery was subsequently observed. Endothelial cell loading predominated with only a few smooth muscle cells seen to contain carboxyfluorescein (Figure 4.5A; n = 3). As the small size of carboxyfluorescein (376Da) enables the molecule to pass through gap junctions the

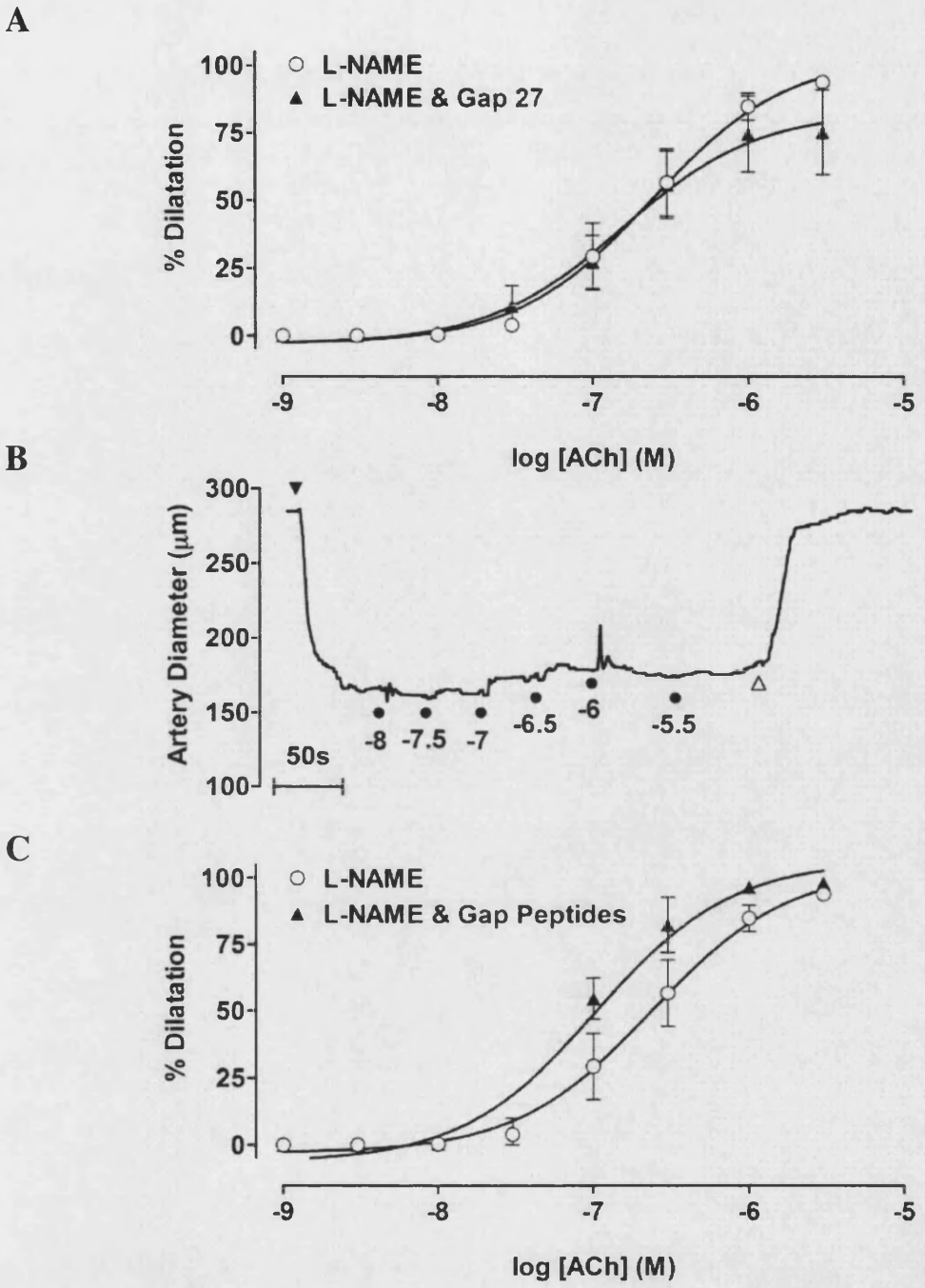

Figure 4.4 Effect of the gap peptides on ACh-evoked dilatation responses

A, C, Mean concentration-dependent dilatation responses to ACh following treatment with **A,** ^{Cx37Cx43} Gap27 (300μM, 120min; *n*=5) and **C**, a triple combination of gap peptides ^{Cx43}Gap26, ^{Cx40}Gap27, and ^{Cx37Cx43}Gap27 (300μM each, total peptide concentration 900μM, 120min; *n*=3-6) *vs* unpaired time-matched controls (*n*=6). **B,** Trace showing the inhibition of ACh-evoked dilatation by ^{Cx37Cx43}Gap27 (300μM, 120min) in *n*=1 artery. The filled triangle shows addition of PE (10μM). The open triangle shows addition of LVK (1μM). L-NAME (100μM) present in all experiments. Please note gap peptides were added to the bath and the lumen of arteries for the entire incubation period.

Treatment	pD_2 ± s.e.mean	R_{max} ± s.e.mean	*n*
L-NAME, 0min	6.5±0.1	97.2±1.3%	6
L-NAME, 120min	6.6±0.1	93.9±1.6%	6
L-NAME, ^{Cx37,Cx43}Gap 27, 120min	6.9±0.2	75.3±15.7	5
L-NAME, ^{Cx43}Gap 26, ^{Cx37,Cx43}Gap 27 & ^{Cx40}Gap27, 120min	6.6±0.2	93.9±1.6	3

Table 4.3. Effect of the gap peptides on ACh-evoked dilatation responses
The effect of incubation with ^{Cx37Cx43}Gap27 (300μM, 120min) and a triple combination of gap peptides ^{Cx43}Gap26, ^{Cx40}Gap27, and ^{Cx37Cx43}Gap27 (300μM each, total peptide concentration 900μM, 120min) on concentration-dependent responses to ACh following maximal PE-evoked constriction (high tone; 3-10μM). R_{max} corresponds to dilatation to 3μM ACh. No statistically significant differences were found using one-way ANOVA. L-NAME (100μM) present in all experiments.

Treatment	pD_2 ± s.e.mean	R_{max} ± s.e.mean	*n*
L-NAME	6.8±0.0	92.0±1.0%	39
L-NAME & Post-Load	6.8±0.1	96.0±1.2%	9
L-NAME & Anti-Connexin37 Antibody	6.7±0.1	93.6±1.4%	9
L-NAME & Anti-Connexin40 Antibody	n/a	36.6±9.5% *P<0.001	14
L-NAME & Anti-Connexin43 Antibody	6.7±0.1	96.5±1.0%	7

Table 4.4. Effect of the luminal pinocytic loading of connexin antibodies on dilatation responses to ACh
The effects of luminal pinocytic loading of vehicle (post-load) anti-connexin 37, anti-connexin 40, and anti-connexin 43 antibodies (all 0.1mg ml^{-1}) on ACh-evoked dilatation responses following maximal PE-evoked constriction (high tone; 3-10μM). R_{max} corresponds to dilatation to 3μM ACh. L-NAME (100μM) present in all experiments. Anti-connexin 40 antibody data are also shown in Table 4.5. Some data shown matches data obtained from arteries used in the evaluation of the effects of luminal pinocytic loading of connexin antibodies on spreading dilatation responses to ACh and LVK (section 5.3). n/a; not applicable, an EC_{50} could not be accurately calculated for this data set so the pD_2 value is excluded. Parts of these data were obtained by Dr. Simon Mather. * Significantly different to L-NAME following a one-way ANOVA with a Bonferroni post-test (P<0.05).

staining observed herein may not accurately reflect the efficacy of the pinocytic loading method. Consequently, the larger molecular weight, gap junction impermeant, compounds FITC-coupled dextran (3000Da) (~6.0mgml^{-1}) and Alexa Fluor® 633-conjugated IgG were loaded into the endothelium using the same protocol. Both FITC-coupled dextran and Alexa Fluor® 633-conjugated IgG were seen to selectively and extensively load into the endothelium (Figures 4.5B and C) when applied luminally using the pinocytic loading protocol.

As expected in experiments carried out to determine the ultrastructural integrity of the arterial wall before, during and after luminal application of the pinocytic loading protocol (section 2.4) an ~4-fold increase in the number of intracellular endothelial cell vesicles (excluding surface caveolae) was observed in the hypertonic stage of the treatment process (Figures 4.6A and B; n = 3). After the protocol was fully completed the number of endothelial cell vesicles returned to levels seen before the treatment process was carried out (Figures 4.6A and 4.6C; n = 3).

4.3.7. Arterial viability and ultrastructural integrity following luminal pinocytic loading

Radial cross-sections were taken through isolated and pressurized (50mmHg) arteries fixed before (Figures 4.6A, 4.7A and 4.7D), during (Figures 4.6B, 4.7B and 4.7E) and after (Figures 4.6C, 4.7C and 4.7F) luminal pinocytic loading (vehicle only) (n = 3). Cellular integrity was maintained throughout the protocol (Figures 4.6 and 4.7A-C) although disruption of gap junctions was apparent during the hypertonic treatment stage (Figure 4.7E) when compared to images of untreated arteries (Figure 4.7D). Gap junction integrity appeared restored upon completion of the full pinocytic loading protocol Figure 4.7F). Smooth muscle cell morphology was unaffected at any stage of the treatment (Figures 4.7A-C). Functional viability was assessed by evaluating concentration-dependent dilatation responses to ACh following maximal PE-evoked constriction (3-10μM) before and after luminal pinocytic loading (vehicle only). Consistent with the intact structural integrity of arteries following the treatment,

A. Endothelial cell loading with carboxyfluorescein

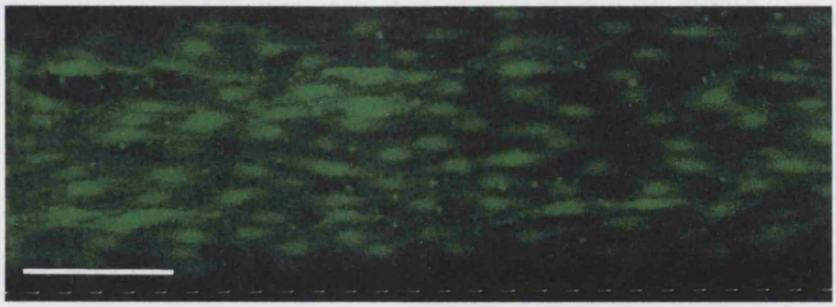

B. Endothelial cell loading with FITC-coupled 3kDa dextran

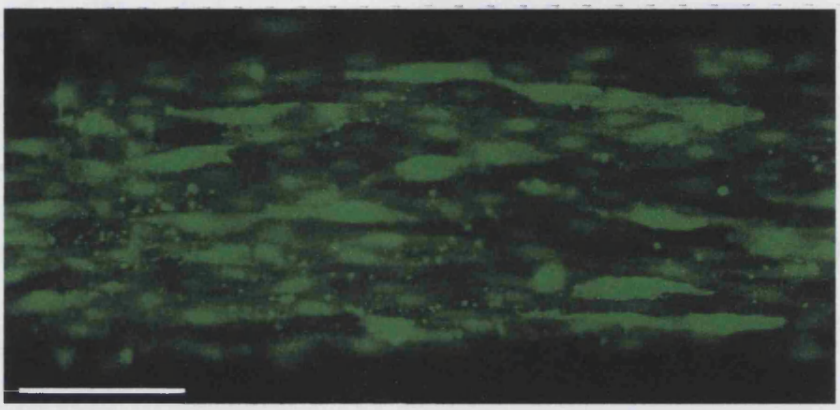

C. Endothelial cell loading with Alexa Fluor® 633-coupled IgG

Figure 4.5 Luminal pinocytic loading of fluorescent molecules into intact vascular cells

Confocal, fluorescent images of rat isolated, pressurized mesenteric arteries showing endothelial cell loading of **A**, carboxyfluorescein (~1mg ml^{-1}), **B**, FITC-coupled 3kDa dextran (~6mg ml^{-1}) and **C**, Alexa Fluor® 633 IgG (0.2mg ml^{-1} luminal solution) following luminal application of the pinocytic loading protocol. Images were taken at 50mmHg using a 20x water-immersion objective. Bar: 100 μm. Please note similar results to **A** (different *n*) are shown in section 3.3 (figure 3.4). Dr. Simon Mather performed the fluorescent antibody loading experiments.

Treatment	pD_2 ± s.e.mean	pD_2 P (n)	R_{max} ± s.e.mean	R_{max} P (n)
Control	6.8±0.0	n.a.	93.6±0.4%	n.a.
L-NAME	6.7±0.1	P>0.05* (6)	87.8±2.2%	P>0.05* (6)
TRAM-34 & Apamin	5.9±0.1	P<0.01* (4)	84.2±2.8%	P>0.05* (4)
L-NAME, TRAM-34 & Apamin	5.8±0.1	P<0.001** (6)	30.1±4.0%	P<0.001** (6) P<0.001***
L-NAME & K^+	n.a.	n.a.	5.6±1.8%	P<0.001** (6)

Table 4.1. Effects of inhibition of K^+ channels on dilatation responses to ACh
The effect of K^+ channel blockade with either a combination of TRAM-34 (1μM, 20min) and apamin (50nM, 1h) or by raising extracellular K^+ (35-45mM) on concentration-dependent responses to ACh. R_{max} corresponds to dilatation to 3μM ACh. *Significantly different to control **significantly different to L-NAME, and *** significantly different to TRAM-34 and apamin following a one-way ANOVA with a Bonferroni post-test (P<0.05). L-NAME (100μM) present where indicated.

Treatment	pD_2 ± s.e.mean	R_{max} ± s.e.mean	n
L-NAME & Low Tone	6.6±0.2	94.7±2.9%	4
L-NAME & High Tone	6.4±0.1	92.5±2.6%	3
L-NAME, Low Tone & Carbenoxolone	6.3±0.3	90.0±1.0%	4
L-NAME & High Tone Carbenoxolone	5.5±0.5	52.0±12.6%	8

Table 4.2. Effects of carbenoxolone treatment on dilatation responses to ACh
The effect of treatment with carbenoxolone (100μM, 30min) on concentration-dependent responses to ACh at high (5-15μM) and low (1-5μM) levels of PE-evoked tone in unpaired arteries. R_{max} corresponds to dilatation to 3μM ACh. No statistically significant differences were found using one-way ANOVA. L-NAME (100μM) present in all experiments.

A. Pre-load

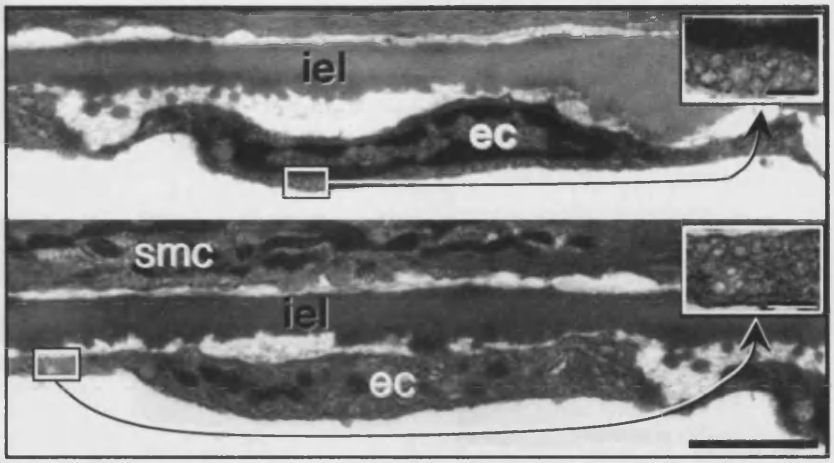

B. Hypertonic stage

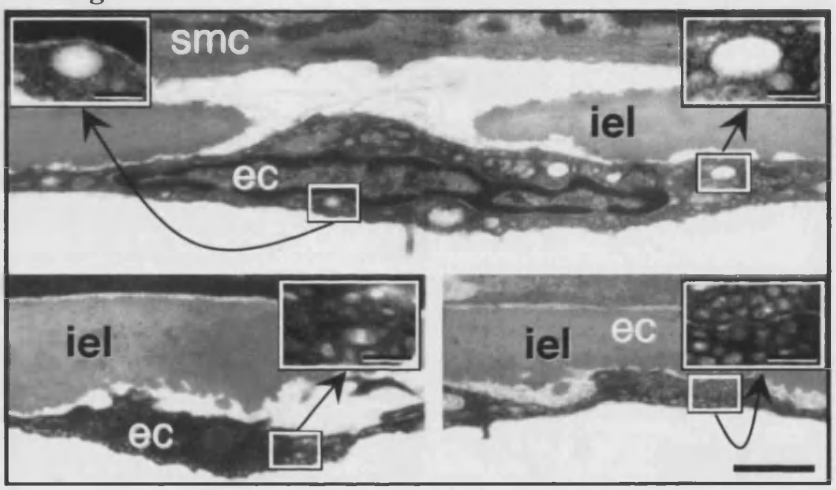

C. Post-load

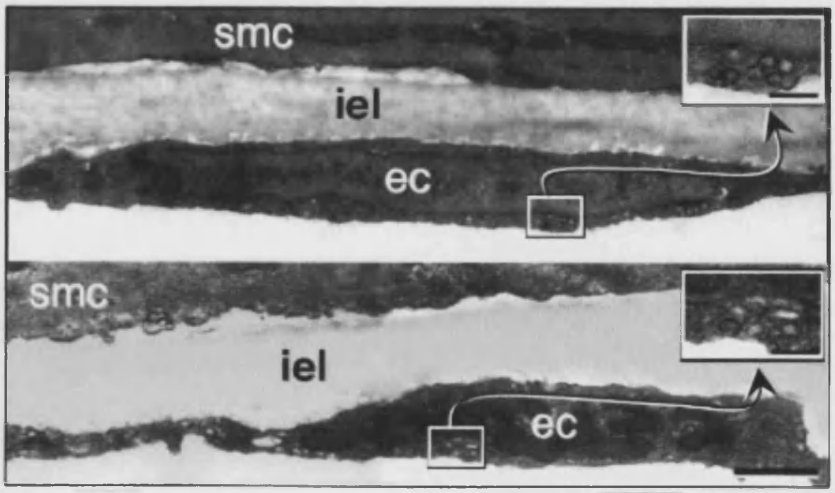

Figure 4.6 Effect of the luminal pinocytic loading protocol on number of intracellular endothelial vesicles

Representative (n=3) electron micrographs of radial cross-sections through isolated, pressurized arteries fixed **A,** before, **B,** during and **C,** after fully completing the pinocytic loading protocol. Bar: Main panels 1μm; insets 200nm. Modified from Mather *et al.*, 2005. All electron microscopy work, image production and vesicle counts were performed by Dr. Shaun Sandow.

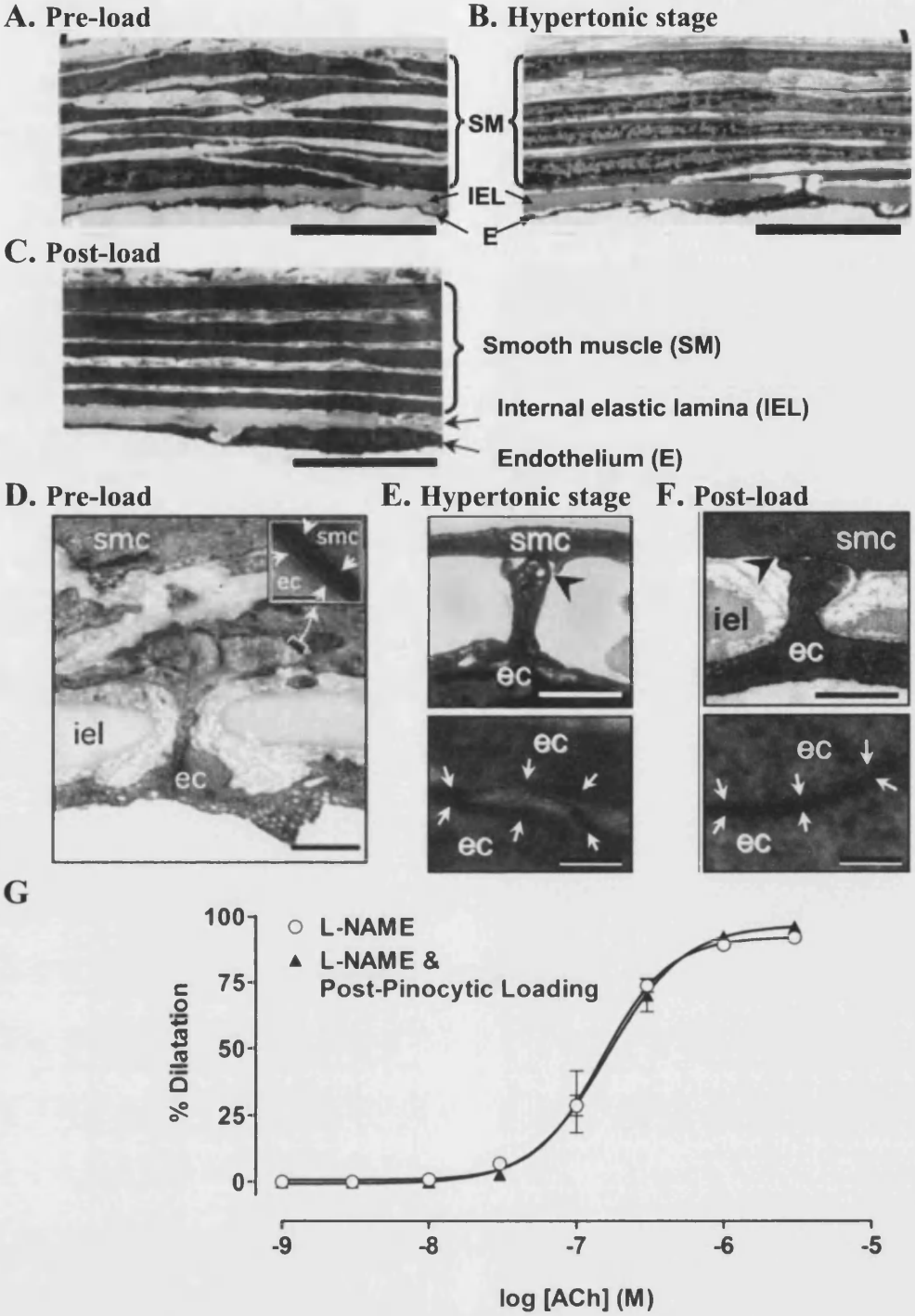

Figure 4.7 Effect of the luminal pinocytic loading protocol on arterial ultrastructural and functional integrity

Representative electron micrographs of radial cross-sections through isolated, pressurized arteries fixed **A, D,** before, **B, E,** during and **C, F** after fully completing the pinocytic loading protocol (n=3). **G,** Effect of the luminal pinocytic loading protocol on dilatation responses to ACh (n=9-39). Bar: **A - C,** 10μm; **D,** 1μm; **E, F,** 50nm; **D,** inset 100nm. **D, E, F,** Arrows indicate gap junction plaques. Modified from Mather *et al.*, (2005). All electron microscopy work, image production and structural analyses were performed by Dr. Shaun Sandow.

dilatation to ACh was unaffected by the pinocytic loading protocol (Figure 4.7G; Table 4.4, n = 9 - 39).

4.3.8. Effect of luminal pinocytic loading of connexin antibodies on ACh-evoked dilatation

Antibodies targeted against the intracellular C-terminus of connexin 37, connexin 40 or connexin 43 were included in the hypertonic solution (0.1mg ml^{-1}) during luminal treatment of isolated, pressurized arteries with the pinocytic loading protocol. Pinocytic loading of anti-connexin 37 (n = 6 - 9) and 43 (n = 3 - 7) antibodies had no effect on concentration-dependent dilatation responses to ACh (Figure 4.8A; Table 4.4). In contrast inclusion of anti-connexin 40 antibodies in the hypertonic solution resulted in a rightward shift in the concentration-response curve to ACh and a significant attenuation of the vasodilatation to 3μM ACh (Figure 4.8A; Table 4.4; n = 2 - 14). Endothelial cell viability remained intact following luminal pinocytic loading of connexin antibodies as evidenced by the minimal endothelial cell staining by propidium iodide (0.01%wv^{-1}) when compared to tissue damaged by cannulation (Figures 4.8C and D).

Experiments were performed to evaluate the influence of the Na^+/K^+ATPase and tone on EDHF-type responses prior to and following pinocytic loading of anti-connexin 40 antibodies. Under conditions of low PE-evoked tone ouabain (1μM; n = 4) evoked a significant rightward shift in the concentration-response curve to ACh. In separate experiments endothelial cell loading of anti-connexin 40 was without effect on ACh-evoked vasodilatation, further supporting a minimal effect of this protocol on cell viability (Figure 4.8B; n = 4). Endothelial cell loading of anti-connexin 40 antibodies in the presence of ouabain did not evoke any further inhibitory effects (Figure 4.8B, n = 4). In contrast under conditions of high PE-evoked tone, the inhibitory effects of endothelial cell loading with anti-connexin 40 were unmasked to a similar extent whether in the presence (n = 4) or absence of ouabain (Figure 4.8B; n = 2 – 14).

Treatment	pD_2 ± s.e.mean	R_{max} ± s.e.mean (*P*)	*n*
Low Tone & L-NAME	7.1±0.1	98.5±0.5%	8
Low Tone, L-NAME & Ouabain	6.3±0.1	99.2±0.7% (*ns*)	4
Low Tone, L-NAME & Anti-Connexin40 Antibody	7.1±0.1	97.6±0.8% (*ns*)	4
High Tone, L-NAME & Anti-Connexin40 Antibody	n/a	36.6±9.5%	14
Low Tone, L-NAME, Anti-Connexin40 Antibody & Ouabain	6.3±0.2 (*n*=3/4)*	96.0±2.2%	4
High Tone, L-NAME, Anti-Connexin40 Antibody & Ouabain	n/a	16.3±4.0% (<0.001)	4

Table 4.5. Effect of PE-evoked tone, ouabain and anti-connexin 40 antibody on dilatation responses to ACh
The effects of luminal pinocytic loading of anti-connexin 40 (0.1mg ml^{-1}), the level of PE-evoked tone (low, 0.3-3μM; High 3-10μM) and the inhibitor of Na^+/K^+-ATPase, ouabain (1μM) on ACh-evoked dilatation responses. R_{max} corresponds to dilatation to 3μM ACh. L-NAME (100μM) present in all experiments. The anti-connexin 40 antibody data has been shown previously (please see Table 4.4). n/a and *, an EC_{50} could not be accurately calculated so the pD_2 value is excluded. Parts of this work were obtained by Dr. Kim Dora and Dr. Simon Mather. * Significantly different to Low Tone & L-NAME following a one-way ANOVA with a Bonferroni post-test (*P*<0.05).

Figure 4.8 Effect of luminal pinocytic loading of anti-connexin antibodies on dilatation responses to ACh
A, B, Concentration-response curves illustrating the effects of luminal pinocytic loading (0.1mg ml^{-1}) of **A,** anti-connexin 37 (*n*=6-9), **A, B,** anti-connexin 40 (*n* =2-14) and **A,** anti-connexin 43 antibodies (*n*=3-7) on ACh-evoked dilatation responses under conditions of high PE-evoked background tone (3-10μM). **B,** The effects of different levels of background PE-evoked tone (low, 0.3-3μM; and high 3-10μM) and the Na^+/K^+-ATPase inhibitor ouabain (1μM) on ACh-evoked dilatation responses prior to and following luminal pinocytic loading of anti-connexin 40 (0.1mg ml^{-1}). L-NAME present throughout all experiments (100μM). **C, D,** Representative images of propidium iodide (0.01%wv^{-1}) staining of damaged endothelial and smooth muscle cells at **C,** the site of cannulation and **D**, the middle of the artery following pinocytic loading of anti-connexin 40 antibodies. **C, D,** bar 50μm. Images were taken using a x40, water immersion objective. Some (*n*=2-6) concentration-response data are also shown in section 5.3. Parts of this work were obtained by Dr. Kim Dora and Dr. Simon Mather. Significant differences from L-NAME were assessed using a one-way ANOVA with a Bonferroni post-test (*P*<0.05).

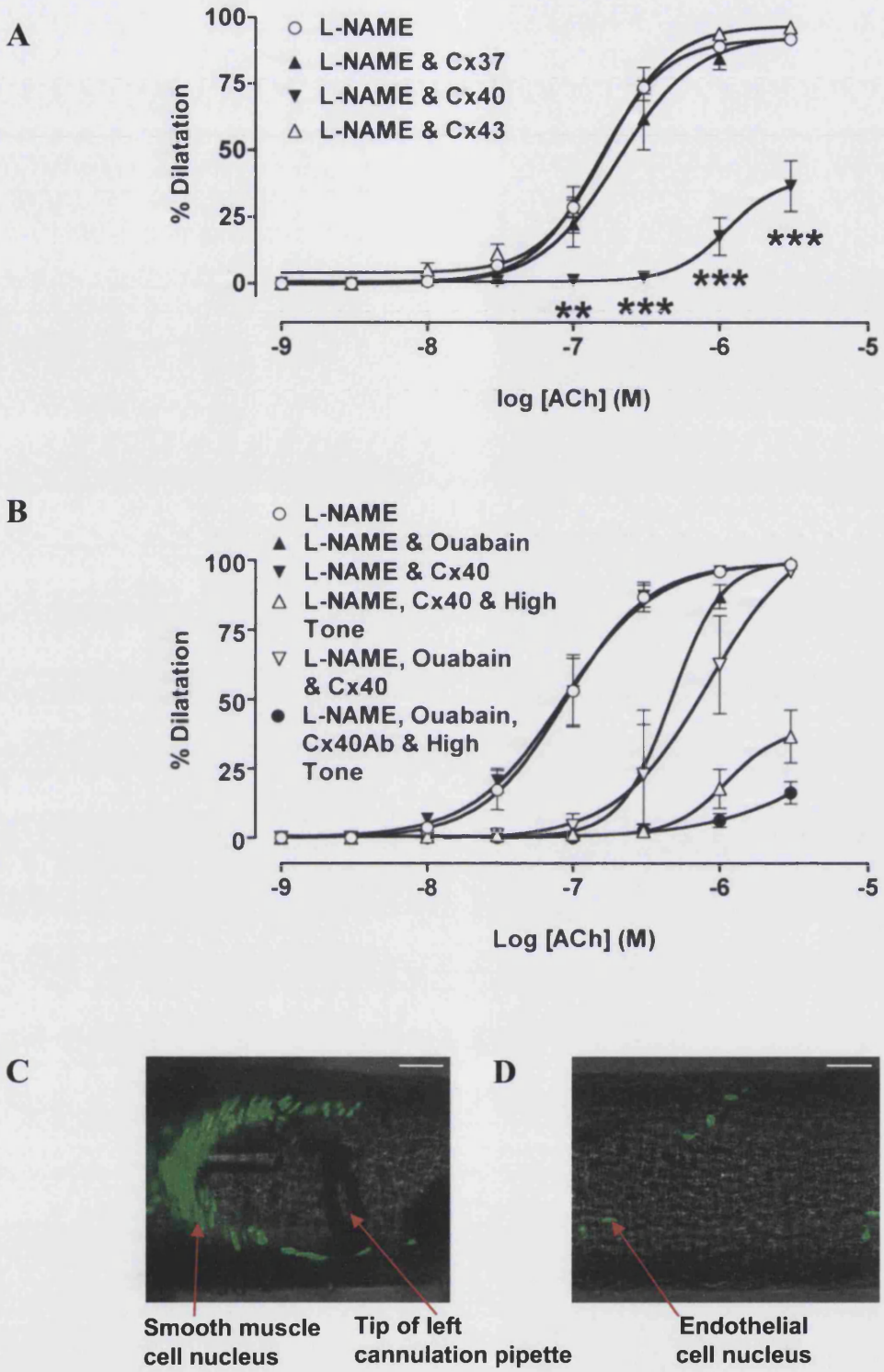
A
100
75
50
25
0
% Dilatation
L-NAME
L-NAME & Cx37
L-NAME & Cx40
L-NAME & Cx43
**
***
***
***
-9
-8
-7
-6
-5
log [ACh] (M)
B
L-NAME
L-NAME & Ouabain
L-NAME & Cx40
L-NAME, Cx40 & High Tone
L-NAME, Ouabain & Cx40
L-NAME, Ouabain, Cx40Ab & High Tone
100
75
50
25
0
% Dilatation
-9
-8
-7
-6
-5
Log [ACh] (M)
C
D
Smooth muscle cell nucleus
Tip of left cannulation pipette
Endothelial cell nucleus

Figure 4.8

4.4. Discussion

Gap junctional communication has been demonstrated to be an integral part of both EDHF-facilitated vasodilatation and spreading dilatation responses by a number of investigators. However the lack of selective inhibitors of either homocellular or heterocellular gap junctions has precluded a definitive assessment of the pathways mediating these responses. Within this study conditions under which EDHF-mediated dilatation and in particular dilatation likely mediated by gap junctional communication were established in rat isolated and pressurized mesenteric arteries. This provided a model for evaluation of the efficacy of established gap junction uncouplers and enabled the effects of endothelial cell pinocytic loading of anti-connexin antibodies to be studied.

Consistent with previous reports, pre-contraction of the rat mesenteric artery to a high level of background tone with PE (3-10μM) in the presence of L-NAME prevented relaxations to K^+ previously reported at lower levels of tension in rat mesenteric arteries (Dora & Garland, 2001; Dora *et al.*, 2000b; Dora *et al.*, 2002; Doughty *et al.*, 2000; Edwards *et al.*, 1998; Richards *et al.*, 2001; Weston *et al.*, 2002). A significant rightward shift of the ACh concentration-response-curve was also observed, which could imply a degree of physiological antagonism of the PE-evoked response. However a number of studies have also demonstrated that the inhibition of K^+-evoked dilatation by raised PE-evoked background tone could be almost completely prevented by treatment with the BK_{Ca} blockers iberiotoxin and charybdotoxin in this preparation. These findings support the hypothesis of maximal $3Na^+/2K^+$ATPase activation by smooth muscle cell K^+ under conditions of high tone and suggest that a K^+ component of the EDHF response to ACh could be prevented under these conditions (Dora & Garland, 2001; Dora *et al.*, 2000b; Dora *et al.*, 2002; Richards *et al.*, 2001).

The complete attenuation of ACh-evoked vasodilatation under high levels of PE-evoked tone in the presence of L-NAME and following blockade of K^+ channels was consistent with the remaining relaxation component being driven by an EDHF, which according to previous studies would most likely comprise a gap junction-facilitated component (Chen & Cheung, 1997; Dora *et al.*, 1999; Doughty *et al.*, 1999; Edwards *et al.*, 1998; Hinton & Langton, 2003; Sandow & Hill, 2000; Sandow *et al.*, 2006; Sandow *et al.*,

2002; Ungvari *et al.*, 2002; Walker *et al.*, 2001; Zygmunt & Hogestatt, 1996). The inconsistent, or even absent blockade of ACh-evoked responses by either carbenoxolone or the gap peptides was therefore surprising. Although the specificity and effectiveness of carbenoxolone may have been questioned (Chaytor *et al.*, 2000; Goto *et al.*, 2002; Griffith, 2004; Matchkov *et al.*, 2004b; Tare *et al.*, 2002) previous reports have clearly demonstrated the efficacy and reliability of the gap peptides as inhibitors of vascular gap junctional communication, particularly when administered as a triple combination of ^{Cx43}Gap 26, ^{Cx37,Cx43}Gap 27 and ^{Cx40}Gap27 (Chaytor *et al.*, 1998; Chaytor *et al.*, 2001; Dora *et al.*, 1999; Doughty *et al.*, 2000; Edwards *et al.*, 1999; Griffith, 2004; Matchkov *et al.*, 2006; Sandow *et al.*, 2003a; Sandow *et al.*, 2002). Inconsistencies in their efficacy have been documented previously and shown not to correlate with the incidence of MEGJ (Dora *et al.*, 2003a). However, such an occurrence is still difficult to mechanistically resolve. Within this study the pH of the peptides was adjusted to physiological levels, an aspect that has not been reported in previous studies and one that may have significant implications on peptide structure and interaction with gap junctions. However, an influence of pH on gap peptide efficacy can only be deemed as speculation and a definitive assessment of the discrepancies, perhaps also evaluating the likelihood of protein digestion or supplier differences would need to be performed to fully understand the results of this study.

Given the poor efficacy of the gap peptides in our hands we employed a new technique that had the capacity to facilitate the selective blockade of endothelial cell gap junctions in the isolated artery preparation. Véquad & Thorin (2001) recently described the use of a commercially available kit to selectively load antibodies into the endothelium by a method of enhanced pinocytosis (please see section 2.4). However, within this laboratory we were unable to maintain the functional integrity of the artery using this method so a technique based on the osmotic lysis of pinocytic vesicles originally developed for cells in culture was adapted for use in the intact artery (please see section 2.4; Mather *et al.*, 2005; Okada & Rechsteiner, 1982).

Inclusion of carboxyfluorescein, FITC-conjugated dextran (3000Da) or Alexa Fluor® 633-conjugated IgG in the hypertonic solution during luminal application of the pinocytic loading protocol demonstrated the selectivity and efficiency with which this

method loads molecules into the endothelium (please also see 3.3.3). The increased number of intracellular vesicles during the hypertonic stage of the process is consistent with the original work of Okada & Rechsteiner (Okada & Rechsteiner, 1982) and supports the proposed mechanism behind the loading protocol whereby the increased osmotic pressure in the presence of a hypertonic solution stimulates the formation of intracellular vesicles containing the extracellular solute (please see section 2.4). Electron micrographs and functional responses to ACh demonstrated the maintained structural integrity and endothelial cell viability following the pinocytic loading protocol.

Subsequent studies evaluating the contribution of gap junctions, and more specifically the known vascular connexins to EDHF responses in the rat isolated mesenteric artery were performed. By luminal pinocytic loading of antibodies directed against the C-terminus of connexin 40 a significant role for connexin 40 in EDHF-type dilatation responses to ACh under conditions of high PE-evoked tone was revealed. Given that the inhibition of EDHF-type responses was without detrimental affects on endothelial cell Ca^{2+} or smooth muscle cell function (Mather *et al.*, 2005) the current study directly supports the contribution of MEGJ to EDHF responses in isolated rat mesenteric arteries.

Ultrastructural and immunohistochemical studies have localized both connexins 37 and 40 to MEGJ plaques in primary and secondary rat mesenteric arteries. Given that MEGJs were shown to occur with a frequency of ~0.79 per endothelial cell in these preparations it is likely that both connexin subtypes could contribute to EDHF-type responses in this vascular bed (Sandow *et al.*, 2006; Sandow *et al.*, 2002). Indeed functional studies performed using $^{Cx37,\ Cx43}$Gap27 (Doughty *et al.*, 2000; Edwards *et al.*, 1999; Sandow *et al.*, 2002) and the triple combination of gap peptides described herein (Matchkov *et al.*, 2006) report a significant attenuation of EDHF-mediated hyperpolarization and relaxation within this preparation. As staining for connexin 43 was much more scarce compared to connexins 37 and 40 in the endothelium of rat mesenteric resistance arteries and connexin 43 was seen to be absent from the MEGJ of the primary mesenteric artery (Kansui *et al.*, 2004; Matchkov *et al.*, 2006; Sandow *et al.*, 2006) it perhaps follows that within this study antibodies directed against connexin

43 were without effect. However, the extensive endothelial cell staining for connexin 37 in the rat mesenteric artery, and its localization to MEGJ (Gustafsson *et al.*, 2003; Kansui *et al.*, 2004; Sandow *et al.*, 2006) would lead us to expect at least a small contribution of connexin 37. The lack of any inhibition of EDHF-type responses by antibodies and peptides directed against various domains of connexin 37 (Mather *et al.*, 2005), including the C-terminus as described herein could therefore reflect a sensitivity of connexin 37 to smooth muscle tone. Indeed under conditions of low PE-evoked background tone the rightward shift in the concentration-response curve to ACh by ouabain was not augmented by pinocytic loading of anti-connexin 40 antibodies. This would suggest that another compensatory mechanism possibly involving gap junctions composed of connexin 37 is providing an alternative pathway for an EDHF-mediated dilatation response.

An important role for connexin 40 in the regulation of vascular function has been previously documented following the development of connexin 40 knockout mice (de Wit *et al.*, 2000; Figueroa *et al.*, 2003). Within the two reports it was found that the knockout mice were hypertensive and showed impaired conducted vasodilatation responses to ACh, bradykinin and electrical stimulation (de Wit *et al.*, 2000; Figueroa *et al.*, 2003). Indeed, consistent with our studies de Wit *et al.* (2000) demonstrated an ~30% attenuation of ACh-evoked vasodilatation responses of cremaster arterioles from connexin 40 knockout animals. However, ongoing developmental changes that may be a result of, or compensate for, the deletion of a connexin channel cannot be dismissed and cannot be differentiated from the supposed direct effects of connexin deletion (Liao *et al.*, 2001). Indeed, in mice in which connexin 43 was selectively deleted from vascular endothelial cells, increased plasma NO levels, bradycardia, hypotension and increased levels of angiotensin I and II were all reported but the influence of connexin 43 deletion on these parameters could not be confirmed (Liao *et al.*, 2001).

Acute, pharmacological dissection of the individual connexin channels mediating either the MEGJ or smooth muscle transfer of hyperpolarization has been attempted previously by elegant use of a range of gap peptides in the rabbit iliac artery (Chaytor *et al.*, 2005). By taking advantage of the larger number of smooth muscle layers in this artery (~10) the authors were able to differentiate between homocellular coupling

mechanisms and heterocellular coupling mechanisms by measuring endothelium-dependent smooth muscle cell hyperpolarization in sub-adventitial and sub-intimal layers of the media respectively. Using this technique combined with the selective application of the gap peptides ($^{Cx37,\ Cx40}$Gap26, ^{Cx40}Gap27, $^{Cx37,\ Cx43}$Gap27 and ^{Cx43}Gap26) the authors were able to dissect a role for connexins 37 and 40 in the heterocellular transfer of hyperpolarization to the sub-intimal smooth muscle layer and a role for connexin 43 in the relay of hyperpolarization throughout the sub-adventitial layers. Furthermore, the electrophysiological data were found to correlate with immunohistochemical staining patterns for each of the connexin subtypes within the rabbit iliac artery wall (Chaytor *et al.*, 2005). Crucially however, no ultrastructural evidence supporting the existence of MEGJ and the localization of connexins 37 and 40 to sites of heterocellular coupling were provided such that definitive conclusions as to the discrete connexin subtypes contributing to the MEGJ could not be made.

To summarize, within this study preliminary steps have been taken to show that the pinocytic loading method may be used as a tool for incorporating large cell-impermeant molecules into the endothelium of intact pressurized arteries. By using this protocol to load antibodies directed against the C-terminus of connexin 40 we have shown that MEGJ at least partly composed of connexin 40, contribute to EDHF-mediated dilatations in rat small mesenteric arteries under conditions of high PE-evoked tone.

4.5. Acknowledgements

I would like to thank Dr. Kim Dora and Dr. Simon Mather for their contributions to this chapter and Dr. Shaun Sandow for carrying out the electron microscopy work and subsequent image analysis. I would also like to thank Professor Chris Garland for the helpful discussion of this work.

5. The role of connexins in conducted vasodilatation responses in rat isolated small mesenteric arteries

5.1. Introduction

Mechanisms associated with the radial endothelium-dependent dilatation response to bath application of agonists such as ACh are continually reported. However focal vasodilatation, at a restricted site of metabolite release for example, may be insufficient to adequately increase blood flow to provide for the metabolic needs of the tissue. Therefore an ascending vasodilatation from the site of stimulation to the level of the feed arteries that occurs independently of stimulus diffusion can more effectively facilitate tissue perfusion due to a greater reduction in vascular resistance (Kurjiaka & Segal, 1995; Segal, 1991; Segal, 2005; Segal & Duling, 1986b). In support of this, these "conducted vasomotor" responses are frequently observed over distances greater than 1mm and have been documented following the release of metabolites such as ATP, adenosine, H^+ and K^+ from the downstream tissue (Berg *et al.*, 1997; Duza & Sarelius, 2003; Folkow *et al.*, 1971; Hilton, 1959; Kajita *et al.*, 1996; McCullough *et al.*, 1997; Murrant & Sarelius, 2000; Segal & Duling, 1986a; Segal & Jacobs, 2001; VanTeeffelen & Segal, 2006).

Spreading vasomotor responses were first documented 85 years ago when in a study on the vasomotor mechanisms of the capillaries of the frog hind leg Krogh *et al.*, (1922) applied silver nitrate to the web between two toes of the frog and observed the spread of vasodilatation to vessels in an adjacent webbed region (Krogh *et al.*, 1922). Cutting of the sciatic nerve was found not to abolish the propagated vasodilatation the authors thus proposing local neuronal mechanisms to mediate the phenomenon (Krogh *et al.*, 1922). Later studies using the cat femoral artery and hamster cheek pouch microcirculation also attributed the spreading vasodilatation to mechanisms intrinsic to the arterial wall, either proposing the direct electrical communication between cells of the arterial wall or the activation of an intrinsic neural pathway (Duling & Berne, 1970; Hilton, 1959).

It has since become apparent that the characteristics of the spreading response such as the extent of propagation upstream and the amplitude of vasodilatation or vasoconstriction can be dependent on the vascular bed, the type of preparation used and the agonist used to evoke the local response suggesting that multiple mechanisms contribute to this apparently conserved vasomotor function (Delashaw & Duling, 1991; Gustafsson & Holstein-Rathlou, 1999; Looft-Wilson *et al.*, 2004; Neild & Crane, 2002;

Segal & Duling, 1989; Segal *et al.*, 1999; Thengchaisri & Rivers, 2005). However, of the proposed mechanisms for spreading vasodilatation the electrotonic conduction of hyperpolarization from the site of stimulation upstream via gap junctions within the endothelium is perhaps the most widely accepted hypothesis (de Wit *et al.*, 2006a; de Wit *et al.*, 2000; Dora *et al.*, 2003b; Emerson & Segal, 2001; Figueroa *et al.*, 2003; Neild & Crane, 2002; Segal & Duling, 1986b; Segal & Duling, 1987; Segal *et al.*, 1999; Takano *et al.*, 2004; Welsh & Segal, 1998; Xia & Duling, 1995).

Hirst & Neild (1978) first documented the longitudinal transfer of current along the guinea-pig mesenteric arteriole, at the time proposing an intrinsic electrical conduction pathway within the arterial wall. Based on accumulating data showing a direct gap junctional mediated pathway between both endothelial and smooth muscle cells and the close approximation of the length constants (the distance over which the response decays to ~37% of its initial value) reported for electrotonic conduction and conducted vasodilatation, Segal & Duling (1991; 1989; 1989; 1986b) proposed that the mechanism of the conducted vasomotor response was associated with a conducted increase in membrane potential, transferred from cell to cell via gap junctions. This crucial role for the conducted change in membrane potential was highlighted by observations that conducted vasomotor responses were associated with agonists that evoked their local response by predominantly electromechanical mechanisms (for example ACh and PE; please see sections 1.2.4.2 and 1.3.2.6). Whereas pharmacomechanically-evoked vasomotor responses (for example sodium nitroprusside) were unable to conduct (Delashaw & Duling, 1991). Parallel conducted depolarization and vasoconstriction responses to KCl and the attenuation of remote vasodilator responses to ACh by upstream application of depolarizing concentrations of K^+ also supported the idea of an electrotonically-conducted response (Segal & Duling, 1989; Xia & Duling, 1995; Xia *et al.*, 1995). However the cell-to-cell pathway mediating the conduction of this increase in membrane potential was unclear.

The longitudinal orientation of the endothelial cells favour a more rapid conduction pathway than that achieved via smooth muscle cell coupling (Haas & Duling, 1997; Yamamoto *et al.*, 2001). Indeed, the circumferential arrangement of the smooth muscle cells observed in the hamster cheek pouch arteriole suggest that an electrical current

would have to pass through the width of 140 smooth muscle cells to cover a 1mm segment of vessel whereas just 6 or 7 endothelial cell lengths would span the same distance (Haas & Duling, 1997). This combined with the equal to high coupling resistance between the smooth muscle cells versus the endothelium suggests that a smooth muscle cell pathway for the spread of the increase in membrane potential is unlikely (Emerson *et al.*, 2002; Yamamoto *et al.*, 2001). Experimentally, complete attenuation of conducted vasodilatation and hyperpolarization responses to both ACh and LVK following mechanical removal of the endothelium in the rat isolated and pressurized mesenteric artery has been described (Goto *et al.*, 2004; Takano *et al.*, 2004). Given that the primary mechanism associated with LVK-evoked vasodilatation is one of direct smooth muscle hyperpolarization (please see section 1.3.1.1) the disruption of the LVK-evoked conducted response highlights an obligatory role for the endothelium. In pressurized hamster retractor muscle feed arteries focal (targeting an ~300μm region) light dye treatment to selectively disrupt conduction through either the endothelium or smooth muscle layers supported an endothelial cell pathway for conduction of the response to ACh. This elegant study described blockade of conducted dilatation and hyperpolarization responses to ACh upon disruption of the endothelium whilst disruption of the smooth muscle had minimal effects (Emerson & Segal, 2000b).

Given the obligatory role for the endothelium in the longitudinal conduction of vasodilatation in the rat mesenteric artery and the extensive anatomical and immunohistochemical evidence for endothelial cell homocellular gap junctions within this vascular bed (please see chaper 3; Goto *et al.*, 2002; Goto *et al.*, 2004; Gustafsson *et al.*, 2003; Kansui *et al.*, 2004; Mather *et al.*, 2005; Sandow & Hill, 2000; Sandow *et al.*, 2006) a gap junctional pathway for the longitudinal transfer of an increased membrane potential would therefore seem likely (Segal *et al.*, 1989; Segal & Duling, 1989; Segal & Duling, 1986b). However to date, despite much evidence in support of the selective and specific blockade of vascular gap junctions with the gap peptides (please see sections 4.1 and 4.4), studies evaluating the contribution of the vascular connexins to conducted vasodilatation by use of these specific gap junction uncouplers have not been reported.

Connexin knockout studies describing the deletion of connexin 40 have documented the attenuation of conducted dilatation responses to ACh, bradykinin (de Wit *et al.*, 2000) and more recently direct electrical stimulation (Figueroa *et al.*, 2003) in mouse cremaster muscle preparations. Indeed, conducted vasoconstrictions to K^+ and electrical stimulation were unaffected (de Wit *et al.*, 2000), implying that different connexins may contribute in a divergent manner to the conduction of either dilator or constrictor vasomotor responses (de Wit *et al.*, 2006b). However, such studies must be regarded with caution as compensatory regulation of other associated channel proteins or even in-direct effects associated with deletion of the channel may occur (please see section 4.4). Furthermore, knock out studies also currently restrict the experimenter to cell culture models or mouse preparations, which given the tissue variability associated with the conducted vasodilatation response, limits the usefulness of this methodology.

The aim of this study was to therefore examine the role of endothelial cell gap junctions on the conducted vasodilatation response to ACh and LVK in the rat isolated and pressurized mesenteric artery. Given the poor efficacy of the gap peptides in our hands (please see chapter 4; Mather *et al.*, 2005) selective endothelial cell pinocytic loading of antibodies targeted against known vascular connexins was used. Characterization of the pinocytic loading protocol and the effects of endothelial cell connexin antibody loading on radial EDHF-type dilatation responses have been described previously (please see chapter 4; Mather *et al.*, 2005) wherein a significant attenuation of the EDHF-type response was observed following endothelial cell loading of connexin 40 antibody under conditions of high tone. Preliminary experiments in this study were therefore designed to evaluate the effects of the pinocytic loading vehicle on the conducted vasodilatation response and evaluate the efficacy of carbenoxolone as an inhibitor of conducted vasodilatation responses. Subsequently, the effects of selective endothelial cell loading of antibodies directed against connexins 37, 40 and 43 were evaluated.

5.2. Methods

5.2.1. Rat mesenteric artery isolation and cannulation

Please see section 2.1 for methods of artery isolation.

5.2.2. Pressure myography

Arteries were mounted in custom-built organ baths (0.5ml; Figure 2.3) specifically designed to prevent upstream flow of focally-applied agonists. For cannulation and equilibration methods please see section 2.2. Endothelial cell viability was assessed as a >90% control dilatation to ACh (1μM) following pre-constriction with PE (1 - 3μM). Arteries were maintained at 50mmHg and 37°C unless otherwise stated.

5.2.3. Cumulative concentration-response curves

All experiments were performed in the presence of L-NAME (100μM, 20min). Inhibition of cyclooxygenase was not required, as indomethacin (10μM) has been shown to have no effect on ACh-evoked dilatation responses within the rat mesenteric artery (please see section 1.3.2.4). Cumulative concentration-response curves to ACh (1nM-3μM) were performed following maximal (~90%; high tone) constriction to PE.

5.2.4. Focal stimulation of pressurized arteries

Please see section 2.3 for details of the methods used for the focal stimulation of arteries. In summary bolus doses of agonists were pressure-pulse ejected to the downstream end of arteries and dilatation responses simultaneously measured at sites up to 2mm upstream.

5.2.5. Pinocytic loading of cell impermeant molecules

For endothelial cell loading, anti-connexin antibodies were diluted (1:10) with hypertonic solution (containing PEG) to give final luminal concentrations of 0.1mg ml^{-1}. Endothelial cell viability was subsequently assessed by inclusion of propidium iodide in the bath solution (0.01% wv^{-1}), which was visualized as previously described (please see section 3.2.7).

5.2.6. Drugs and solutions

All drugs and solutions were prepared as detailed previously (please see section 2.6).

For experiments assessing vascular responses to focal stimulation PE, L-NAME and carbenoxolone were added to the superfusate reservoir prior to artery superfusion. L-NAME (100μM) was present throughout all experiments.

5.2.7. Antibodies

The antibodies used were described previously (please see section 4.2.8).

5.2.8. Data analysis

Data were initially collected and analysed as has been described previously (please see sections 2.5 and 2.7). To enable simultaneous observation of the local (0μm) and remote (500μm, 1000μm, 1500μm and 2000μm) sites full visualization (>2mm) of the artery required the use of a 4x objective, which limited the resolution of the images to ~5μm, circa 1.5% of the maximum diameter of the arteries. However, for the purposes of this study the capability of measuring spreading dilatation to a single application of agonist (not repeated stimuli visualized along the artery at multiple sites) outweighed the disadvantage of reduced image resolution. The ability to pair each remote response to the local dilatation response more clearly demonstrated the extent of decay over distance of the conducted vasodilatation response.

This approach also enabled us to evaluate the time taken for each artery to commence dilatation by 10μm at each of the remote sites (Figures 5.2C, 5.2D, 5.3C and 5.3D). Due to the latency and complexity of the evoked pathways associated with the dilatation response at the local site, measurements were only compared to the initiation of dilatation at the 500μm remote site (Emerson *et al.*, 2002). However even with this parameter accounted for, the analyses performed herein cannot be taken as a measurement of the electrical conduction as we did not attempt to concomitantly measure membrane potential or endothelial cell resistance. Indeed it is hoped that these data may simply provide a further indication of the effects of endothelial cell loading of anti-connexin antibodies. For example, were the endothelial cell loading of connexin antibodies to block inter-endothelial cell gap junctions only (Figure 5.1), we would expect a radial EDHF response at the site of stimulation, but minimal longitudinal communication of the response via the smooth muscle (Emerson *et al.*, 2002; Haas & Duling, 1997; Yamamoto *et al.*, 2001). Due to the high density of connexin expression

at the endothelial cell borders (please see chapter 3)(Mather *et al.*, 2005; Sandow *et al.*, 2006) it is unlikely that we would be able to inhibit all gap junctions. Therefore, we may only reduce the speed of the dilatation response rather than the magnitude. As we do not know how many gap junctions are required to enable the spread of current this, however, would be difficult to predict. Alternatively were the endothelial cell loading of connexin antibodies only to block MEGJ (Figure 5.1), which is highly unlikely under conditions of low tone given the expression of both connexins 37 and 40 at the MEGJ and endothelial cell border (Mather *et al.*, 2005; Sandow *et al.*, 2006), local (radial) and conducted (longitudinal) dilatation responses to ACh would be reduced as the smooth muscle would not be stimulated at either the local or conducted sites. However a local response to LVK possibly coupled to a small spread of dilatation through smooth muscle gap junctions would be expected. Finally were we to block smooth muscle cell gap junctions only, the current would be dissipated less through the smooth muscle layers and so the magnitude of the conducted endothelial cell response would likely be increased. However, if the reduced passage of current though the smooth muscle cells would limit the number of smooth muscle cells able to relax this could be seen as a limited dilatation response.

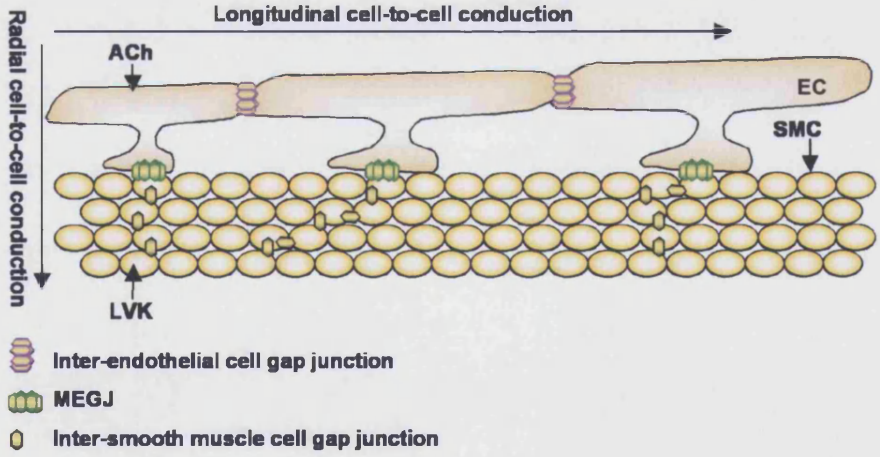

Figure 5.1 Cell-to-cell conduction within the artery wall
Cartoon illustrating the gap junction cell-to-cell conduction pathways within the artery wall. EC, endothelial cell; SM, smooth muscle cell.

5.3. Results

5.3.1. ACh and LVK-evoked conducted vasodilatation responses

L-NAME (100μM) was present throughout this study. Agonists were pressure-pulse ejected as a bolus dose through micropipettes positioned abluminally at the downstream end of the artery. Focal application of ACh (1mM, 1 – 100ms) stimulated robust dilatation at the local site (0μm, 81.5 ± 4.5%, n = 5; Figures 5.2A and 5.2B) that conducted rapidly upstream to more distal sites (please see Figure 2.5; 500 - 2000μm; Figures 5.2C and 5.2D) with little decay in the amplitude of dilatation (2000μm, 56.8 ± 9.2%; Figures 5.2A and 5.2B). Focal application of LVK (1mM, 3 – 30ms,) also evoked a large local dilatation response (0μm, 92.9 ± 2.8%, n = 4; Figures 5.3A and 5.3B) that decayed to a similar extent as ACh (2000μm, 43.3 ± 4.4%; Figures 5.3A and 5.3B). However in contrast to ACh-evoked responses the time course of both the local and spreading dilatation responses was much slower (Figures 5.3C and D). Treatment of arteries with the pinocytic loading protocol (vehicle only) had no significant effects on either the time taken to dilate (Figures 5.2D and 5.3D) or the extent of dilatation at local and distal sites (Figures 5.2B and 5.3B) following focal stimulation with either ACh (n = 5 – 6) or LVK (n = 4).

Figure 5.2 Spreading responses evoked by abluminal application of ACh
ACh was pressure-pulse ejected as a bolus dose with a micropipette positioned at the downstream end of the artery. **A, C,** Representative traces (1mM, 30ms) **B,** mean peak amplitude of spreading dilatation responses (1mM, 1-100ms; n=5-6, unpaired experiments) and **D,** mean time taken to dilate by 10μm (1mM, 1-100ms; n =4-5, unpaired experiments) at the local (0μm) and upstream (500-2000μm) sites under **A, B, C, D,** control conditions and **B, D,** immediately following the pinocytic loading protocol. **C,** Expanded view of the initial dilatation response to ACh as shown **A,** in full. Images were acquired at 12Hz. Diameter was measured simultaneously at all positions along the artery. Dashed lines indicate the measurements taken to evaluate the time taken to dilate by 10μm. L-NAME (100μM) present in all experiments.

Figure 5.3 Spreading responses evoked by abluminal application of LVK
LVK was pressure-pulse ejected as a bolus dose with a micropipette positioned at the downstream end of the artery. **A, C,** Representative traces (1mM, 3ms) **B,** mean peak amplitude of spreading dilatation responses (1mM, 3-30ms; n=4, unpaired experiments) and **D,** mean time taken to dilate by 10μm (1mM, 3-30ms; n=4, unpaired experiments) at the local (0μm) and upstream (500-2000μm) sites under **A, B, C, D,** control conditions and **B, D,** immediately following the pinocytic loading protocol. **C,** Expanded view of the initial dilatation response to LVK as shown **A,** in full. Images were acquired at 12Hz. Diameter was measured simultaneously at all positions along the artery. Dashed lines indicate the measurements taken to evaluate the time taken to dilate by 10μm. L-NAME (100μM) present in all experiments.

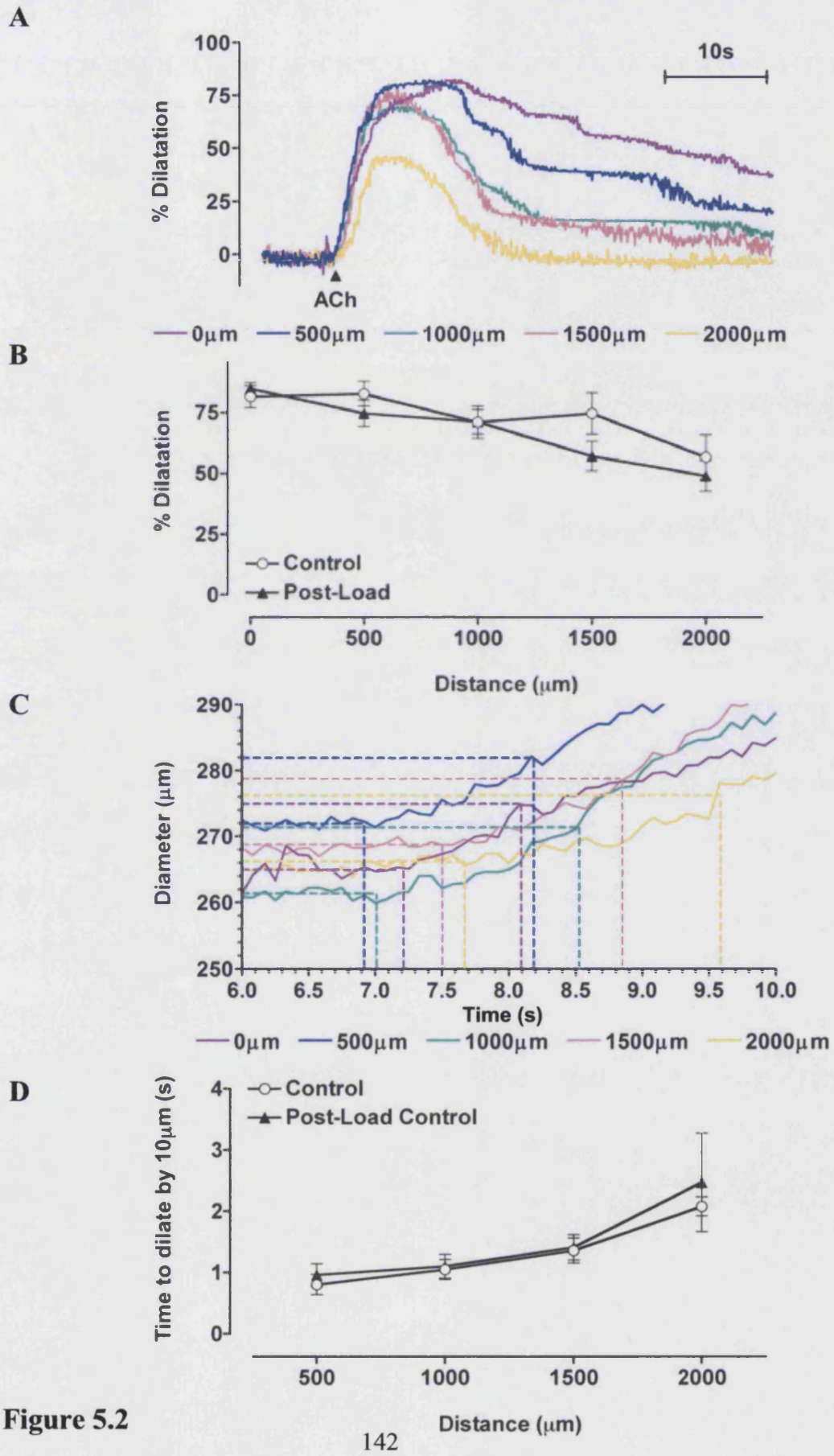
A
100
75
50
25
0
% Dilatation
10s
ACh
0µm
500µm
1000µm
1500µm
2000µm
B
% Dilatation
75
50
25
0
Control
Post-Load
0
500
1000
1500
2000
Distance (µm)
C
290
280
270
260
250
Diameter (µm)
6.0
6.5
7.0
7.5
8.0
8.5
9.0
9.5
10.0
Time (s)
0µm
500µm
1000µm
1500µm
2000µm
D
Time to dilate by 10µm (s)
4
3
2
1
0
Control
Post-Load Control
500
1000
1500
2000
Distance (µm)

Figure 5.2

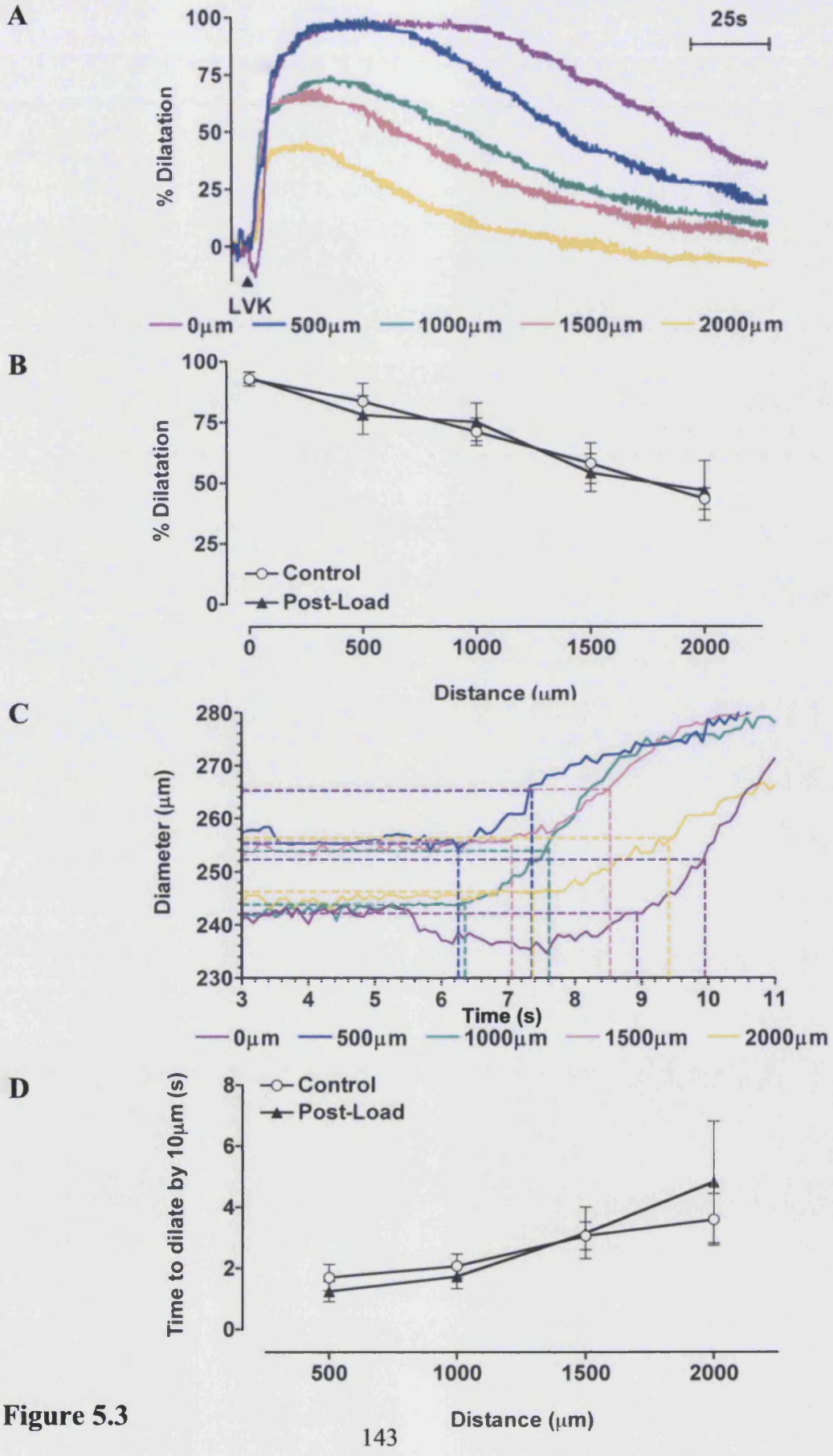
A
100
75
50
25
0
% Dilatation
25s
LVK
0µm
500µm
1000µm
1500µm
2000µm
B
100
75
50
25
0
% Dilatation
Control
Post-Load
0
500
1000
1500
2000
Distance (µm)
C
280
270
260
250
240
230
Diameter (µm)
3
4
5
6
7
8
9
10
11
Time (s)
0µm
500µm
1000µm
1500µm
2000µm
D
8
6
4
2
0
Time to dilate by 10µm (s)
Control
Post-Load
500
1000
1500
2000
Distance (µm)

Figure 5.3

5.3.2. Effect of carbenoxolone treatment on dilatation responses to ACh and LVK

The effect of treatment with carbenoxolone (100μM, 30min; n = 2) on spreading dilatation responses to ACh was difficult to ascertain (Figure 5.4A) as the extent of the conducted dilatation response was dependent on the magnitude of the local response, which itself, was affected by carbenoxolone treatment. Focal application of LVK, by the nature of its direct action on smooth muscle cells, was more able to evoke a local dilatation response and so the effect of carbenoxolone on conducted responses could be evaluated. Carbenoxolone treatment caused a marked increase in the decay of the spreading dilatation response to LVK at all upstream sites (500 - 2000μm; n = 3; Figure 5.4B).

5.3.3. Effect of pinocytic loading of connexin antibodies into the endothelium on conducted vasodilatation responses evoked by ACh and LVK

Inclusion of antibodies targeted against the intracellular C-terminus of connexin 37, connexin 40 or connexin 43 in the hypertonic solution (0.1mg ml^{-1}) during luminal treatment with the pinocytic loading protocol had no significant effect on the magnitude of spreading dilatation responses to ACh (connexin 37, 1mM, 3 – 60ms, n = 6; connexin 40, 1mM, 1 – 10ms; n = 3; connexin 43, 1mM, 1 – 30ms, n = 4; Figure 5.5). The time taken to dilate by 10μm at both local and distal sites in response to focal ACh application was also not significantly affected (Figure 5.6), however a tendency towards a decreased 10μm dilatation time was observed in 2 out of 4 arteries treated with the anti-connexin 43 antibody. Spreading dilatation responses to focal application of LVK following anti-connexin 37 antibody treatment tended towards a reduced magnitude of dilatation (2000μm, 23.1 ± 6.1%, 1mM, 3 - 100ms; n = 6; Figure 5.7A). The magnitude of dilatation of arteries treated with anti-connexin 40 antibody (1mM, 3 – 10ms; n = 2; Figure 5.7B) or anti-connexin 43 antibody (1mM, 10ms; n = 3; Figure 5.7C) was not affected. Further analysis of the time taken for the arteries to dilate by 10μm in each of the treatment groups showed that each of the antibody treatments showed a tendency towards increasing the initial time course of the dilatation response to LVK (Figure 5.8), however connexin 37 and connexin 43 antibody treatments appeared to have the most marked affects on LVK-evoked responses (connexin 37, 2000μm, 10.0 ± 2.9s, n = 4; connexin 40, 2000μm, 5.16 ± 1.8s, n = 2; connexin 43, 2000μm, 7.8 ± 3.2s, n = 2).

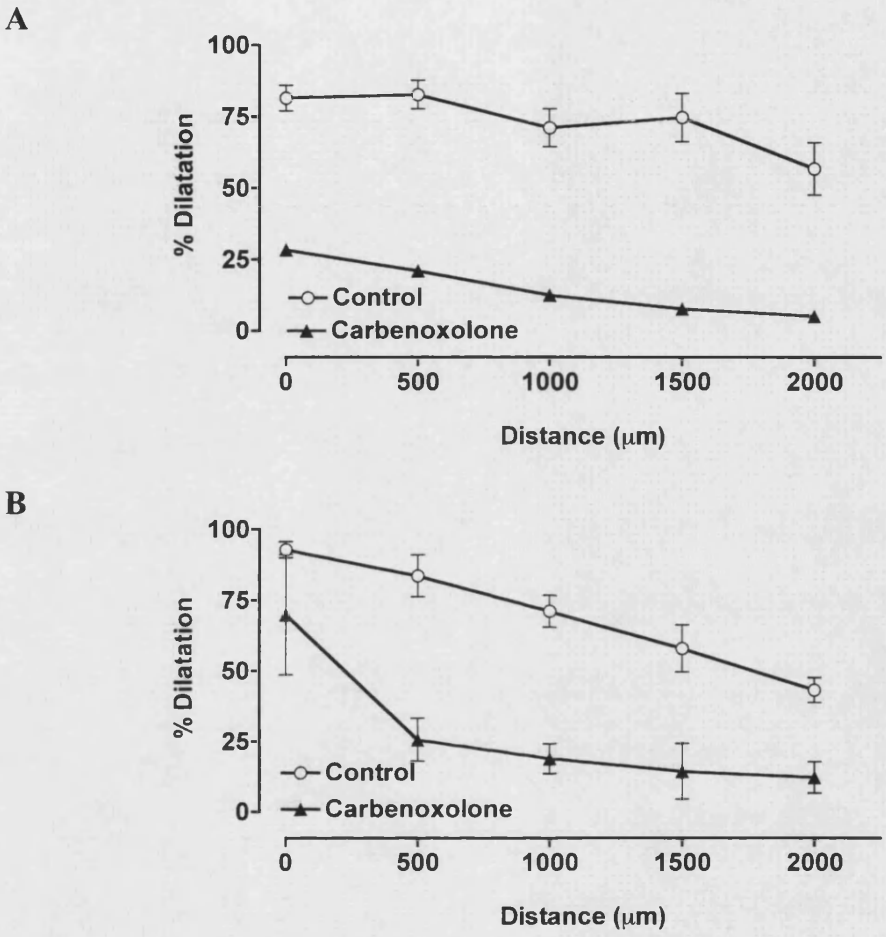

Figure 5.4 Effect of carbenoxolone treatment on spreading responses evoked by abluminal application of ACh and LVK

A, B, Mean spreading dilatation responses at the local (0μm) and upstream (500-2000μm) sites following downstream abluminal application of **A,** ACh and **B,** LVK under control conditions (**A**, ACh, *n*=5, 1mM, 1-100ms; **B,** LVK, *n*=4, 1mM, 3-30ms) and following treatment with carbenoxolone (100μM, 30min; **A,** ACh, *n*=2, 1mM, 30ms; LVK, *n*=3, 1mM, 100-300ms). Images were acquired at 12Hz. Diameter was measured simultaneously at all positions along the artery. L-NAME (100μM) present in all experiments. ACh-evoked responses are paired to LVK-evoked responses. Control and carbenoxolone treated arteries are unpaired but ACh and LVK-evoked responses were paired. Control data is also shown in Figures 5.2 and 5.3.

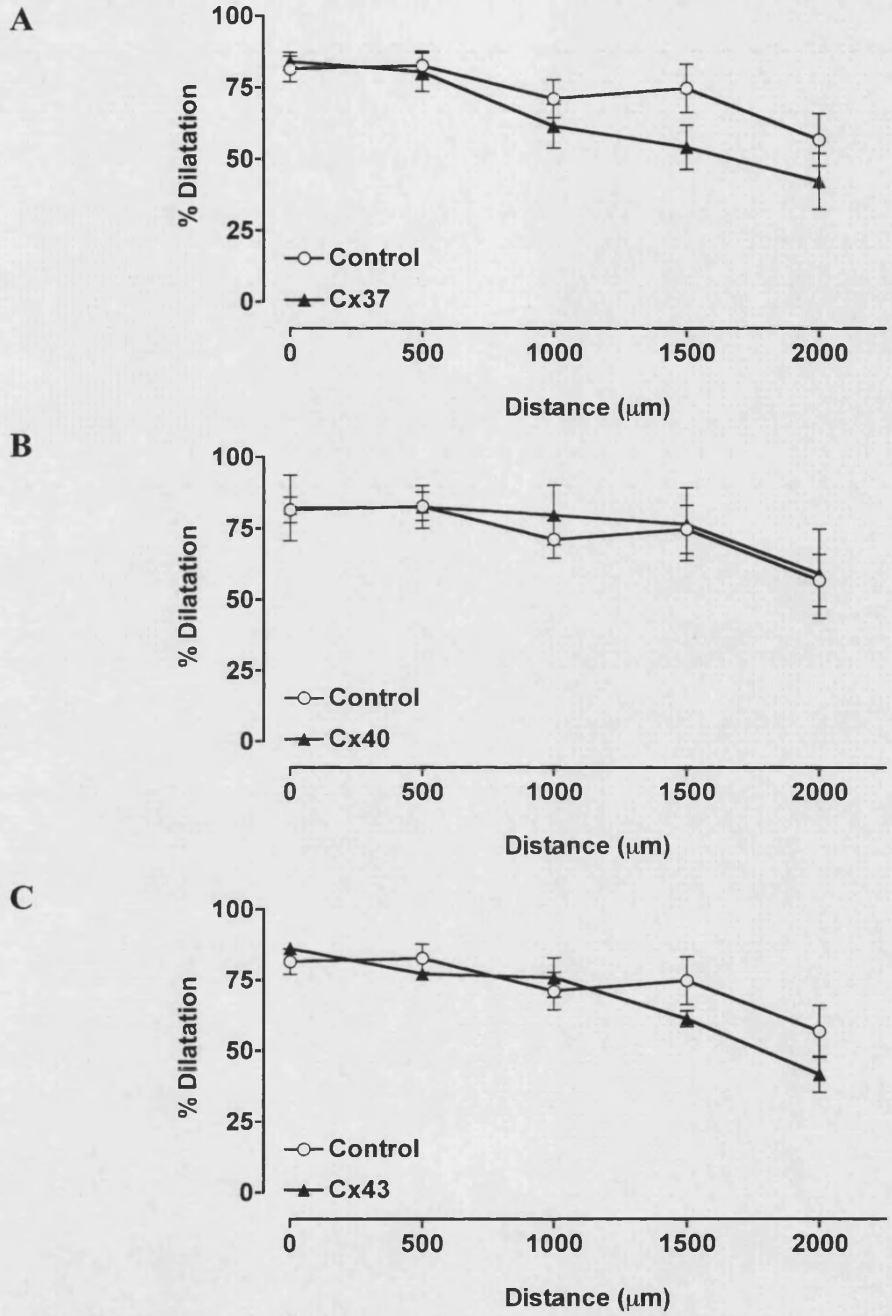

Figure 5.5 Effect of luminal anti-connexin antibody loading on spreading responses evoked by abluminal application of ACh

A, B, C, Mean spreading dilatation responses at the local (0μm) and upstream (500-2000μm) sites following downstream abluminal application of ACh under **A, B, C**, control conditions (n=5; 1mM, 10-100ms) and following luminal pinocytic loading of **A,** anti-connexin 37 antibody (n=6; 1mM, 3-60ms) **B,** anti-connexin 40 antibody (n=3; 1mM, 1-10ms) **C,** anti-connexin 43 antibody (n=4; 1mM, 1-30ms). Images were acquired at 12Hz. Diameter was measured simultaneously at all positions along the artery. L-NAME (100μM) present in all experiments. Control data is also shown in Figures 5.2 and 5.3.

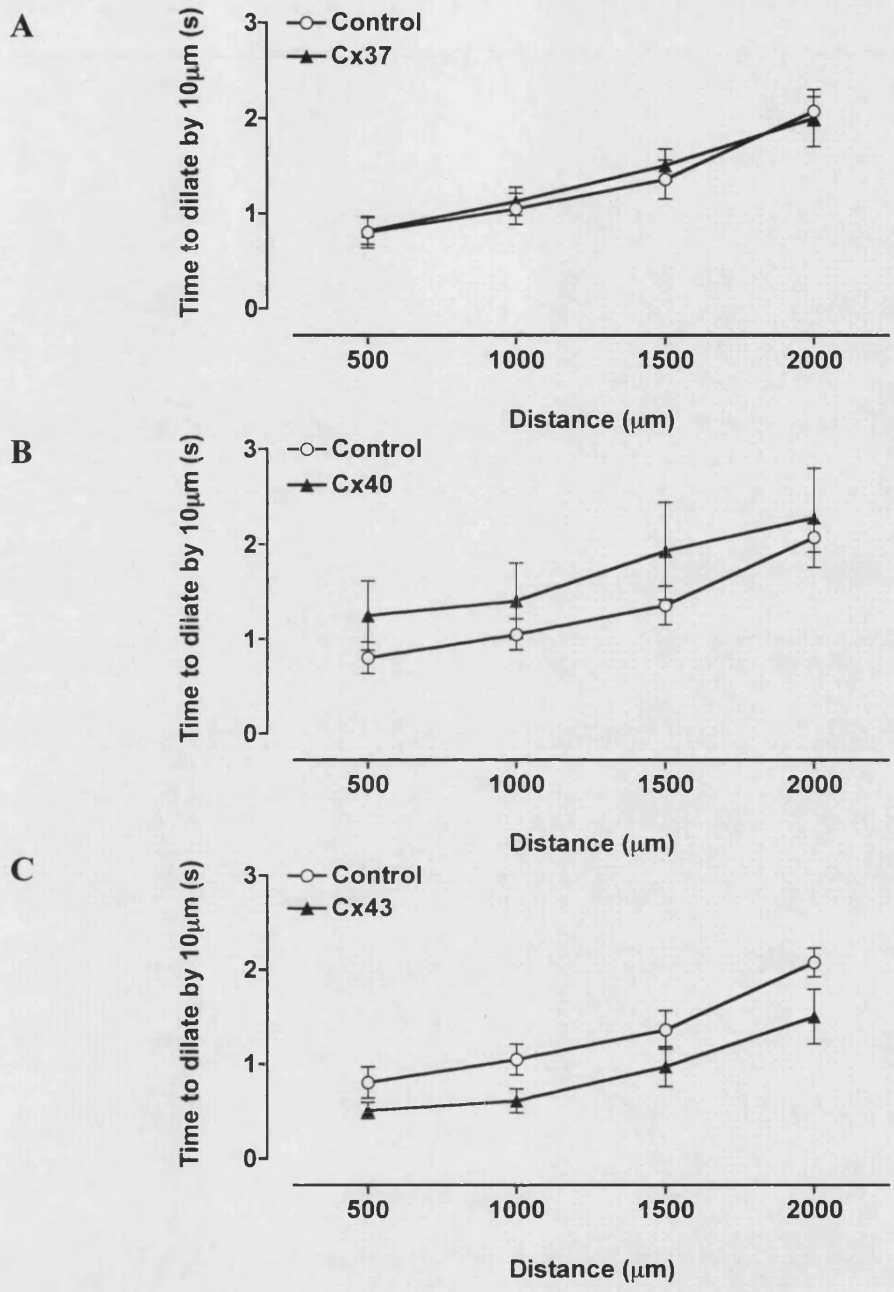

Figure 5.6 Effect of luminal anti-connexin antibody loading on the initial dilatation rate of spreading responses evoked by abluminal application of ACh

A, B, C, Mean time taken to dilate by 10μm at the local (0μm) and upstream (500-2000μm) sites following downstream abluminal application of ACh under **A, B, C**, control conditions (n=5; 1mM, 10-100ms) and following luminal pinocytic loading of **A,** anti-connexin 37 antibody (n=5-6; 1mM, 3-60ms) **B,** anti-connexin 40 antibody (n=3; 1mM, 1-10ms) **C,** anti-connexin 43 antibody (n=4; 1mM, 1-30ms). Images were acquired at 12Hz. Diameter was measured simultaneously at all positions along the artery. L-NAME (100μM) present in all experiments. Control data is also shown in Figures 5.2 and 5.3.

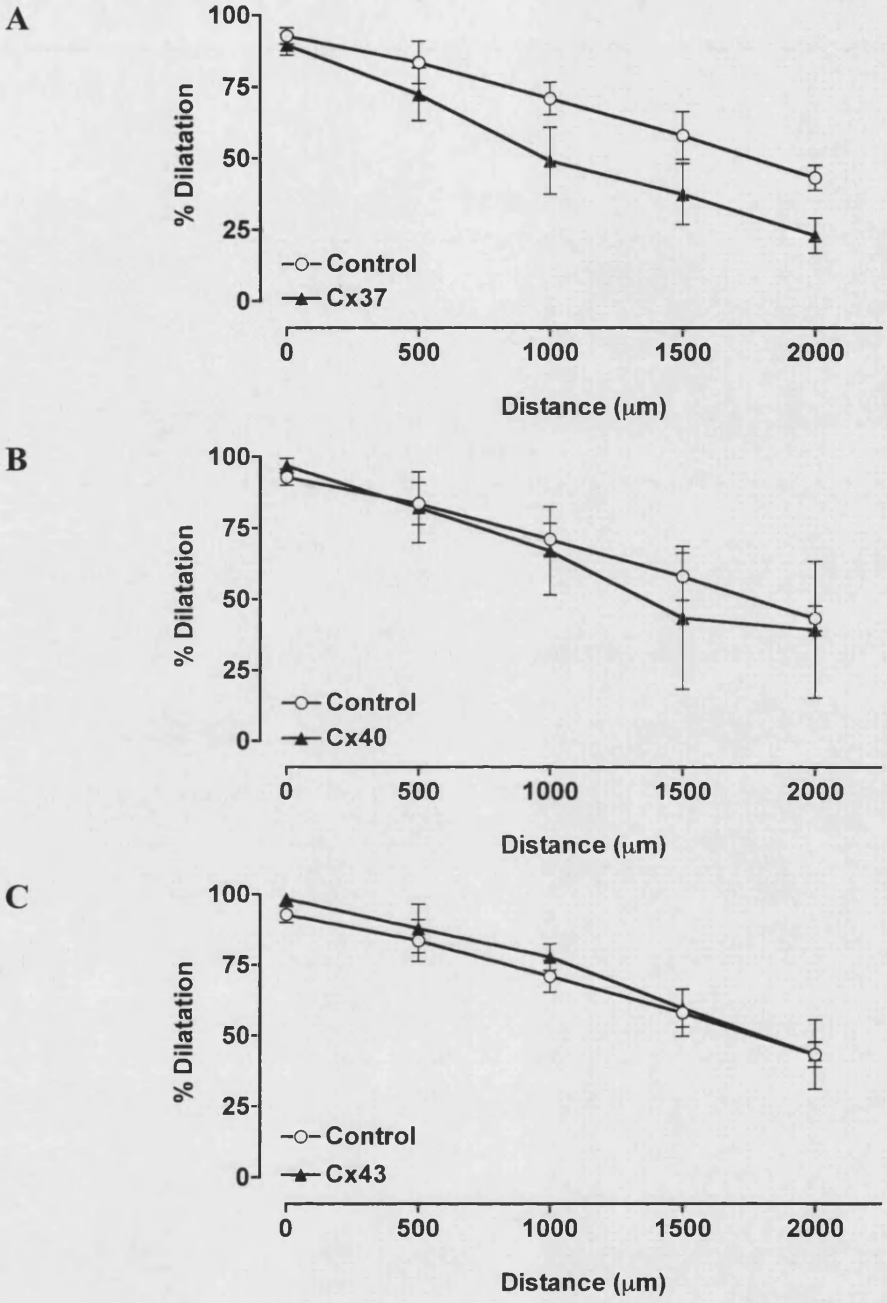

Figure 5.7 Effect of luminal anti-connexin antibody loading on spreading responses evoked by abluminal application of LVK

A, B, C, Mean spreading dilatation responses at the local (0μm) and upstream (500-2000μm) sites following downstream abluminal application of LVK under **A, B, C**, control conditions (n=4; 1mM, 3-30ms) and following luminal pinocytic loading of **A,** anti-connexin 37 antibody (n=6; 1mM, 3-100ms) **B,** anti-connexin 40 antibody (n=2; 1mM, 3-10ms) **C,** anti-connexin 43 antibody (n=3; 1mM, 10ms). Images were acquired at 12Hz. Diameter was measured simultaneously at all positions along the artery.L-NAME (100μM) present in all experiments. Control data is also shown in Figures 5.2 and 5.3.

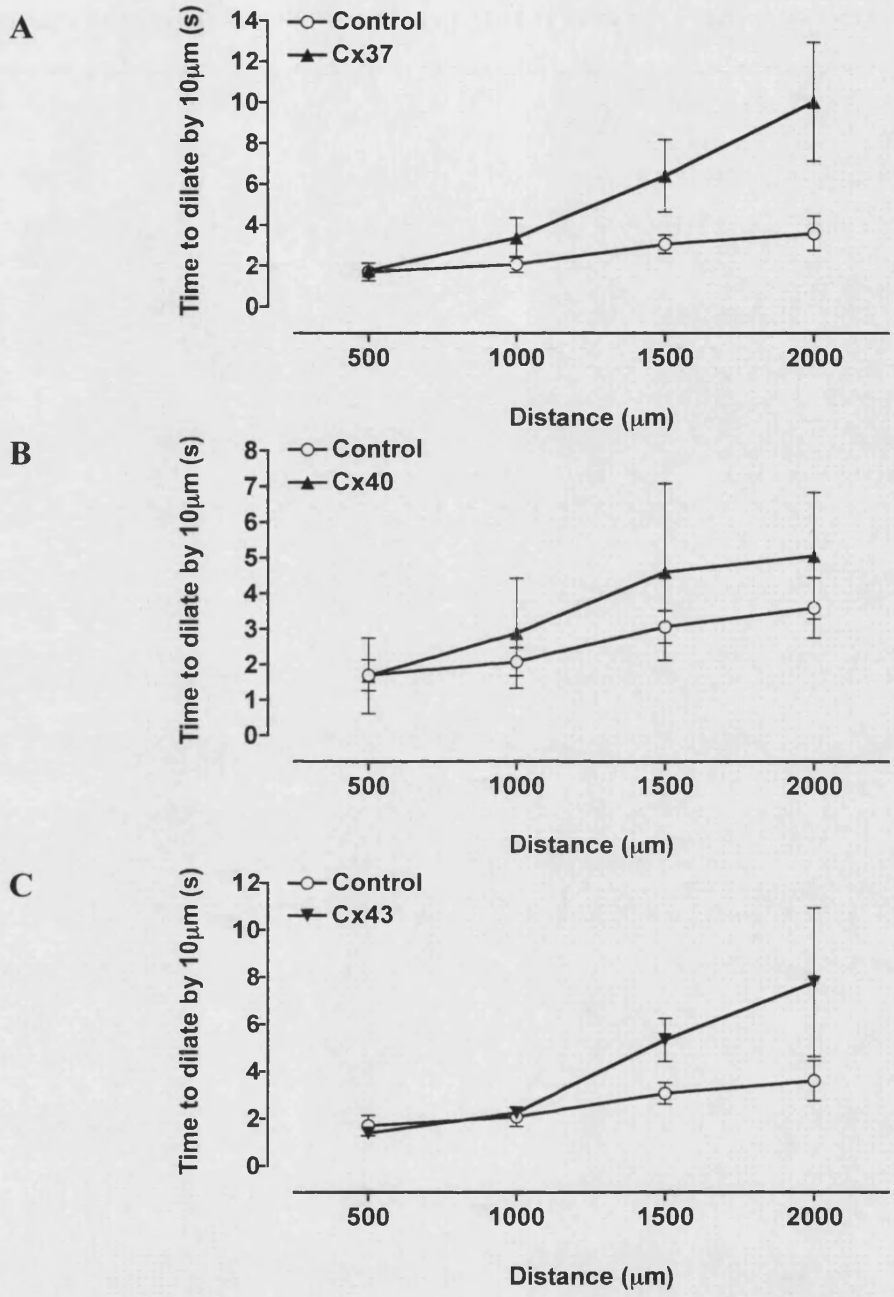

Figure 5.8 Effect of luminal anti-connexin antibody loading on the initial dilatation rate of spreading responses evoked by abluminal application of LVK

A, B, C, Mean time taken to dilate by 10μm at the local (0μm) and upstream (500-2000μm) sites following downstream abluminal application of LVK under **A, B, C**, control conditions (n=3-4; 1mM, 3-30ms) and following luminal pinocytic loading of **A,** anti-connexin 37 antibody (n=4-6; 1mM, 3-100ms) **B,** anti-connexin 40 antibody (n=2; 1mM, 3-10ms) **C,** anti-connexin 43 antibody (n=2-3; 1mM, 10ms). Images were acquired at 12Hz. Diameter was measured simultaneously at all positions along the artery.L-NAME (100μM) present in all experiments. Control data is also shown in Figures 5.2 and 5.3.

Concentration-response curves to ACh were assessed following evaluation of the effects of endothelial cell loading with anti-connexin antibodies on conducted dilatation responses. Endothelial cell loading with antibodies directed against either connexin 37 (n = 6) or connexin 43 (n = 4) had no clear effect on concentration-dependent dilatation responses to ACh (Figure 5.9B). In contrast loading of antibodies directed against connexin 40 (n = 2 - 3) caused a rightward shift in the concentration-response curve to ACh and a depression of the maximal response attained with 3μM ACh (Figures 5.9A and B). Endothelial cell viability remained intact following luminal pinocytic loading of connexin antibodies as evidenced by the minimal endothelial cell staining by propidium iodide (0.01%wv^{-1}) when compared to tissue damaged by cannulation (Figure 5.9C). Please note that the data obtained from these arteries also contributed to the concentration-response data illustrated in section 4.3.8.

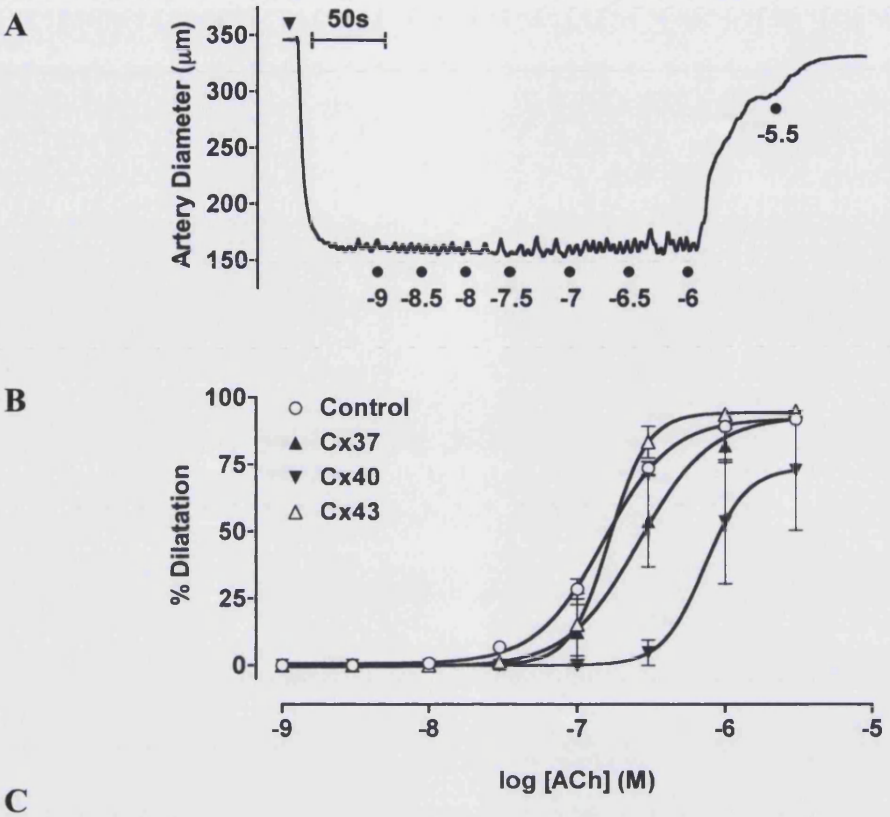

Figure 5.9 Effect of luminal pinocytic loading of connexin antibodies on dilatation responses to ACh

A, Representative trace and **B,** concentration-response curves illustrating the effects of luminal pinocytic loading of **B, a**nti-connexin 37 (n=6), **A, B,** anti-connexin 40 (n =2-3) and **B**, anti-connexin 43 antibodies (n=3) on ACh-evoked dilatation responses. **C,** Representative images of propidium iodide (0.01%wv^{-1}) staining of damaged endothelial and smooth muscle cells at the site of cannulation (left hand panel; merged images) and the middle of the artery (middle and right hand panels) following pinocytic loading of anti-connexin 40 antibodies. All data is paired to spreading response experiments. L-NAME (100μM) present in all experiments. **A,** Triangle indicates addition of PE. **C,** bar 50μm. Images were taken using a x40, water immersion objective.

5.4. Discussion

The electrotonic conduction of hyperpolarization though the endothelium via gap junctions is thought to make a significant contribution to the longitudinal spread of vasodilatation. Indeed recent knock out studies in which the deletion of connexin 40 was shown to abrogate both ACh- and electrically-evoked spreading vasodilatations support such a hypothesis (de Wit *et al.*, 2000; Figueroa *et al.*, 2003). However direct evidence by short-term manipulation of the gap junctions has not been described. Within the present study selective endothelial cell loading of antibodies directed against the known vascular connexins was therefore performed (please see chapter 4) in an attempt to evaluate the contribution of each connexin to the spreading vasodilatation response in rat isolated and pressurized small mesenteric arteries.

5.4.1. Characteristics of the conducted vasodilatation response to ACh and LVK

In the present study focal stimulation of rat small mesenteric arteries with either ACh or LVK was shown to evoke a robust local and spreading vasodilatation consistent with previous observations (Goto *et al.*, 2004; Takano *et al.*, 2004) that together may be indicative of the importance of ascending vasodilatation responses throughout the circulation (Takano *et al.*, 2005). In contrast to previous studies however, the rate of decay appeared qualitatively slower (Takano *et al.*, 2004). Based on previous reports (Dietrich *et al.*, 1996) it is unlikely that the marginally increased spritz duration used within the present study facilitated an increased diffusion of the agonist upstream. Indeed small beads were included in the superfusate at various stages of the experimental protocol to enable direct observation of the flow direction. Furthermore, the severe attenuation of the conducted response to LVK in the presence of carbenoxolone documented herein would suggest that agonists were unable to diffuse to the upstream sites.

Passive, longitudinal cell-to-cell conduction of the hyperpolarization response is often characterised by a decay of ~70% at a distance ~1500μm from the site of stimulation. Given the intrinsic link between vascular tone and membrane potential (please see section 1.2.4; Takano *et al.*, 2004) this is likely also reflected by a pronounced decay of the spreading dilatation response at that site (Hirst & Neild, 1978; Segal *et al.*, 1999; Takano *et al.*, 2004). The slow decay of the responses documented in the current study

may therefore be indicative of an active electrotonic conduction process, possibly associated with an additional or regenerative current source that is associated with the opening of ion channels but is not directly activated by agonist stimulation and/or improved cell-to-cell coupling (Neild & Crane, 2002; Segal & Neild, 1996; Segal *et al.*, 1999; Takano *et al.*, 2004).

Importantly, facilitation of the conducted dilatation responses to agonists such as ACh occurs independently of the magnitude of the local hyperpolarization response (Emerson *et al.*, 2002). Emerson *et al* (2002) demonstrated that despite identical local hyperpolarization responses, the length constant of the spreading response to ACh was almost 60% greater than that seen for current injection. Thus it has subsequently been proposed that some of the downstream signalling cascades activated by either ACh or LVK (please see sections 1.3.1.1 and 1.3.2) may contribute to amplification of the conducted dilatation response (Emerson *et al.*, 2002; Takano *et al.*, 2004).

Numerous reports examining the contribution of a neural mechanism to the conducted vasomotor response have described a minimal sensitivity of the spreading dilatation response to the Na^+ channel inhibitor tetrodotoxin and thus rejected the hypothesis of a of a role for an intrinsic neuronal conduction of the vasomotor response (Berg et al., 1997; Figueroa et al., 2003; Segal, 1994; Segal & Duling, 1989; Segal & Duling, 1987; Segal et al., 1999). More recently however, it has been suggested that a neural component may still be present, but one associated with the activation of sensory nerve fibres (Thengchaisri & Rivers, 2005). In support of such a mechanism Mupanomunda *et al* (1998) have described clear visualization of the perivascular nerves of the rat mesenteric artery following immunohistochemical staining for CGRP. However, the complete attenuation of conducted dilatation responses to ACh and LVK following denudation of the endothelium (Takano et al., 2004) would suggest that were this mechanism present, its contribution to conducted dilatation responses would not be significant, unless the endothelium was involved secondarily to nerve stimulation.

The influence of flow and shear stress on spreading vasodilatation in larger conduit arteries is well established and could perhaps also contribute to conducted vasomotor responses in the smaller resistance arteries and arterioles (Gustafsson & Holstein-

Rathlou, 1999; Joannides et al., 1994; Lie et al., 1970; Pohl et al., 1986; Segal & Jacobs, 2001; Thorsgaard et al., 2003). Indeed Thorsgaard *et al* (2003) have described a flow-dependent local vasodilatation response within the rat small mesenteric artery. However, an obligatory role for a flow-mediated mechanism of spreading vasodilatation is unlikely as conducted vasomotor responses in both isolated arteries and within *in vi*vo and *in situ* preparations in which flow or pressure have been eliminated are unaffected (Duling & Berne, 1970; Hilton, 1959; Rivers, 1997b; Segal, 1994; Segal & Duling, 1986a; Segal & Duling, 1987; Segal *et al.*, 1999; Takano *et al.*, 2004).

Multiple endothelium-dependent pathways could feasibly contribute to the conducted vasodilatation. Indeed many reports cite an obligatory role for both endothelial cell hyperpolarization and NO in the spreading vasodilatation response (Domeier & Segal, 2007; Doyle & Duling, 1997; Rivers, 1997a; Segal *et al.*, 1999). A recent report from Domeier & Segal (2007) demonstrated that at least in the hamster retractor muscle two interacting phases of the conducted vasodilatation response could be distinguished pharmacologically: The rapid initiation and amplitude of the response, sensitive to TRAM-34 and apamin termed the 'electromechanical' response followed by a second 'slow' conducted vasodilator component visualized as the sustained phase of the response and mediated by the endothelium and Ca^{2+}-dependent production of autacoids such as NO. This hypothesis is consistent with the results of Doyle & Duling (1997) and Segal *et al* (1999) who both described an attenuation of the duration of the conducted response following selective blockade of eNOS but no change in response amplitude. Given that our experiments were conducted in the presence of L-NAME and used relatively short pulse durations (Doyle & Duling, 1997) it is likely that we are only evaluating the contribution of the 'fast' hyperpolarization-dependent component. It would therefore seem that some mechanism able to regenerate the hyperpolarization or limit its dissipation as it is conducted upstream is apparent (Takano *et al.*, 2004).

A role for endothelial cell K_{ir} in the conducted hyperpolarization response has been proposed, which given their increased conductance following hyperpolarization is indeed conceivable (Goto *et al.*, 2004; Jantzi *et al.*, 2006; Neild & Crane, 2002; Rivers *et al.*, 2001; Takano *et al.*, 2004). Within both porcine coronary arterioles (Rivers *et al.*, 2001) and hamster retractor muscle feed arteries (Jantzi *et al.*, 2006) conducted

dilatation responses to KCl and bradykinin were attenuated by the K_{ir} channel blocker barium. Goto *et al* (2004) also documented a significant attenuation of ACh-evoked spreading hyperpolarization and vasodilatation responses in the rat primary mesenteric artery following incubation with barium (Goto *et al.*, 2004). Results from this laboratory however, show that barium has no effect on the conducted dilatation responses to either LVK or ACh in the rat small mesenteric artery suggesting that within this preparation the conducted dilatation response is facilitated by at least one other mechanism (Takano *et al.*, 2004).

The importance of endothelial cell intracellular calcium in regulating local vasomotor responses to ACh is clear (please see section 1.3.2; Freay *et al.*, 1989; Fukao *et al.*, 1997b; McSherry *et al.*, 2005; Oishi *et al.*, 2001). A role for Ca^{2+} in the propagation of the vasodilatation response is, however, more ambiguous. A number of reports, including studies conducted within the isolated rat mesenteric artery, have shown that conducted hyperpolarization and vasodilatation responses are not accompanied by a remote rise in endothelial cell Ca^{2+} (Dora et al., 2003b; Segal & Duling, 1989; Takano et al., 2004). However, conversely, reports of a conducted rise in endothelial cell Ca^{2+}, albeit associated with a slower, NO-dependent dilatation component have also been published (Domeier & Segal, 2007; Duza & Sarelius, 2003; Uhrenholt *et al.*, 2007). Importantly, the studies of Segal *et al* (Domeier & Segal, 2007; Uhrenholt *et al.*, 2007) demonstrated that the longitudinal conduction of the Ca^{2+} signal through the endothelium occurred after the decrease in smooth muscle cell Ca^{2+} and the longitudinal transfer of hyperpolarization, implying that these mechanisms are likely to be distinct from the conducted hyperpolarizing responses to LVK and ACh observed in the rat mesenteric preparation (Takano *et al.*, 2004). However, discrete rises in endothelial cell Ca^{2+}, for example in Ca^{2+} microdomains within the arterial wall would not be apparent by the Ca^{2+}-imaging methods previously described (Domeier & Segal, 2007; Takano *et al.*, 2004). Thus it is possible that elevations of Ca^{2+} in distinct microdomains, perhaps associated with the connexin channels themselves or with enzymes such as PLA_2, could facilitate the production of endothelial cell factors such as 11,12-EETs, which could contribute to the magnitude of the distal vasodilatation response (Popp et al., 2002). Indeed, inter-endothelial cell and heterocellular gap junctional communication have been shown to be upregulated by PKA downstream of 11,12-EET production within

sheets of porcine coronary artery endothelial cells (Popp *et al.*, 2002) and by cAMP within the rabbit iliac artery respectively (Griffith *et al.*, 2002).

5.4.2. The role of cell-to-cell coupling in the conducted vasodilatation response

As documented previously (please see chapter 4 (Goto *et al.*, 2002; Mather *et al.*, 2005)) carbenoxolone resulted in disruption of the ACh-evoked response at the local site. However, this could not be overcome sufficiently to match the local vasodilatation seen under control conditions consequently impairing an accurate assessment of the conducted response. In contrast, LVK evoked a local dilatation response that was well maintained in the presence of the putative gap junction uncoupler, consistent with its direct hyperpolarizing action on the smooth muscle (please see section 1.3.1.1). The spreading vasodilatation response to LVK was however, severely attenuated by carbenoxolone, indicative of a gap junctional facilitated transfer of the response upstream. However, the endothelium-dependent nature of the conducted hyperpolarization to LVK (Takano *et al.*, 2004) also meant that carbenoxolone may have attenuated the local transfer of hyperpolarization from the smooth muscle to the endothelium, disrupting the conducted response at the initiation site. Indeed, without any measurements of endothelial cell membrane potential, selective inhibition of the homocellular gap junctions cannot be assumed. Thus in order to more closely examine the effects of endothelial cell gap junction blockade we employed the pinocytic loading technique to selectively load antibodies targeted against known endothelial cell connexins into the endothelium (please see chapter 4; Mather *et al.*, 2005).

The negligible effects of the pinocytic loading protocol on the conducted dilatation response crucially demonstrated that the blockade of conducted vasomotor responses that may occur using hypertonic sucrose solutions (Murrant & Sarelius, 2000; Segal & Duling, 1989) was either transient and restricted to the loading stage of the protocol or was not apparent within the present study. Indeed, selective endothelial cell loading of antibodies directed against connexins 37, 40 or 43 had no significant effect on the amplitude of the conducted vasodilatation responses to either ACh or, with the exception of connexin 37, LVK.

A slight reduction in magnitude and increase in time taken for the arteries to dilate to LVK stimulation was seen at positions distal to the site of agonist application following loading of antibodies directed against connexin 37. However, this was non-significant and such a comparison of the time taken to dilate is instilled with inaccuracies associated with the mechanisms required to reverse smooth muscle cell contraction (please see section 1.3; Emerson *et al.*, 2002). Indeed, the present observation that the time taken to dilate by 10μm in response to ACh was almost twice as fast as that with LVK likely reflects the differential dilatation mechanisms associated with each agonist (please see sections 1.3.1.1 and 1.3.2), i.e. the rate of dilatation at the local site was slower for LVK, therefore dilatation at the remote sites dilate would also take longer. Given that hyperpolarization is so intrinsically linked to the remote dilatation responses to both ACh and LVK (Takano *et al.*, 2004) the increased time taken to dilate by 10μm in response to LVK following loading of anti-connexin 37 antibodies may however, very loosely, reflect a decreased rate of conduction of the hyperpolarization response.

In contrast to previous results (Chapter 4; Mather *et al.*, 2005) only a small suppression of the maximal dilatation response to bath application of ACh (3μM) was seen following endothelial cell loading of anti-connexin 40 antibodies. The robust spreading responses observed herein might therefore reflect limited loading of the antibodies into the endothelium. Indeed without the use of fluorescently tagged connexin specific antibodies in the present study it is impossible to demonstrate that the antibodies are actually present at the time of agonist stimulation. Differences in antibody loading could reflect transport of the anti-connexin antibodies out of the endothelium, or despite previous reports to the contrary, the lysosomal degradation of the antibodies over the time taken to achieve the correct conditions for evaluation of the conducted dilatation response (Chakrabarti *et al.*, 1989; Ober *et al.*, 2004; Okada & Rechsteiner, 1982; Predescu *et al.*, 2004). Repeated ACh concentration-response curves following selective endothelial cell loading of antibodies directed against connexin 40 could therefore be performed to evaluate whether the inhibitory effects of this protocol that were previously described are reversed over time (please see chapter 4; Mather *et al.*, 2005).

Importantly, the concentrations of ACh used to evoke the conducted dilatation responses, although likely diluted at the time of focal application, are potentially far

higher than the micromolar concentrations used previously when studying the effects of anti-connexin antibodies on the radial ACh-evoked dilatation response (Chapter 4; Mather *et al.*, 2005). It is therefore conceivable that any effects of the connexin antibodies were masked by the near-maximal nature of the conducted dilatation response, or at least subtle changes could not be measured. Within this laboratory a novel triple cannulation method has recently been developed for the evaluation of conducted dilatation responses to luminally applied purinoceptor agonists (please see chapter 7; Figure 7.1) that may be of use for further development of the current study. Using a third cannulation pipette, the branch at an arterial bifurcation is cannulated, through which perfusate containing the agonist and carboxyfluorescein is infused. By applying a low level of flow (50μL min^{-1}) through the lumen of the feed artery diffusion of the agonist upstream is prevented (as visualized by the fluorescence of the carboxyfluorescein) and a conducted dilatation response spreading from the side branch upstream into the feed artery may be observed. By applying the agonist luminally, direct and maintained contact of the agonist with the endothelium occurs, enabling the use of a lower agonist concentration to evoke a sustained spreading response. Combining this approach with application of the pinocytic loading protocol to the feed artery would leave the local dilatation response in the branch unaffected, and as such the significance of any inhibitory effects observed at the remote sites can be measured reliably and in more detail.

A third explanation for the poor inhibitory effects of the anti-connexin antibodies is that maximal endothelial cell loading of the connexin antibodies did occur but the number of antibodies loaded was not sufficient to block every gap junction channel within the large homocellular plaques prevalent within the endothelium of this preparation (Sandow & Hill, 2000). Indeed, the small attenuation of the conducted response to LVK observed following treatment with the anti-connexin 37 antibody and the extensive endothelial cell border staining for connexin 37 would support such a hypothesis (Goto *et al.*, 2004; Gustafsson *et al.*, 2003; Kansui *et al.*, 2004; Sandow *et al.*, 2006). However, a simpler explanation may be that blockade of more than one connexin isoform is necessary to block conducted vasodilatation. Given the incomplete blockade of the radial EDHF-type dilatation response by endothelial cell loading of anti-connexin 40 antibodies under conditions of low tone but in the presence of ouabain it is also

likely that multiple connexins could contribute to both the radial and longitudinally-transferred (Figure 5.1) dilatation responses under the low tone conditions used within the present study (Chapter 4; Doughty *et al.*, 2000; Edwards *et al.*, 1999; Matchkov *et al.*, 2006; Mather *et al.*, 2005; Sandow *et al.*, 2006; Sandow *et al.*, 2002). It is therefore proposed that experiments be performed to assess the effects of the loading protocol on smooth muscle cell hyperpolarization responses to ACh under conditions of high tone, enabling a direct assessment of the effects of the protocol on the radial conduction of the hyperpolarization response. Subsequently, a re-evaluation of the pinocytic loading method would also be performed to enable selective endothelial cell loading of a greater volume of antibody to facilitate increasing the concentration of antibodies loaded and the targeting of multiple connexin subtypes.

To summarize, the present report describes the simultaneous observation of local and remote vasodilatation responses to ACh and LVK at distances up to 2mm from the point of stimulation that showed little decay in the extent of vasodilatation with distance. Incubation with the non-selective gap junction uncoupler carbenoxolone attenuated conducted dilatation responses to LVK and both local and conducted responses to ACh. In contrast selective endothelial cell loading of antibodies directed against the known endothelial cell connexins had minimal effects on the conducted vasodilatation responses to either agonist. Due to the preliminary nature of the gap junction uncoupler methods presented, exact conclusions as to the nature of the cell-to-cell coupling response cannot be made and further work is proposed.

5.5. Acknowledgments

I would like to thank Professor Chris Garland for the helpful discussion of this work.

6. Characterisation of nucleotide-evoked dilatation responses

6.1. Introduction

The contribution of endothelium-dependent dilatation responses to the regulation of vascular tone is now well established. Key roles for the diffusible factors NO, EDHF, PGI_2 and the direct cell-to-cell transfer of hyperpolarization from the endothelium to the smooth muscle via MEGJs have been identified (please see section 1.3.2; Chen *et al.*, 1988; Ignarro *et al.*, 1987; Mather *et al.*, 2005; Moncada & Vane, 1978; Palmer *et al.*, 1987; Sandow & Hill, 2000; Taylor *et al.*, 1988; Vane, 1994). The activation of these mechanisms is associated with a variety of stimuli including the mechanical forces associated with shear stress and both the direct and indirect actions of various agonists on the endothelium (Busse *et al.*, 2002; Busse & Fleming, 2003; Dora *et al.*, 1997; Dora *et al.*, 2000b; Fleming & Busse, 2003; Ledoux *et al.*, 2006; McGuire *et al.*, 2001; White & Hiley, 1997b).

Historically, ACh has been used to evoke the endothelium-dependent dilatation response for its study (Furchgott & Zawadzki, 1980). The robust nature of the ACh-evoked response and the selectivity of the agonist for the endothelium make it an ideal candidate for the study of endothelium-dependent dilatation. Indeed such robust vasoactive responses could be construed as supporting the physiological relevance of this agonist. However, despite localization of acetylcholinesterase to the adrenergic perivascular nerves of the rat mesentery no direct cholinergic innervation of this vascular bed could be seen (Furness, 1973). Atropine-sensitive dilatation responses of the hamster retractor muscle microcirculation have been reported (VanTeeffelen & Segal, 2006). However, plasma concentrations of ACh in the rat and human were found to be in the low nanomolar range (Fujii *et al.*, 1995), rather than the high nanomolar/ low micromolar range associated with robust endothelium-dependent dilatations. Although release of ACh from circulating cells directly adjacent to target cells such as the endothelium would minimise degradation by acetylcholinesterase possibly enabling concentrations to reach levels sufficient to evoke a response (Fujii *et al.*, 1995), these findings have yet to be verified.

In contrast, the release of purinoceptor agonists such as ATP, adenosine diphosphate (ADP) and UTP into the vasculature has been documented and shown to come from a variety of sources (Dubyak & el-Moatassim, 1993; Ralevic & Burnstock, 1998). These

include sympathetic and sensory nerve terminals (Su, 1983), circulating cells within the lumen of the vessel, particularly red blood cells responding to low PO_2 and platelets (Beigi *et al.*, 1999; Dietrich *et al.*, 2000; Ellsworth, 2004; Ellsworth *et al.*, 1995; Gonzalez-Alonso *et al.*, 2002; Lazarowski & Harden, 1999; Motte *et al.*, 1995), damaged cells and the vascular endothelium itself (Bodin & Burnstock, 2001; Milner *et al.*, 1992; Pearson, 1979; Saiag, 1995; Yamamoto *et al.*, 2003). Indeed, during exercise, micromolar concentrations of plasma ATP have been measured in the femoral circulation of humans (Rosenmeier *et al.*, 2004). The action of these nucleotides on the P2X and P2Y receptors present within the vascular wall may therefore represent a key mechanism for the physiological regulation of vascular tone.

Previous studies have suggested the presence of the $P2X_1$, $P2X_4$, $P2X_5$, and $P2X_7$ nucleotide-gated ion channels and the $P2Y_1$, $P2Y_2$, $P2Y_4$, $P2Y_6$ and $P2Y_{11}$ G protein-coupled receptors within the rat mesenteric arterial bed. Of these $P2Y_1$, $P2Y_2$, $P2Y_4$, $P2Y_{11}$, $P2X_1$ and $P2X_7$ have been associated with vasodilator responses (Buvinic *et al.*, 2006; Galligan *et al.*, 2001; Gitterman & Evans, 2000; Harrington & Mitchell, 2004; Lewis & Evans, 2000; Liu *et al.*, 2004; Malmsjo *et al.*, 2000a; Malmsjo *et al.*, 2002; Malmsjo *et al.*, 2000b; Malmsjo *et al.*, 1999; Mistry *et al.*, 2003). However of the studies described, many employed wire myograph techniques that can limit the investigator to bath application of agonists. This leads to activation of smooth muscle purinoceptors and subsequent vasoconstriction. More recently however, this complication has been overcome by the luminal application of purinoceptor agonists in the pressurized artery set-up (Liu *et al.*, 2004). Luminal perfusion of agonists such as ATP and UTP evoked an apparently flow-dependent dilatation response via activation of both P2Y and P2X receptors. The dilatation response to ATP was shown to be dependent on the release of a raised K^+-sensitive, EDHF-like, H_2O_2 component (Liu *et al.*, 2004; Liu *et al.*, 2006a) and is consistent with previous studies documenting the contribution of both NO and EDHF to the vasodilator and hyperpolarization responses to purinoceptor agonists within rat mesenteric arteries (Malmsjo *et al.*, 1999; Mistry *et al.*, 2003). However, the individual contribution of the two characteristic K^+ channels activated in the EDHF response (please see section 1.3.2.6), the IK_{Ca} and SK_{Ca} channels, has not been ascertained for purinoceptor-mediated vasodilatation responses. Therefore, within the present study the relative contributions of IK_{Ca} and SK_{Ca} to the

EDHF-type responses evoked by ATP, UTP and the non-hydrolyzable ADP analogue, ADPβS were investigated in rat isolated and pressurized small mesenteric arteries. Using the selective $P2Y_1$ inhibitor MRS2179, the contribution of $P2Y_1$ receptor activation to the dilatation response to luminal perfusion of the three agonists was also evaluated.

In addition to the EDHF-type response evoked by the luminal perfusion of purinoceptor agonists, Liu *et al* (2004) documented an attenuation of the dilatation response to the non-hydrolyzable purinoceptor agonists ATPγS and adenosine 5'-(β,γ-imido)triphosphate tetralithium salt hydrate (AMP-PNP) upon repeated agonist exposure. The decay of the response was attributed to a lower concentration of agonist at the cell surface upon each successive period of flow (agonist delivery) as a result of limited ectonucleotidase breakdown (Liu *et al.*, 2004). However, it could also be explained by desensitization of the receptors. Given previous reports detailing a role for PKC in the desensitization of the $P2Y_1$ and $P2Y_2$ purinoceptors (Chen & Lin, 1999; Hardy *et al.*, 2005) the possible influence of PKC on the profile of the responses to ATP, UTP, ADPβS and ATPγS was also examined in the present study.

Parts of this work have been reported previously (Winter & Dora, 2006b; Winter & Dora, 2005).

6.2. Methods

6.2.1. Rat mesenteric artery isolation and cannulation

Please see section 2.1.

6.2.2. Pressure myography

Arteries were mounted in a commercially available pressure myograph (10ml; 120CP, Danish Myo Technology, Denmark; Figure 2.1). For cannulation and equilibration methods please see section 2.2. Endothelial cell viability was assessed as a >90% control dilatation to ACh (1μM) following pre-constriction with PE (1 - 3μM). Arteries were maintained at 50mmHg and 37°C unless otherwise stated.

6.2.3. Concentration-response curves

All experiments were performed in the presence of L-NAME (100μM, 20min). Inhibition of cyclooxygenase was not required, as indomethacin (10μM) has been shown to have no effect on purinoceptor agonist or ACh-evoked dilatation responses within the rat mesenteric artery (please see section 1.3.2.4)(Mistry *et al.*, 2003).

6.2.3.1. ACh concentration-dependent responses

Cumulative concentration-response curves to ACh (1nM-3μM) were performed following submaximal (~70%) constriction to PE (0.5-10μM).

6.2.3.2. Purinoceptor agonist concentration-dependent responses

The purinoceptor agonists were perfused through the lumen at ~90 μL/min for two 2min periods (unless otherwise stated), interspersed with one 2min no flow period using a BeeHive® syringe pump system (Figure 6.1; Bioanalytical systems, West Lafayette, Indiana, USA). This perfusion flow rate equates to a shear stress of ~10 dyn/cm^2 in fully dilated arteries. Consecutive, non-cumulative concentration-responses to ATP (10nM - 3μM), UTP (0.3μM - 30μM), ADPβS (30nM - 1μM) and ATPγS (1 and 3μM) were obtained upon stabilization of submaximal levels of PE-evoked background tone (~70%; 0.5 - 10μM). Arteries were luminally-perfused with MOPS and left to equilibrate for 10min between each agonist and concentration-response curve to minimise receptor desensitization. Indeed, reversal of the desensitization response is

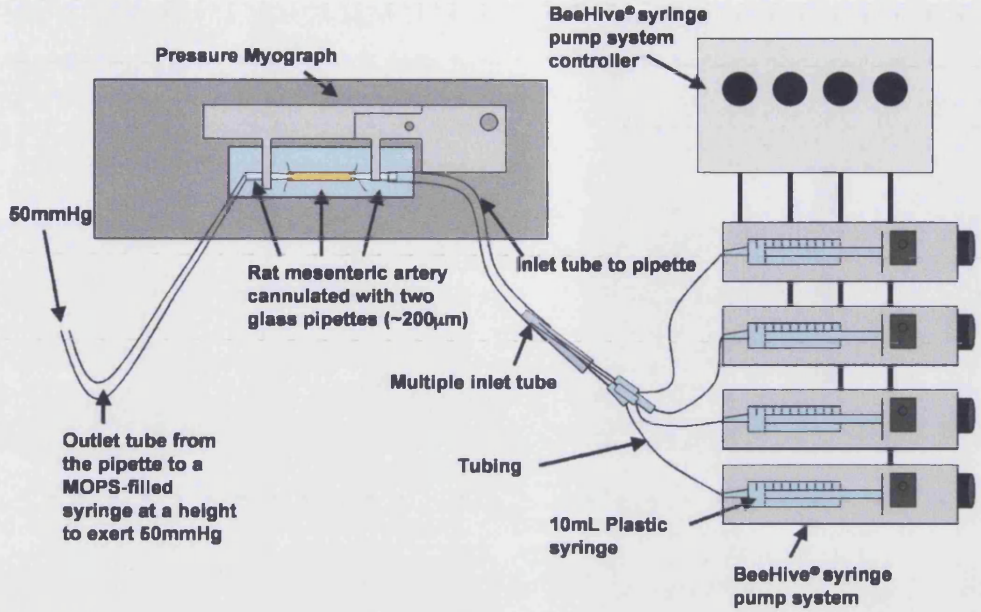

Figure 6.1

The BeeHive® syringe pump system for luminal perfusion

Cartoon illustration of the pressure myograph with BeeHive® syringe pump system set-up for luminal perfusion of a range of purinoceptor agonists, or concentrations of agonist.

thought to be mediated within ~5min following removal of the agonist (Otero *et al.*, 2000)

6.2.4. Drugs

All drugs and solutions were prepared as detailed previously (please see section 2.6).

6.2.5. Data analysis

Arteries were visualized and data analysed as described previously (please see sections 2.5.1 and 2.7). Peak vasodilatation responses were taken from the first period of luminal perfusion.

6.3. Results

6.3.1. Dilatation responses to luminal perfusion of nucleotides

Following pre-contraction with PE (0.5 - 10μM) luminal flow of MOPS-buffered salt solution had no effect on arterial diameter (Figure 6.2A; n = 5). In contrast, luminal perfusion of ATP evoked a concentration- and flow-dependent dilatation (pD2: 6.4 ± 0.1, R_{max} = 87.1 ± 5.3%, n = 5 - 14; Figures 6.2B and C) that was preceded by a short delay of ~30s reflecting the time taken to void the tubing and pipette dead-space volume. Once evoked, dilatation was maintained until cessation of flow when an immediate contraction of the artery was observed. Dilatation responses of similar magnitude were evoked almost immediately upon the second instigation of luminal ATP perfusion (R_{max} = 96.1 ± 2.7%, n = 5 - 11). The NOS inhibitor, L-NAME (100μM) had no effect on ATP-evoked dilatation (Figure 6.2C).

Luminal perfusion of UTP evoked concentration- and flow-dependent dilatation responses that had a similar profile to those seen with ATP (Figure 6.3A) but were evoked at higher agonist concentrations (pD_2: 5.5 ± 0.1, R_{max} = 87.1 ± 5.3%, n = 4 - 5; Figure 6.3C). The potency of the non-hydrolyzable analogue of ADP, ADPβS, was only slightly lower than ATP (pD_2: 6.2 ± 0.1, R_{max} = 94.2 %, n = 2; Figure 6.3C) but the time course of dilatation was markedly different: A transient dilatation was evoked during the first period of luminal perfusion, the magnitude of which could not be reproduced with repeated ADPβS (1μM) exposure (Figure 6.3B). Using submaximal concentrations, both UTP (3μM) and ADPβS (1μM)-evoked responses were unaffected by eNOS inhibition (L-NAME, 100μM; $UTP_{Control}$: 66.7 ± 10.0%, n = 12; $UTP_{L\text{-}NAME}$: 53.9 ± 13.1%, n = 7; $ADP\beta S_{Control}$: 69.7 ± 5.8, n = 12; $ADP\beta S_{L\text{-}NAME}$: 61.5 ± 5.0, n = 8).

The effects of endothelium removal on dilatation responses to the purinoceptor agonists are not described in the present study as this work has been reported previously (Buvinic *et al.*, 2002; Malmsjo *et al.*, 2000a; Malmsjo *et al.*, 2002; Malmsjo *et al.*, 1998; Malmsjo *et al.*, 2000b; Malmsjo *et al.*, 1999; Mistry *et al.*, 2003). However, on occasion when the endothelium was removed by passage of an air bubble through the lumen the dilatation response to luminally-perfused UTP was abolished and a concentration-dependent vasoconstrictor response was observed (results not shown).

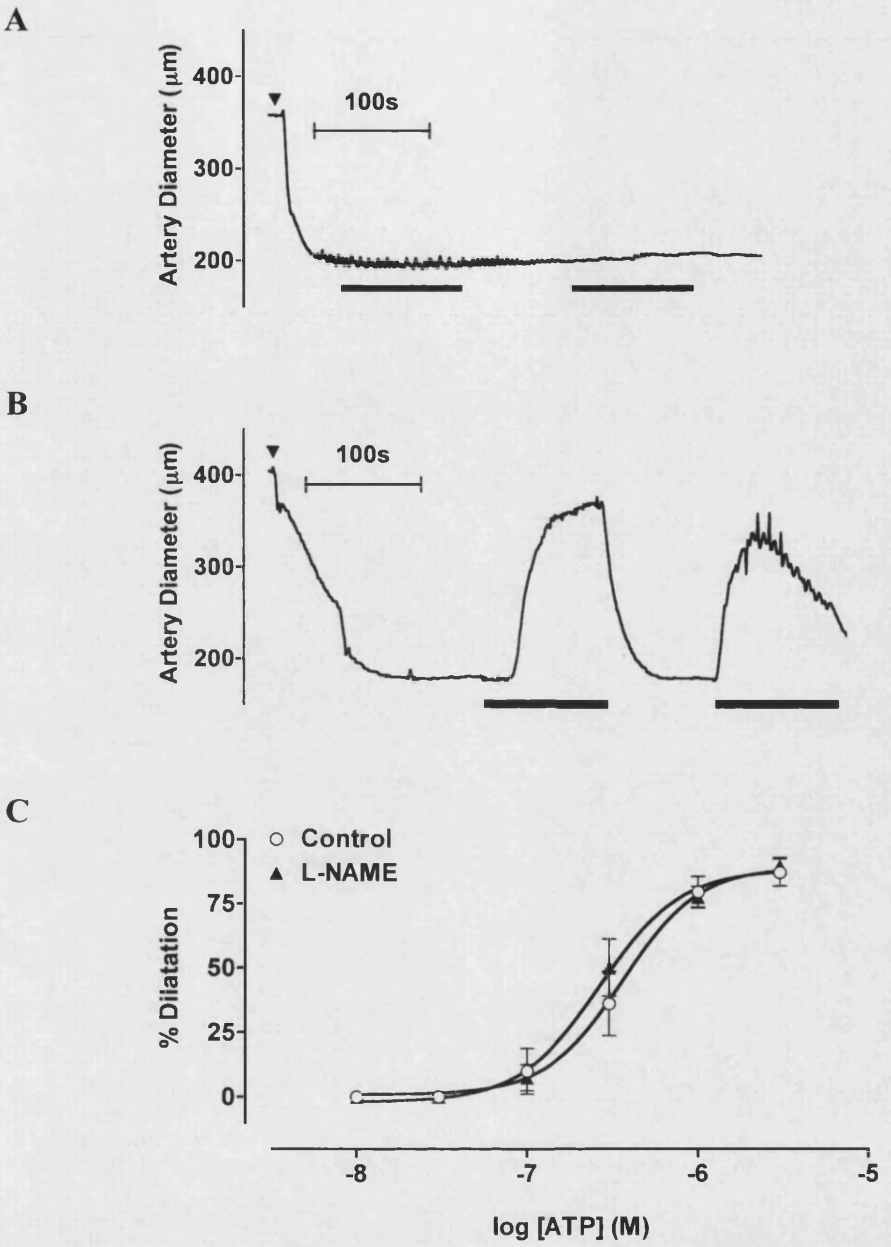

Figure 6.2 Dilatation responses to luminal perfusion of ATP
A, B, Representative traces illustrating the effects of luminal perfusion of isolated rat small mesenteric arteries with **A**, MOPS-buffered salt solution and **B**, ATP (1μM). Filled triangles indicate addition of PE. Bars indicate periods of luminal perfusion of **A**, MOPS or **B**, ATP (1μM). L-NAME (100μM) present in **B**. **C,** Consecutive, non-cumulative concentration-dependent responses to ATP following constriction with PE (0.5-10μM) under control conditions and in the presence of L-NAME (100μM). Values are mean±s.e.mean *n*=4-14 responses. Arteries were perfused with MOPS between each concentration of agonist.

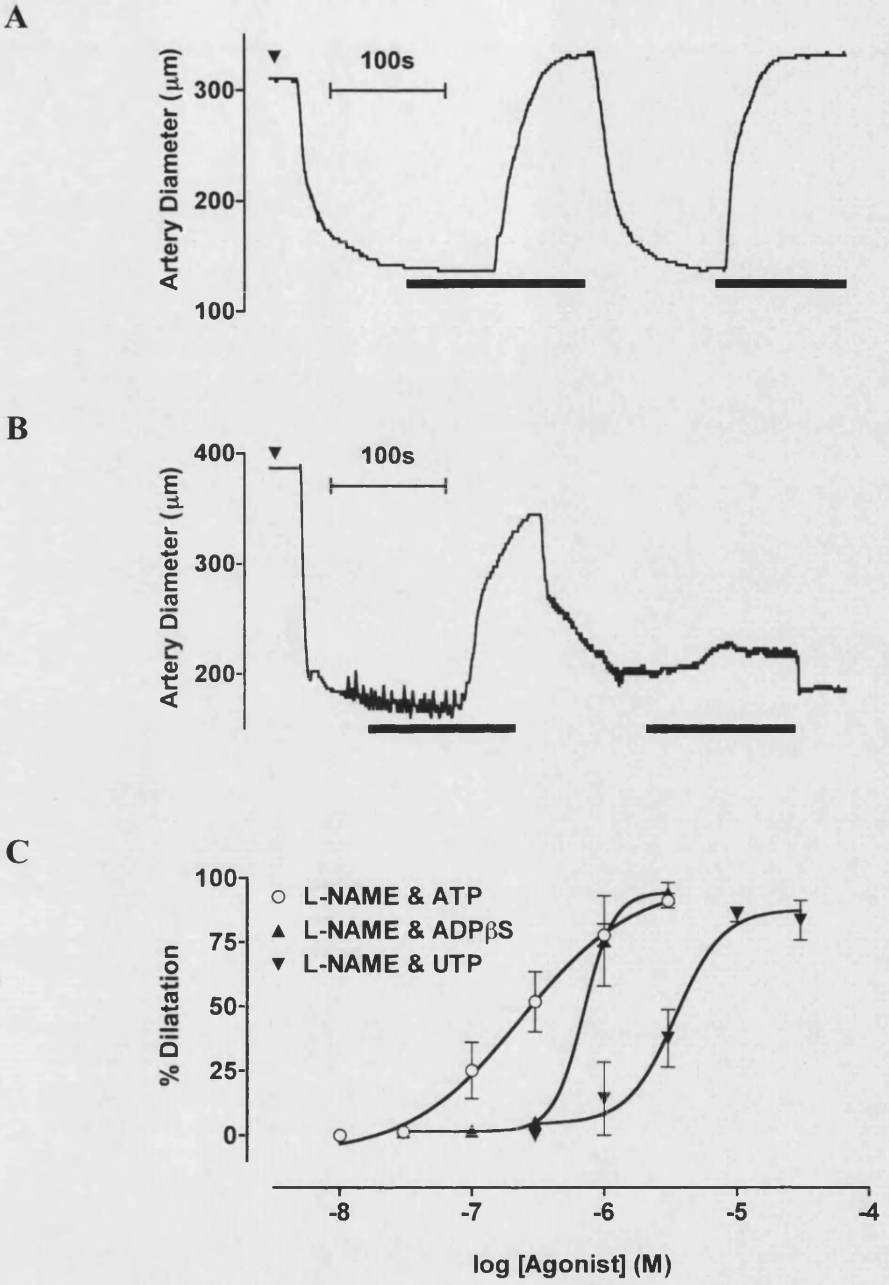

Figure 6.3 Dilatation responses to luminal perfusion of ATP, UTP and ADPβS

A, B, Representative traces illustrating the effects of luminal perfusion of **A,** UTP (3μM) and **B**, ADPβS (1μM) following constriction with PE (0.5-10μM) . Filled triangles indicate addition of PE. Bars indicate periods of luminal agonist perfusion. **C**, Summary data illustrating mean consecutive, non-cumulative concentration-dependent responses to luminal perfusion of ATP (n =3-10), UTP (n=4-5) and ADPβS (n=2). Arteries were perfused with MOPS between each agonist concentration. L-NAME (100μM) present in all experiments.

6.3.2. Activation of $P2Y_1$ and K_{Ca} by luminally-perfused agonists

The $P2Y_1$ receptor antagonist MRS2179 (1μM) significantly inhibited ATP (1μM; Figures 6.4A and C) and ADPβS (1μM; Figures 6.4B and C)-evoked dilatation responses but dilatations to UTP (3μM) and the M_3 receptor agonist ACh (1μM) remained unaffected (Figure 6.4C).

In the presence of L-NAME (100μM), incubation with the selective IK_{Ca} channel blocker, TRAM-34 (1μM), had no effect on dilatation to luminally-perfused ATP (10nM - 3μM; n = 5 - 6), UTP (3μM; n = 8) or ADPβS (1μM; n = 8) (Figure 6.5). In contrast, incubation with the selective SK_{Ca} channel blocker, apamin (50nM), inhibited ATP-evoked vasodilatation causing a rightward shift of the concentration-response curve (Figure 6.5A; n = 5 - 10). This inhibition of ATP-evoked dilatation was most apparent when comparing responses to submaximal concentrations of ATP (1μM; Control: 77.4 ± 4.2, n = 9; Apamin: 33.6 ± 10.3%, n = 12; Figure 6.5B). Apamin had no significant effect on dilatation responses to either UTP (n = 10) or ADPβS (n = 11). Blockade of both IK_{Ca} and SK_{Ca} channels with a combination of TRAM-34 and apamin significantly inhibited dilatation responses to ATP, UTP and ADPβS (ATP: 12.9 ± 3.5%, n = 9; UTP: 12.7 ± 6.1%, n = 9; ADPβS: 12.9 ± 3.5%, n = 9; Figure 6.5). This level of blockade by TRAM-34 and apamin is similar to that seen with ACh-evoked dilatation (1μM; Control: 89.6 ± 1.0%, n = 38; TRAM-34 and apamin: 21.1 ± 6.4%, n = 20).

Raising extracellular K^+ (35 - 40mM) in the presence of L-NAME (100μM) in both the bath and the lumen of isolated arteries completely abolished the relaxation response to each of the luminally-perfused purinoceptor agonists (n = 3) and ACh (1μM; n = 11).

6.3.3. Contribution of PKC to regulation of nucleotide-evoked vasodilatation responses

Experiments using a range of purinoceptor agonists were subsequently performed in an attempt to clarify some of the mechanisms contributing to the reversal of the dilatation response to ADPβS during the agonist perfusion period. To enable sufficient time for

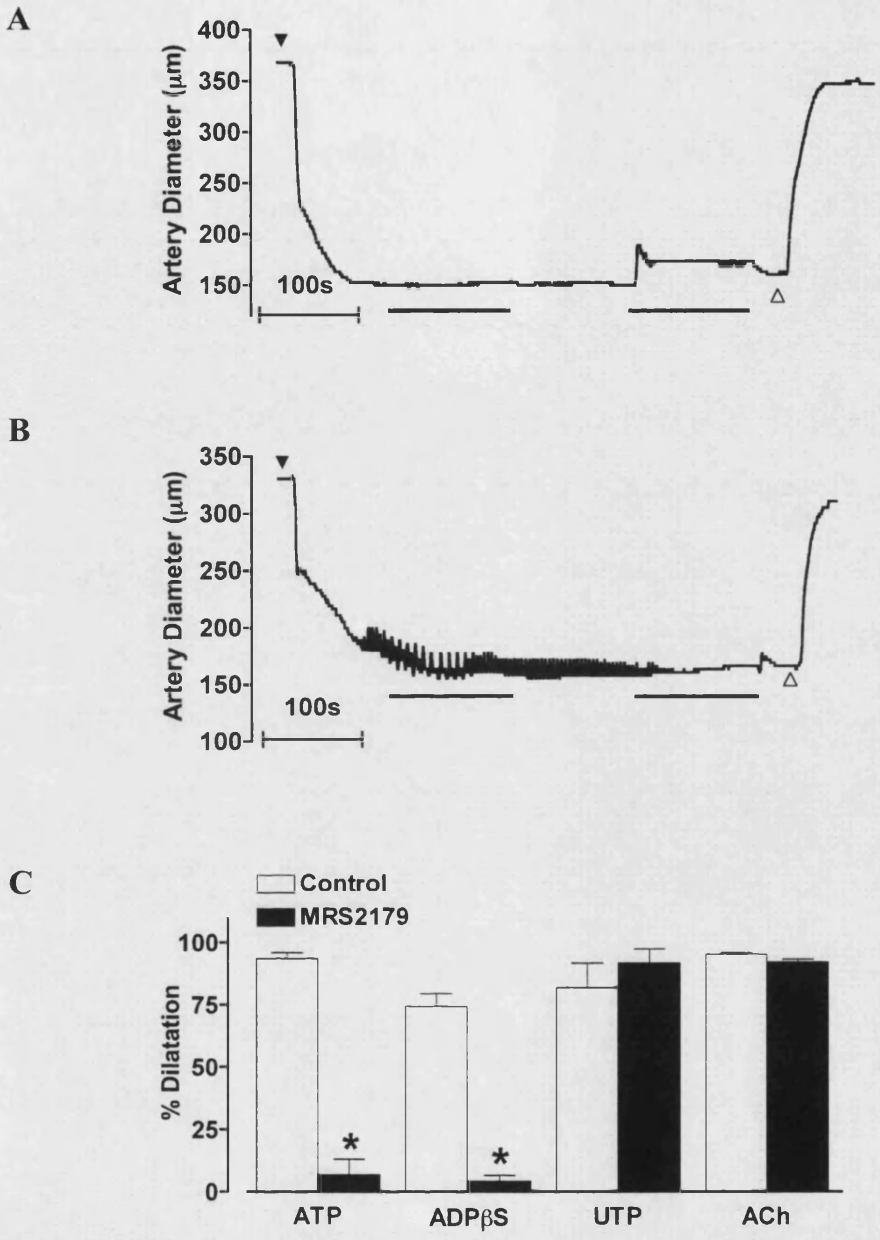

Figure 6.4 Effect of selective inhibition of $P2Y_1$ on dilatation to luminal perfusion of nucleotides

A, **B**, representative traces and **C**, summary data of paired responses illustrating the effect of the selective $P2Y_1$ inhibitor MRS2179 (1μM) on dilatation responses to luminal perfusion of **A**, **C**, ATP (1μM; n = 3), **B**, **C**, ADPβS (1μM; n = 7) and **C**, UTP (3μM; n = 3) and ACh (1μM; n = 6). Bars indicate periods of luminal agonist perfusion. Filled triangle indicates addition of PE. Clear triangle indicates addition of ACh. *, Significantly different to control following a paired t-test.

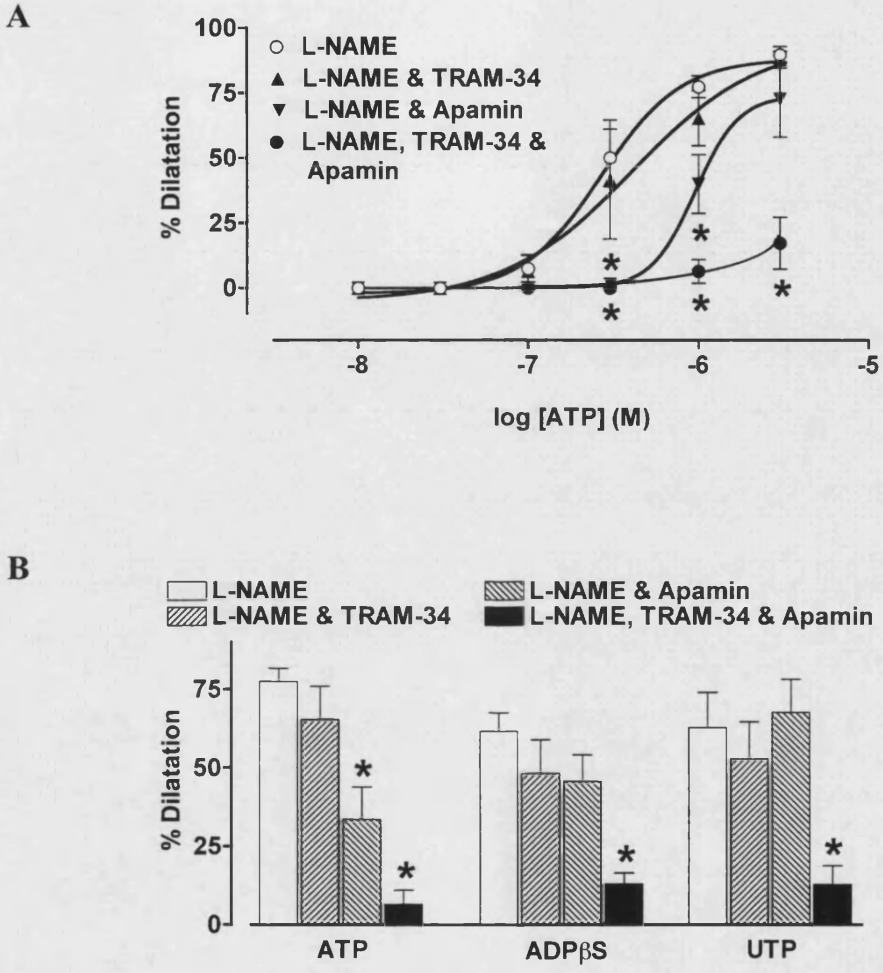

Figure 6.5 Effect of K^+ channel inhibition on dilatation to luminal perfusion of nucleotides

Summary data of unpaired responses showing **A**, the effects of TRAM-34 (1μM) and apamin (50nM) on consecutive, non-cumulative, concentration-dependent responses to ATP (*n*=3-14), and to compare, **B**, submaximal concentrations of ATP (1μM; *n*=6-12), ADPβS (1μM; *n*=8-11) and UTP (3μM; *n*=6-10). **A, B**, L-NAME (100μM) present in all experiments. *, Significantly different to control using the Kruskal-Wallis test followed by Dunn's multiple comparison post-test. Experiments performed by Dr. Kim Dora and Miss Hanna Norris contributed to the data collected for the ATP-evoked responses.

reversal of the vasodilatation response, the first period of agonist luminal perfusion was extended such that upon attainment of the peak dilatation response luminal perfusion was continued for 4min. All experiments were performed in the presence of L-NAME (100μM).

6.3.3.1. ATP

When the period of ATP perfusion was extended compared to that shown in Figure 6.2B, the initial peak dilatation response to ATP (1μM; 50.4 ± 6.1%, *n*=9) rapidly (within ~1min) reversed to a plateau value of 31.1 ± 5.3% maximal diameter. Cessation of flow completely reversed the dilatation response. During a second period of luminal perfusion dilatation responses were limited to the extent observed during the plateau phase of the first perfusion period (Figures 6.6A and C). Increasing the concentration of ATP to 3μM however, resulted in a dilatation response that was maintained at peak level (91.3 ± 1.5%, *n*=3) for the duration of the first and second luminal perfusion periods (Figures 6.7A and C). Cessation of flow resulted in a small reversal of the ATP (3μM) dilatation response.

In paired experiments, luminal incubation (to minimize smooth muscle effects) with the selective PKC inhibitor BIS I (1μM) tended to augment the vasodilatation to 1μM ATP (Figure 6.6). This was observed together with a delay in the onset of the reversal of dilatation, a reduced reversal during the flow off period, and a rapid dilatation during the second flow on period (Figure 6.6). Thus BIS I tended to make the profile of the response to 1μM ATP more closely match that of the control response to 3μM ATP (Figures 6.6B and 6.7A).

Incubation with BIS I during luminal perfusion of increased concentrations of ATP (3μM; *n*=3, paired to L-NAME controls) reduced the extent of reversal of the vasodilatation response during the flow off period such that a dilatation of 82.0 ± 7.9% (compared to 47.4 ± 15.0% under control conditions) could still be achieved after 2min without flow (Figures 6.7B and C). No effects of BIS I on the vasodilatation to ATP (3μM) during the periods of luminal perfusion were observed.

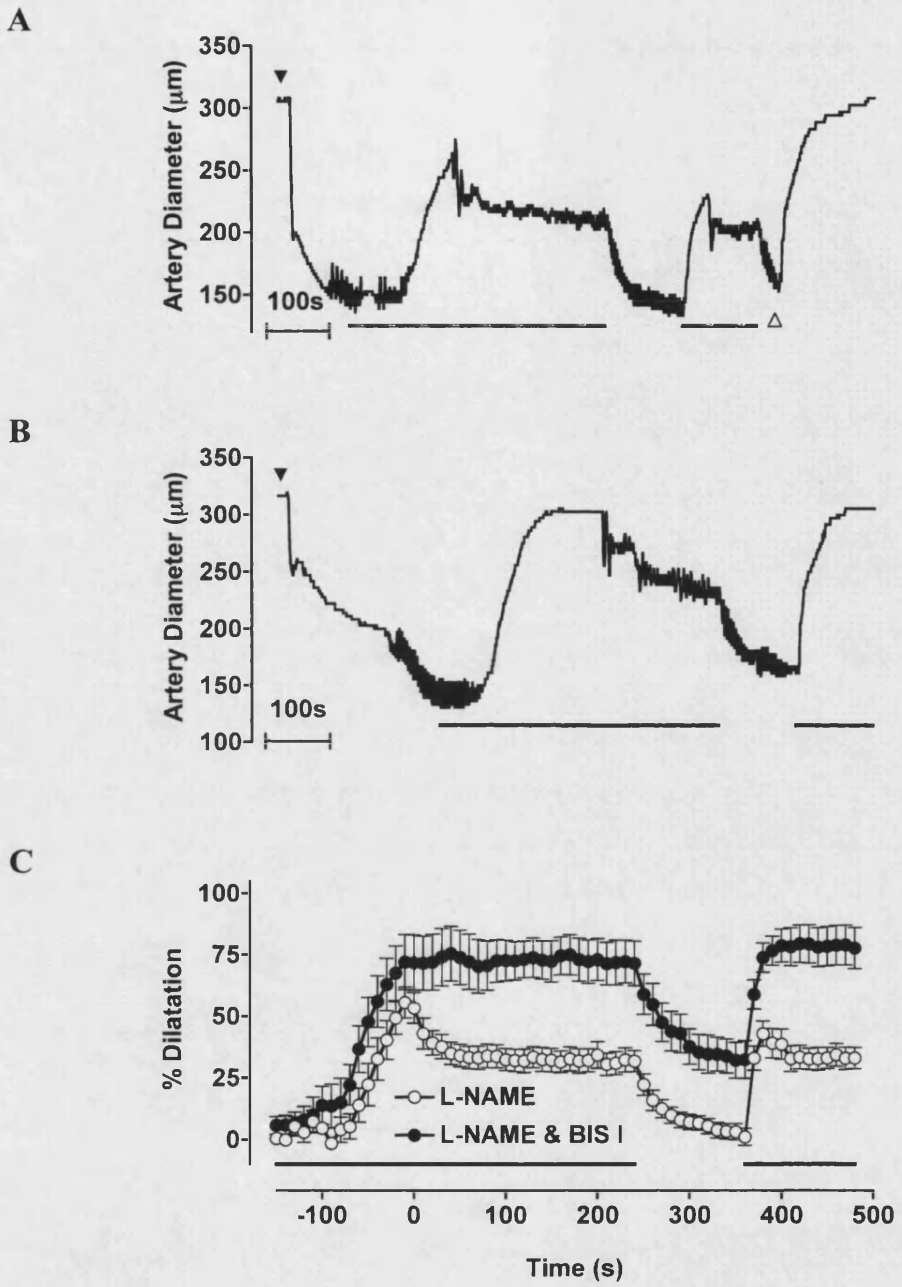

Figure 6.6 Effect of selective inhibition of PKC on dilatation to luminal perfusion of ATP (1μM)

Paired **A**, **B**, representative traces and **C**, meaned (n=9) data illustrating dilatation responses to extended luminal perfusion of ATP (1μM) in the presence of **A, B, C,** L-NAME (100μM) and **B, C,** following incubation with the selective PKC inhibitor BIS I (1μM) under **A, B, C,** submaximal levels of PE-evoked tone (0.1-1μM). **A, B, C,** Bars represent periods of ATP (1μM) luminal perfusion. **A**, **B**, Filled triangle indicates addition of PE. **A**, Open triangle indicates addition of ACh (1μM). **C,** Time = 0s corresponds to start of 4min post-peak period.

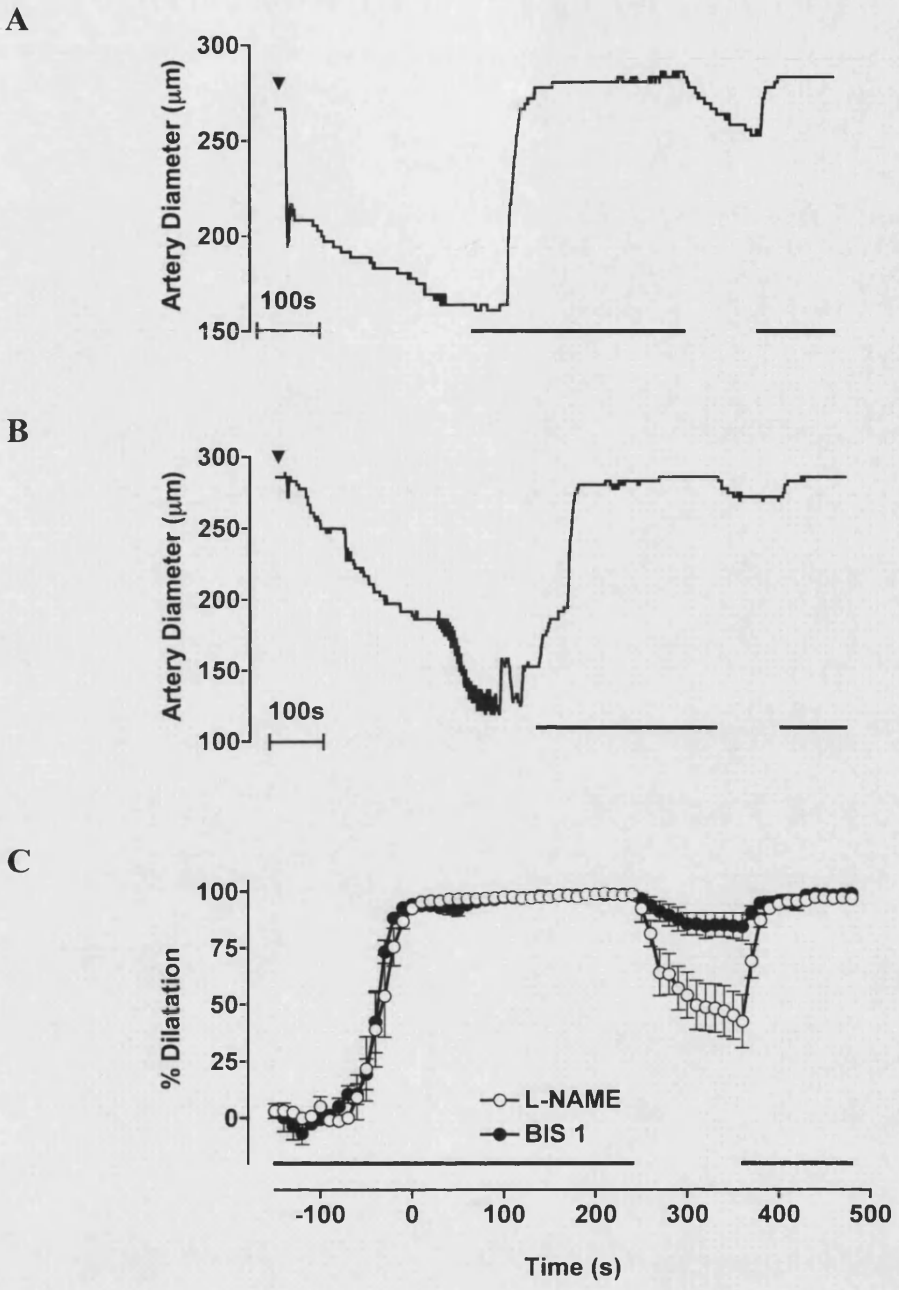

Figure 6.7 Effect of selective inhibition of PKC on dilatation to luminal perfusion of ATP (3μM)

Paired **A**, **B**, representative traces and **C**, meaned (n=3) data illustrating dilatation responses to extended luminal perfusion of ATP (3μM) in the presence of **A, B, C,** L-NAME (100μM) and **B, C,** following incubation with the selective PKC inhibitor BIS I (1μM) under **A, B, C,** submaximal levels of PE-evoked tone (0.3-1.8μM). **A, B, C,** Bars represent periods of ATP (3μM) luminal perfusion. **A**, **B**, Filled triangle indicates addition of PE. **C,** Time = 0s corresponds to start of 4min post-peak period.

6.3.3.2. ADPβS

As demonstrated previously (Figure 6.3B), immediately upon reaching the peak vasodilatation response to luminal perfusion of ADPβS (1μM; 70.0 ± 6.6%, *n*=7) the dilatation was rapidly reversed such that within 2min of the peak response a plateau dilatation response of 41.5 ± 6.1% was observed. In contrast to 1μM ATP, this plateau was maintained following cessation of flow and during the second period of luminal perfusion (Figures 6.8A and C). In paired experiments, subsequent luminal incubation with BIS I increased the amplitude of the peak vasodilatation response (94.8 ± 1.0%) and delayed the reversal of the vasodilatation to ADPβS by ~2min so that in contrast to the L-NAME control, no change in artery diameter could be observed during the first 2min of the first luminal perfusion period. However, BIS I treatment had no effects on the dilatation responses observed during the second period of ADPβS perfusion.

6.3.3.3. UTP

The profile of responses evoked by the extended luminal perfusion of UTP (3μM; *n*=3) were similar to those seen following perfusion of ATP (3μM) such that any effects of BIS I (*n*=3, paired to L-NAME control) could only be observed during the flow off period where a decrease in the reversal rate of the relaxation response could be observed (Figure 6.9). Consequently, the effects of BIS I on the time course of vasodilatation evoked by luminal perfusion of a lower concentration of UTP (1μM; *n*=3) were investigated in further paired experiments (Figure 6.10). In contrast to ADPβS (1μM) and ATP (1μM)-evoked vasodilatation responses the amplitude (23.2 ± 10.8%) or time course of vasodilatation to UTP (1μM) during the first luminal perfusion period was not significantly increased following luminal incubation with BIS 1 (1μM; 38.2 ± 17.8%). However, during the flow off and second luminal perfusion periods an increase in the amplitude of vasodilatation could be observed (Figure 6.10).

6.3.3.4. ATPγS

In the rat mesenteric artery it is thought that UTP evokes its vasodilator actions through stimulation of $P2Y_2$ receptors on the endothelium (Buvinic *et al.*, 2002; Malmsjo *et al.*, 2000a; Malmsjo *et al.*, 2000b). To more fully investigate the profile of $P2Y_2$ receptor activation in the rat mesenteric artery, the effects of BIS I on responses to

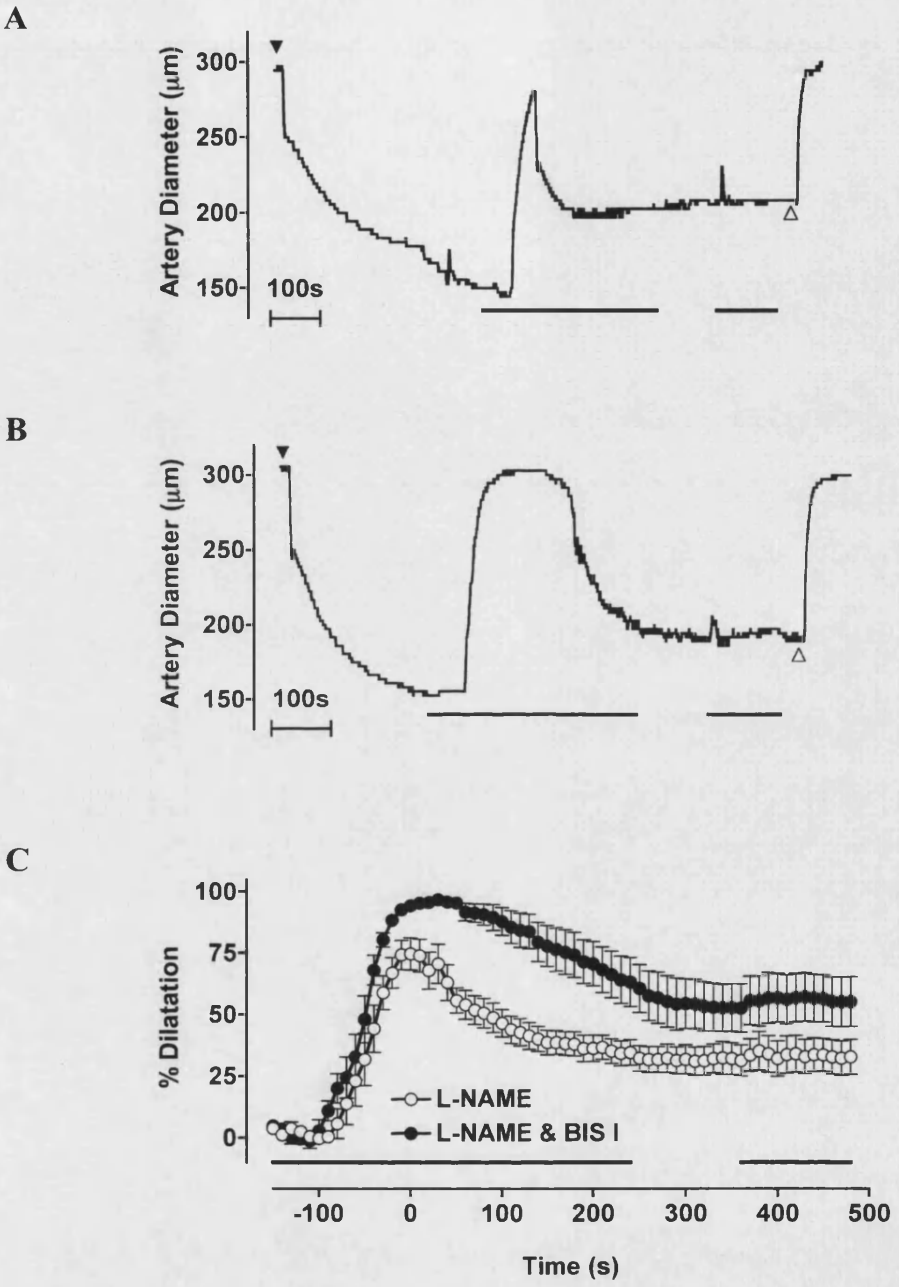

Figure 6.8 Effect of selective inhibition of PKC on dilatation to luminal perfusion of ADPβS (1μM)

Paired **A**, **B**, representative traces and **C**, meaned (n=7) data illustrating dilatation responses to extended luminal perfusion of ADPβS (1μM) in the presence of **A, B, C,** L-NAME (100μM) and **B, C,** following incubation with the selective PKC inhibitor BIS I (1μM) under **A, B, C,** submaximal levels of PE-evoked tone (0.2-1.7μM). **A, B, C,** Bars represent periods of ADPβS (1μM) luminal perfusion. **A**, **B**, Filled triangle indicates addition of PE. Open triangle indicates addition of ACh (1μM). **C,** Time = 0s corresponds to start of 4min post-peak period.

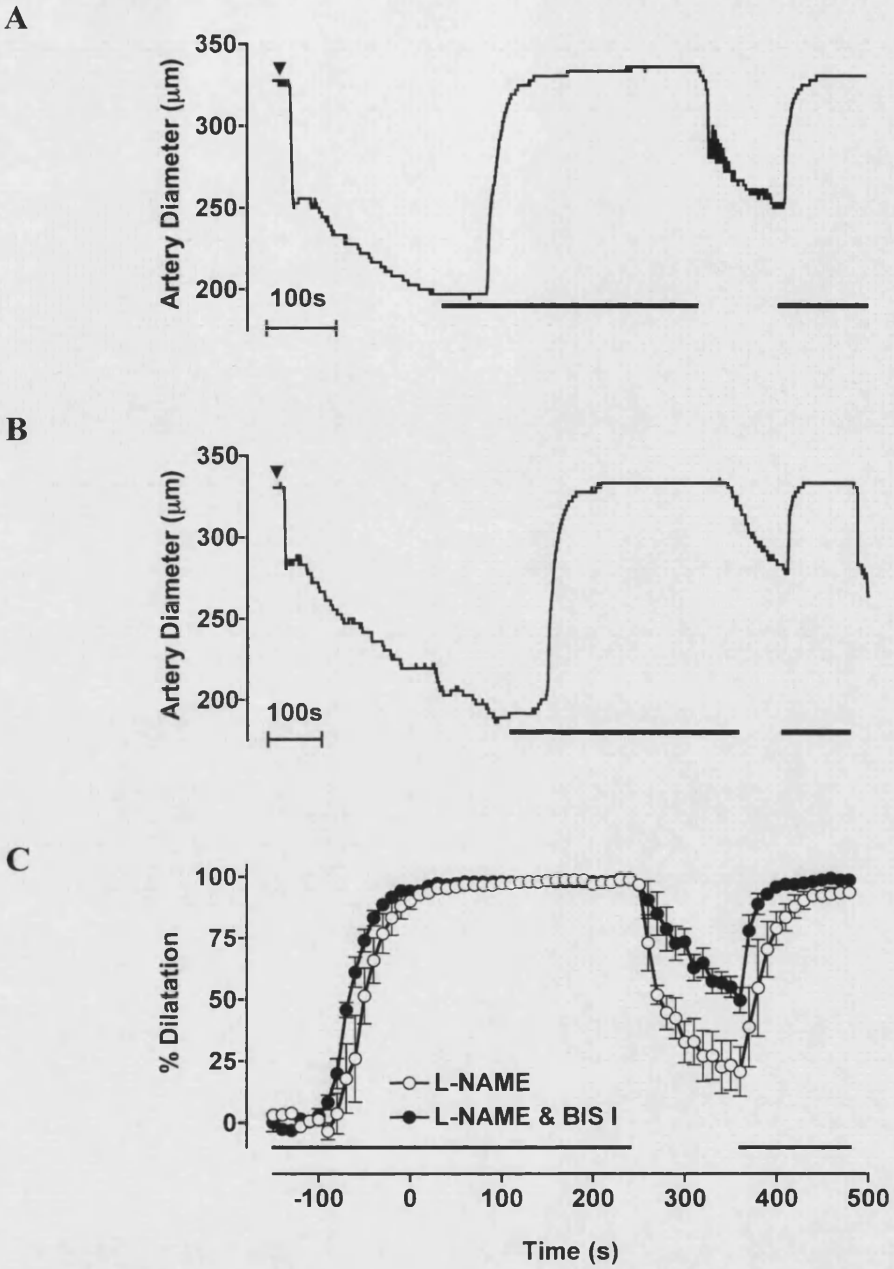

Figure 6.9 Effect of selective inhibition of PKC on dilatation to luminal perfusion of UTP (3μM)

Paired **A**, **B**, representative traces and **C**, meaned (n=3) data illustrating dilatation responses to extended luminal perfusion of UTP (3μM) in the presence of **A, B, C,** L-NAME (100μM) and **B, C,** following incubation with the selective PKC inhibitor BIS I (1μM) under **A, B, C,** submaximal levels of PE-evoked tone (0.5-1.6μM). **A, B, C,** Bars represent periods of UTP (3μM) luminal perfusion. **A, B,** Filled triangle indicates addition of PE. **C,** Time = 0s corresponds to start of 4min post-peak period.

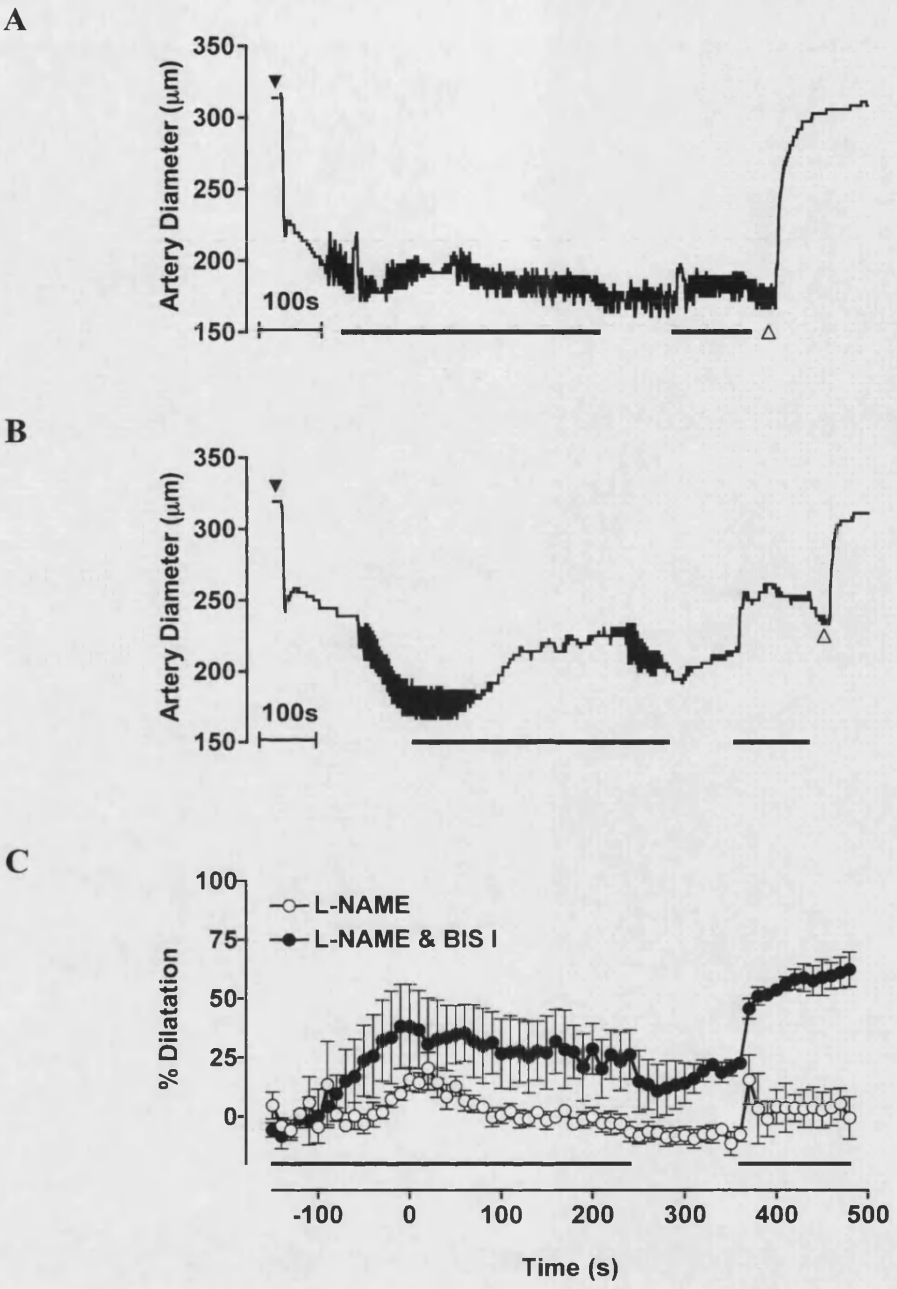

Figure 6.10 Effect of selective inhibition of PKC on dilatation to luminal perfusion of UTP (1μM)

Paired **A**, **B**, representative traces and **C**, meaned (n=3) data illustrating dilatation responses to extended luminal perfusion of UTP (1μM) in the presence of **A, B, C,** L-NAME (100μM) and **B, C,** following incubation with the selective PKC inhibitor BIS I (1μM) under **A, B, C,** submaximal levels of PE-evoked tone (0.5-1.3μM). **A, B, C,** Bars represent periods of luminal UTP (1μM) perfusion. **A**, **B**, Filled triangle indicates addition of PE. Open triangle indicates addition of ACh (1μM). **C,** Time = 0s corresponds to start of 4min post-peak period.

luminal perfusion of the non-hydrolyzable $P2Y_2$ agonist ATPγS (Malmsjo *et al.*, 2000a) were investigated.

Initiation of ATPγS perfusion (1μM; *n*=4; Figures 6.11A and C) evoked a rapid dilatation response that after peaking (70.6 ± 9.1%) was reversed to reach a plateau of 41.1 ± 4.5% maximum diameter. Upon cessation of flow the dilatation response was completely and rapidly reversed. During the second luminal perfusion period a small dilatation response was seen. As observed for ATP (1μM)-evoked responses, the amplitude of this response was limited to the diameter attained during the plateau phase of the first luminal perfusion period (Figures 6.11A and C). Increasing the concentration of ATPγS within the luminal perfusate to 3μM (*n*=5) evoked a vasodilatation response (80.5 ± 4.0%) that was maintained for nearly the duration of the 4min primary luminal perfusion period (Figures 6.12A and C). As seen for the 1μM ATPγS-evoked response cessation of flow caused a rapid reversal of the dilatation response, however this was not complete and slowed towards the end of the 2min period. The extent of vasodilatation upon re-application of luminal perfusion was then limited to the amplitude of dilatation observed towards the end of the first luminal perfusion period (53.1 ± 6.5%; Figures 6.12A and 6.12C).

Inclusion of BIS 1 in the 1μM (*n*=4; paired to L-NAME controls) and 3μM (*n*=5; paired to L-NAME controls) ATPγS perfusate solutions facilitated a maintained peak vasodilatation response throughout both periods of luminal perfusion (Figures 6.11B, 6.11C, 6.12B and 6.12C). Upon cessation of flow an initial rapid reversal of the dilatation response was observed in the case of both agonist concentrations, however this quickly plateaued at ~60% maximum diameter for both 1μM and 3μM ATPγS.

6.3.3.5. ACh

To ascertain whether inhibition of PKC with BIS I directly enhanced EDHF-type vasodilatation responses the effects of BIS I on concentration-dependent dilatation responses to ACh (1nM - 3μM; *n*=7) were evaluated. There was no significant effect of BIS I on the cumulative concentration-response curve to ACh (Figure 6.13).

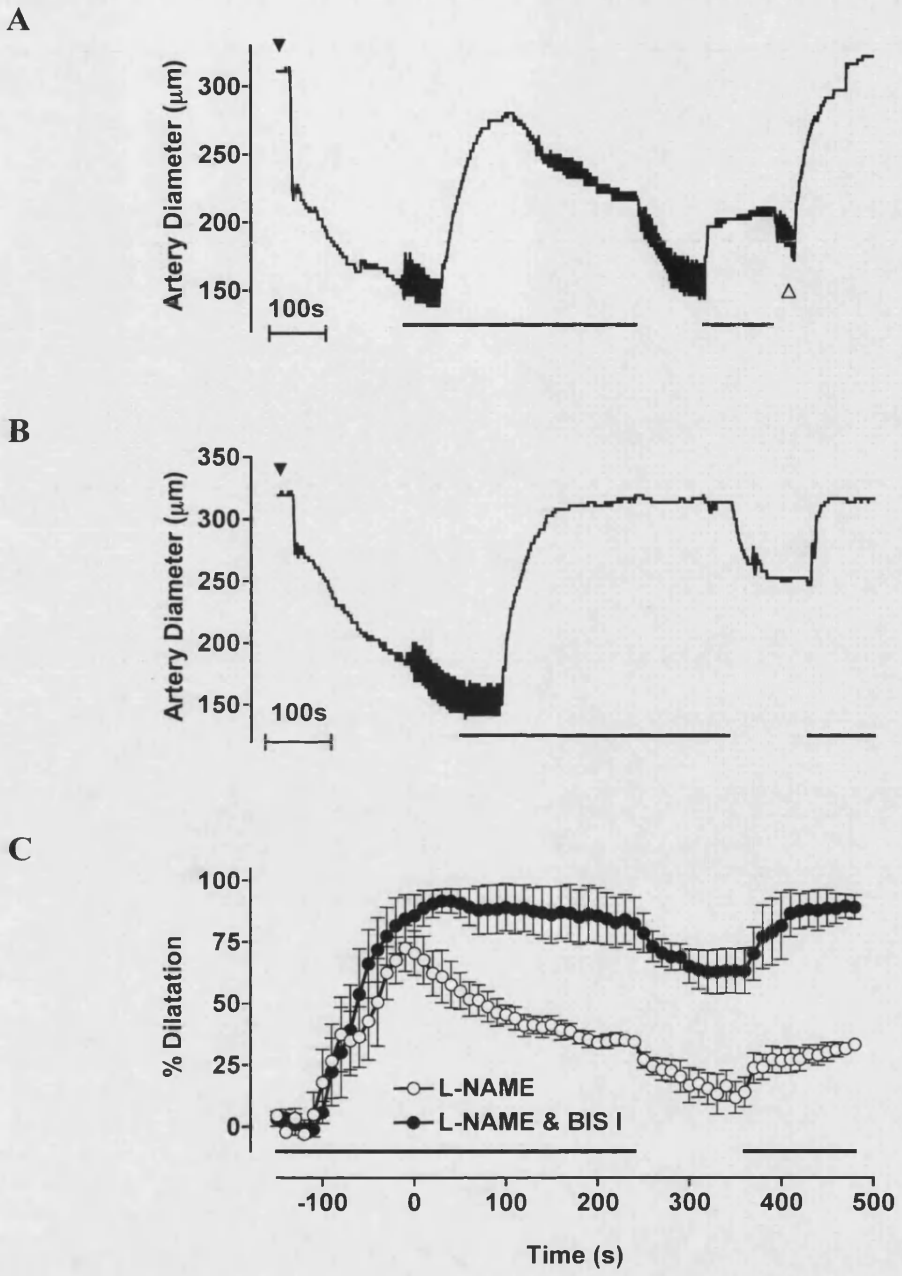

Figure 6.11 Effect of selective inhibition of PKC on dilatation to luminal perfusion of ATPγS (1μM)

Paired **A**, **B**, representative traces and **C**, meaned (n=4) data illustrating dilatation responses to extended luminal perfusion of ATPγS (1μM) in the presence of **A, B, C,** L-NAME (100μM) and **B, C,** following incubation with the selective PKC inhibitor BIS I (1μM) under **A, B, C,** submaximal levels of PE-evoked tone (0.3-0.9μM). **A, B, C,** Bars represent periods of luminal ATPγS (1μM) perfusion. **A**, **B**, Filled triangle indicates addition of PE. **A**, Open triangle indicates addition of ACh (1μM). **C,** Time = 0s corresponds to start of 4min post-peak period.

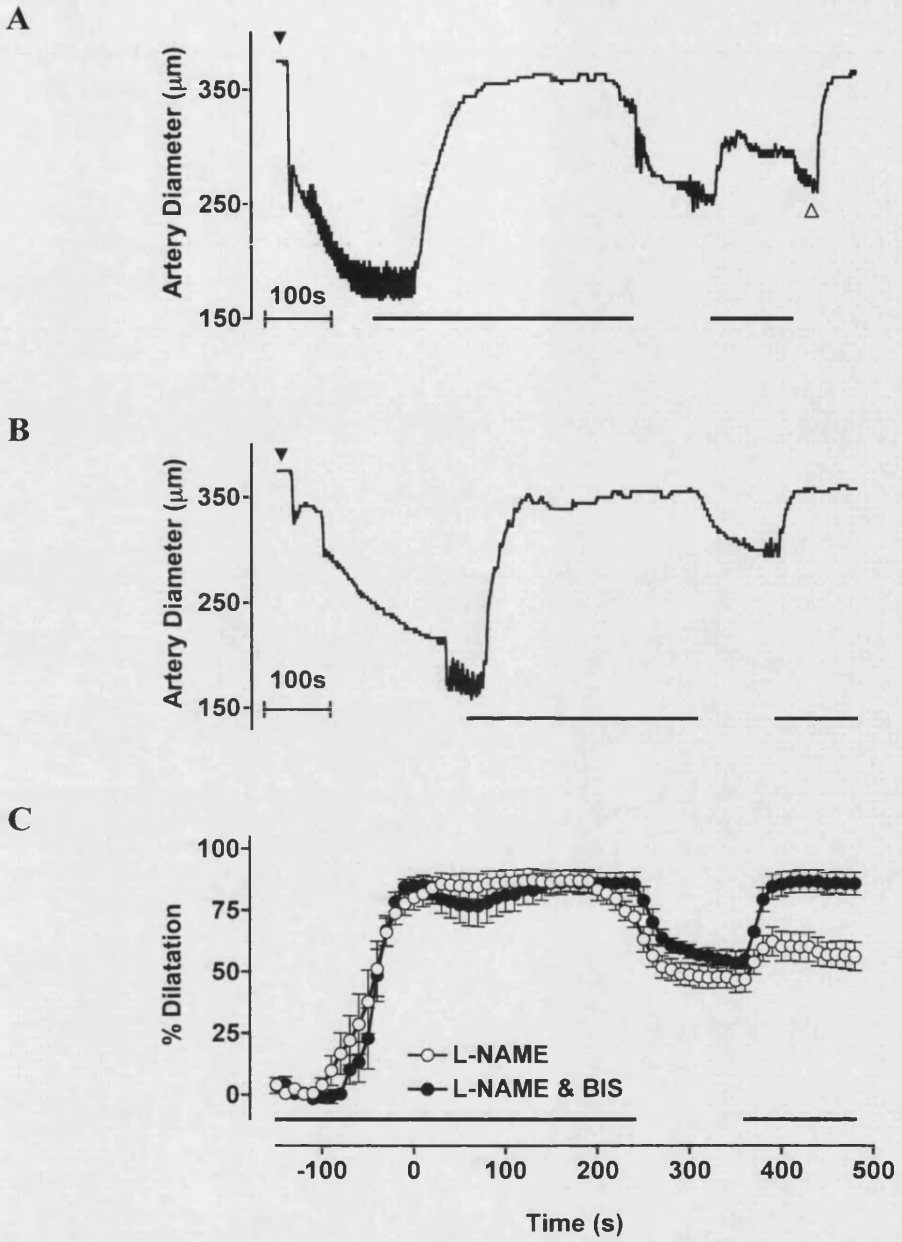

Figure 6.12 Effect of selective inhibition of PKC on dilatation to luminal perfusion of ATPγS (3μM)

Paired **A**, **B**, representative traces and **C**, meaned (*n*=5) data illustrating dilatation responses to extended luminal perfusion of ATPγS (3μM) in the presence of **A, B, C,** L-NAME (100μM) and **B, C,** following incubation with the selective PKC inhibitor BIS I (1μM) under **A, B, C,** submaximal levels of PE-evoked tone (0.4-1.7μM). **A, B, C,** Bars represent periods of luminal ATPγS (3μM) perfusion. **A**, **B**, Filled triangle indicates addition of PE. **A**, Open triangle indicates addition of ACh (1μM). **C,** Time = 0s corresponds to start of 4min post-peak period.

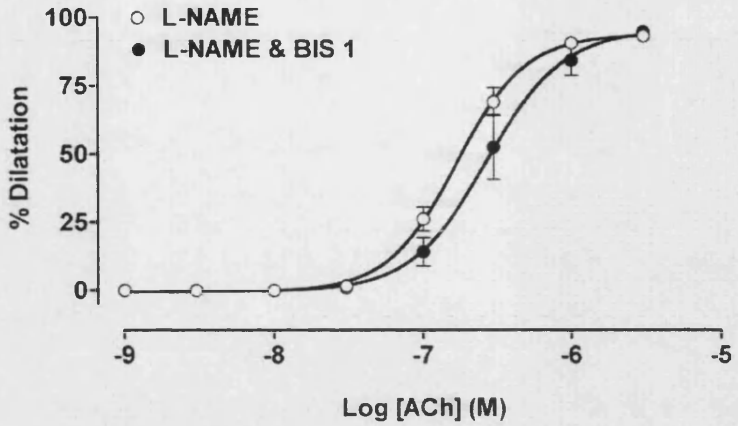

Figure 6.13 Effects of selective inhibition of PKC on ACh-evoked vasodilatation. The effects of luminal BIS I (1μM) on concentration-dependent dilatation responses to cumulative additions of ACh (1nM-3μM; *n*=7) following submaximal pre-constriction with PE (0.5-1.5μM). L-NAME (100μM) present throughout. ACh and PE were added abluminally.

6.4. Discussion

Aspects of the experiments detailed herein are consistent with previous reports: Luminal application of the $P2Y_1$ receptor agonists ATP, ADPβS and the likely $P2Y_2$ receptor agonist UTP evoked robust vasodilatation responses, which were shown to comprise a significant EDHF-facilitated component (Buvinic *et al.*, 2002; Liu *et al.*, 2004; Liu *et al.*, 2006a; Malmsjo *et al.*, 2000a; Malmsjo *et al.*, 2002; Malmsjo *et al.*, 1998; Malmsjo *et al.*, 2000b; Malmsjo *et al.*, 1999; Mistry *et al.*, 2003). On closer examination, however, EDHF-type dilatation responses to the luminal perfusion of purinoceptor agonists were also found to be differentially sensitive to inhibition of IK_{Ca} and SK_{Ca}. Submaximal concentrations of ATP evoked responses requiring SK_{Ca} activation in order to evoke a full dilatation whilst UTP-, and to a large extent ADPβS-evoked dilatations were achieved by activation of either IK_{Ca} or SK_{Ca} alone. Additionally, experiments performed to begin to characterize the profile of the ATP-, ADPβS-, UTP- and ATPγS-evoked vasodilatations found PKC contribute to both the decay and blunting of the responses.

Within the present study ATP-evoked responses were almost completely attenuated by treatment with the selective $P2Y_1$ inhibitor MRS2179 (1μM) (Boyer *et al.*, 1998). Previous reports citing inhibition of ATP-evoked dilatation responses in the rat mesenteric arterial bed document incomplete blockade with MRS2179, attributing the remainder of the dilatation response to activation of $P2Y_2$ receptors (Buvinic *et al.*, 2002; Malmsjo *et al.*, 2002). However, within the present report ATP was approximately 10-fold more potent than UTP, which could tentatively (given the variability associated with ectonucleotidase activity; Chen & Chen, 1997) rule out a predominant role for $P2Y_2$ activation in the ATP-evoked response (Buvinic *et al.*, 2002; Malmsjo *et al.*, 2002; Ralevic & Burnstock, 1998). UTP- and ACh-evoked responses were both unaffected by MRS2179 suggesting that the concentration used would appear selective for $P2Y_1$ as demonstrated previously (Boyer *et al.*, 1998). Thus the present results probably reflect the breakdown of ATP to ADP by endothelial cell ectonucleotidases (Figure 1.10) prior to its action on the endothelium (Alvarado-Castillo *et al.*, 2005; Koziak *et al.*, 1999). Why such activity should be observed in the present study and not in that of Buvinic *et al* (2002) is unclear. Further experiments employing the ectonucleotidase inhibitor ARL67156 to prevent ATP breakdown with

subsequent evaluation of the MRS2179 sensitivity of the dilatation response are required to establish this.

6.4.1. The contribution of IK_{Ca} and SK_{Ca} to nucleotide-evoked dilatation responses

The contributions of EDHF and NO to purinoceptor-mediated dilatation responses in the rat mesenteric artery are well documented. Thus the complete attenuation of ATP, ADPβS and UTP-evoked dilatation responses by selective inhibition of eNOS, IK_{Ca} and SK_{Ca} would support such data (Buvinic *et al.*, 2002; Liu *et al.*, 2004; Liu *et al.*, 2006a; Malmsjo *et al.*, 2002; Malmsjo *et al.*, 1998; Malmsjo *et al.*, 1999; Mistry *et al.*, 2003). However, the differential contribution of the IK_{Ca} and SK_{Ca} channels to the $P2Y_1$ and $P2Y_2$-evoked dilatation responses perhaps highlights a facet of EDHF-type dilatation responses, the differential contribution of IK_{Ca} and SK_{Ca}, that is becoming increasingly well recognised (Crane *et al.*, 2003a; Sandow *et al.*, 2006). Patch clamp studies have reported that ATP-evoked endothelial cell hyperpolarization was dependent on activation of SK_{Ca}, attributing the lack of an IK_{Ca} current to a spatial compartmentalization of the ATP-evoked Ca^{2+} response (Marchenko, 2002). More recently reports have been published (Sandow *et al.*, 2006) that support the differential localization of SK_{Ca} and IK_{Ca} within the endothelium: SK_{Ca} localized to endothelial cell borders, whilst IK_{Ca} is localized to areas adjacent to holes in the IEL. It is therefore possible that the differential contribution of the two K_{Ca} channels to ATP and UTP-evoked dilatations is associated with a discrete localization of the $P2Y_1$ and $P2Y_2$ receptors themselves, or their associated Ca^{2+} responses (Figure 6.14).

A recent report from Marrelli *et al* (2006) using rat isolated and pressurized middle cerebral arteries describes an association of UTP-evoked dilatation responses with both apical and baso-lateral increases in endothelial cell Ca^{2+}. Given the activation of EDHF-type responses in the current report by either IK_{Ca} or SK_{Ca} and the localization of IK_{Ca} to the MEGJ, it is thus speculated, albeit with caution given results to the contrary in cultured calf pulmonary endothelial cells (Madge *et al.*, 1997), that within the rat mesenteric artery similar baso-lateral and apical increases in endothelial cell Ca^{2+} in response to UTP would be observed. Interestingly, Marrelli *et al* (2006) documented a PLA_2- and $TRPV_4$-dependency of the baso-lateral increase in endothelial cell Ca^{2+} that

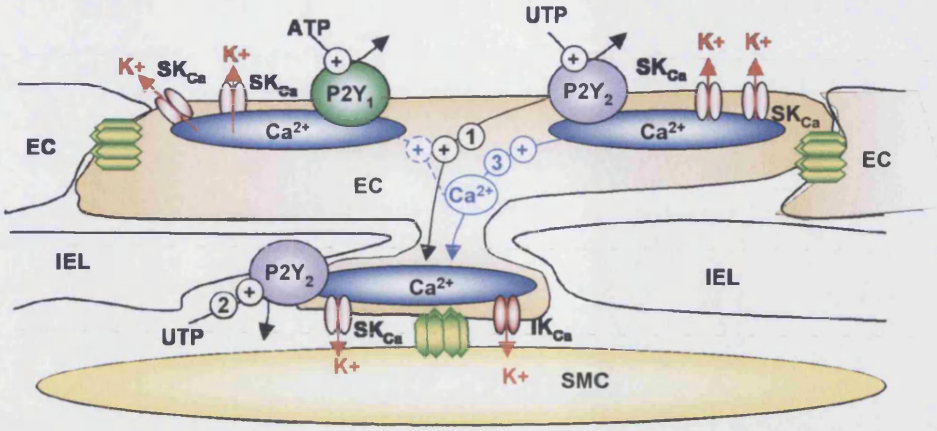

Figure 6.14. Proposed pathways leading to the differential activation of IK_{Ca} and SK_{Ca} downstream of ATP and UTP stimulation
Cartoon illustrating the mechanisms by which ATP and UTP could differentially activate IK_{Ca} and SK_{Ca} channels downstream of receptor activation. ATP-evoked hyperpolarization and dilatation would be predominantly evoked by an apical increase in intracellular Ca^{2+} in the vicinity of SK_{Ca} localized to the endothelial cell border (Marchenko, 2002; Sandow *et al.*, 2006). A small IK_{Ca} component could be facilitated by diffusion of Ca^{2+} to the MEGJ (dashed line). In contrast, UTP would facilitate endothelial cell hyperpolarization and dilatation by apical activation of SK_{Ca} followed by a baso-lateral mechanism of Ca^{2+} release and activation of MEGJ IK_{Ca} (Marelli *et al.*, 2006; Sandow *et al.*, 2006). The latter occurring by; 1), diffusion of signalling molecules and activation of a distinct Ca^{2+} release mechanism; 2), direct stimulation of $P2Y_2$ receptors on the baso-lateral surface of the endothelium; or 3), by diffusion of the Ca^{2+} response from the apical surface.

was not characteristic of the apical Ca^{2+} response. ATP-evoked endothelial cell increases in cytosolic Ca^{2+} have been described, and their dependence on SOCC and IP_3-mediated release from intracellular stores documented (please see section 1.2.3; Chen *et al.*, 1996; Liu *et al.*, 2006a; Madge *et al.*, 1997). However, a role for PLA_2 in the ATP-evoked Ca^{2+}-dependent response has not. It would therefore be of interest to evaluate the sub-cellular localization of endothelial cell Ca^{2+} responses to both ATP and UTP within the rat mesenteric artery and elucidate the sensitivity of these responses to PLA_2 inhibition.

Compartmentalization of endothelial P2Y receptors has been reported within guinea-pig aortic ring preparations (Kaiser *et al.*, 2002). Upon β-methyl-cyclodextrin treatment to disrupt cholesterol-rich microdomains, Ca^{2+} release and NO-dependent dilatation responses to the P2Y agonists 2-methylthio-ATP, ADP, ATP and UTP were disrupted.

In contrast Ca^{2+} responses to bradykinin or ACh and dilatation to the Ca^{2+} ionophore A23187 were unaffected, implying an association of P2Y receptors with cholesterol-rich microdomains (Kaiser *et al.*, 2002). A recent report from Weerth *et al* (2007) detailing Ca^{2+} responses in rat glial cells in response to activation of $P2Y_1$ documented the co-immunoprecipitation and expression of signalling proteins such as PLCβ1, IP_3R2, PKCα, and $TRPC_1$ to these microdomains, detailing that the number of signalling proteins in the microdomains increased upon $P2Y_1$ stimulation (Weerth *et al.*, 2007). One component of the report of Weerth *et al* (2007) of interest is therefore the question whether complete association of all of the $P2Y_1$ downstream signalling proteins is required to evoke even the smallest increases in intracellular Ca^{2+}? Can the degree of receptor stimulation influence the extent of signalling protein association and subsequently have a graded influence on the spatiotemporal characteristics of the downstream Ca^{2+} response? If so, this would highlight a mechanism by which the cell may differentiate between the apparently promiscuous physiological P2Y agonists.

Were our hypothesis of a differential contribution of IK_{Ca} and SK_{Ca} to $P2Y_1$ and $P2Y_2$-evoked responses to be true, the responses to ADPβS and ATP should be similarly dependent on activation of SK_{Ca}. However, the results of the present study would suggest that the ADPβS-evoked dilatation response is facilitated by activation of either SK_{Ca} or IK_{Ca} alone. Such differences between the ATP and ADPβS response are unlikely to be associated with their differing capacity for breakdown by luminal ectonucleotidases as the flow-dependent nature of the UTP-evoked response could be facilitated by activation of either SK_{Ca} or IK_{Ca}. It is therefore proposed that these results may reflect a differential activity of ATP and ADPβS at the $P2Y_1$ receptor (Gallagher & Salter, 2003).

Addition of the thiol group to the β phosphate moiety of the adenine nucleotide may instill ADPβS with a greater affinity for the $P2Y_1$ receptor than ATP (ADP) by increasing the strength of binding of the negatively charged phosphate moieties with the positively charged binding site (Jiang *et al.*, 1997). As a result ADPβS may associate with the $P2Y_1$ receptor for longer or evoke different conformational changes in the receptor upon binding. This may result in an increased association of downstream

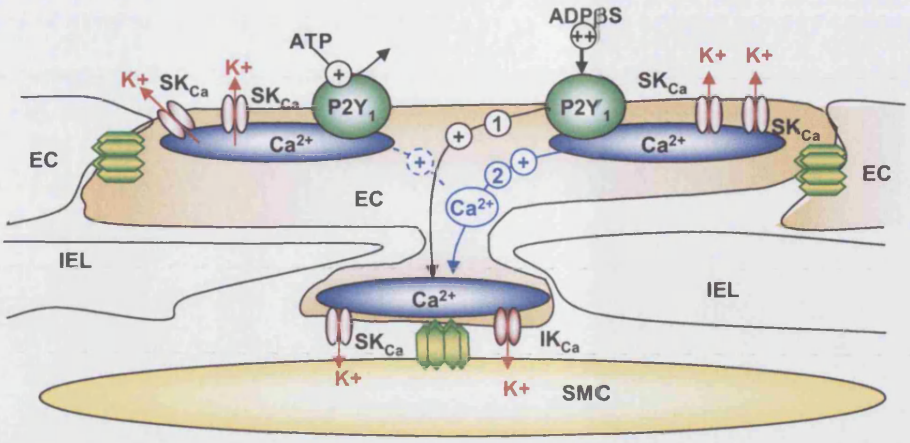

Figure 6.15. Proposed pathways leading to the differential activation of IK_{Ca} and SK_{Ca} downstream of ATP and ADPβS stimulation

Cartoon illustrating the mechanisms by which ATP and ADPβS could differentially activate IK_{Ca} and SK_{Ca} channels downstream of receptor activation. ATP-evoked hyperpolarization and dilatation would be predominantly evoked by an apical increase in intracellular Ca^{2+} in the vicinity of SK_{Ca} localized to the endothelial cell border (Marchenko, 2002; Sandow *et al.*, 2006). A small IK_{Ca} component could be facilitated by diffusion of Ca^{2+} to the MEGJ (dashed line). In contrast, due to differential binding characteristics ADPβS, would facilitate endothelial cell hyperpolarization and dilatation by both apical activation of SK_{Ca} followed by a baso-lateral mechanism of Ca^{2+} release and activation of MEGJ IK_{Ca} (Sandow *et al.*, 2006). The latter occurring by; 1), diffusion of signalling molecules and activation of a distinct Ca^{2+} release mechanism; or, 2), diffusion of the Ca^{2+} response from the apical surface.

signalling proteins with the receptor and a larger or more diffuse endothelial cell Ca^{2+} response. Diffusion of Ca^{2+} to the baso-lateral portion of the endothelial cell, whether by signalling intermediates or by direct spread of Ca^{2+} would then facilitate activation of both SK_{Ca} and IK_{Ca} (Figure 6.15; Sandow *et al.*, 2006).

To test such a hypothesis it would be essential to study the Ca^{2+} signal downstream of $P2Y_1$ and $P2Y_2$ receptor activation by ATP, ADPβS, and UTP, possibly using the Rhod Ca^{2+} indicators in conjunction with Lucifer yellow staining of the IEL as has been described (please see chapter 3). However acceptance of such proposals for the differential activation of IK_{Ca} and SK_{Ca} by ATP, UTP and ADPβS is also limited by the lack of selective antibodies for the P2Y purinoceptors and therefore, the limited knowledge with regards to the *in vitro* localization of the receptors within the arterial wall. Therefore it is proposed that upon development of selective antibodies for the

$P2Y_1$ and $P2Y_2$ receptors, further experiments be performed to elucidate the localization of the $P2Y_1$ and $P2Y_2$ receptors relative to the IK_{Ca} and SK_{Ca} channels.

6.4.2. Contribution of PKC to desensitization of the nucleotide-evoked dilatation response

In contrast to previous reports (Liu *et al.*, 2004) dilatation responses in the present study could not be evoked by flow alone ($n = 5$). Given the large n value (99) documented by Liu *et al* (2004), the present results probably reflect the inconsistency with which flow-dependent responses are evoked in this preparation (54% of arteries tested; Liu *et al.*, 2004). Upon inclusion of ATP or UTP in the perfusate, dilatation responses were observed that were of a similar profile to those described previously (Liu *et al.*, 2004) and as such are consistent with the idea that the flow-dependent nature of the responses reflects the breakdown of ATP and UTP by ectonucleotidases in the absence of flow. Luminal perfusion of the nucleotides increases the effective concentration at the endothelial cell surface thus increasing the likelihood of receptor activation (Berra-Romani *et al.*, 2004). However, a flow-independent reduction in the dilatation response to the non-hydrolyzable analogues of ADPβS was also observed. Given the limited dilatation upon repeated luminal perfusion of ADPβS such a reduction in the dilatation response likely reflects a desensitization of the response that cannot be overcome. The limited breakdown of the ADPβS by ectonucleotidases minimizing the differences in agonist concentration seen in the presence and absence of flow (Liu *et al.*, 2004).

The requirement for ATP and UTP to be continually perfused through the lumen in order to evoke a robust vasodilatation response reflects the nature with which the nucleotides may be released into the lumen physiologically. A decrease in PO_2 in response to increased tissue metabolism would stimulate nucleotide release from circulating red blood cells, which would lead to vasodilatation (reflected by our luminal perfusion period). The subsequently increased blood flow would then increase the PO_2, inhibiting nucleotide release and reversing the vasodilatation response (reflected by our 'flow off' period) (Dietrich *et al.*, 2000; Ellsworth, 2004; Ellsworth *et al.*, 1995; Gonzalez-Alonso *et al.*, 2002). The desensitization of the dilatation response to the non-hydrolyzable agonists thus possibly reflects a negative feedback mechanism that may be

associated with limiting this vasodilatation response to ensure that adequate blood flow to other tissues is maintained.

Desensitization of $P2Y_1$ and $P2Y_2$-evoked responses by various isoforms of PKC has been proposed for a number of cell types, including bovine pulmonary artery endothelial cells, mouse neuroblastoma cells, human platelets and rat renal mesangial cells (Chen & Lin, 1999; Chen & Chen, 1997; Hardy *et al.*, 2005; Pfeilschifter & Huwiler, 1996; Ralevic & Burnstock, 1998). As yet there are no other reports documenting the modulation of endogenous $P2Y_1$ and $P2Y_2$ receptors by PKC in intact arteries. The reduction of GPCR activity by PKC is associated with the phosphorylation of the C-terminus or third intracellular loop of the activated GPCR by the serine-threonine kinase, which prevents the association of the receptor with downstream signalling proteins. Receptor internalization and degradation are not associated with the PKC-mediated desensitization of agonist-evoked responses (Bailey *et al.*, 2006; Gainetdinov *et al.*, 2004; Garrad *et al.*, 1998; Otero *et al.*, 2000). At least 12 isoforms of PKC have been identified which are localized to and contribute differently to cell function depending on the cell type and receptor under study (Chen & Lin, 1999). Each isoform may belong to one of three classes, the conventional PKC isoforms (α, $\beta1$, $\beta2$ and γ), the new isoforms (δ, ε, η and θ) and the atypical isoforms (ζ, λ, ι and μ) (Chen & Chen, 1997). BIS I, a non-isoform selective PKC inhibitor was used in the present study, as the non-selective effects of the inhibitor on other protein kinases are relatively minimal (Davies *et al.*, 2000).

Previous reports have shown that within bovine pulmonary artery endothelial cells PKC$\beta1$, ε and μ translocate to the cell membrane upon activation and that PKC$\beta1$ mediates the rapid desensitization of $P2Y_1$ and $P2Y_2$-evoked dilatation responses (Chen & Lin, 1999). The present results are therefore consistent with such an observation as the reversal of the $P2Y_1$ and $P2Y_2$ receptor-stimulated responses were at least partly dependent on the activation of PKC. However, within the current study selective activation of $P2Y_2$ receptors with ATPγS was the only dilatation response that could be fully maintained in the presence of flow following inhibition of PKC. Given that both the ATPγS- and UTP-evoked dilatation responses are most likely associated with endothelial cell $P2Y_2$ receptor activation (Buvinic *et al.*, 2002; Malmsjo *et al.*, 2000a),

dilatation responses to UTP would be expected to be similarly affected by BIS I. However, the differences between the dilatation responses to the two agonists could reflect concentration differences at the endothelial surface due to the breakdown of UTP. Indeed the ability of UTP to evoke a full and sustained dilatation response at 3μM (identical to the profile of dilatation to 3μM ATPγS) would support such a theory. In contrast, the remaining reversal of the dilatation response to both ATP and ADPβS in the presence of BIS I could possibly indicate an influence of other protein kinases such as PKA and the G protein receptor-coupled kinases (GRKs) on the $P2Y_1$ purinoceptor (Gainetdinov *et al.*, 2004).

In contrast to the present report, Otero *et al* (2000) have advanced the suggestion that the regulation of $P2Y_2$ receptors may be partly mediated by GRKs whilst Hardy *et al* (2005) have documented that desensitization of the $P2Y_1$ receptor is fully mediated by activation of PKC. These differences in the documented contributions of PKC to P2Y receptor desensitization most likely reflect the fact that the contribution of each protein kinase to the dilatation response is dependent on the agonist used to evoke receptor activation, the level of desensitization observed, the cell type studied and the duration of agonist exposure (Bailey *et al.*, 2006; Gainetdinov *et al.*, 2004; Garrad *et al.*, 1998; Otero *et al.*, 2000).

Within the present study therefore, where agonists are applied luminally and the response controlled from the attainment of peak vasodilatation, a degree of experimental error must arise from the actual contact time of the agonist with the endothelium and the real concentration of agonist at the endothelial cell surface. Indeed, the lack of desensitization of the 3μM ATP, 3μM ATPγS and 3μM UTP-evoked responses suggest that concentration-dependent effects appear also to be involved. A limitation of the current technique was the inability to assess desensitization over the first 1 – 2min of agonist perfusion, due to the dead space volume (~100μl) that needed to be cleared before the agonists reached the artery lumen. Therefore if rapid desensitization occurred, the current set-up could not measure it. A more detailed interpretation of the contribution of PKC, or indeed other protein kinases to the dilatation response would therefore most likely be achieved by minimizing the dead space volume between the lumen of the artery and the start point of agonist perfusion

and by analyzing the initial part of the dilatation response. Further improvements to the protocol may then also be achieved by inclusion of a fluorescent dye in the purinoceptor agonist solution. Using concurrent visualization of luminal fluorescence and artery diameter it would be possible to measure the rate of agonist delivery in the lumen of the artery and subsequently also the duration of agonist exposure, minimising variability within the experimental protocol.

In conclusion the present report demonstrates that EDHF-type dilatation responses evoked by ATP, UTP and ADPβS were differentially dependent on IK_{Ca} and SK_{Ca}. Pending the results of further work, we propose that the differential contribution of the two K_{Ca} may reflect differential activation of endothelial cell P2Y receptors and the subsequent activation of discrete spatiotemporal Ca^{2+} signals. Further preliminary results suggest that both $P2Y_1$ and $P2Y_2$ responses are modulated by downstream activation of PKC although a role for other protein kinases is not discounted by the results of the present study.

6.5. Acknowledgments

I would like to thank Dr. Amanda MacKenzie for her advice thoughout this study and Dr. Kim Dora and Miss Hannah Norris for their contributions to the data obtained for the ATP concentration-response curves.

7. Nucleotide-evoked conducted dilatation responses

7.1. Introduction

Conducted vasodilatation responses are essential for the maintenance of sufficient tissue perfusion during periods of increased tissue metabolism and hypoxia (Dora *et al.*, 2000a; Kurjiaka & Segal, 1995; Segal, 2005; Segal & Duling, 1986a). As such, extensive studies have been performed to elucidate the mechanisms associated with these responses (please see chapter 5). Of the mechanisms described most investigators conclude cell-to-cell conduction of hyperpolarization through gap junctions within the endothelium to be the most significant (de Wit *et al.*, 2000; de Wit *et al.*, 2006b; Emerson & Segal, 2001; Emerson & Segal, 2000b; Figueroa *et al.*, 2003; Takano *et al.*, 2004).

The majority of experiments performed to investigate this phenomenon employ the robust agonist ACh to evoke the local vasodilatation response. Conducted dilatation responses to more physiologically relevant agonists such as ATP and UTP, both of which may be prevalent in the blood stream under exercising conditions and instances of tissue ischaemia (please see section 6.1; Erlinge *et al.*, 2005; Rosenmeier *et al.*, 2004; Wihlborg *et al.*, 2006) have, however, been scarcely documented. A few studies of conducted vasodilatation responses to ATP and adenosine have been performed within the small arterioles and vascular beds of the microcirculation (Delashaw & Duling, 1991; Dietrich *et al.*, 1996; Duza & Sarelius, 2003; Kajita *et al.*, 1996; McCullough *et al.*, 1997). However, given that the larger resistance-sized arteries of the vasculature may also contribute significantly to the regulation of total peripheral resistance (please see section 1.1.1; Fenger-Gron *et al.*, 1997; Fenger-Gron *et al.*, 1995; Mulvany & Aalkjaer, 1990) it would seem crucial that such responses are also investigated in vessels of this size.

Conducted vasodilatation responses to both ACh and LVK have been documented within the larger resistance arteries of the rat mesenteric bed and are most likely present to maintain perfusion to the smaller downstream feed arteries (please see chapter 5; Dora *et al.*, 2000a; Goto *et al.*, 2004; Kurjiaka & Segal, 1995; Takano *et al.*, 2004). Importantly, radial EDHF-type dilatation and hyperpolarization responses, the latter a prerequisite for the conducted vasodilatation response, have also been documented within this preparation following application of a range of purinoceptor agonists (please

see chapter 6; Delashaw & Duling, 1991; Dora *et al.*, 2003b; Liu *et al.*, 2006a; Malmsjo *et al.*, 1999; Mistry *et al.*, 2003; Neild & Crane, 2002; Takano *et al.*, 2005). Therefore within the present study, experiments were performed to explore whether the vasodilatation response of the rat small mesenteric artery to purinoceptor agonists could propagate longitudinally through the wall of these resistance arteries to evoke a spreading vasodilatation s previously observed for ACh and LVK (please see chapter 5; Goto *et al.*, 2004; Takano *et al.*, 2004). As many purinoceptor agonists also evoke vasoconstriction responses when applied abluminally (Galligan *et al.*, 2001; Gitterman & Evans, 2000; Harrington & Mitchell, 2004; Malmsjo *et al.*, 2000a) conducted dilatation responses to luminally-perfused purinoceptor agonists were also evaluated using a novel triple cannulation technique.

Aspects of this work have been described previously (Winter & Dora, 2006a).

7.2. Methods

7.2.1. Rat mesenteric artery isolation and cannulation

Please see section 2.1 for methods of artery isolation.

7.2.2. Pressure myography

Arteries were mounted in custom-built organ baths (0.5ml; Figure 2.2). For cannulation and equilibration methods please see section 2.2. Endothelial cell viability was assessed as a >90% control dilatation to ACh (1μM) following pre-constriction with PE (1 - 3μM). Arteries were maintained at 50mmHg and 37°C unless otherwise stated.

7.2.3. Focal abluminal stimulation of pressurized arteries

Please see section 2.3 for details of the methods used for the focal stimulation of arteries. In summary bolus doses of agonists were pressure-pulse ejected to the downstream end of arteries and dilatation responses simultaneously measured at sites up to 2mm upstream.

7.2.4. Focal luminal application of agonists

The three ends of arteries with a bifurcation at the downstream end were cannulated and mounted in a heated, 2ml chamber (Warner Instruments) and continuously superfused at 2ml min^{-1}. The upstream and downstream perfusion pressures through the feed artery were adjusted to generate luminal flow (7 – 9cmH_2O gradient, 30 - 50μl min^{-1}), whilst maintaining a constant pressure at the bifurcation to avoid upstream flow of infused agonists. Agonist solutions were luminally-perfused into one of the side branches for at least 2min at 50μl min^{-1} using a BeeHive® syringe pump system (Bioanalytical systems, USA). In all experiments the movement of perfusion solution was monitored by including 0.1μM carboxyfluorescein in the agonist solution (Figure 7.1).

7.2.5. Drugs and solutions

All drugs and solutions were prepared as detailed previously (please see section 2.6). Drugs used to characterise conducted dilatation responses were added to the superfusate reservoir prior to artery superfusion. Inhibitors were only applied luminally where necessary (please see section 2.6). L-NAME (100μM) was present throughout all experiments. Inhibition of cyclooxygenase was not required, as indomethacin (10μM)

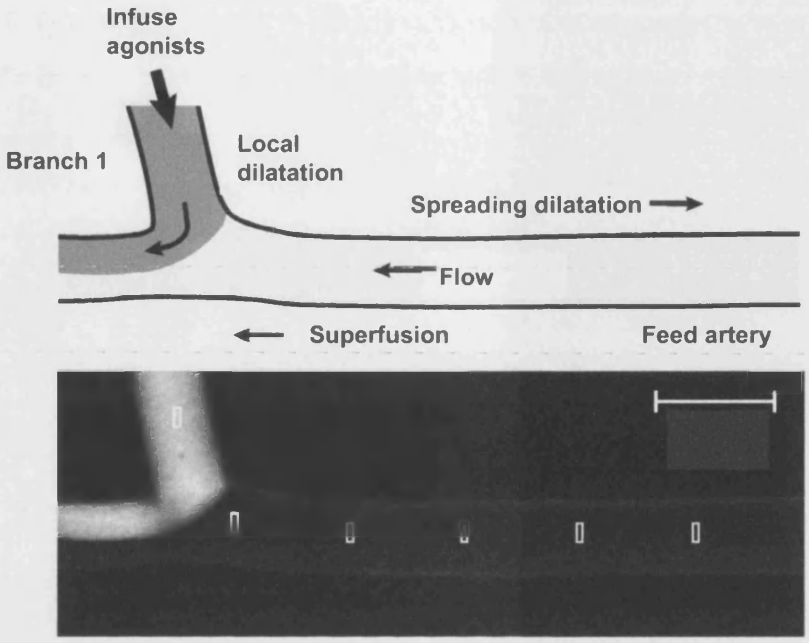

Figure 7.1 The triple cannulation technique for evaluation of spreading dilatation responses to luminally-perfused agonists
Diagrammatic representation and representative image of a triple cannulated rat small mesenteric artery for the study of conducted dilatation responses to luminally-perfused agonists. Using a third cannulating pipette, one branch at an arterial bifurcation (Branch 1) was cannulated, through which perfusate containing agonists and carboxyfluorescein (0.1μM) was infused. The second panel illustrates the limited upstream diffusion of the agonist using this method (the arterial wall visible due to autofluorescence), the small boxes indicating the positions of fluorescence measurement, and relate to the positions at which diameter was measured from the simultaneous brightfield images, 2000μm being the furthest upstream. Bar=500μm.

has been shown to have no effect on purinoceptor agonist or ACh-evoked dilatation responses within the rat mesenteric artery (please see section 1.3.2.4; Mistry *et al.*, 2003).

7.2.6. Data analysis

Data for conducted dilatation responses to abluminally-applied agonists were collected and analysed as has been described previously (please see section 5.2.8) with the exception that analysis of the speed of the conducted dilatation response was not performed. For analysis of conducted dilatation responses to luminally-perfused purinoceptor agonists arteries were visualized using a laser scanning confocal microscope (FV500-SU, Olympus, Japan, excitation 488nm, emission 505nm) to enable

simultaneous fluorescence and brightfield imaging, with a 4x/0.13NA objective (UplanFl, Olympus, Japan), and images were recorded with Fluoview software (Olympus, USA) at 1Hz. As mentioned previously (please see section 5.2.8) the resolution of the system using the 4x/0.13NA objective was 5μm (equivalent to 1 pixel, circa 1.5% of the maximum diameter of the arteries). There was a short delay in observing responses to luminal perfusion of agonists due to voiding the tubing and pipette dead-space volume.

For all spreading dilatation responses artery outer diameter was analysed using motion analysis software (Metamorph, Universal Imaging, USA) as has been described previously (please see section 2.5.2). For spreading dilatation responses to luminally-applied agonists fluorescence intensity was also measured offline simultaneously at multiple positions in the lumen of arteries and subsequently matched to the diameter measurements also made at those positions but on the outer edge of the artery wall (Figure 7.1). Fluorescence intensity (F) relative to the maximum fluorescence obtained during perfusion periods (F_{max}) was expressed as the relative change (F/F_{max}) for each luminal region of interest.

7.3. Results

All experiments were performed in the presence of the selective eNOS inhibitor L-NAME (100μM).

7.3.1. Spreading dilatation to focal abluminal application of nucleotides

When applied focally to the outside of isolated, pressurized arteries at a downstream position ATP (1mM, 30 - 300ms, n = 4) stimulated a biphasic response comprising a robust vasoconstriction (0μm; 50.2 ± 6.6%) immediately followed by a small vasodilatation (0μm; 17.53 ± 7.5%; Figures 7.2A and 7.4). Both phases were conducted upstream (2000μm; Constriction, 13.7 ± 1.5%, Dilatation, 21.1 ± 11.5%; n = 3; Figure 7.4) such that local (0μm) and spreading (500 - 2000μm) responses occurred synchronously (Figure 7.2A). In contrast, focal abluminal application of UTP (1mM, 30 - 1000ms, n = 4) caused only a spreading vasoconstriction (0μm, 66.2 ± 13.9, n = 4; 2000: 11.0 ± 4.8%, n = 3; Figures 7.2B and 7.4) that was synchronous at both local and upstream sites (Figure 7.2B).

In order to evaluate if the relatively small dilatation response to abluminal (versus luminal; Figures 6.2 and 7.8) application of ATP was due to its breakdown at the smooth muscle surface before it could reach the endothelium as either ATP or ADP, the response to focal abluminal application of ADPβS (1mM, 30ms, n = 4) was studied. The dilatation response to ADPβS was greater in amplitude at the local site than that seen for ATP (90.29 ± 5.9%) and, but for a small transient local constriction (23.1 ± 3.7%), more closely resembled ACh-evoked spreading responses at local and distal sites (Figures 7.3A and 7.4). In contrast when similar experiments were carried out to evaluate the efficacy of ATPγS (1mM, 10 - 100ms, n = 4) as a dilator (rather than UTP, which may be broken down at the smooth muscle surface) a response akin to that seen with ATP was observed: A biphasic response constituting an initial spreading constriction (0μm: 54.2 ± 16.9%; 2000μm: 16.7 ± 7.4) followed by a spreading dilatation that in some cases appeared masked at the local site by the extensive constriction (0μm: 14.5 ± 7.9%; 2000μm: 33.6 ± 2.9; Figures 7.3B and 7.4).

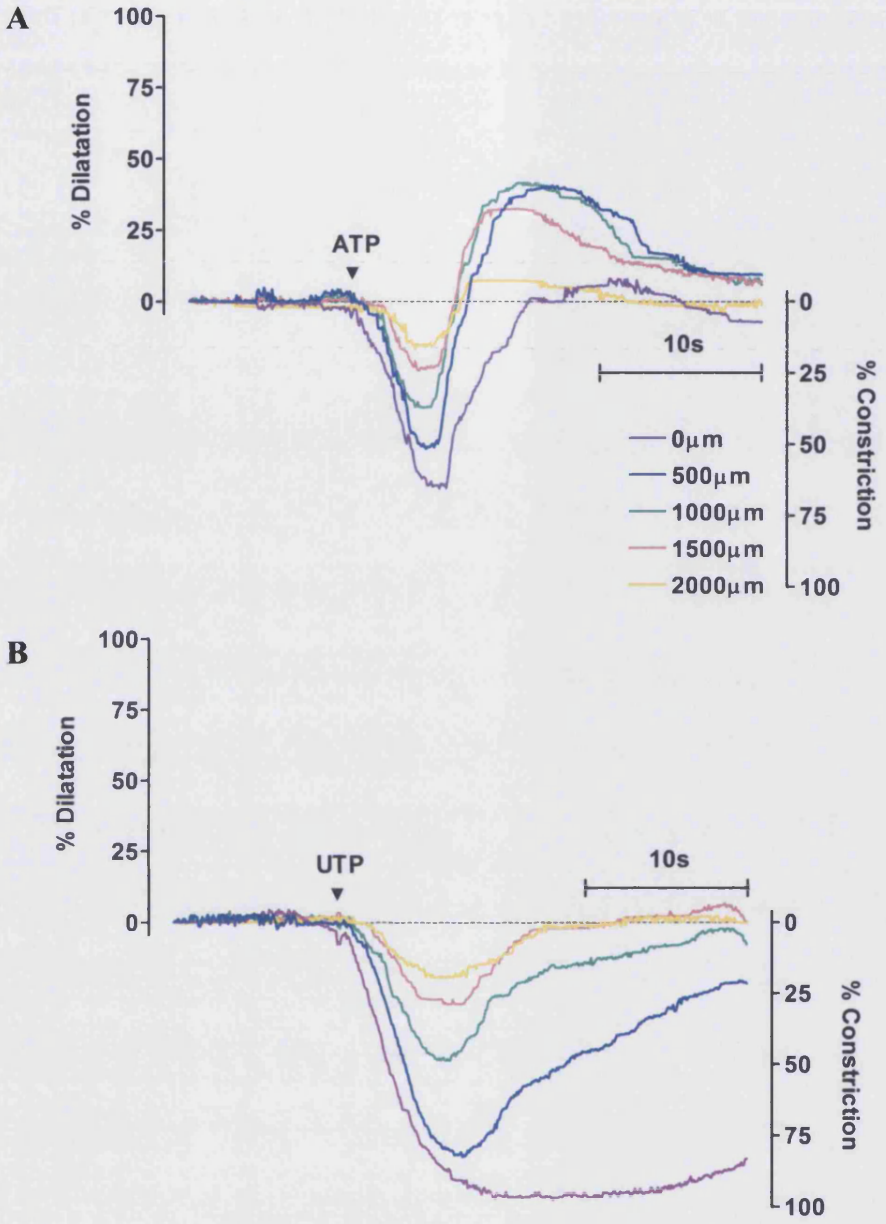

Figure 7.2 Local and spreading dilatation and constriction responses to abluminal application of ATP and UTP

Using a micropipette positioned at the downstream end of the artery, agonists were pressure-pulse ejected as bolus doses. The figure shows representative traces of the local (0µm) and spreading (500 - 2000µm) responses to **A,** ATP (1mM, 100ms) and **B,** UTP (1mM, 300ms). Images were acquired at 12Hz. Diameter was measured simultaneously at all positions along the artery. L-NAME (100µM) present in all experiments.

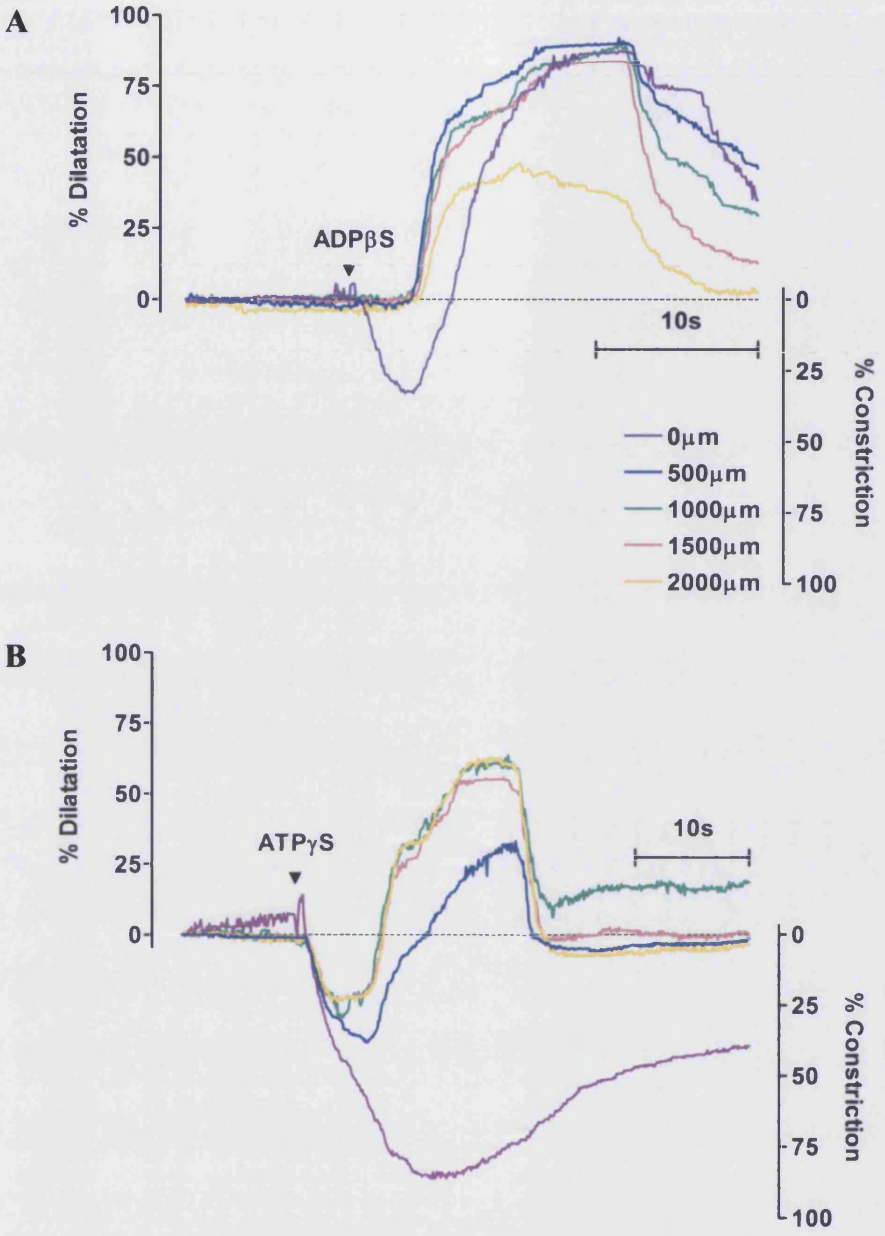

Figure 7.3 Local and spreading dilatation and constriction responses to abluminal application of ADPβS and ATPγS.

Using a micropipette positioned at the downstream end of the artery, agonists were pressure-pulse ejected as bolus doses. The figure shows representative traces of the local (0μm) and spreading (500 - 2000μm) responses to **A,** ADPβS (1mM, 100ms) and **B,** ATPγS (1mM, 300ms). Images were acquired at 12Hz. Diameter was measured simultaneously at all positions along the artery. L-NAME (100μM) present in all experiments.

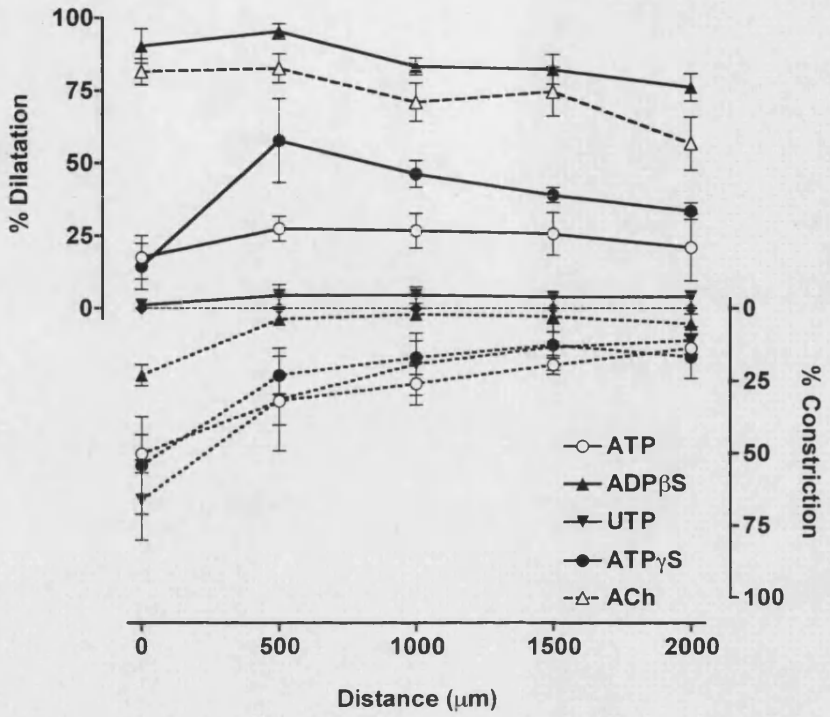

Figure 7.4 Summary of local and spreading dilatation and constriction responses to abluminal application of nucleotides
Summary data showing mean spreading responses to abluminal application of ATP (1mM, 30 - 300ms, *n*=4), ADPβS (1mM, 30ms, *n*=4), UTP (1mM, 30-1000ms, *n*=4), ATPγS (1mM, 10-100ms, *n*=4) and, for comparison, ACh (1mM, 30-100ms, *n*=5). The biphasic nature of the conducted responses to the nucleotides is represented by the peak dilatation (solid lines) and constriction (broken lines) responses to each agonist. L-NAME (100μM) present in all experiments.

7.3.2. Effects of $P2Y_1$ and K_{Ca} inhibition on nucleotide-evoked spreading responses

Spreading dilatation responses evoked by abluminal application of bolus doses of ATP (1mM, 30ms, n = 3) and ADPβS (1mM, 10 - 30ms, n = 3) were reduced by selective inhibition of $P2Y_1$ receptors with MRS2179 (1μM; Figure 7.5). In contrast constriction responses to either agonist were not influenced by treatment with MRS2179 (Figure 7.5). Dilatation responses to ATPγS (1mM, 10 - 30ms, n = 3) and ACh (1mM, 3 - 100ms, n = 3) were also largely unaffected although a larger ATPγS-evoked constriction response was observed at the local site (Figure 7.6).

Selective blockade of IK_{Ca} and SK_{Ca} with TRAM-34 (1μM) and apamin (50nM) completely blocked spreading dilatation responses to ATP (1mM, 100ms, n = 3; Figure 7.7A) and ADPβS (1mM, 10-30ms, n = 3; Figure 7.7B).

7.3.3. Spreading dilatation to luminally-perfused nucleotides

Luminal perfusion of ATP (1 or 3μM; Figure 7.8A), UTP (3 or 10μM) or ADPβS (1 or 3μM) into a side branch of a triple cannulated artery evoked a robust local (Branch 1; ATP, 90.0 ± 3.7%, n = 6; UTP, 81.5 ± 6.7%, n = 6; ADPβS, 85.8 ± 5.0% n = 6; Figure 7.8B) dilatation response that was only slightly, if at all, reduced as it passed into the feed artery (0μm; ATP, 80.8 ± 3.5%; UTP, 75.8 ± 10.8%; ADPβS, 80.0 ± 6.6%; Figure 7.8B). Dilatation responses to ATP, UTP and ADPβS all spread upstream into the feed artery to remote regions not directly stimulated by the agonist (Figure 7.8). Although the spreading dilatation responses decayed with distance (2000μm; ATP, 8.7 ± 2.5%; UTP, 9.8 ± 1.1%; ADPβS, 9.3 ± 4.2%; Figure 7.8B) small dilatation responses were still observed at distances greater than 2mm from the site of stimulation. In contrast, local dilatation responses to concentrations of adenosine (100μM) sufficient to evoke a matched dilatation in Branch 1 (76.7 ± 5.0%) decayed to an extent such that even the local dilatation response in the feed artery was greatly reduced (0μm, 39.6 ± 7.1%). Local (Branch 1 and 0μm) and spreading dilatation (500 - 2000μm) responses to all agonists occurred synchronously (Figure 7.8A).

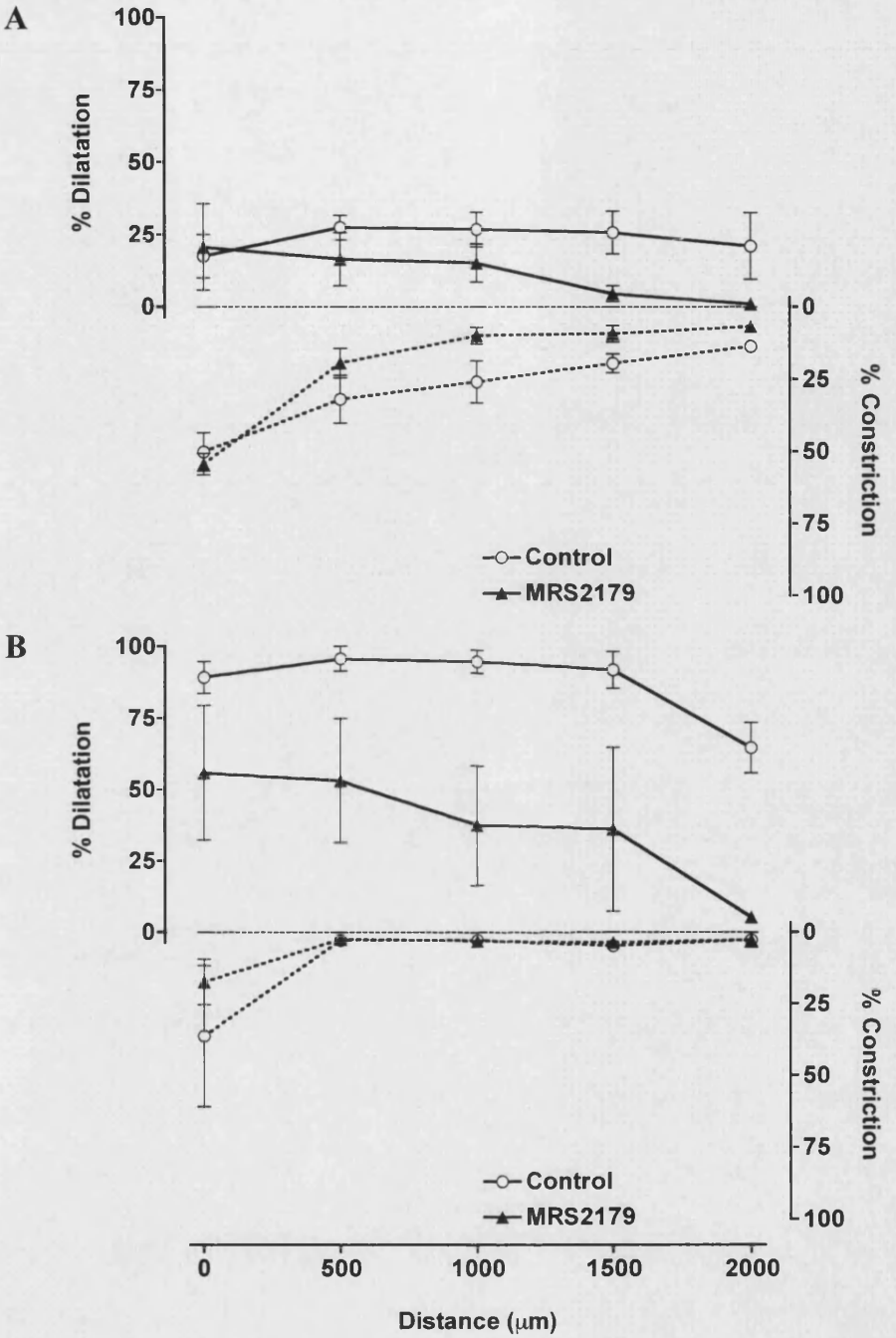

Figure 7.5 Effect of MRS2179 on local and spreading dilatation and constriction responses to abluminally-applied ATP and ADPβS
Summary data illustrating the effect of luminal and abluminal incubation with MRS2179 (1μM) on mean spreading responses to **A**, ATP (1mM, 30ms, *n*=3, unpaired), and **B**, ADPβS (1mM, 10 - 30ms, *n*=3, paired). The biphasic nature of the responses is represented by the peak dilatation (solid lines) and constriction (dotted lines) responses to each agonist. L-NAME (100μM) present in all experiments. Please note that the control data for ATP-evoked responses has been shown previously (Figure 5.5).

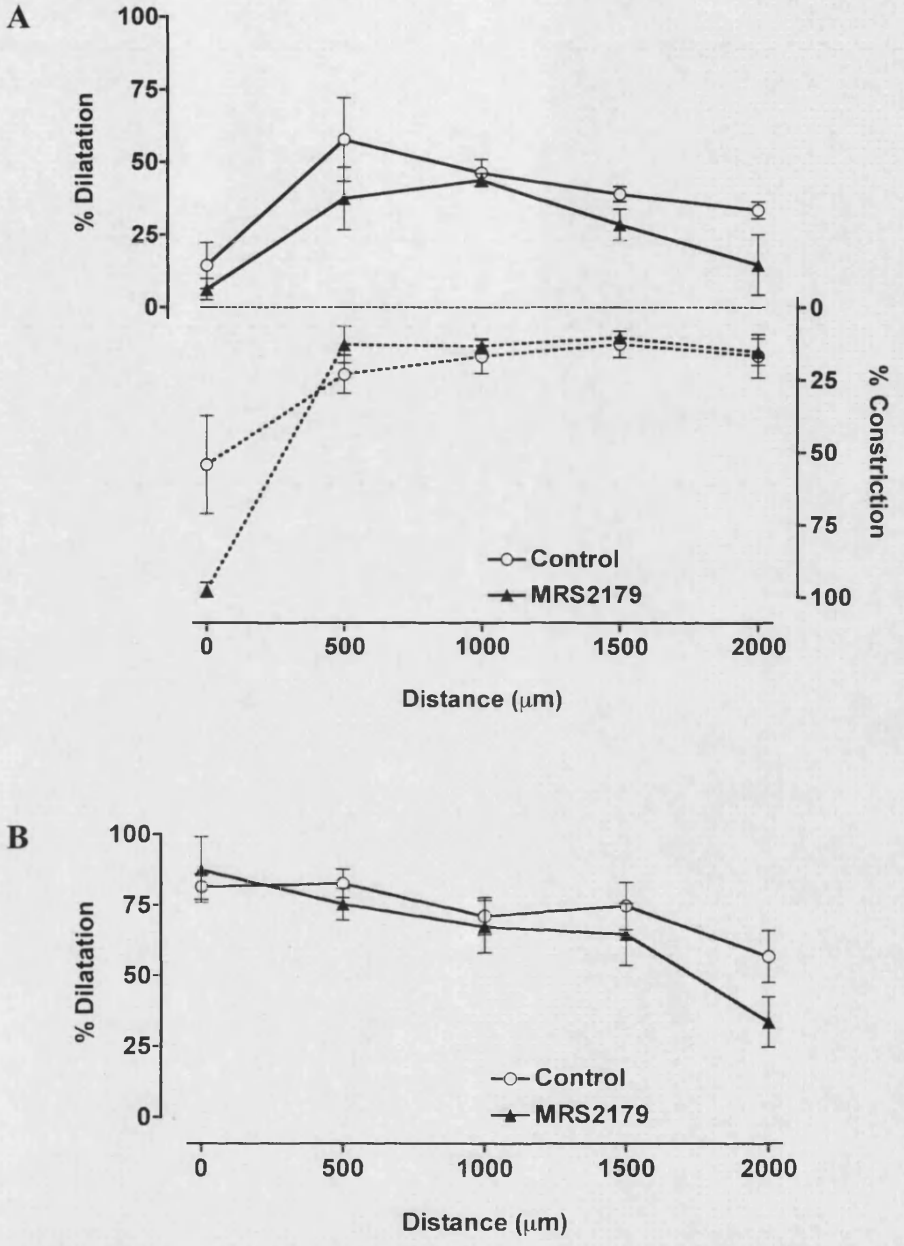

Figure 7.6 Effect of MRS2179 on local and spreading dilatation and constriction responses to abluminally-applied ATPγS and ACh
Summary data illustrating the effect of luminal and abluminal incubation with MRS2179 (1μM) on spreading responses to **A**, ATPγS (1mM, 10 - 30ms, *n*=3, unpaired), and **B**, ACh (1mM, 3 - 100ms, *n*=3, unpaired). The biphasic nature of the responses is represented by the peak dilatation (solid lines) and constriction (dotted lines) responses to each agonist. L-NAME (100μM) present in all experiments. Please note that all control data has been shown previously (Figure 5.5).

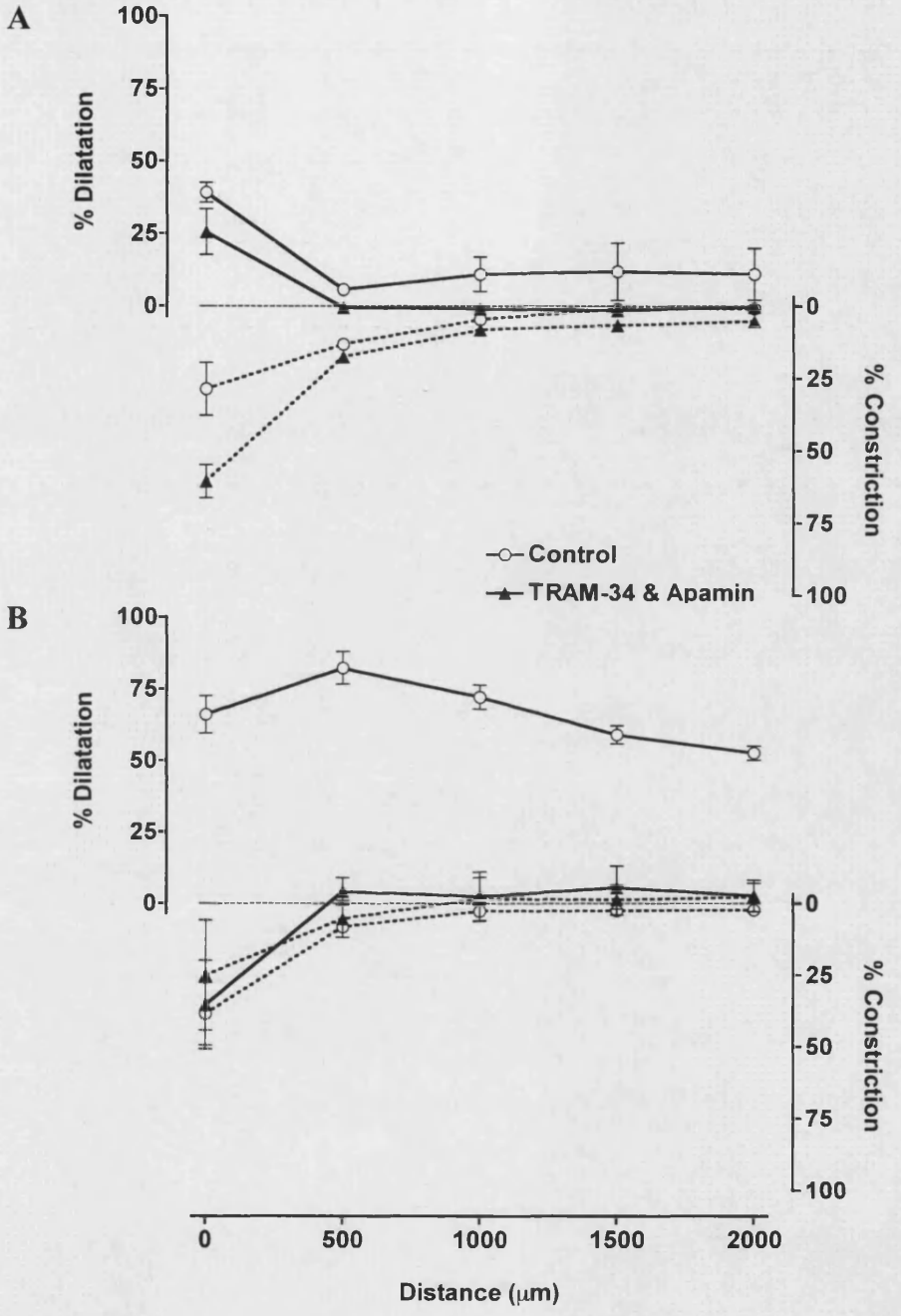

Figure 7.7 Effect of TRAM-34 and apamin on local and spreading dilatation and constriction responses to abluminally-applied nucleotides
Summary data illustrating the effect of luminal and abluminal incubation with TRAM-34 (1μM) and apamin (50nM) on spreading responses to **A**, ATP (1mM, 100ms, *n*=3, paired), and **B**, ADPβS (1mM, 10-30ms, *n*=3, paired). The biphasic nature of the responses is represented by the peak dilatation (solid lines) and constriction (dotted lines) responses to each agonist. L-NAME (100μM) present in all experiments. All experiments were performed by Dr. Kim Dora.

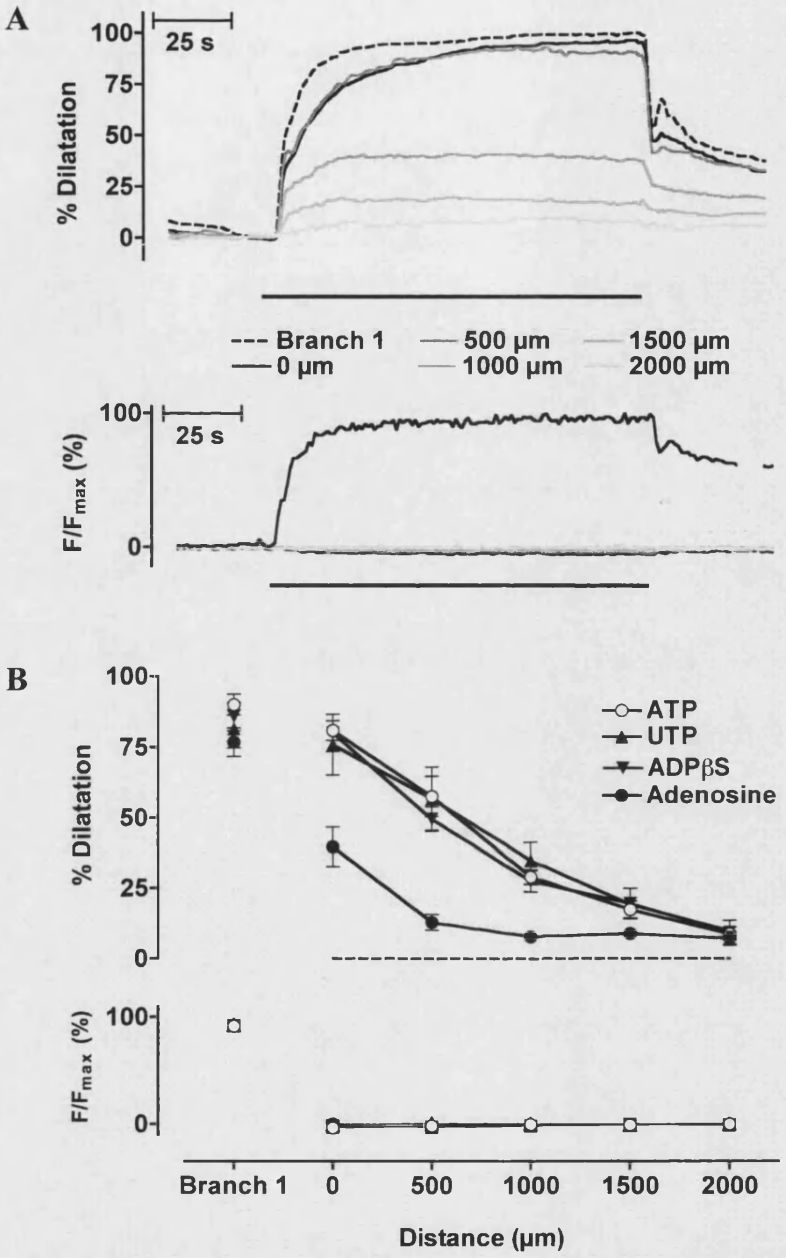

Figure 7.8 Spreading dilatation responses to luminal perfusion of nucleotides

A, Representative traces and **B**, summary data of arterial dilatation (upper panels) and relative fluorescence (F/F_{max} in Branch 1, lower panels) simultaneously measured at local (Branch 1 and 0µm) and remote (500-2000µm) sites in response to luminal perfusion of **A,** ATP (3µM), **B,** ATP (1 or 3 µM, *n*=6), ADPβS (1 or 3µM, *n*=6), UTP (3 or 10 µM, *n*=6), adenosine (100µM, *n*=5) and **A, B**, carboxyfluorescein (0.1µM) into Branch 1. Images were acquired at 1Hz. Bars indicate periods of luminal perfusion. L-NAME (100µM) present in all experiments. All experiments were performed by Dr. Kim Dora.

7.4. Discussion

Within the present report conducted responses to the purinoceptor agonists ATP, UTP, ADPβS and ATPγS were studied and for the first time in an artery of this size, spreading dilatation responses to both abluminally- and luminally-applied nucleotides were revealed. Similar experiments have been performed previously wherein conducted vasomotor responses to ATP and adenosine were studied in the smaller vessels of the hamster retractor muscle preparation and the rat cerebral arteriole. However, with the exception of one study in which ATP was luminally applied with a micropipette (McCullough *et al.*, 1997) all experiments were performed following abluminal application of either ATP or adenosine (Dietrich *et al.*, 1996; Duza & Sarelius, 2003; Kajita *et al.*, 1996).

The biphasic spreading response to focal abluminal application of ATP observed in the present study was locally of a similar profile to that previously documented in the microcirculation (Dietrich *et al.*, 1996; Duza & Sarelius, 2003; Kajita *et al.*, 1996; McCullough *et al.*, 1997). However, in contrast to previous reports the vasoconstriction evoked by ATP spread to remote sites such that at a distance of 1500μm from the site of application a significant reduction in artery diameter was observed. Given the NO-dependent attenuation of conducted vasoconstriction responses to KCl recently observed in the mouse cremaster muscle preparation such a difference may be explained by the use of L-NAME in the present study (McCullough *et al.*, 1997; Rodenwaldt *et al.*, 2007). The spreading vasoconstriction to ATP would be facilitated by the activation of P2X (most likely $P2X_1$) receptors on the smooth muscle and the subsequent depolarization caused by the inward current through these non-selective cation channels (Gitterman & Evans, 2000; Harrington & Mitchell, 2004; Lewis & Evans, 2000; Malmsjo *et al.*, 2000a; Malmsjo *et al.*, 2000b). However, the robust vasoconstriction to the $P2Y_2$ agonist ATPγS, a response that has been shown previously to be insensitive to P2X desensitization with αβ-methylene-ATP, suggests that a $P2Y_2$ component may also contribute to the response (Malmsjo *et al.*, 2000a). Studies performed to investigate $P2Y_1$, $P2Y_2$ and $P2Y_4$ receptor mRNA expression within the rat mesenteric bed suggest that only $P2Y_6$ is present in the smooth muscle (Buvinic *et al.*, 2002). Given the high concentrations of ATPγS and ATP used in the present study activation of the $P2Y_6$ receptor although unlikely, cannot be ruled out (Malmsjo *et al.*, 2000a). Further

experiments following desensitization of P2X receptors with αβ-methylene-ATP and inhibition of P2Y6 with MRS2578 would be required to establish which receptor(s) facilitate the ATP-evoked vasoconstriction (Alexander *et al.*, 2006; Malmsjo *et al.*, 2000a).

A secondary small spreading vasodilatation was also evident following focal abluminal application of ATP; the temporal characteristics of which were probably indicative of the time taken for ATP to diffuse to the endothelium (Dietrich *et al.*, 1996; McCullough *et al.*, 1997). However, locally the extent and time course of the local vasoconstriction masked any vasodilatation response to abluminally-applied ATP (Dietrich *et al.*, 1996; Malmsjo *et al.*, 2000b; McCullough *et al.*, 1997). Given that the vasoconstrictor component was enhanced following incubation with TRAM-34 and apamin, the current observation would suggest that the profile of the ATP-evoked response depends on the balance between the locally-evoked hyperpolarization response downstream of endothelial cell K_{Ca} activation and the extent of smooth muscle cell depolarization (Malmsjo *et al.*, 2000b; Malmsjo *et al.*, 1999).

The relatively small size of the conducted dilatation response, compared to that seen following luminal application of ATP, possibly also reflects the breakdown of the nucleotide by ectonucleotidases (please see section 1.3.1.2) as it passed though the adventitial and medial layers of the artery and the reduction in the active concentration of either ATP or ADP at the endothelium (Burnstock, 2006; Duza & Sarelius, 2003; Gorlach, 2005; Malmsjo *et al.*, 2000a). Indeed, the robust nature of the spreading vasodilatation responses to abluminally-applied ADPβS, a non-hydrolyzable analogue of ATP, would support such a hypothesis.

Adenosine has been shown to evoke significant dilatation responses within rat mesenteric artery preparations (Mian & Marshall, 1995), and is capable of evoking, albeit inconsistently (Delashaw & Duling, 1991; McCullough *et al.*, 1997), a conducted dilatation response within a variety of arteriolar and microcirculation preparations (Delashaw & Duling, 1991; Duza & Sarelius, 2003; Kajita *et al.*, 1996; Rivers & Frame, 1999). Indeed, as a metabolite of ATP that is capable of evoking an endothelium-dependent vasodilatation and K_{ATP}-facilitated hyperpolarization in the rat

aorta, adenosine may conceivably also contribute to the conducted dilatation response to ATP in the present study (please see section 1.3.1.2; Ray *et al.*, 2002; Ray & Marshall, 2005; Ray & Marshall, 2006). However, the rapid decay of the conducted dilatation response to luminally-applied adenosine over distances greater than 500μm would suggest that ATP-evoked spreading dilatation responses (whether following abluminal or luminal application of ATP) were not significantly dependent on an adenosine component.

Given the robust nature of the ADPβS-evoked conducted dilatation response (whether applied luminally or abluminally), and the MRS2179 sensitivity of local dilatations to luminally-perfused ATP and ADPβS in previous experiments (please see chapter 6), spreading vasodilatation responses to abluminally-applied ATP were evaluated in the presence of MRS2179 in an attempt to establish the involvement of the $P2Y_1$ receptor. Owing to the masked nature of the local vasodilatation response, the competitive nature of the antagonist (Boyer *et al.*, 1998) and the difficulties associated with evaluating the concentration of ATP released with each spritz the significance of these experiments is limited. However, using a concentration of MRS2179 previously demonstrated to abolish the dilatation response to luminally-perfused ATP (please see chapter 6) spreading dilatation responses to abluminal application of both ATP and ADPβS appeared attenuated, implying some action of endothelial $P2Y_1$ receptors in the conducted dilatation response.

Luminal application of ATP has been achieved previously by impaling an arteriole of the exteriorized hamster retractor muscle preparation with a pipette and then spritzing ATP onto the surface of the lumen by pressure-pulse ejection (McCullough *et al.*, 1997). Dilatation responses up to a distance of 1200μm from the stimulation site were recorded and were, in contrast to the present report found to be sensitive to eNOS inhibition with L-NAME. Luminal perfusion of ATP in the present study evoked an extensive, L-NAME-insensitive spreading dilatation response that persisted for the duration of agonist perfusion. Such a response is consistent with the robust nature of the radial dilatation response to the luminally perfused agonists and thus is also likely dependent on the activation of $P2Y_1$ receptors (please see chapter 6; Liu *et al.*, 2004).

Given the extensive vasodilatation response to luminally-applied UTP previously described (please see chapter 6; Liu *et al.*, 2004) experiments were subsequently performed to establish whether $P2Y_2$ activation could evoke a conducted vasodilatation. Luminal perfusion of UTP evoked a spreading dilatation response of equal magnitude and with equal decay characteristics as that observed for ADPβS and ATP, suggesting that stimulation of endothelial cell $P2Y_2$ receptors (Buvinic *et al.*, 2002; Malmsjo *et al.*, 2000a) is indeed capable of evoking a robust conducted dilatation response. However, abluminal application of UTP evoked only a local and spreading vasoconstriction that was likely reflective of smooth muscle P2Y receptor activation with minimal actions of the nucleotide on the endothelium (Buvinic *et al.*, 2006; Gitterman & Evans, 2000; Malmsjo *et al.*, 2000a). Unlike ATP, the products of ectonucleotidase metabolism of UTP have negligible vasodilatation capabilities within this artery, even at millimolar concentrations, so the absence of a vasodilatation component should perhaps be expected (Burnstock, 2006; Malmsjo *et al.*, 2000a; Malmsjo *et al.*, 2002). This observation is confirmed by the more robust nature of the ATPγS evoked conducted dilatation response, which in contrast to UTP, when applied abluminally is not broken down as it diffuses to the endothelium to activate $P2Y_2$ receptors.

Conducted dilatation responses to abluminally-applied ATP and ADPβS were completely attenuated by blockade of SK_{Ca} and IK_{Ca} channels with TRAM-34 and apamin. Furthermore, although conducted dilatation responses were not directly examined, local dilatation responses to luminally-perfused agonists were blocked by raising extracellular K^+ or by the combined blockade of SK_{Ca} and IK_{Ca} supporting the significant contribution of an endothelial cell hyperpolarization component to the local $P2Y_1$ and $P2Y_2$ receptor-evoked dilatation response (please see chapter 6; Malmsjo *et al.*, 1999; Mistry *et al.*, 2003). Given that longitudinal conduction of the hyperpolarization response within the rat mesenteric artery may occur irrespective of the agonist used to evoke the local increase in membrane potential (Takano *et al.*, 2004) the $P2Y_1$- and $P2Y_2$-evoked spreading dilatation responses observed in the present study likely reflect the transfer of hyperpolarization upstream through the endothelium as previously described for ACh and LVK in the rat mesenteric artery (Goto *et al.*, 2004; Takano *et al.*, 2004). Indeed the matched rate of decay for the ACh- and ADPβS-

evoked spreading dilatation responses would support such a hypothesis (Delashaw & Duling, 1991; Segal & Duling, 1989).

Conceivably the inhibition of the conducted dilatation response to ATP and ADPβS by TRAM-34 and apamin could reflect a blockade of the radial hyperpolarization response at the remote site and not an inhibition of the conducted hyperpolarization response. A local rise in endothelial cell Ca^{2+} has been documented within this preparation in response to luminal perfusion of micromolar concentrations of ATP (Liu *et al.*, 2006a) that is consistent with the local Ca^{2+} response to abluminal application of ACh (McSherry *et al.*, 2005; Takano *et al.*, 2004) that facilitates the activation of endothelial cell IK_{Ca} and SK_{Ca} (Malmsjo *et al.*, 1999; McSherry *et al.*, 2005; Mistry *et al.*, 2003). Conducted dilatation responses to both ACh and ATP within hamster retractor muscle feed arteries and hamster cheek pouch arterioles respectively have been shown to be dependent on a conducted endothelial cell Ca^{2+} response (Domeier & Segal, 2007; Duza & Sarelius, 2003; Uhrenholt *et al.*, 2007). However, these responses were also dependent on an NO component, which was not required for the spreading dilatation responses observed within the present study. Crucially, within rat mesenteric arteries the conducted hyperpolarization response does not parallel a conducted rise in endothelial cell Ca^{2+}, suggesting that the cell-to-cell transfer of hyperpolarization likely observed in the present study was independent of a remote rise in endothelial cell Ca^{2+}, and thus was also independent of the remote activation of IK_{Ca} and SK_{Ca} channels.

Nucleotides may be released into the vasculature from a range of sources including circulating cells under conditions of low PO_2 (Dietrich *et al.*, 2000; Ellsworth, 2004; Ellsworth *et al.*, 1995; Miseta *et al.*, 1993), surrounding ischaemic tissues (Erlinge *et al.*, 2005; Wihlborg *et al.*, 2006) and sympathetic nerve terminals (Burnstock, 2006; Su, 1983). As such they are considered to be key to the physiological regulation of vascular tone and thus have an inherent role in the regulation of tissue perfusion and total peripheral resistance. To ensure nucleotide-evoked dilatation responses are sufficient to maintain an increase in tissue blood flow and oxygen supply the response may be conducted upstream to the feed arteries (Dora *et al.*, 2000a; Kurjiaka & Segal, 1995; McCullough *et al.*, 1997).

The conducted dilatation responses to luminally-applied nucleotides observed in the present study demonstrate that the physiological release of nucleotides from circulating cells under conditions of low PO_2 could possibly be sufficient to evoke a conducted dilatation response within the resistance vasculature and thus also possibly increase blood flow to the downstream tissue (Rosenmeier *et al.*, 2004). The maintenance of the conducted dilatation response for the duration of luminal nucleotide perfusion supports the hypothesis that under low levels of PO_2 arterial perfusion with red blood cells will stimulate an ascending vasodilatation response via nucleotide activation of endothelial cell P2Y receptors that will be maintained for as long as the continual entry of the red blood cells into the artery is maintained. Only upon increased levels of PO_2 and cessation of nucleotide release would the conducted dilatation response end (McCullough *et al.*, 1997). The biphasic conducted response to abluminally-applied ATP observed in the present study thus reflects the fine balance that is likely to be present *in vivo* between the vasoconstriction evoked upon sympathetic nerve stimulation and the vasodilatation responses to luminally-released nucleotides just described: the balance between the hyperpolarizing and depolarizing influences having the final influence over tissue blood flow (Burnstock, 2006; Dietrich *et al.*, 2000; Duza & Sarelius, 2003; Ellsworth, 2004; Ellsworth *et al.*, 1995; Malmsjo *et al.*, 2000b; Malmsjo *et al.*, 1999; McCullough *et al.*, 1997; Miseta *et al.*, 1993; Rosenmeier *et al.*, 2004; Su, 1983).

7.5. Acknowledgements

I would like to thank Dr. Richard Rivers for the helpful discussion of this work and Dr. Kim Dora for her contributions to the study.

8. Conclusion

The studies documented within this thesis have explored how direct cell-to-cell communication within the arterial wall can facilitate EDHF-type radial and longitudinal dilatation responses in resistance arteries.

A correlation between the incidence of MEGJ and endothelium-derived hyperpolarizing responses is well established in a number of resistance arteries suggesting that myoendothelial cell-to-cell coupling is an important mechanism in the control of artery diameter (Sandow *et al.*, 2004; Sandow *et al.*, 2002). Indeed the inhibition of the EDHF-type dilatation response by carbenoxolone and selective endothelial cell pinocytic loading of anti-connexin 40 antibodies as described herein and in other reports (Edwards *et al.*, 1999; Goto *et al.*, 2002; Mather *et al.*, 2005) would support such a proposal. However, crucially, the results of the present study also highlight the difficulties that may be associated with trying to selectively inhibit gap junctions.

In contrast to a number of reports using the rat mesenteric artery (Matchkov *et al.*, 2006; Sandow *et al.*, 2002) the connexin-specific gap peptides were ineffective in the present study, even when used as a triple combination that targeted each of the known rat mesenteric artery connexins. Spreading dilatation responses, thought to at least partially rely on the longitudinal cell-to-cell conduction of hyperpolarization through gap junctions (de Wit *et al.*, 2000; Figueroa *et al.*, 2003; Segal *et al.*, 1989; Segal & Duling, 1989; Segal & Duling, 1986b), were also unaffected by endothelial cell loading of the anti-connexin antibodies. The heterogeneity in the connexin composition at each gap junction means that presently at least, selective pharmacological inhibition of either inter-endothelial or myoendothelial gap junction channels is virtually impossible. However, a number of other factors also preclude a definitive assessment of the efficacy of any of the inhibitors in the present study. In particular, the lack of electrophysiological data and the ambiguity associated with whether the antibodies are actually present at the site of cell-to-cell coupling.

Preliminary morphological studies described herein illustrated how the structure of the arterial wall could potentially facilitate the transfer of hyperpolarization from the endothelium to the smooth muscle and the longitudinal conduction of hyperpolarization. Staining of the rat mesenteric artery with di-8-ANEPPS revealed the narrow elongated

shape of the endothelial cells, which were aligned along the longitudinal axis of the artery wall and spanned ~12 smooth muscle widths. The extensive endothelial cell border staining for connexin 40 observed in the present study and that of others therefore suggests that the endothelial cell-to-cell coupling within this preparation is potentially adequate for a low resistance longitudinal conduction pathway (Goto *et al.*, 2004; Kansui *et al.*, 2004; Mather *et al.*, 2005; Sandow *et al.*, 2006). The co-localization of connexin 40, SK_{Ca} and IK_{Ca} channels with holes in the IEL was also consistent with a role for myoendothelial projections as key signalling domains for the radial cell-to-cell communication of the EDHF-type dilatation response, supporting the functional data described herein (Mather *et al.*, 2005; Sandow *et al.*, 2006).

The physiological importance of these observations is however difficult to reconcile, particularly given that traditionally EDHF-type dilatation responses are commonly characterised following inhibition of NO and prostacyclin-dependent pathways, whereas under physiological conditions these other pathways may be active. Indeed, within the rat mesenteric arterial bed *in vivo* EDHF is not thought to contribute to the regulation of basal blood flow. A significant contribution is, however, observed under conditions of agonist-evoked dilatation (Coleman *et al.*, 2004). This could possibly reflect an important role for the EDHF pathway under conditions of hypoxia or increased tissue metabolism where an increase in tissue blood flow may be associated with the release of vasodilator substances such as ATP (Dietrich *et al.*, 2000; Ellsworth, 2004). Indeed, within this study and others (Malmsjo *et al.*, 1999; Mistry *et al.*, 2003) EDHF-type dilatation and hyperpolarization responses have been observed in response to nucleotide application. Furthermore luminal perfusion of the physiological nucleotides ATP and UTP was able to evoke a robust spreading dilatation response suggesting that the nucleotides may also activate longitudinal cell-to-cell communication pathways within the rat small mesenteric artery, which could contribute to the maintenance of adequate tissue perfusion (Dora *et al.*, 2000a; Kurjiaka & Segal, 1995; Segal, 2005; Segal & Duling, 1986a).

Morphological data presented within this study made it apparent that SK_{Ca} and connexin 40, not IK_{Ca} were visible at sites of inter-endothelial cell-to-cell contact. The preliminary nature of these experiments precluded robust conclusions. However, a

recent report from Sandow *et al.* (2006) reported similar findings and advanced the suggestion that the differential IK_{Ca} and SK_{Ca} staining possibly reflected the differential contribution of these two channels to the ACh-evoked EDHF response in the rat mesenteric artery under different levels of PE-evoked tone (Crane *et al.*, 2003a; Sandow *et al.*, 2006). Within the current study the contribution of the IK_{Ca} and SK_{Ca} channels to the purinoceptor-evoked EDHF-type dilatation response was also shown to vary suggesting that the $P2Y_1$ and $P2Y_2$ receptors could perhaps evoke differential Ca^{2+} signals upon agonist stimulation leading to the differential activation of the two K_{Ca} channels. Indeed, compartmentalization of the P2Y receptors has been documented previously (Kaiser *et al.*, 2002). A role for PKC as a modulator of the nucleotide-evoked EDHF-type dilatation response was made apparent within this thesis and, although these and the K_{Ca} data are by no means conclusive they highlight the complexity associated with the EDHF-type dilatation response, particularly suggesting that the mechanisms associated with regulation of this response may be unique to each agonist. This could have significant implications for the study of EDHF type responses to nucleotides, particularly within the rat mesenteric artery preparation and thus should be considered in future studies.

Given that IK_{Ca} knockout and SK_{Ca} knockout mice were both hypertensive (Si *et al.*, 2006; Taylor *et al.*, 2003) and an altered expression and function of both IK_{Ca} and SK_{Ca} channels has been documented within various disease state models including cirrhosis, balloon catheter injury, chronic renal failure and diabetes (Barriere *et al.*, 2001; Burnham *et al.*, 2006; Ding *et al.*, 2005; Kohler *et al.*, 2001; Kohler *et al.*, 2005), an understanding of how each ion channel contributes to the dilatation response could have potentially beneficial effects for the therapeutic modulation of vascular tone. If the results of the present study and those of previous reports documenting the hypertensive state of connexin 40 knockout mice are also taken into account (de Wit *et al.*, 2000; Figueroa *et al.*, 2003), ion channel expression and function at points of cell-to-cell contact apparently plays an important role in the modulation of vascular tone. Crucially, however, the results of this study also suggest that improved pharmacological tools are required to accurately evaluate the contribution of cell-to-cell communication to the regulation of vascular tone.

9. References

AALKJAER, C. & MULVANY, M.J. (1985). Effect of ouabain on tone, membrane potential and sodium efflux compared with [3H]ouabain binding in rat resistance vessels. *J Physiol*, **362,** 215-31.

ABDEL-LATIF, A.A. (2001). Cross talk between cyclic nucleotides and polyphosphoinositide hydrolysis, protein kinases, and contraction in smooth muscle. *Exp Biol Med (Maywood)*, **226,** 153-63.

ADAMS, D.J., BARAKEH, J., LASKEY, R. & VAN BREEMEN, C. (1989). Ion channels and regulation of intracellular calcium in vascular endothelial cells. *Faseb J*, **3,** 2389-400.

ADELSTEIN, R.S., CONTI, M.A., HATHAWAY, D.R. & KLEE, C.B. (1978). Phosphorylation of smooth muscle myosin light chain kinase by the catalytic subunit of adenosine 3': 5'-monophosphate-dependent protein kinase. *J Biol Chem*, **253,** 8347-50.

AHLUWALIA, A. & HOBBS, A.J. (2005). Endothelium-derived C-type natriuretic peptide: more than just a hyperpolarizing factor. *Trends Pharmacol Sci*, **26,** 162-7.

AHLUWALIA, A., VILLAR, I., SCOTLAND, R.S. & HOBBS, A. (2005). The natriuretic peptide receptor-C antagonist, M372049, blocks C-type natriuretic peptide and endothelium-derived hyperpolaizing factor-induced relaxation of resistance arteries. In *Experimental Biology 2005 and XXXV International Congress of Physiological Sciences*. pp. 879.2. San Diego.

ALBERT, A.P. & LARGE, W.A. (2004). Inhibitory regulation of constitutive transient receptor potential-like cation channels in rabbit ear artery myocytes. *J Physiol*, **560,** 169-80.

ALBERT, A.P. & LARGE, W.A. (2003). Synergism between inositol phosphates and diacylglycerol on native TRPC6-like channels in rabbit portal vein myocytes. *J Physiol*, **552,** 789-95.

ALEXANDER, S.P., MATHIE, A. & PETERS, J.A. (2006). Guide to receptors and channels, 2nd edition. *Br J Pharmacol*, **147 Suppl 3,** S1-168.

ALVARADO-CASTILLO, C., HARDEN, T.K. & BOYER, J.L. (2005). Regulation of P2Y1 receptor-mediated signaling by the ectonucleoside triphosphate diphosphohydrolase isozymes NTPDase1 and NTPDase2. *Mol Pharmacol*, **67,** 114-22.

ANDRIANTSITOHAINA, R., LAGAUD, G.J., ANDRE, A., MULLER, B. & STOCLET, J.C. (1995). Effects of cGMP on calcium handling in ATP-stimulated rat resistance arteries. *Am J Physiol*, **268,** H1223-31.

ANGUS, J.A., BROUGHTON, A. & MULVANY, M.J. (1988). Role of alpha-adrenoceptors in constrictor responses of rat, guinea-pig and rabbit small arteries to neural activation. *J Physiol*, **403,** 495-510.

ARCHER, S.L., HUANG, J.M., HAMPL, V., NELSON, D.P., SHULTZ, P.J. & WEIR, E.K. (1994). Nitric oxide and cGMP cause vasorelaxation by activation of a charybdotoxin-sensitive K channel by cGMP-dependent protein kinase. *Proc Natl Acad Sci U S A*, **91,** 7583-7.

ASANO, M. & NOMURA, Y. (2003). Comparison of inhibitory effects of Y-27632, a Rho kinase inhibitor, in strips of small and large mesenteric arteries from spontaneously hypertensive and normotensive Wistar-Kyoto rats. *Hypertens Res*, **26,** 97-106.

ASLANOGLU, M. & AYNE, G. (2004). Voltammetric studies of the interaction of quinacrine with DNA. *Anal Bioanal Chem*, **380,** 658-63.

AZNAR-SALATTI, J., BASTIDA, E., BUCHANAN, M.R., CASTILLO, R., ORDINAS, A. & ESCOLAR, G. (1990). Differential localization of von Willebrand factor,

fibronectin and 13-HODE in human endothelial cell cultures. *Histochemistry*, **93,** 507-11.

BABA, Y., HAYASHI, K., FUJII, Y., MIZUSHIMA, A., WATARAI, H., WAKAMORI, M., NUMAGA, T., MORI, Y., IINO, M., HIKIDA, M. & KUROSAKI, T. (2006). Coupling of STIM1 to store-operated Ca2+ entry through its constitutive and inducible movement in the endoplasmic reticulum. *Proc Natl Acad Sci U S A*, **103,** 16704-9.

BAILEY, C.P., SMITH, F.L., KELLY, E., DEWEY, W.L. & HENDERSON, G. (2006). How important is protein kinase C in mu-opioid receptor desensitization and morphine tolerance? *Trends Pharmacol Sci*, **27,** 558-65.

BALDINI, G., DOGLIA, S., DOLCI, S. & SASSI, G. (1981). Fluorescence-determined preferential binding of quinacrine to DNA. *Biophys J*, **36,** 465-77.

BARLOW, R.S. & WHITE, R.E. (1998). Hydrogen peroxide relaxes porcine coronary arteries by stimulating BKCa channel activity. *Am J Physiol*, **275,** H1283-9.

BARRIERE, E., TAZI, K.A., PESSIONE, F., HELLER, J., POIREL, O., LEBREC, D. & MOREAU, R. (2001). Role of small-conductance Ca2+-dependent K+ channels in in vitro nitric oxide-mediated aortic hyporeactivity to alpha-adrenergic vasoconstriction in rats with cirrhosis. *J Hepatol*, **35,** 350-7.

BASTIDE, B., JARRY-GUICHARD, T., BRIAND, J.P., DELEZE, J. & GROS, D. (1996). Effect of antipeptide antibodies directed against three domains of connexin43 on the gap junctional permeability of cultured heart cells. *J Membr Biol*, **150,** 243-53.

BEACH, J.M., MCGAHREN, E.D. & DULING, B.R. (1998). Capillaries and arterioles are electrically coupled in hamster cheek pouch. *Am J Physiol*, **275,** H1489-96.

BEACH, J.M., MCGAHREN, E.D., XIA, J. & DULING, B.R. (1996). Ratiometric measurement of endothelial depolarization in arterioles with a potential-sensitive dye. *Am J Physiol*, **270,** H2216-27.

BEIGI, R., KOBATAKE, E., AIZAWA, M. & DUBYAK, G.R. (1999). Detection of local ATP release from activated platelets using cell surface-attached firefly luciferase. *Am J Physiol*, **276,** C267-78.

BENHAM, C.D. & BOLTON, T.B. (1986). Spontaneous transient outward currents in single visceral and vascular smooth muscle cells of the rabbit. *J Physiol*, **381,** 385-406.

BENY, J.L. & PACICCA, C. (1994). Bidirectional electrical communication between smooth muscle and endothelial cells in the pig coronary artery. *Am J Physiol*, **266,** H1465-72.

BENY, J.L., ZHU, P. & HAEFLIGER, I.O. (1997). Lack of bradykinin-induced smooth muscle cell hyperpolarization despite heterocellular dye coupling and endothelial cell hyperpolarization in porcine ciliary artery. *J Vasc Res*, **34,** 344-50.

BERG, B.R., COHEN, K.D. & SARELIUS, I.H. (1997). Direct coupling between blood flow and metabolism at the capillary level in striated muscle. *Am J Physiol*, **272,** H2693-700.

BERMAN, R.S., MARTIN, P.E., EVANS, W.H. & GRIFFITH, T.M. (2002). Relative contributions of NO and gap junctional communication to endothelium-dependent relaxations of rabbit resistance arteries vary with vessel size. *Microvasc Res*, **63,** 115-28.

BERRA-ROMANI, R., BLAUSTEIN, M.P. & MATTESON, D.R. (2005). TTX-sensitive voltage-gated Na+ channels are expressed in mesenteric artery smooth muscle cells. *Am J Physiol Heart Circ Physiol*, **289,** H137-45.

BERRA-ROMANI, R., RINALDI, C., RAQEEB, A., CASTELLI, L., MAGISTRETTI, J., TAGLIETTI, V. & TANZI, F. (2004). The duration and amplitude of the plateau phase of ATP- and ADP-evoked Ca(2+) signals are modulated by ectonucleotidases in in situ endothelial cells of rat aorta. *J Vasc Res*, **41,** 166-73.

BERRIDGE, M.J. (1993). Inositol trisphosphate and calcium signalling. *Nature*, **361,** 315-25.

BERRIDGE, M.J. & IRVINE, R.F. (1989). Inositol phosphates and cell signalling. *Nature*, **341,** 197-205.

BLIN, N., YUN, J. & WESS, J. (1995). Mapping of single amino acid residues required for selective activation of Gq/11 by the m3 muscarinic acetylcholine receptor. *J Biol Chem*, **270,** 17741-8.

BODIN, P., BAILEY, D. & BURNSTOCK, G. (1991). Increased flow-induced ATP release from isolated vascular endothelial cells but not smooth muscle cells. *Br J Pharmacol*, **103,** 1203-5.

BODIN, P. & BURNSTOCK, G. (2001). Evidence that release of adenosine triphosphate from endothelial cells during increased shear stress is vesicular. *J Cardiovasc Pharmacol*, **38,** 900-8.

BOLOTINA, V.M., NAJIBI, S., PALACINO, J.J., PAGANO, P.J. & COHEN, R.A. (1994). Nitric oxide directly activates calcium-dependent potassium channels in vascular smooth muscle. *Nature*, **368,** 850-3.

BOLTON, T.B. (1979). Mechanisms of action of transmitters and other substances on smooth muscle. *Physiol Rev*, **59,** 606-718.

BONDARENKO, A. (2004). Sodium-calcium exchanger contributes to membrane hyperpolarization of intact endothelial cells from rat aorta during acetylcholine stimulation. *Br J Pharmacol*, **143,** 9-18.

BONEV, A.D. & NELSON, M.T. (1996). Vasoconstrictors inhibit ATP-sensitive K+ channels in arterial smooth muscle through protein kinase C. *J Gen Physiol*, **108,** 315-23.

BOO, Y.C. & JO, H. (2003). Flow-dependent regulation of endothelial nitric oxide synthase: role of protein kinases. *Am J Physiol Cell Physiol*, **285,** C499-508.

BORIC, M.P., FIGUEROA, X.F., DONOSO, M.V., PAREDES, A., POBLETE, I. & HUIDOBRO-TORO, J.P. (1999). Rise in endothelium-derived NO after stimulation of rat perivascular sympathetic mesenteric nerves. *Am J Physiol Heart Circ Physiol*, **277,** H1027-1035.

BOYER, J.L., MOHANRAM, A., CAMAIONI, E., JACOBSON, K.A. & HARDEN, T.K. (1998). Competitive and selective antagonism of P2Y1 receptors by N6-methyl 2[prime]-deoxyadenosine 3[prime],5[prime]-bisphosphate. **124,** 1-3.

BRAIN, S.D. & GRANT, A.D. (2004). Vascular actions of calcitonin gene-related peptide and adrenomedullin. *Physiol Rev*, **84,** 903-34.

BRAYDEN, J.E. (2002). Functional roles of KATP channels in vascular smooth muscle. *Clin Exp Pharmacol Physiol*, **29,** 312-6.

BREDT, D.S. & SNYDER, S.H. (1990). Isolation of nitric oxide synthetase, a calmodulin-requiring enzyme. *Proc Natl Acad Sci U S A*, **87,** 682-5.

BREYER, R.M., BAGDASSARIAN, C.K., MYERS, S.A. & BREYER, M.D. (2001). Prostanoid receptors: subtypes and signaling. *Annu Rev Pharmacol Toxicol*, **41,** 661-90.

BRIONES, A.M., DALY, C.J., JIMENEZ-ALTAYO, F., MARTINEZ-REVELLES, S., GONZALEZ, J.M., MCGRATH, J.C. & VILA, E. (2005). Direct demonstration of beta1- and evidence against beta2- and beta3-adrenoceptors, in smooth muscle cells of rat small mesenteric arteries. *Br J Pharmacol*, **146,** 679-91.

BRIONES, A.M., GONZALEZ, J.M., SOMOZA, B., GIRALDO, J., DALY, C.J., VILA, E., GONZALEZ, M.C., MCGRATH, J.C. & ARRIBAS, S.M. (2003). Role of elastin in spontaneously hypertensive rat small mesenteric artery remodelling. *J Physiol*, **552,** 185-95.

BRUEGGEMANN, L.I., MARKUN, D.R., HENDERSON, K.K., CRIBBS, L.L. & BYRON, K.L. (2006). Pharmacological and electrophysiological characterization of store-operated currents and capacitative Ca(2+) entry in vascular smooth muscle cells. *J Pharmacol Exp Ther*, **317,** 488-99.

BRYAN, P.T. & MARSHALL, J.M. (1999a). Adenosine receptor subtypes and vasodilatation in rat skeletal muscle during systemic hypoxia: a role for A1 receptors. *J Physiol*, **514 (Pt 1),** 151-62.

BRYAN, P.T. & MARSHALL, J.M. (1999b). Cellular mechanisms by which adenosine induces vasodilatation in rat skeletal muscle: significance for systemic hypoxia. *J Physiol*, **514 (Pt 1),** 163-75.

BRYAN, R.M., JR., YOU, J., PHILLIPS, S.C., ANDRESEN, J.J., LLOYD, E.E., ROGERS, P.A., DRYER, S.E. & MARRELLI, S.P. (2006). Evidence for two-pore domain potassium channels in rat cerebral arteries. *Am J Physiol Heart Circ Physiol*, **291,** H770-80.

BUDEL, S., BARTLETT, I.S. & SEGAL, S.S. (2003). Homocellular Conduction Along Endothelium and Smooth Muscle of Arterioles in Hamster Cheek Pouch: Unmasking an NO Wave. *Circ Res*, **93,** 61-68.

BUDZYN, K., PAULL, M., MARLEY, P.D. & SOBEY, C.G. (2006). Segmental Differences in the Roles of Rho-Kinase and Protein Kinase C in Mediating Vasoconstriction. *J Pharmacol Exp Ther*, **317,** 791-796.

BUKAUSKAS, F.F., JORDAN, K., BUKAUSKIENE, A., BENNETT, M.V., LAMPE, P.D., LAIRD, D.W. & VERSELIS, V.K. (2000). Clustering of connexin 43-enhanced green fluorescent protein gap junction channels and functional coupling in living cells. *Proc Natl Acad Sci U S A*, **97,** 2556-61.

BURNHAM, M.P., JOHNSON, I.T. & WESTON, A.H. (2006). Impaired small-conductance Ca2+-activated K+ channel-dependent EDHF responses in Type II diabetic ZDF rats. *Br J Pharmacol*, **148,** 434-41.

BURNSTOCK, G. (2006). Historical review: ATP as a neurotransmitter. *Trends Pharmacol Sci*, **27,** 166-76.

BURNSTOCK, G. (1999). Release of vasoactive substances from endothelial cells by shear stress and purinergic mechanosensory transduction. *J Anat*, **194 (Pt 3),** 335-42.

BURT, J.M. & STEELE, T.D. (2003). Selective effect of PDGF on connexin43 versus connexin40 comprised gap junction channels. *Cell Commun Adhes*, **10,** 287-91.

BUSSE, R., EDWARDS, G., FELETOU, M., FLEMING, I., VANHOUTTE, P.M. & WESTON, A.H. (2002). EDHF: bringing the concepts together. *Trends Pharmacol Sci*, **23,** 374-80.

BUSSE, R., FICHTNER, H., LUCKHOFF, A. & KOHLHARDT, M. (1988). Hyperpolarization and increased free calcium in acetylcholine-stimulated endothelial cells. *Am J Physiol*, **255,** H965-9.

BUSSE, R. & FLEMING, I. (2003). Regulation of endothelium-derived vasoactive autacoid production by hemodynamic forces. *Trends Pharmacol Sci*, **24,** 24-9.

BUTLER, T.M. & SIEGMAN, M.J. (1998). Control of cross-bridge cycling by myosin light chain phosphorylation in mammalian smooth muscle. *Acta Physiol Scand*, **164,** 389-400.

BUUS, C.L., AALKJAER, C., NILSSON, H., JUUL, B., MOLLER, J.V. & MULVANY, M.J. (1998). Mechanisms of Ca2+ sensitization of force production by noradrenaline in rat mesenteric small arteries. *J Physiol*, **510 (Pt 2),** 577-90.

BUVINIC, S., BRIONES, R. & HUIDOBRO-TORO, J.P. (2002). P2Y(1) and P2Y(2) receptors are coupled to the NO/cGMP pathway to vasodilate the rat arterial mesenteric bed. *Br J Pharmacol*, **136,** 847-56.

BUVINIC, S., POBLETE, M.I., DONOSO, M.V., DELPIANO, A.M., BRIONES, R., MIRANDA, R. & HUIDOBRO-TORO, J.P. (2006). P2Y1 and P2Y2 receptor distribution varies along the human placental vascular tree: role of nucleotides in vascular tone regulation. *J Physiol*, **573,** 427-43.

BUYUKAFSAR, K., ARIKAN, O., ARK, M., SECILMIS, A., UN, I. & SINGIRIK, E. (2004). Rho-kinase expression and its contribution to the control of perfusion pressure in the isolated rat mesenteric vascular bed. *Eur J Pharmacol*, **485,** 263-8.

BYCHKOV, R., PIEPER, K., RIED, C., MILOSHEVA, M., BYCHKOV, E., LUFT, F.C. & HALLER, H. (1999). Hydrogen peroxide, potassium currents, and membrane potential in human endothelial cells. *Circulation*, **99,** 1719-25.

CAMPBELL, D.L., STRAUSS, H.C. & WHORTON, A.R. (1991). Voltage dependence of bovine pulmonary artery endothelial cell function. *J Mol Cell Cardiol*, **23 Suppl 1,** 133-44.

CAMPBELL, W.B., GEBREMEDHIN, D., PRATT, P.F. & HARDER, D.R. (1996). Identification of epoxyeicosatrienoic acids as endothelium-derived hyperpolarizing factors. *Circ Res*, **78,** 415-23.

CANNELL, M.B. & SAGE, S.O. (1989). Bradykinin-evoked changes in cytosolic calcium and membrane currents in cultured bovine pulmonary artery endothelial cells. *J Physiol*, **419,** 555-68.

CARVAJAL, J.A., GERMAIN, A.M., HUIDOBRO-TORO, J.P. & WEINER, C.P. (2000). Molecular mechanism of cGMP-mediated smooth muscle relaxation. *J Cell Physiol*, **184,** 409-20.

CHACKO, S. & ROSENFELD, A. (1982). Regulation of actin-activated ATP hydrolysis by arterial myosin. *Proc Natl Acad Sci U S A*, **79,** 292-6.

CHAKRABARTI, R., PFEIFFER, N.E., WYLIE, D.E. & SCHUSTER, S.M. (1989). Incorporation of monoclonal antibodies into cells by osmotic permeabilization. Effect on cellular metabolism. *J Biol Chem*, **264,** 8214-21.

CHAMPION, H.C., PIERCE, R.L., BIVALACQUA, T.J., MURPHY, W.A., COY, D.H. & KADOWITZ, P.J. (2001). Analysis of responses to hAmylin, hCGRP, and hADM in isolated resistance arteries from the mesenteric vascular bed of the rat. *Peptides*, **22,** 1427-34.

CHATAIGNEAU, T., FELETOU, M., DUHAULT, J. & VANHOUTTE, P.M. (1998). Epoxyeicosatrienoic acids, potassium channel blockers and endothelium-dependent hyperpolarization in the guinea-pig carotid artery. *Br J Pharmacol*, **123,** 574-80.

CHAUHAN, S., RAHMAN, A., NILSSON, H., CLAPP, L., MACALLISTER, R. & AHLUWALIA, A. (2003a). NO contributes to EDHF-like responses in rat small arteries: a role for NO stores. *Cardiovasc Res*, **57,** 207-16.

CHAUHAN, S.D., NILSSON, H., AHLUWALIA, A. & HOBBS, A.J. (2003b). Release of C-type natriuretic peptide accounts for the biological activity of endothelium-derived hyperpolarizing factor. *Proc Natl Acad Sci U S A*, **100,** 1426-31.

CHAYTOR, A.T., BAKKER, L.M., EDWARDS, D.H. & GRIFFITH, T.M. (2005). Connexin-mimetic peptides dissociate electrotonic EDHF-type signalling via

myoendothelial and smooth muscle gap junctions in the rabbit iliac artery. *Br J Pharmacol*, **144,** 108-14.

CHAYTOR, A.T., EDWARDS, D.H., BAKKER, L.M. & GRIFFITH, T.M. (2003). Distinct hyperpolarizing and relaxant roles for gap junctions and endothelium-derived H2O2 in NO-independent relaxations of rabbit arteries. *Proc Natl Acad Sci U S A.*

CHAYTOR, A.T., EVANS, W.H. & GRIFFITH, T.M. (1998). Central role of heterocellular gap junctional communication in endothelium-dependent relaxations of rabbit arteries. *J Physiol*, **508 (Pt 2),** 561-73.

CHAYTOR, A.T., EVANS, W.H. & GRIFFITH, T.M. (1997). Peptides homologous to extracellular loop motifs of connexin 43 reversibly abolish rhythmic contractile activity in rabbit arteries. *J Physiol*, **503 (Pt 1),** 99-110.

CHAYTOR, A.T., MARSH, W.L., HUTCHESON, I.R. & GRIFFITH, T.M. (2000). Comparison of glycyrrhetinic acid isoforms and carbenoxolone as inhibitors of EDHF-type relaxations mediated via gap junctions. *Endothelium*, **7,** 265-78.

CHAYTOR, A.T., MARTIN, P.E., EDWARDS, D.H. & GRIFFITH, T.M. (2001). Gap junctional communication underpins EDHF-type relaxations evoked by ACh in the rat hepatic artery. *Am J Physiol Heart Circ Physiol*, **280,** H2441-50.

CHEN, B.C., LEE, C.M., LEE, Y.T. & LIN, W.W. (1996). Characterization of signaling pathways of P2Y and P2U purinoceptors in bovine pulmonary artery endothelial cells. *J Cardiovasc Pharmacol*, **28,** 192-9.

CHEN, B.C. & LIN, W.W. (1999). PKCbetaI mediates the inhibition of P2Y receptor-induced inositol phosphate formation in endothelial cells. *Br J Pharmacol*, **127,** 1908-14.

CHEN, C.C. & CHEN, W.C. (1997). P2Y receptor linked to phospholipase C: stimulation of neuro 2A cells by UTP and ATP and possible regulation by protein kinase C subtype epsilon. *J Neurochem*, **69,** 1409-16.

CHEN, G. & CHEUNG, D.W. (1997). Effect of K(+)-channel blockers on ACh-induced hyperpolarization and relaxation in mesenteric arteries. *Am J Physiol*, **272,** H2306-12.

CHEN, G., SUZUKI, H. & WESTON, A.H. (1988). Acetylcholine releases endothelium-derived hyperpolarizing factor and EDRF from rat blood vessels. *Br J Pharmacol*, **95,** 1165-74.

CHEN, H.H. & BURNETT, J.C., JR. (1998). C-type natriuretic peptide: the endothelial component of the natriuretic peptide system. *J Cardiovasc Pharmacol*, **32 Suppl 3,** S22-8.

CHEN, Y. & RIVERS, R.J. (2001). Measurement of membrane potential and intracellular Ca(2+) of arteriolar endothelium and smooth muscle in vivo. *Microvasc Res*, **62,** 55-62.

CHENG, Y., NDISANG, J.F., TANG, G., CAO, K. & WANG, R. (2004). Hydrogen sulfide-induced relaxation of resistance mesenteric artery beds of rats. *Am J Physiol Heart Circ Physiol*, **287,** H2316-23.

CHIKUMI, H., VAZQUEZ-PRADO, J., SERVITJA, J.M., MIYAZAKI, H. & GUTKIND, J.S. (2002). Potent activation of RhoA by Galpha q and Gq-coupled receptors. *J Biol Chem*, **277,** 27130-4.

CHRIST, G.J., SPRAY, D.C., EL-SABBAN, M., MOORE, L.K. & BRINK, P.R. (1996). Gap junctions in vascular tissues. Evaluating the role of intercellular communication in the modulation of vasomotor tone. *Circ Res*, **79,** 631-46.

CLAPHAM, D.E. (2003). TRP channels as cellular sensors. *Nature*, **426,** 517-24.

CLAPHAM, D.E. & NEER, E.J. (1997). G protein beta gamma subunits. *Annu Rev Pharmacol Toxicol*, **37,** 167-203.

COATS, P. & HILLIER, C. (1999). Determination of an optimal axial-length tension for the study of isolated resistance arteries on a pressure myograph. *Exp Physiol*, **84,** 1085-94.

COATS, P., JARAJAPU, Y.P., HILLIER, C., MCGRATH, J.C. & DALY, C. (2003). The use of fluorescent nuclear dyes and laser scanning confocal microscopy to study the cellular aspects of arterial remodelling in human subjects with critical limb ischaemia. *Exp Physiol*, **88,** 547-54.

COHEN, K.D. & JACKSON, W.F. (2005). Membrane hyperpolarization is not required for sustained muscarinic agonist-induced increases in intracellular Ca2+ in arteriolar endothelial cells. *Microcirculation*, **12,** 169-82.

COHEN, R.A., PLANE, F., NAJIBI, S., HUK, I., MALINSKI, T. & GARLAND, C.J. (1997). Nitric oxide is the mediator of both endothelium-dependent relaxation and hyperpolarization of the rabbit carotid artery. *Proc Natl Acad Sci U S A*, **94,** 4193-8.

COLDEN-STANFIELD, M., SCHILLING, W.P., RITCHIE, A.K., ESKIN, S.G., NAVARRO, L.T. & KUNZE, D.L. (1987). Bradykinin-induced increases in cytosolic calcium and ionic currents in cultured bovine aortic endothelial cells. *Circ Res*, **61,** 632-40.

COLE, W.C. & CLEMENT-CHOMIENNE, O. (2003). ATP-sensitive K+ channels of vascular smooth muscle cells. *J Cardiovasc Electrophysiol*, **14,** 94-103.

COLE, W.C., MALCOLM, T., WALSH, M.P. & LIGHT, P.E. (2000). Inhibition by protein kinase C of the K(NDP) subtype of vascular smooth muscle ATP-sensitive potassium channel. *Circ Res*, **87,** 112-7.

COLEMAN, H.A., TARE, M. & PARKINGTON, H.C. (2004). Endothelial potassium channels, endothelium-dependent hyperpolarization and the regulation of vascular tone in health and disease. *Clinical and Experimental Pharmacology Physiolology*, **31,** 641-649.

COLEMAN, H.A., TARE, M. & PARKINGTON, H.C. (2001). K+ currents underlying the action of endothelium-derived hyperpolarizing factor in guinea-pig, rat and human blood vessels. *J Physiol*, **531,** 359-73.

CONNER, S.D. & SCHMID, S.L. (2003). Regulated portals of entry into the cell. *Nature*, **422,** 37-44.

CONTRERAS, J.E., SAEZ, J.C., BUKAUSKAS, F.F. & BENNETT, M.V.L. (2003). Gating and regulation of connexin 43 (Cx43) hemichannels. *PNAS*, **100,** 11388-11393.

COOK, N.S. (1988). The pharmacology of potassium channels and their therapeutic potential. *Trends Pharmacol Sci*, **9,** 21-8.

CORSON, M.A., JAMES, N.L., LATTA, S.E., NEREM, R.M., BERK, B.C. & HARRISON, D.G. (1996). Phosphorylation of endothelial nitric oxide synthase in response to fluid shear stress. *Circ Res*, **79,** 984-91.

CRANE, G.J., GALLAGHER, N., DORA, K.A. & GARLAND, C.J. (2003a). Small- and intermediate-conductance calcium-activated K+ channels provide different facets of endothelium-dependent hyperpolarization in rat mesenteric artery. *J Physiol*, **553,** 183-9.

CRANE, G.J., WALKER, S.D., DORA, K.A. & GARLAND, C.J. (2003b). Evidence for a differential cellular distribution of inward rectifier K channels in the rat isolated mesenteric artery. *J Vasc Res*, **40,** 159-68.

CRIBBS, L.L. (2006). T-type Ca2+ channels in vascular smooth muscle: Multiple functions. *Cell Calcium*

T-type calcium channels: from old physiology to novel functions, **40,** 221-230.

CRIDDLE, D.N., GREENWOOD, I.A. & WESTON, A.H. (1994). Levcromakalim-induced modulation of membrane potassium currents, intracellular calcium and mechanical activity in rat mesenteric artery. *Naunyn Schmiedebergs Arch Pharmacol*, **349,** 422-30.

DART, C. & STANDEN, N.B. (1993). Adenosine-activated potassium current in smooth muscle cells isolated from the pig coronary artery. *J Physiol*, **471,** 767-86.

DAVIES, P.F., RENNKE, H.G. & COTRAN, R.S. (1981). Influence of molecular charge upon the endocytosis and intracellular fate of peroxidase activity in cultured arterial endothelium. *J Cell Sci*, **49,** 69-86.

DAVIES, S.P., REDDY, H., CAIVANO, M. & COHEN, P. (2000). Specificity and mechanism of action of some commonly used protein kinase inhibitors. *Biochem J*, **351,** 95-105.

DE WIT, C., HOEPFL, B. & WOLFLE, S.E. (2006a). Endothelial mediators and communication through vascular gap junctions. *Biol Chem*, **387,** 3-9.

DE WIT, C., ROOS, F., BOLZ, S.-S., KIRCHHOFF, S., KRUGER, O., WILLECKE, K. & POHL, U. (2000). Impaired Conduction of Vasodilation Along Arterioles in Connexin40-Deficient Mice. *Circ Res*, **86,** 649-655.

DE WIT, C., WOLFLE, S.E. & HOPFL, B. (2006b). Connexin-dependent communication within the vascular wall: contribution to the control of arteriolar diameter. *Adv Cardiol*, **42,** 268-83.

DEL PUP, L., DE ANGELI, S., CONCONI, M.T., GRANDI, C., GAMBA, P.G., PARNIGOTTO, P.P. & NUSSDORFER, G.G. (2002). New human embryo liver cell lines obtained by stabilization and immortalization enhance in vitro clonal growth of cordonal blood cells. *Int J Mol Med*, **10,** 561-8.

DELASHAW, J.B. & DULING, B.R. (1991). Heterogeneity in conducted arteriolar vasomotor response is agonist dependent. *Am J Physiol Heart Circ Physiol*, **260,** H1276-1282.

DIETRICH, H.H., ELLSWORTH, M.L., SPRAGUE, R.S. & DACEY, R.G., JR. (2000). Red blood cell regulation of microvascular tone through adenosine triphosphate. *Am J Physiol Heart Circ Physiol*, **278,** H1294-1298.

DIETRICH, H.H., KAJITA, Y. & DACEY, R.G., JR (1996). Local and conducted vasomotor responses in isolated rat cerebral arterioles. *Am J Physiol Heart Circ Physiol*, **271,** H1109-1116.

DIMMELER, S., FLEMING, I., FISSLTHALER, B., HERMANN, C., BUSSE, R. & ZEIHER, A.M. (1999). Activation of nitric oxide synthase in endothelial cells by Akt-dependent phosphorylation. *Nature*, **399,** 601-5.

DING, H., HASHEM, M., WIEHLER, W.B., LAU, W., MARTIN, J., REID, J. & TRIGGLE, C. (2005). Endothelial dysfunction in the streptozotocin-induced diabetic apoE-deficient mouse. *Br J Pharmacol*, **146,** 1110-8.

DOCHERTY, J.R. (1998). Subtypes of functional alpha1- and alpha2-adrenoceptors. *Eur J Pharmacol*, **361,** 1-15.

DOMEIER, T.L. & SEGAL, S.S. (2007). Electromechanical and pharmacomechanical signalling pathways for conducted vasodilatation along endothelium of hamster feed arteries. *J Physiol*, **579,** 175-86.

DORA, K.A., DAMON, D.N. & DULING, B.R. (2000a). Microvascular dilation in response to occlusion: a coordinating role for conducted vasomotor responses. *Am J Physiol Heart Circ Physiol*, **279,** H279-84.

DORA, K.A., DOYLE, M.P. & DULING, B.R. (1997). Elevation of intracellular calcium in smooth muscle causes endothelial cell generation of NO in arterioles. *Proc Natl Acad Sci U S A*, **94,** 6529-34.

DORA, K.A. & DULING, B.R. (1998). Use of fluorescent reporters in the quantitation of microvascular function. *Microcirculation*, **5,** 95-100.

DORA, K.A. & GARLAND, C.J. (2001). Properties of smooth muscle hyperpolarization and relaxation to K+ in the rat isolated mesenteric artery. *Am J Physiol Heart Circ Physiol*, **280,** H2424-9.

DORA, K.A., HINTON, J.M., WALKER, S.D. & GARLAND, C.J. (2000b). An indirect influence of phenylephrine on the release of endothelium-derived vasodilators in rat small mesenteric artery. *Br J Pharmacol*, **129,** 381-7.

DORA, K.A., INGS, N.T. & GARLAND, C.J. (2002). K(Ca) channel blockers reveal hyperpolarization and relaxation to K+ in rat isolated mesenteric artery. *Am J Physiol Heart Circ Physiol*, **283,** H606-14.

DORA, K.A., MARTIN, P.E., CHAYTOR, A.T., EVANS, W.H., GARLAND, C.J. & GRIFFITH, T.M. (1999). Role of heterocellular Gap junctional communication in endothelium-dependent smooth muscle hyperpolarization: inhibition by a connexin-mimetic peptide. *Biochem Biophys Res Commun*, **254,** 27-31.

DORA, K.A., SANDOW, S.L., GALLAGHER, N.T., TAKANO, H., RUMMERY, N.M., HILL, C.E. & GARLAND, C.J. (2003a). Myoendothelial Gap Junctions May Provide the Pathway for EDHF in Mouse Mesenteric Artery. *J Vasc Res*, **40,** 480-490.

DORA, K.A., XIA, J. & DULING, B.R. (2003b). Endothelial cell signaling during conducted vasomotor responses. *Am J Physiol Heart Circ Physiol*, **285,** H119-126.

DOUGHTY, J.M., BOYLE, J.P. & LANGTON, P.D. (2001). Blockade of chloride channels reveals relaxations of rat small mesenteric arteries to raised potassium. *Br J Pharmacol*, **132,** 293-301.

DOUGHTY, J.M., BOYLE, J.P. & LANGTON, P.D. (2000). Potassium does not mimic EDHF in rat mesenteric arteries. *Br J Pharmacol*, **130,** 1174-82.

DOUGHTY, J.M., PLANE, F. & LANGTON, P.D. (1999). Charybdotoxin and apamin block EDHF in rat mesenteric artery if selectively applied to the endothelium. *Am J Physiol*, **276,** H1107-12.

DOYLE, M.P. & DULING, B.R. (1997). Acetylcholine induces conducted vasodilation by nitric oxide-dependent and -independent mechanisms. *Am J Physiol*, **272,** H1364-71.

DUBYAK, G.R. & EL-MOATASSIM, C. (1993). Signal transduction via P2-purinergic receptors for extracellular ATP and other nucleotides. *Am J Physiol*, **265,** C577-606.

DUIVENVOORDEN, W.C., SCHAFER, R., PFEIFER, A.M., PIQUET, D. & MAIER, P. (1995). Nuclear matrix condensation and c-myc and c-fos expression are specifically altered in culture rat hepatocytes after exposure to cyproterone acetate and phenobarbital. *Biochem Biophys Res Commun*, **215,** 598-605.

DULING, B.R. & BERNE, R.M. (1970). Propagated vasodilation in the microcirculation of the hamster cheek pouch. *Circ Res*, **26,** 163-70.

DULING, B.R., GORE, R.W., DACEY, R.G., JR. & DAMON, D.N. (1981). Methods for isolation, cannulation, and in vitro study of single microvessels. *Am J Physiol*, **241,** H108-116.

DUSSERRE, N., L'HEUREUX, N., BELL, K.S., STEVENS, H.Y., YEH, J., OTTE, L.A., LOUFRANI, L. & FRANGOS, J.A. (2004). PECAM-1 interacts with nitric oxide synthase in human endothelial cells: implication for flow-induced nitric oxide synthase activation. *Arterioscler Thromb Vasc Biol*, **24,** 1796-802.

DUZA, T. & SARELIUS, I.H. (2003). Conducted dilations initiated by purines in arterioles are endothelium dependent and require endothelial Ca2+. *Am J Physiol Heart Circ Physiol*, **285,** H26-37.

EARLEY, S., HEPPNER, T.J., NELSON, M.T. & BRAYDEN, J.E. (2005). TRPV4 forms a novel Ca2+ signaling complex with ryanodine receptors and BKCa channels. *Circ Res*, **97,** 1270-9.

EARLEY, S., PASTUSZYN, A. & WALKER, B.R. (2003). Cytochrome p-450 epoxygenase products contribute to attenuated vasoconstriction after chronic hypoxia. *Am J Physiol Heart Circ Physiol*, **285,** H127-36.

EDWARDS, G., DORA, K.A., GARDENER, M.J., GARLAND, C.J. & WESTON, A.H. (1998). K+ is an endothelium-derived hyperpolarizing factor in rat arteries. *Nature*, **396,** 269-72.

EDWARDS, G., FELETOU, M., GARDENER, M.J., THOLLON, C., VANHOUTTE, P.M. & WESTON, A.H. (1999). Role of gap junctions in the responses to EDHF in rat and guinea-pig small arteries. *Br J Pharmacol*, **128,** 1788-94.

EDWARDS, G., THOLLON, C., GARDENER, M.J., FELETOU, M., VILAINE, J., VANHOUTTE, P.M. & WESTON, A.H. (2000). Role of gap junctions and EETs in endothelium-dependent hyperpolarization of porcine coronary artery. *Br J Pharmacol*, **129,** 1145-54.

EDWARDS, G. & WESTON, A.H. (2004). Potassium and potassium clouds in endothelium-dependent hyperpolarizations. *Pharmacol Res*, **49,** 535-41.

EICHLER, I., WIBAWA, J., GRGIC, I., KNORR, A., BRAKEMEIER, S., PRIES, A.R., HOYER, J. & KOHLER, R. (2003). Selective blockade of endothelial Ca2+-activated small- and intermediate-conductance K+-channels suppresses EDHF-mediated vasodilation. *Br J Pharmacol*, **138,** 594-601.

ELLIS, A., PANNIRSELVAM, M., ANDERSON, T.J. & TRIGGLE, C.R. (2003). Catalase has negligible inhibitory effects on endothelium-dependent relaxations in mouse isolated aorta and small mesenteric artery. *Br J Pharmacol*, **140,** 1193-200.

ELLIS, A. & TRIGGLE, C.R. (2003). Endothelium-derived reactive oxygen species: their relationship to endothelium-dependent hyperpolarization and vascular tone. *Can J Physiol Pharmacol*, **81,** 1013-28.

ELLSWORTH, M.L. (2004). Red blood cell-derived ATP as a regulator of skeletal muscle perfusion. *Med Sci Sports Exerc*, **36,** 35-41.

ELLSWORTH, M.L., FORRESTER, T., ELLIS, C.G. & DIETRICH, H.H. (1995). The erythrocyte as a regulator of vascular tone. *Am J Physiol*, **269,** H2155-61.

EMERSON, G.G., NEILD, T.O. & SEGAL, S.S. (2002). Conduction of hyperpolarization along hamster feed arteries: augmentation by acetylcholine. *Am J Physiol Heart Circ Physiol*, **283,** H102-9.

EMERSON, G.G. & SEGAL, S.S. (2001). Electrical activation of endothelium evokes vasodilation and hyperpolarization along hamster feed arteries. *Am J Physiol Heart Circ Physiol*, **280,** H160-7.

EMERSON, G.G. & SEGAL, S.S. (2000a). Electrical coupling between endothelial cells and smooth muscle cells in hamster feed arteries: role in vasomotor control. *Circ Res*, **87,** 474-9.

EMERSON, G.G. & SEGAL, S.S. (2000b). Endothelial cell pathway for conduction of hyperpolarization and vasodilation along hamster feed artery. *Circ Res*, **86,** 94-100.

ERLINGE, D., HARNEK, J., VAN HEUSDEN, C., OLIVECRONA, G., JERN, S. & LAZAROWSKI, E. (2005). Uridine triphosphate (UTP) is released during cardiac ischemia. *Int J Cardiol*, **100,** 427-33.

EVANS, W.H. & BOITANO, S. (2001). Connexin mimetic peptides: specific inhibitors of gap-junctional intercellular communication. *Biochem Soc Trans*, **29,** 606-12.

EVANS, W.H., DE VUYST, E. & LEYBAERT, L. (2006). The gap junction cellular internet: connexin hemichannels enter the signalling limelight. *Biochem J*, **397,** 1-14.

EVANS, W.H. & MARTIN, P.E. (2002). Gap junctions: structure and function (Review). *Mol Membr Biol*, **19,** 121-36.

FELEDER, E.C. & ADLER-GRASCHINSKY, E. (1997). Endothelium-mediated and N omega-nitro-L-arginine methyl ester-sensitive responses to cromakalim and diazoxide in the rat mesenteric bed. *Eur J Pharmacol*, **319,** 229-38.

FELETOU, M. & VANHOUTTE, P.M. (2004). EDHF: new therapeutic targets? *Pharmacol Res*, **49,** 565-80.

FELETOU, M. & VANHOUTTE, P.M. (1988). Endothelium-dependent hyperpolarization of canine coronary smooth muscle. *Br J Pharmacol*, **93,** 515-24.

FELETOU, M. & VANHOUTTE, P.M. (2006). Endothelium-derived hyperpolarizing factor: where are we now? *Arterioscler Thromb Vasc Biol*, **26,** 1215-25.

FENGER-GRON, J., MULVANY, M.J. & CHRISTENSEN, K.L. (1997). Intestinal blood flow is controlled by both feed arteries and microcirculatory resistance vessels in freely moving rats. *J Physiol*, **498 (Pt 1),** 215-24.

FENGER-GRON, J., MULVANY, M.J. & CHRISTENSEN, K.L. (1995). Mesenteric blood pressure profile of conscious, freely moving rats. *J Physiol*, **488 (Pt 3),** 753-60.

FERRER, M., MARIN, J. & BALFAGON, G. (2000). Diabetes alters neuronal nitric oxide release from rat mesenteric arteries. Role of protein kinase C. *Life Sci*, **66,** 337-45.

FESKE, S., GWACK, Y., PRAKRIYA, M., SRIKANTH, S., PUPPEL, S.H., TANASA, B., HOGAN, P.G., LEWIS, R.S., DALY, M. & RAO, A. (2006). A mutation in Orai1 causes immune deficiency by abrogating CRAC channel function. *Nature*, **441,** 179-85.

FIGUEROA, X.F., ISAKSON, B.E. & DULING, B.R. (2006). Vascular gap junctions in hypertension. *Hypertension*, **48,** 804-11.

FIGUEROA, X.F., PAUL, D.L., SIMON, A.M., GOODENOUGH, D.A., DAY, K.H., DAMON, D.N. & DULING, B.R. (2003). Central Role of Connexin40 in the Propagation of Electrically Activated Vasodilation in Mouse Cremasteric Arterioles In Vivo. *Circ Res*, **92,** 793-800.

FISSLTHALER, B., POPP, R., KISS, L., POTENTE, M., HARDER, D.R., FLEMING, I. & BUSSE, R. (1999). Cytochrome P450 2C is an EDHF synthase in coronary arteries. *Nature*, **401,** 493-7.

FLEMING, I. (2004). Cytochrome P450 epoxygenases as EDHF synthase(s). *Pharmacol Res*, **49,** 525-33.

FLEMING, I. & BUSSE, R. (2006). Endothelium-derived epoxyeicosatrienoic acids and vascular function. *Hypertension*, **47,** 629-33.

FLEMING, I. & BUSSE, R. (2003). Molecular mechanisms involved in the regulation of the endothelial nitric oxide synthase. *Am J Physiol Regul Integr Comp Physiol*, **284,** R1-12.

FLEMING, I., FISSLTHALER, B., DIXIT, M. & BUSSE, R. (2005). Role of PECAM-1 in the shear-stress-induced activation of Akt and the endothelial nitric oxide synthase (eNOS) in endothelial cells. *J Cell Sci*, **118,** 4103-11.

FOLKOW, B., SONNENSCHEIN, R.R. & WRIGHT, D.L. (1971). Loci of neurogenic and metabolic effects on precapillary vessels of skeletal muscle. *Acta Physiol Scand*, **81,** 459-71.

FORD, A.P., DANIELS, D.V., CHANG, D.J., GEVER, J.R., JASPER, J.R., LESNICK, J.D. & CLARKE, D.E. (1997). Pharmacological pleiotropism of the human recombinant alpha1A-adrenoceptor: implications for alpha1-adrenoceptor classification. *Br J Pharmacol*, **121,** 1127-35.

FRANK, P.G., WOODMAN, S.E., PARK, D.S. & LISANTI, M.P. (2003). Caveolin, Caveolae, and Endothelial Cell Function. *Arterioscler Thromb Vasc Biol*, **23,** 1161-1168.

FREAY, A., JOHNS, A., ADAMS, D.J., RYAN, U.S. & VAN BREEMEN, C. (1989). Bradykinin and inositol 1,4,5-trisphosphate-stimulated calcium release from intracellular stores in cultured bovine endothelial cells. *Pflugers Arch*, **414,** 377-84.

FREICHEL, M., SUH, S.H., PFEIFER, A., SCHWEIG, U., TROST, C., WEISSGERBER, P., BIEL, M., PHILIPP, S., FREISE, D., DROOGMANS, G., HOFMANN, F., FLOCKERZI, V. & NILIUS, B. (2001). Lack of an endothelial store-operated Ca2+ current impairs agonist-dependent vasorelaxation in TRP4-/- mice. *Nat Cell Biol*, **3,** 121-7.

FUJII, T., YAMADA, S., YAMAGUCHI, N., FUJIMOTO, K., SUZUKI, T. & KAWASHIMA, K. (1995). Species differences in the concentration of acetylcholine, a neurotransmitter, in whole blood and plasma. *Neurosci Lett*, **201,** 207-10.

FUJIMOTO, S. & MATSUDA, T. (1991). M3 cholinoceptors and P2y purinoceptors mediating relaxation of arteries in spontaneously hypertensive rats at prehypertensive stages. *Eur J Pharmacol*, **202,** 9-15.

FUJITA, A., TAKEUCHI, T., SAITOH, N., HANAI, J. & HATA, F. (2001). Expression of Ca(2+)-activated K(+) channels, SK3, in the interstitial cells of Cajal in the gastrointestinal tract. *Am J Physiol Cell Physiol*, **281,** C1727-33.

FUKAO, M., HATTORI, Y., KANNO, M., SAKUMA, I. & KITABATAKE, A. (1997a). Evidence against a role of cytochrome P450-derived arachidonic acid metabolites in endothelium-dependent hyperpolarization by acetylcholine in rat isolated mesenteric artery. *Br J Pharmacol*, **120,** 439-46.

FUKAO, M., HATTORI, Y., KANNO, M., SAKUMA, I. & KITABATAKE, A. (1997b). Sources of Ca2+ in relation to generation of acetylcholine-induced endothelium-dependent hyperpolarization in rat mesenteric artery. *Br J Pharmacol*, **120,** 1328-34.

FUKAO, M., WATANABE, H., TAKEUCHI, K., TOMIOKA, H. & HATTORI, Y. (2001). Effects of SK&F 96365 and mefenamic acid on Ca2+ influx in stimulated endothelial cells and on endothelium-derived hyperpolarizing factor-mediated arterial hyperpolarization and relaxation. *J Cardiovasc Pharmacol*, **38,** 130-40.

FUKATA, Y., AMANO, M. & KAIBUCHI, K. (2001). Rho-Rho-kinase pathway in smooth muscle contraction and cytoskeletal reorganization of non-muscle cells. *Trends Pharmacol Sci*, **22,** 32-9.

FUKUDA, N., IZUMI, Y., SOMA, M., WATANABE, Y., WATANABE, M. & HATANO, M. (1992). Effects of L-NG-monomethyl arginine on the cyclic GMP formations in rat mesenteric arteries. *Jpn J Pharmacol*, **58,** 55-60.

FURCHGOTT, R.F. (1983). Role of endothelium in responses of vascular smooth muscle. *Circ Res*, **53,** 557-73.

FURCHGOTT, R.F. & ZAWADZKI, J.V. (1980). The obligatory role of endothelial cells in the relaxation of arterial smooth muscle by acetylcholine. *Nature*, **288,** 373-6.

FURNESS, J.B. (1973). Arrangement of blood vessels and their relation with adrenergic nerves in the rat mesentery. *J Anat*, **115,** 347-64.

GAIETTA, G., DEERINCK, T.J., ADAMS, S.R., BOUWER, J., TOUR, O., LAIRD, D.W., SOSINSKY, G.E., TSIEN, R.Y. & ELLISMAN, M.H. (2002). Multicolor and electron microscopic imaging of connexin trafficking. *Science*, **296,** 503-7.

GAINETDINOV, R.R., PREMONT, R.T., BOHN, L.M., LEFKOWITZ, R.J. & CARON, M.G. (2004). Desensitization of G protein-coupled receptors and neuronal functions. *Annu Rev Neurosci*, **27,** 107-44.

GALLAGHER, C.J. & SALTER, M.W. (2003). Differential properties of astrocyte calcium waves mediated by P2Y1 and P2Y2 receptors. *J Neurosci*, **23,** 6728-39.

GALLIGAN, J.J., HESS, M.C., MILLER, S.B. & FINK, G.D. (2001). Differential localization of P2 receptor subtypes in mesenteric arteries and veins of normotensive and hypertensive rats. *J Pharmacol Exp Ther*, **296,** 478-85.

GANONG, W.F. (1999). *Review of medical physiology*. Stamford, Conn.: Appleton & Lange ; London : Prentice Hall International.

GANZ, P., SANDROCK, A.W., LANDIS, S.C., LEOPOLD, J., GIMBRONE, M.A., JR. & ALEXANDER, R.W. (1986). Vasoactive intestinal peptide: vasodilatation and cyclic AMP generation. *Am J Physiol*, **250,** H755-60.

GAO, Y.J., HIROTA, S., ZHANG, D.W., JANSSEN, L.J. & LEE, R.M. (2003). Mechanisms of hydrogen-peroxide-induced biphasic response in rat mesenteric artery. *Br J Pharmacol*, **138,** 1085-92.

GARDENER, M.J., JOHNSON, I.T., BURNHAM, M.P., EDWARDS, G., HEAGERTY, A.M. & WESTON, A.H. (2004). Functional evidence of a role for two-pore domain potassium channels in rat mesenteric and pulmonary arteries. *Br J Pharmacol*, **142,** 192-202.

GARDINER, S.M., KEMP, P.A., MARCH, J.E., FALLGREN, B. & BENNETT, T. (1996). Effects of glibenclamide on the regional haemodynamic actions of alpha-trinositol and its influence on responses to vasodilators in conscious rats. *Br J Pharmacol*, **117,** 507-515.

GARLAND, C.J. & PLANE, F. (1996). Relative importance of endothelium-derived hyperpolarizing factor for the relaxation of vascular smooth muscle in different arterial beds. In *Endothelium-derived Hyperpolarizing Factor*. ed Vanhoutte, P.M. pp. 173-179. London: Harwood Academic.

GARLAND, J.G. & MCPHERSON, G.A. (1992). Evidence that nitric oxide does not mediate the hyperpolarization and relaxation to acetylcholine in the rat small mesenteric artery. *Br J Pharmacol*, **105,** 429-35.

GARRAD, R.C., OTERO, M.A., ERB, L., THEISS, P.M., CLARKE, L.L., GONZALEZ, F.A., TURNER, J.T. & WEISMAN, G.A. (1998). Structural basis of agonist-induced desensitization and sequestration of the P2Y2 nucleotide receptor. Consequences of truncation of the C terminus. *J Biol Chem*, **273,** 29437-44.

GITTERMAN, D.P. & EVANS, R.J. (2000). Properties of P2X and P2Y receptors are dependent on artery diameter in the rat mesenteric bed. *Br J Pharmacol*, **131,** 1561-8.

GLUAIS, P., EDWARDS, G., WESTON, A.H., FALCK, J.R., VANHOUTTE, P.M. & FELETOU, M. (2005). Role of SK(Ca) and IK(Ca) in endothelium-dependent hyperpolarizations of the guinea-pig isolated carotid artery. *Br J Pharmacol*, **144,** 477-85.

GOHLA, A., SCHULTZ, G. & OFFERMANNS, S. (2000). Role for G(12)/G(13) in agonist-induced vascular smooth muscle cell contraction. *Circ Res*, **87,** 221-7.

GONZALEZ, J.M., BRIONES, A.M., STARCHER, B., CONDE, M.V., SOMOZA, B., DALY, C., VILA, E., MCGRATH, I., GONZALEZ, M.C. & ARRIBAS, S.M. (2005). Influence of elastin on rat small artery mechanical properties. *Exp Physiol*, **90,** 463-8.

GONZALEZ-ALONSO, J., OLSEN, D.B. & SALTIN, B. (2002). Erythrocyte and the regulation of human skeletal muscle blood flow and oxygen delivery: role of circulating ATP. *Circ Res*, **91,** 1046-55.

GOODENOUGH, D.A. & PAUL, D.L. (2003). Beyond the gap: functions of unpaired connexon channels. *Nat Rev Mol Cell Biol*, **4,** 285-94.

GORLACH, A. (2005). Control of adenosine transport by hypoxia. *Circ Res*, **97,** 1-3.

GOTO, K., FUJII, K., KANSUI, Y., ABE, I. & IIDA, M. (2002). Critical role of gap junctions in endothelium-dependent hyperpolarization in rat mesenteric arteries. *Clin Exp Pharmacol Physiol*, **29,** 595-602.

GOTO, K., RUMMERY, N.M., GRAYSON, T.H. & HILL, C.E. (2004). Attenuation of conducted vasodilatation in rat mesenteric arteries during hypertension: role of inwardly rectifying potassium channels. *J Physiol*, **561,** 215-31.

GRAYSON, T.H., HADDOCK, R.E., MURRAY, T.P., WOJCIKIEWICZ, R.J. & HILL, C.E. (2004). Inositol 1,4,5-trisphosphate receptor subtypes are differentially distributed between smooth muscle and endothelial layers of rat arteries. *Cell Calcium*, **36,** 447-58.

GRIFFITH, T.M. (2004). Endothelium-dependent smooth muscle hyperpolarization: do gap junctions provide a unifying hypothesis? *Br J Pharmacol*, **141,** 881-903.

GRIFFITH, T.M., CHAYTOR, A.T., EDWARDS, D.H., DAVERIO, F. & MCGUIGAN, C. (2004). Enhanced inhibition of the EDHF phenomenon by a phenyl methoxyalaninyl phosphoramidate derivative of dideoxyadenosine. *Br J Pharmacol*, **142,** 27-30.

GRIFFITH, T.M., CHAYTOR, A.T., TAYLOR, H.J., GIDDINGS, B.D. & EDWARDS, D.H. (2002). cAMP facilitates EDHF-type relaxations in conduit arteries by enhancing electrotonic conduction via gap junctions. *Proc Natl Acad Sci U S A*, **99,** 6392-7.

GROSCHNER, K., GRAIER, W.F. & KUKOVETZ, W.R. (1994). Histamine induces K+, Ca2+, and Cl- currents in human vascular endothelial cells. Role of ionic currents in stimulation of nitric oxide biosynthesis. *Circ Res*, **75,** 304-14.

GROSCHNER, K., HINGEL, S., LINTSCHINGER, B., BALZER, M., ROMANIN, C., ZHU, X. & SCHREIBMAYER, W. (1998). Trp proteins form store-operated cation channels in human vascular endothelial cells. *FEBS Lett*, **437,** 101-6.

GUSTAFSSON, F., ANDREASEN, D., SALOMONSSON, M., JENSEN, B.L. & HOLSTEIN-RATHLOU, N. (2001). Conducted vasoconstriction in rat mesenteric arterioles: role for dihydropyridine-insensitive Ca(2+) channels. *Am J Physiol Heart Circ Physiol*, **280,** H582-90.

GUSTAFSSON, F. & HOLSTEIN-RATHLOU, N. (1999). Conducted vasomotor responses in arterioles: characteristics, mechanisms and physiological significance. *Acta Physiol Scand*, **167,** 11-21.

GUSTAFSSON, F., MIKKELSEN, H.B., ARENSBAK, B., THUNEBERG, L., NEVE, S., JENSEN, L.J. & HOLSTEIN-RATHLOU, N.H. (2003). Expression of connexin 37, 40 and 43 in rat mesenteric arterioles and resistance arteries. *Histochem Cell Biol*, **119,** 139-48.

HAAS, T.L. & DULING, B.R. (1997). Morphology favors an endothelial cell pathway for longitudinal conduction within arterioles. *Microvasc Res*, **53,** 113-20.

HADDOCK, R.E., GRAYSON, T.H., BRACKENBURY, T.D., MEANEY, K.R., NEYLON, C.B., SANDOW, S.L. & HILL, C.E. (2006). Endothelial coordination of cerebral vasomotion via myoendothelial gap junctions containing connexins 37 and 40. *Am J Physiol Heart Circ Physiol*, **291,** H2047-56.

HALLAM, T.J. & PEARSON, J.D. (1986). Exogenous ATP raises cytoplasmic free calcium in fura-2 loaded piglet aortic endothelial cells. *FEBS Lett*, **207,** 95-9.

HANSEN, P.R. & OLESEN, S.P. (1997). Relaxation of rat resistance arteries by acetylcholine involves a dual mechanism: activation of K+ channels and formation of nitric oxide. *Pharmacol Toxicol*, **80,** 280-5.

HARDY, A.R., CONLEY, P.B., LUO, J., BENOVIC, J.L., POOLE, A.W. & MUNDELL, S.J. (2005). P2Y1 and P2Y12 receptors for ADP desensitize by distinct kinase-dependent mechanisms. *Blood*, **105,** 3552-60.

HARRINGTON, L.S. & MITCHELL, J.A. (2004). Novel role for P2X receptor activation in endothelium-dependent vasodilation. *Br J Pharmacol*, **143,** 611-7.

HARRIS, A.L. (2001). Emerging issues of connexin channels: biophysics fills the gap. *Q Rev Biophys*, **34,** 325-472.

HARRIS, D., MCCULLOCH, A.I., KENDALL, D.A. & RANDALL, M.D. (2002). Characterization of vasorelaxant responses to anandamide in the rat mesenteric arterial bed. *J Physiol*, **539,** 893-902.

HAYABUCHI, Y., DART, C. & STANDEN, N.B. (2001). Evidence for involvement of A-kinase anchoring protein in activation of rat arterial K(ATP) channels by protein kinase A. *J Physiol*, **536,** 421-7.

HELLIWELL, R.M. & LARGE, W.A. (1997). Alpha 1-adrenoceptor activation of a non-selective cation current in rabbit portal vein by 1,2-diacyl-sn-glycerol. *J Physiol*, **499 (Pt 2),** 417-28.

HERVE, J.-C. (2005). The connexins. *Biochimica et Biophysica Acta (BBA) - Biomembranes The Connexins Part II*, **1711,** 97-98.

HILEY, C.R., BOTTRILL, F.E., WARNOCK, J. & RICHARDSON, P.J. (1995). Effects of pH on responses to adenosine, CGS 21680, carbachol and nitroprusside in the isolated perfused superior mesenteric arterial bed of the rat. *Br J Pharmacol*, **116,** 2641-6.

HILL, A.J., HINTON, J.M., CHENG, H., GAO, Z., BATES, D.O., HANCOX, J.C., LANGTON, P.D. & JAMES, A.F. (2006). A TRPC-like non-selective cation current activated by [alpha]1-adrenoceptors in rat mesenteric artery smooth muscle cells. *Cell Calcium*, **40,** 29-40.

HILL, C.E., HICKEY, H. & SANDOW, S.L. (2000). Role of gap junctions in acetylcholine-induced vasodilation of proximal and distal arteries of the rat mesentery. *J Auton Nerv Syst*, **81,** 122-7.

HILL, C.E., PHILLIPS, J.K. & SANDOW, S.L. (2001). Heterogeneous control of blood flow amongst different vascular beds. *Med Res Rev*, **21,** 1-60.

HILL, C.E., RUMMERY, N., HICKEY, H. & SANDOW, S.L. (2002). Heterogeneity in the distribution of vascular gap junctions and connexins: implications for function. *Clin Exp Pharmacol Physiol*, **29,** 620-5.

HILTON, S.M. (1959). A peripheral arterial conducting mechanism underlying dilatation of the femoral artery and concerned in functional vasodilatation in skeletal muscle. *J Physiol*, **149,** 93-111.

HINTON, J.M. & LANGTON, P.D. (2003). Inhibition of EDHF by two new combinations of K+-channel inhibitors in rat isolated mesenteric arteries. *Br J Pharmacol*, **138,** 1031-1035.

HIRST, G.D. & EDWARDS, F.R. (1989). Sympathetic neuroeffector transmission in arteries and arterioles. *Physiol Rev*, **69,** 546-604.

HIRST, G.D. & NEILD, T.O. (1978). An analysis of excitatory junctional potentials recorded from arterioles. *J Physiol*, **280,** 87-104.

HO, W.S. & HILEY, C.R. (2003a). Endothelium-independent relaxation to cannabinoids in rat-isolated mesenteric artery and role of Ca2+ influx. *Br J Pharmacol*, **139,** 585-97.

HO, W.S. & HILEY, C.R. (2003b). Vasodilator actions of abnormal-cannabidiol in rat isolated small mesenteric artery. *Br J Pharmacol*, **138,** 1320-32.

HO, W.S. & HILEY, C.R. (2004). Vasorelaxant activities of the putative endocannabinoid virodhamine in rat isolated small mesenteric artery. *J Pharm Pharmacol*, **56,** 869-75.

HOI, P.M. & HILEY, C.R. (2006). Vasorelaxant effects of oleamide in rat small mesenteric artery indicate action at a novel cannabinoid receptor. *Br J Pharmacol*, **147,** 560-8.

HONG, T. & HILL, C.E. (1998). Restricted expression of the gap junctional protein connexin 43 in the arterial system of the rat. *J Anat*, **192 (Pt 4),** 583-93.

HONING, M.L., SMITS, P., MORRISON, P.J., BURNETT, J.C., JR. & RABELINK, T.J. (2001). C-type natriuretic peptide-induced vasodilation is dependent on hyperpolarization in human forearm resistance vessels. *Hypertension*, **37,** 1179-83.

HUANG, A., SUN, D., JACOBSON, A., CARROLL, M.A., FALCK, J.R. & KALEY, G. (2005). Epoxyeicosatrienoic Acids Are Released to Mediate Shear Stress-Dependent Hyperpolarization of Arteriolar Smooth Muscle. *Circ Res*, **96,** 376-383.

HUSER, J., HOLDA, J.R., KOCKSKAMPER, J. & BLATTER, L.A. (1999). Focal agonist stimulation results in spatially restricted Ca2+ release and capacitative Ca2+ entry in bovine vascular endothelial cells. *J Physiol*, **514 (Pt 1),** 101-9.

HUSSAIN, M.B. & MARSHALL, I. (1997). Characterization of alpha1-adrenoceptor subtypes mediating contractions to phenylephrine in rat thoracic aorta, mesenteric artery and pulmonary artery. *Br J Pharmacol*, **122,** 849-58.

HWA, J.J., GHIBAUDI, L., WILLIAMS, P. & CHATTERJEE, M. (1994). Comparison of acetylcholine-dependent relaxation in large and small arteries of rat mesenteric vascular bed. *Am J Physiol*, **266,** H952-8.

IESAKI, T., OKADA, T., SHIMADA, I., YAMAGUCHI, H. & OCHI, R. (1996). Decrease in Ca2+ sensitivity as a mechanism of hydrogen peroxide-induced relaxation of rabbit aorta. *Cardiovasc Res*, **31,** 820-5.

IGNARRO, L.J., BUGA, G.M., WOOD, K.S., BYRNS, R.E. & CHAUDHURI, G. (1987). Endothelium-derived relaxing factor produced and released from artery and vein is nitric oxide. *Proc Natl Acad Sci U S A*, **84,** 9265-9.

IINO, M. & ENDO, M. (1992). Calcium-dependent immediate feedback control of inositol 1,4,5-triphosphate-induced Ca2+ release. *Nature*, **360,** 76-8.

INOUE, R., OKADA, T., ONOUE, H., HARA, Y., SHIMIZU, S., NAITOH, S., ITO, Y. & MORI, Y. (2001). The transient receptor potential protein homologue TRP6 is the essential component of vascular alpha(1)-adrenoceptor-activated Ca(2+)-permeable cation channel. *Circ Res*, **88,** 325-32.

INVITROGEN (2006). The handbook - A guide to fluorescent probes and labeling technologies: Invitrogen - Molecular probes

IRVIN, J.L. & IRVIN, E.M. (1954). The interaction of quinacrine with adenine nucleotides. *J Biol Chem*, **210,** 45-56.

ISOMOTO, S., KONDO, C., YAMADA, M., MATSUMOTO, S., HIGASHIGUCHI, O., HORIO, Y., MATSUZAWA, Y. & KURACHI, Y. (1996). A novel sulfonylurea receptor forms with BIR (Kir6.2) a smooth muscle type ATP-sensitive K+ channel. *J Biol Chem*, **271,** 24321-4.

ITO, S., KAJIKURI, J., ITOH, T. & KURIYAMA, H. (1991). Effects of lemakalim on changes in Ca2+ concentration and mechanical activity induced by noradrenaline in the rabbit mesenteric artery. *Br J Pharmacol*, **104,** 227-33.

ITOH, H., SHIMOMURA, A., OKUBO, S., ICHIKAWA, K., ITO, M., KONISHI, T. & NAKANO, T. (1993). Inhibition of myosin light chain phosphatase during Ca(2+)-independent vasocontraction. *Am J Physiol*, **265,** C1319-24.

JACKSON, W.F. (2000). Ion channels and vascular tone. *Hypertension*, **35,** 173-8.

JACKSON, W.F. (2005). Potassium channels in the peripheral microcirculation. *Microcirculation*, **12,** 113-27.

JAGGAR, J.H., WELLMAN, G.C., HEPPNER, T.J., PORTER, V.A., PEREZ, G.J., GOLLASCH, M., KLEPPISCH, T., RUBART, M., STEVENSON, A.S., LEDERER, W.J., KNOT, H.J., BONEV, A.D. & NELSON, M.T. (1998). Ca2+ channels, ryanodine receptors and Ca(2+)-activated K+ channels: a functional unit for regulating arterial tone. *Acta Physiol Scand*, **164,** 577-87.

JANTZI, M.C., BRETT, S.E., JACKSON, W.F., CORTELING, R.L., VIGMOND, E.J. & WELSH, D.G. (2006). Inward Rectifying Potassium Channels Facilitate Cell-to-Cell Communication in Hamster Retractor Muscle Feed Arteries. *Am J Physiol Heart Circ Physiol.*

JENSEN, L.J., SALOMONSSON, M., JENSEN, B.L. & HOLSTEIN-RATHLOU, N.H. (2004). Depolarization-induced calcium influx in rat mesenteric small arterioles is mediated exclusively via mibefradil-sensitive calcium channels. *Br J Pharmacol*, **142,** 709-18.

JIANG, Q., GUO, D., LEE, B.X., VAN RHEE, A.M., KIM, Y.C., NICHOLAS, R.A., SCHACHTER, J.B., HARDEN, T.K. & JACOBSON, K.A. (1997). A mutational analysis of residues essential for ligand recognition at the human P2Y1 receptor. *Mol Pharmacol*, **52,** 499-507.

JOANNIDES, R., HAEFELI, W.E., LINDER, L., RICHARD, V., THUILLEZ, C. & LUSCHER, T.F. (1994). [Role of nitric oxide in flow-dependent vasodilation of human peripheral arteries in vivo]. *Arch Mal Coeur Vaiss*, **87,** 983-5.

JONES, K.H. & KNISS, D.A. (1987). Propidium iodide as a nuclear counterstain for immunofluorescence studies on cells in culture. *J Histochem Cytochem*, **35,** 123-5.

KAISER, R.A., OXHORN, B.C., ANDREWS, G. & BUXTON, I.L. (2002). Functional compartmentation of endothelial P2Y receptor signaling. *Circ Res*, **91,** 292-9.

KAJITA, Y., DIETRICH, H.H. & DACEY, R.G., JR. (1996). Effects of oxyhemoglobin on local and propagated vasodilatory responses induced by adenosine, adenosine diphosphate, and adenosine triphosphate in rat cerebral arterioles. *J Neurosurg*, **85,** 908-16.

KAMENETSKY, M., MIDDELHAUFE, S., BANK, E.M., LEVIN, L.R., BUCK, J. & STEEGBORN, C. (2006). Molecular details of cAMP generation in mammalian cells: a tale of two systems. *J Mol Biol*, **362,** 623-39.

KAMM, K.E. & STULL, J.T. (1985). The function of myosin and myosin light chain kinase phosphorylation in smooth muscle. *Annu Rev Pharmacol Toxicol*, **25,** 593-620.

KANSUI, Y., FUJII, K., NAKAMURA, K., GOTO, K., ONIKI, H., ABE, I., SHIBATA, Y. & IIDA, M. (2004). Angiotensin II receptor blockade corrects altered expression of gap junctions in vascular endothelial cells from hypertensive rats. *Am J Physiol Heart Circ Physiol*, **287,** H216-24.

KAWADA, T., TOYOSATO, A., ISLAM, M.O., YOSHIDA, Y. & IMAI, S. (1997). cGMP-kinase mediates cGMP- and cAMP-induced Ca2+ desensitization of skinned rat artery. *Eur J Pharmacol*, **323,** 75-82.

KEMP, B.K. & COCKS, T.M. (1997). Evidence that mechanisms dependent and independent of nitric oxide mediate endothelium-dependent relaxation to bradykinin in human small resistance-like coronary arteries. *Br J Pharmacol*, **120,** 757-62.

KISHIMOTO, A., TAKAI, Y., MORI, T., KIKKAWA, U. & NISHIZUKA, Y. (1980). Activation of calcium and phospholipid-dependent protein kinase by diacylglycerol, its possible relation to phosphatidylinositol turnover. *J Biol Chem*, **255,** 2273-6.

KITAZAWA, T., ETO, M., WOODSOME, T.P. & BRAUTIGAN, D.L. (2000). Agonists trigger G protein-mediated activation of the CPI-17 inhibitor phosphoprotein of myosin light chain phosphatase to enhance vascular smooth muscle contractility. *J Biol Chem*, **275,** 9897-900.

KLEPPISCH, T. & NELSON, M.T. (1995). Adenosine activates ATP-sensitive potassium channels in arterial myocytes via A2 receptors and cAMP-dependent protein kinase. *Proc Natl Acad Sci U S A*, **92,** 12441-5.

KOHLER, R., BRAKEMEIER, S., KUHN, M., BEHRENS, C., REAL, R., DEGENHARDT, C., ORZECHOWSKI, H.D., PRIES, A.R., PAUL, M. & HOYER, J. (2001). Impaired hyperpolarization in regenerated endothelium after balloon catheter injury. *Circ Res*, **89,** 174-9.

KOHLER, R., EICHLER, I., SCHONFELDER, H., GRGIC, I., HEINAU, P., SI, H. & HOYER, J. (2005). Impaired EDHF-mediated vasodilation and function of endothelial Ca-activated K channels in uremic rats. *Kidney Int*, **67,** 2280-7.

KOMALAVILAS, P. & LINCOLN, T.M. (1996). Phosphorylation of the inositol 1,4,5-trisphosphate receptor. Cyclic GMP-dependent protein kinase mediates cAMP and cGMP dependent phosphorylation in the intact rat aorta. *J Biol Chem*, **271,** 21933-8.

KOTLIKOFF, M.I. (2005). EDHF redux: EETs, TRPV4, and Ca2+ sparks. *Circ Res*, **97,** 1209-10.

KOYAMA, M., ITO, M., FENG, J., SEKO, T., SHIRAKI, K., TAKASE, K., HARTSHORNE, D.J. & NAKANO, T. (2000). Phosphorylation of CPI-17, an inhibitory phosphoprotein of smooth muscle myosin phosphatase, by Rho-kinase. *FEBS Lett*, **475,** 197-200.

KOZIAK, K., SEVIGNY, J., ROBSON, S.C., SIEGEL, J.B. & KACZMAREK, E. (1999). Analysis of CD39/ATP diphosphohydrolase (ATPDase) expression in endothelial cells, platelets and leukocytes. *Thromb Haemost*, **82,** 1538-44.

KROGH, A., HARROP, G.A. & REHBERG, P.B. (1922). Studies on the physiology of capillaries: III. The innervation of the blood vessels in the hind legs of the frog. *J Physiol*, **56,** 179-189.

KUBO, M., QUAYLE, J.M. & STANDEN, N.B. (1997). Angiotensin II inhibition of ATP-sensitive K+ currents in rat arterial smooth muscle cells through protein kinase C. *J Physiol*, **503 (Pt 3),** 489-96.

KURJIAKA, D.T. & SEGAL, S.S. (1995). Conducted vasodilation elevates flow in arteriole networks of hamster striated muscle. *Am J Physiol Heart Circ Physiol*, **269,** H1723-1728.

LACY, P.S., PILKINGTON, G., HANVESAKUL, R., FISH, H.J., BOYLE, J.P. & THURSTON, H. (2000). Evidence against potassium as an endothelium-derived hyperpolarizing factor in rat mesenteric small arteries. *Br J Pharmacol*, **129,** 605-11.

LAGAUD, G.J., RANDRIAMBOAVONJY, V., ROUL, G., STOCLET, J.C. & ANDRIANTSITOHAINA, R. (1999). Mechanism of Ca2+ release and entry during contraction elicited by norepinephrine in rat resistance arteries. *Am J Physiol*, **276,** H300-8.

LAMONT, C. & WIER, W.G. (2004). Different roles of ryanodine receptors and inositol (1,4,5)-trisphosphate receptors in adrenergically stimulated contractions of small arteries. *Am J Physiol Heart Circ Physiol*, **287,** H617-25.

LAMPE, P.D. & LAU, A.F. (2000). Regulation of gap junctions by phosphorylation of connexins. *Arch Biochem Biophys*, **384,** 205-15.

LARSON, D.M. & SHERIDAN, J.D. (1982). Intercellular junctions and transfer of small molecules in primary vascular endothelial cultures. *J Cell Biol*, **92,** 183-91.

LAUF, U., GIEPMANS, B.N.G., LOPEZ, P., BRACONNOT, S., CHEN, S.-C. & FALK, M.M. (2002). Dynamic trafficking and delivery of connexons to the plasma membrane and accretion to gap junctions in living cells. *PNAS*, **99,** 10446-10451.

LAZAROWSKI, E.R. & HARDEN, T.K. (1999). Quantitation of extracellular UTP using a sensitive enzymatic assay. *Br J Pharmacol*, **127,** 1272-8.

LEDOUX, J., WERNER, M.E., BRAYDEN, J.E. & NELSON, M.T. (2006). Calcium-activated potassium channels and the regulation of vascular tone. *Physiology (Bethesda)*, **21,** 69-78.

LEE, C.H., PARK, D., WU, D., RHEE, S.G. & SIMON, M.I. (1992). Members of the Gq alpha subunit gene family activate phospholipase C beta isozymes. *J Biol Chem*, **267,** 16044-7.

LEUNG, P.C., CHENG, K.T., LIU, C., CHEUNG, W.T., KWAN, H.Y., LAU, K.L., HUANG, Y. & YAO, X. (2006). Mechanism of non-capacitative Ca2+ influx in response to bradykinin in vascular endothelial cells. *J Vasc Res*, **43,** 367-76.

LEVY, M.N. (1979). The cardiac and vascular factors that determine systemic blood flow. *Circ Res*, **44,** 739-47.

LEWIS, C.J. & EVANS, R.J. (2000). Lack of run-down of smooth muscle P2X receptor currents recorded with the amphotericin permeabilized patch technique, physiological and pharmacological characterization of the properties of mesenteric artery P2X receptor ion channels. *Br J Pharmacol*, **131,** 1659-66.

LI, P.L. & CAMPBELL, W.B. (1997). Epoxyeicosatrienoic acids activate K+ channels in coronary smooth muscle through a guanine nucleotide binding protein. *Circ Res*, **80,** 877-84.

LIAO, Y., DAY, K.H., DAMON, D.N. & DULING, B.R. (2001). Endothelial cell-specific knockout of connexin 43 causes hypotension and bradycardia in mice. *Proc Natl Acad Sci U S A*, **98,** 9989-94.

LICHTMAN, J.W. & CONCHELLO, J.A. (2005). Fluorescence microscopy. *Nat Methods*, **2,** 910-9.

LIE, M., SEJERSTED, O.M. & KIIL, F. (1970). Local regulation of vascular cross section during changes in femoral arterial blood flow in dogs. *Circ Res*, **27,** 727-37.

LINCOLN, T.M., CORNWELL, T.L. & TAYLOR, A.E. (1990). cGMP-dependent protein kinase mediates the reduction of Ca2+ by cAMP in vascular smooth muscle cells. *Am J Physiol*, **258,** C399-407.

LIOU, J., KIM, M.L., HEO, W.D., JONES, J.T., MYERS, J.W., FERRELL, J.E., JR. & MEYER, T. (2005). STIM is a Ca2+ sensor essential for Ca2+-store-depletion-triggered Ca2+ influx. *Curr Biol*, **15,** 1235-41.

LIPOWSKY, H.H. (2005). Microvascular rheology and hemodynamics. *Microcirculation*, **12,** 5-15.

LITTLE, T.L., XIA, J. & DULING, B.R. (1995). Dye tracers define differential endothelial and smooth muscle coupling patterns within the arteriolar wall. *Circ Res*, **76,** 498-504.

LIU, C., MATHER, S., HUANG, Y., GARLAND, C.J. & YAO, X. (2004). Extracellular ATP facilitates flow-induced vasodilatation in rat small mesenteric arteries. *Am J Physiol Heart Circ Physiol*, **286,** H1688-95.

LIU, C., NGAI, C.Y., HUANG, Y., KO, W.H., WU, M., HE, G.W., GARLAND, C.J., DORA, K.A. & YAO, X. (2006a). Depletion of intracellular Ca2+ stores enhances flow-induced vascular dilatation in rat small mesenteric artery. *Br J Pharmacol*, **147,** 506-15.

LIU, C.L., HUANG, Y., NGAI, C.Y., LEUNG, Y.K. & YAO, X.Q. (2006b). TRPC3 is involved in flow- and bradykinin-induced vasodilation in rat small mesenteric arteries. *Acta Pharmacol Sin*, **27,** 981-90.

LONG, C.J. & STONE, T.W. (1985). The release of endothelium-derived relaxant factor is calcium dependent. *Blood Vessels*, **22,** 205-8.

LOOFT-WILSON, R.C., HAUG, S.J., NEUFER, P.D. & SEGAL, S.S. (2004). Independence of connexin expression and vasomotor conduction from sympathetic innervation in hamster feed arteries. *Microcirculation*, **11,** 397-408.

LUCKHOFF, A. & BUSSE, R. (1990a). Activators of potassium channels enhance calcium influx into endothelial cells as a consequence of potassium currents. *Naunyn Schmiedebergs Arch Pharmacol*, **342,** 94-9.

LUCKHOFF, A. & BUSSE, R. (1990b). Calcium influx into endothelial cells and formation of endothelium-derived relaxing factor is controlled by the membrane potential. *Pflugers Arch*, **416,** 305-11.

LUCKHOFF, A., POHL, U., MULSCH, A. & BUSSE, R. (1988). Differential role of extra- and intracellular calcium in the release of EDRF and prostacyclin from cultured endothelial cells. *Br J Pharmacol*, **95,** 189-96.

MACDONALD, J.A., BORMAN, M.A., MURANYI, A., SOMLYO, A.V., HARTSHORNE, D.J. & HAYSTEAD, T.A. (2001a). Identification of the endogenous smooth muscle myosin phosphatase-associated kinase. *Proc Natl Acad Sci U S A*, **98,** 2419-24.

MACDONALD, J.A., ETO, M., BORMAN, M.A., BRAUTIGAN, D.L. & HAYSTEAD, T.A. (2001b). Dual Ser and Thr phosphorylation of CPI-17, an inhibitor of myosin phosphatase, by MYPT-associated kinase. *FEBS Lett*, **493,** 91-4.

MACLEOD, K.M., NG, D.D., HARRIS, K.H. & DIAMOND, J. (1987). Evidence that cGMP is the mediator of endothelium-dependent inhibition of contractile responses of rat arteries to alpha-adrenoceptor stimulation. *Mol Pharmacol*, **32,** 59-64.

MADGE, L., MARSHALL, I.C. & TAYLOR, C.W. (1997). Delayed autoregulation of the Ca2+ signals resulting from capacitative Ca2+ entry in bovine pulmonary artery endothelial cells. *J Physiol*, **498 (Pt 2),** 351-69.

MALMSJO, M., ADNER, M., HARDEN, T.K., PENDERGAST, W., EDVINSSON, L. & ERLINGE, D. (2000a). The stable pyrimidines UDPbetaS and UTPgammaS discriminate between the P2 receptors that mediate vascular contraction and relaxation of the rat mesenteric artery. *Br J Pharmacol*, **131,** 51-6.

MALMSJO, M., CHU, Z.M., CROFT, K., ERLINGE, D., EDVINSSON, L. & BEILIN, L.J. (2002). P2Y receptor-induced EDHF vasodilatation is of primary importance for the regulation of perfusion pressure in the peripheral circulation of the rat. *Acta Physiol Scand*, **174,** 301-9.

MALMSJO, M., EDVINSSON, L. & ERLINGE, D. (1998). P2U-receptor mediated endothelium-dependent but nitric oxide-independent vascular relaxation. **123,** 719-729.

MALMSJO, M., EDVINSSON, L. & ERLINGE, D. (2000b). P2X receptors counteract the vasodilatory effects of endothelium derived hyperpolarising factor. *Eur J Pharmacol*, **390,** 173-80.

MALMSJO, M., ERLINGE, D., HOGESTATT, E.D. & ZYGMUNT, P.M. (1999). Endothelial P2Y receptors induce hyperpolarisation of vascular smooth muscle by release of endothelium-derived hyperpolarising factor. *Eur J Pharmacol*, **364,** 169-73.

MARCHENKO, S.M. (2002). Acetylcholine and ATP hyperpolarize endothelium via activation of different types of Ca(2+)-activated K+ channels. *Bull Exp Biol Med*, **134,** 422-4.

MARCHENKO, S.M. & SAGE, S.O. (1993). Electrical properties of resting and acetylcholine-stimulated endothelium in intact rat aorta. *J Physiol*, **462,** 735-51.

MARRELLI, S.P., ECKMANN, M.S. & HUNTE, M.S. (2003). Role of endothelial intermediate conductance KCa channels in cerebral EDHF-mediated dilations. *Am J Physiol Heart Circ Physiol*, **285,** H1590-9.

MARRELLI, S.P., O'NEIL R, G., BROWN, R.C. & BRYAN, R.M. (2006). PLA2 and TRPV4 channels regulate endothelial calcium in cerebral arteries. *Am J Physiol Heart Circ Physiol.*

MARTI, D., MIQUEL, R., ZIANI, K., GISBERT, R., IVORRA, M.D., ANSELMI, E., MORENO, L., VILLAGRASA, V., BARETTINO, D. & D'OCON, P. (2005). Correlation between mRNA levels and functional role of alpha1-adrenoceptor subtypes in arteries: evidence of alpha1L as a functional isoform of the alpha1A-adrenoceptor. *Am J Physiol Heart Circ Physiol*, **289,** H1923-32.

MARTIN, P.E., WALL, C. & GRIFFITH, T.M. (2005). Effects of connexin-mimetic peptides on gap junction functionality and connexin expression in cultured vascular cells. *Br J Pharmacol*, **144,** 617-27.

MARTIN, W., VILLANI, G.M., JOTHIANANDAN, D. & FURCHGOTT, R.F. (1985). Blockade of endothelium-dependent and glyceryl trinitrate-induced relaxation of rabbit aorta by certain ferrous hemoproteins. *J Pharmacol Exp Ther*, **233,** 679-85.

MATCHKOV, V.V., AALKJAER, C. & NILSSON, H. (2004a). A cyclic GMP-dependent calcium-activated chloride current in smooth-muscle cells from rat mesenteric resistance arteries. *J Gen Physiol*, **123,** 121-34.

MATCHKOV, V.V., RAHMAN, A., BAKKER, L.M., GRIFFITH, T.M., NILSSON, H. & AALKJAER, C. (2006). Analysis of effects of connexin-mimetic peptides in rat mesenteric small arteries. *Am J Physiol Heart Circ Physiol*, **291,** H357-367.

MATCHKOV, V.V., RAHMAN, A., PENG, H., NILSSON, H. & AALKJAER, C. (2004b). Junctional and nonjunctional effects of heptanol and glycyrrhetinic acid derivates in rat mesenteric small arteries. *Br J Pharmacol*, **142,** 961-72.

MATHER, S., DORA, K.A., SANDOW, S.L., WINTER, P. & GARLAND, C.J. (2005). Rapid Endothelial Cell-Selective Loading of Connexin 40 Antibody Blocks Endothelium-Derived Hyperpolarizing Factor Dilation in Rat Small Mesenteric Arteries. *Circ Res.*

MATOBA, T., SHIMOKAWA, H., NAKASHIMA, M., HIRAKAWA, Y., MUKAI, Y., HIRANO, K., KANAIDE, H. & TAKESHITA, A. (2000). Hydrogen peroxide is an endothelium-derived hyperpolarizing factor in mice. *J Clin Invest*, **106,** 1521-30.

MAUBAN, J.R., LAMONT, C., BALKE, C.W. & WIER, W.G. (2001). Adrenergic stimulation of rat resistance arteries affects Ca(2+) sparks, Ca(2+) waves, and Ca(2+) oscillations. *Am J Physiol Heart Circ Physiol*, **280,** H2399-405.

MAUBAN, J.R. & WIER, W.G. (2004). Essential role of EDHF in the initiation and maintenance of adrenergic vasomotion in rat mesenteric arteries. *Am J Physiol Heart Circ Physiol*, **287,** H608-16.

MCCULLOCH, A.I. & RANDALL, M.D. (1996). Modulation of vasorelaxant responses to potassium channel openers by basal nitric oxide in the rat isolated superior mesenteric arterial bed. *Br J Pharmacol*, **117,** 859-66.

MCCULLOUGH, W.T., COLLINS, D.M. & ELLSWORTH, M.L. (1997). Arteriolar responses to extracellular ATP in striated muscle. *Am J Physiol*, **272,** H1886-91.

MCFADZEAN, I. & GIBSON, A. (2002). The developing relationship between receptor-operated and store-operated calcium channels in smooth muscle. *Br J Pharmacol*, **135,** 1-13.

MCGAHREN, E.D., BEACH, J.M. & DULING, B.R. (1998). Capillaries demonstrate changes in membrane potential in response to pharmacological stimuli. *Am J Physiol*, **274,** H60-5.

MCGUIRE, J.J., DING, H. & TRIGGLE, C.R. (2001). Endothelium-derived relaxing factors: a focus on endothelium-derived hyperpolarizing factor(s). *Can J Physiol Pharmacol*, **79,** 443-70.

MCPHERSON, G.A. & ANGUS, J.A. (1991). Evidence that acetylcholine-mediated hyperpolarization of the rat small mesenteric artery does not involve the K+ channel opened by cromakalim. *Br J Pharmacol*, **103,** 1184-90.

MCSHERRY, I.N., SANDOW, S.L., CAMPBELL, W.B., FALCK, J.R., HILL, M.A. & DORA, K.A. (2006). A role for heterocellular coupling and EETs in dilation of rat cremaster arteries. *Microcirculation*, **13,** 119-30.

MCSHERRY, I.N., SPITALER, M.M., TAKANO, H. & DORA, K.A. (2005). Endothelial cell Ca2+ increases are independent of membrane potential in pressurized rat mesenteric arteries. *Cell Calcium*, **38,** 23-33.

MIAN, K.B. & MARTIN, W. (1997). Hydrogen peroxide-induced impairment of reactivity in rat isolated aorta: potentiation by 3-amino-1,2,4-triazole. *Br J Pharmacol*, **121,** 813-9.

MIAN, R. & MARSHALL, J.M. (1995). The role of adenosine in mediating vasodilatation in mesenteric circulation of the rat in acute and chronic hypoxia. *J Physiol*, **489 (Pt 1),** 225-34.

MICHEL, J.J. & SCOTT, J.D. (2002). AKAP mediated signal transduction. *Annu Rev Pharmacol Toxicol*, **42,** 235-57.

MILNER, P., BODIN, P., LOESCH, A. & BURNSTOCK, G. (1992). Increased shear stress leads to differential release of endothelin and ATP from isolated endothelial cells from 4- and 12-month-old male rabbit aorta. *J Vasc Res*, **29,** 420-5.

MINNEMAN, K.P. (1988). Alpha 1-adrenergic receptor subtypes, inositol phosphates, and sources of cell Ca2+. *Pharmacol Rev*, **40,** 87-119.

MISETA, A., BOGNER, P., BERENYI, E., KELLERMAYER, M., GALAMBOS, C., WHEATLEY, D.N. & CAMERON, I.L. (1993). Relationship between cellular ATP, potassium, sodium and magnesium concentrations in mammalian and avian erythrocytes. *Biochim Biophys Acta*, **1175,** 133-9.

MISTRY, D.K. & GARLAND, C.J. (1998). Nitric oxide (NO)-induced activation of large conductance Ca2+-dependent K+ channels (BK(Ca)) in smooth muscle cells isolated from the rat mesenteric artery. *Br J Pharmacol*, **124,** 1131-40.

MISTRY, H., GITLIN, J.M., MITCHELL, J.A. & HILEY, C.R. (2003). Endothelium-dependent relaxation and endothelial hyperpolarization by P2Y receptor agonists in rat-isolated mesenteric artery. *Br J Pharmacol*, **139,** 661-71.

MITCHELL, C.H., CARRE, D.A., MCGLINN, A.M., STONE, R.A. & CIVAN, M.M. (1998). A release mechanism for stored ATP in ocular ciliary epithelial cells. *Proc Natl Acad Sci U S A*, **95,** 7174-8.

MONCADA, S. & VANE, J.R. (1978). Pharmacology and endogenous roles of prostaglandin endoperoxides, thromboxane A2, and prostacyclin. *Pharmacol Rev*, **30,** 293-331.

MOREAU, C., PROST, A.L., DERAND, R. & VIVAUDOU, M. (2005). SUR, ABC proteins targeted by KATP channel openers. *J Mol Cell Cardiol*, **38,** 951-63.

MORGAN, K.G. & LEINWEBER, B.D. (1998). PKC-dependent signalling mechanisms in differentiated smooth muscle. *Acta Physiol Scand*, **164,** 495-505.

MOSER, G.C., FALLON, R.J. & MEISS, H.K. (1981). Fluorimetric measurements and chromatin condensation patterns of nuclei from 3T3 cells throughout G1. *J Cell Physiol*, **106,** 293-301.

MOTTE, S., COMMUNI, D., PIROTTON, S. & BOEYNAEMS, J.M. (1995). Involvement of multiple receptors in the actions of extracellular ATP: the example of vascular endothelial cells. *Int J Biochem Cell Biol*, **27,** 1-7.

MULLER, J.M., DAVIS, M.J., KUO, L. & CHILIAN, W.M. (1999). Changes in coronary endothelial cell Ca2+ concentration during shear stress- and agonist-induced vasodilation. *Am J Physiol*, **276,** H1706-14.

MULVANY, M.J. & AALKJAER, C. (1990). Structure and function of small arteries. *Physiol Rev*, **70,** 921-61.

MULVANY, M.J., AALKJAER, C. & PETERSEN, T.T. (1984). Intracellular sodium, membrane potential, and contractility of rat mesenteric small arteries. *Circ Res*, **54,** 740-9.

MULVANY, M.J., NILSSON, H. & FLATMAN, J.A. (1982). Role of membrane potential in the response of rat small mesenteric arteries to exogenous noradrenaline stimulation. *J Physiol*, **332,** 363-73.

MUPANOMUNDA, M.M., WANG, Y. & BUKOSKI, R.D. (1998). Effect of chronic sensory denervation on Ca(2+)-induced relaxation of isolated mesenteric resistance arteries. *Am J Physiol*, **274,** H1655-61.

MURAI, T., MURAKI, K., IMAIZUMI, Y. & WATANABE, M. (1999). Levcromakalim causes indirect endothelial hyperpolarization via a myo-endothelial pathway. *Br J Pharmacol*, **128,** 1491-6.

MURPHY, R.A. & WALKER, J.S. (1998). Inhibitory mechanisms for cross-bridge cycling: the nitric oxide-cGMP signal transduction pathway in smooth muscle relaxation. *Acta Physiol Scand*, **164,** 373-80.

MURPHY, T.V., SPURRELL, B.E. & HILL, M.A. (2001). Tyrosine phosphorylation following alterations in arteriolar intraluminal pressure and wall tension. *Am J Physiol Heart Circ Physiol*, **281,** H1047-56.

MURRANT, C.L. & SARELIUS, I.H. (2000). Local and remote arteriolar dilations initiated by skeletal muscle contraction. *Am J Physiol Heart Circ Physiol*, **279,** H2285-2294.

MURRANT, C.L. & SARELIUS, I.H. (2002). Multiple dilator pathways in skeletal muscle contraction-induced arteriolar dilations. *Am J Physiol Regul Integr Comp Physiol*, **282,** R969-78.

MURTHY, K.S., ZHOU, H., GRIDER, J.R. & MAKHLOUF, G.M. (2003). Inhibition of sustained smooth muscle contraction by PKA and PKG preferentially mediated by phosphorylation of RhoA. *Am J Physiol Gastrointest Liver Physiol*, **284,** G1006-16.

NEILD, T.O. & CRANE, G.J. (2002). Cellular coupling and conducted vasomotor responses. *Clin Exp Pharmacol Physiol*, **29,** 626-9.

NELSON, M.T., CHENG, H., RUBART, M., SANTANA, L.F., BONEV, A.D., KNOT, H.J. & LEDERER, W.J. (1995). Relaxation of arterial smooth muscle by calcium sparks. *Science*, **270,** 633-7.

NELSON, M.T. & QUAYLE, J.M. (1995). Physiological roles and properties of potassium channels in arterial smooth muscle. *Am J Physiol*, **268,** C799-822.

NELSON, M.T., STANDEN, N.B., BRAYDEN, J.E. & WORLEY, J.F., 3RD (1988). Noradrenaline contracts arteries by activating voltage-dependent calcium channels. *Nature*, **336,** 382-5.

NEWBY, A.C. & HENDERSON, A.H. (1990). Stimulus-secretion coupling in vascular endothelial cells. *Annu Rev Physiol*, **52,** 661-74.

NEYLON, C.B., RICHARDS, S.M., LARSEN, M.A., AGROTIS, A. & BOBIK, A. (1995). Multiple types of ryanodine receptor/Ca2+ release channels are expressed in vascular smooth muscle. *Biochem Biophys Res Commun*, **215,** 814-21.

NILIUS, B. & DROOGMANS, G. (2001). Ion channels and their functional role in vascular endothelium. *Physiol Rev*, **81,** 1415-59.

NILIUS, B., DROOGMANS, G. & WONDERGEM, R. (2003). Transient receptor potential channels in endothelium: solving the calcium entry puzzle? *Endothelium*, **10,** 5-15.

NILSSON, H. (1998). Interactions between membrane potential and intracellular calcium concentration in vascular smooth muscle. *Acta Physiol Scand*, **164,** 559-66.

NILSSON, H., JENSEN, P.E. & MULVANY, M.J. (1994). Minor role for direct adrenoceptor-mediated calcium entry in rat mesenteric small arteries. *J Vasc Res*, **31,** 314-21.

NILSSON, H., VIDEBAEK, L.M., TOMA, C. & MULVANY, M.J. (1998). Role of intracellular calcium for noradrenaline-induced depolarization in rat mesenteric small arteries. *J Vasc Res*, **35,** 36-44.

NISHIMURA, J. (2006). Topics on the Na+/Ca2+ exchanger: involvement of Na+/Ca2+ exchanger in the vasodilator-induced vasorelaxation. *J Pharmacol Sci*, **102,** 27-31.

NISHIMURA, J. & VAN BREEMEN, C. (1989). Direct regulation of smooth muscle contractile elements by second messengers. *Biochem Biophys Res Commun*, **163,** 929-35.

NORTHOVER, A.M. & NORTHOVER, B.J. (1997). Some cyclic nucleotides reduce phenylephrine-induced and phorbol ester-induced constriction of the rat anterior mesenteric artery. *Gen Pharmacol*, **28,** 139-43.

O'SULLIVAN, S.E., KENDALL, D.A. & RANDALL, M.D. (2004). Characterisation of the vasorelaxant properties of the novel endocannabinoid N-arachidonoyl-dopamine (NADA). *Br J Pharmacol*, **141,** 803-12.

OBER, R.J., MARTINEZ, C., VACCARO, C., ZHOU, J. & WARD, E.S. (2004). Visualizing the site and dynamics of IgG salvage by the MHC class I-related receptor, FcRn. *J Immunol*, **172,** 2021-9.

OHANIAN, V., OHANIAN, J., SHAW, L., SCARTH, S., PARKER, P.J. & HEAGERTY, A.M. (1996). Identification of protein kinase C isoforms in rat mesenteric small arteries and their possible role in agonist-induced contraction. *Circ Res*, **78,** 806-12.

OHASHI, M., SATOH, K. & ITOH, T. (1999). Acetylcholine-induced membrane potential changes in endothelial cells of rabbit aortic valve. *Br J Pharmacol*, **126,** 19-26.

OISHI, H., BUDEL, S., SCHUSTER, A., STERGIOPULOS, N., MEISTER, J.J. & BENY, J.L. (2001). Cytosolic-free calcium in smooth-muscle and endothelial cells in an intact arterial wall from rat mesenteric artery in vitro. *Cell Calcium*, **30,** 261-7.

OKADA, C.Y. & RECHSTEINER, M. (1982). Introduction of macromolecules into cultured mammalian cells by osmotic lysis of pinocytic vesicles. *Cell*, **29,** 33-41.

OLESEN, S.P., DAVIES, P.F. & CLAPHAM, D.E. (1988). Muscarinic-activated K+ current in bovine aortic endothelial cells. *Circ Res*, **62,** 1059-64.

OMAR, R., BOTTRILL, F.E., HILEY, C.R. & WHITE, R. (2000). Interaction of cyclic AMP modulating agents with levcromakalim in the relaxation of rat isolated mesenteric artery. *Eur J Pharmacol*, **401,** 85-96.

OTERO, M., GARRAD, R.C., VELAZQUEZ, B., HERNANDEZ-PEREZ, M.G., CAMDEN, J.M., ERB, L., CLARKE, L.L., TURNER, J.T., WEISMAN, G.A. & GONZALEZ, F.A. (2000). Mechanisms of agonist-dependent and -independent desensitization of a recombinant P2Y2 nucleotide receptor. *Mol Cell Biochem*, **205,** 115-23.

PALMER, R.M., ASHTON, D.S. & MONCADA, S. (1988). Vascular endothelial cells synthesize nitric oxide from L-arginine. *Nature*, **333,** 664-6.

PALMER, R.M., FERRIGE, A.G. & MONCADA, S. (1987). Nitric oxide release accounts for the biological activity of endothelium-derived relaxing factor. *Nature*, **327,** 524-6.

PARKINGTON, H.C., COLEMAN, H.A. & TARE, M. (2004). Prostacyclin and endothelium-dependent hyperpolarization. *Pharmacol Res*, **49,** 509-14.

PEARCE, M.J., MCINTYRE, T.M., PRESCOTT, S.M., ZIMMERMAN, G.A. & WHATLEY, R.E. (1996). Shear Stress Activates Cytosolic Phospholipase A2(cPLA2) and MAP Kinase in Human Endothelial Cells. *Biochemical and Biophysical Research Communications*, **218,** 500-504.

PEARSON, J.G., JL (1979). vascular enothelial and smooth muscle cells in culture selectively release adenine nucleotides. *Nature*, **281,** 384-386.

PEEL, S.E., LIU, B. & HALL, I.P. (2006). A key role for STIM1 in store operated calcium channel activation in airway smooth muscle. *Respir Res*, **7,** 119.

PEINELT, C., VIG, M., KOOMOA, D.L., BECK, A., NADLER, M.J., KOBLAN-HUBERSON, M., LIS, A., FLEIG, A., PENNER, R. & KINET, J.P. (2006). Amplification of CRAC current by STIM1 and CRACM1 (Orai1). *Nat Cell Biol*, **8,** 771-3.

PENG, H., MATCHKOV, V., IVARSEN, A., AALKJAER, C. & NILSSON, H. (2001). Hypothesis for the initiation of vasomotion. *Circ Res*, **88,** 810-5.

PEREZ, G.J., BONEV, A.D. & NELSON, M.T. (2001). Micromolar Ca(2+) from sparks activates Ca(2+)-sensitive K(+) channels in rat cerebral artery smooth muscle. *Am J Physiol Cell Physiol*, **281,** C1769-75.

PEREZ, G.J., BONEV, A.D., PATLAK, J.B. & NELSON, M.T. (1999). Functional coupling of ryanodine receptors to KCa channels in smooth muscle cells from rat cerebral arteries. *J Gen Physiol*, **113,** 229-38.

PETERSSON, J., ZYGMUNT, P.M. & HOGESTATT, E.D. (1997). Characterization of the potassium channels involved in EDHF-mediated relaxation in cerebral arteries. *Br J Pharmacol*, **120,** 1344-50.

PFEILSCHIFTER, J. & HUWILER, A. (1996). Regulatory functions of protein kinase C isoenzymes in purinoceptor signalling in mesangial cells. *J Auton Pharmacol*, **16,** 315-8.

PIPER, A.S. & LARGE, W.A. (2004). Single cGMP-activated Ca(+)-dependent Cl(-) channels in rat mesenteric artery smooth muscle cells. *J Physiol*, **555,** 397-408.

PIROTTON, S., RASPE, E., DEMOLLE, D., ERNEUX, C. & BOEYNAEMS, J.M. (1987). Involvement of inositol 1,4,5-trisphosphate and calcium in the action of adenine nucleotides on aortic endothelial cells. *J Biol Chem*, **262,** 17461-6.

PLANE, F., HOLLAND, M., WALDRON, G.J., GARLAND, C.J. & BOYLE, J.P. (1997). Evidence that anandamide and EDHF act via different mechanisms in rat isolated mesenteric arteries. *Br J Pharmacol*, **121,** 1509-11.

PLANE, F., HURRELL, A., JEREMY, J.Y. & GARLAND, C.J. (1996). Evidence that potassium channels make a major contribution to SIN-1-evoked relaxation of rat isolated mesenteric artery. *Br J Pharmacol*, **119,** 1557-62.

PLANE, F., SAMPSON, L.J., SMITH, J.J. & GARLAND, C.J. (2001). Relaxation to authentic nitric oxide and SIN-1 in rat isolated mesenteric arteries: variable role for smooth muscle hyperpolarization. *Br J Pharmacol*, **133,** 665-72.

POHL, U., HOLTZ, J., BUSSE, R. & BASSENGE, E. (1986). Crucial role of endothelium in the vasodilator response to increased flow in vivo. *Hypertension*, **8,** 37-44.

POPP, R., BAUERSACHS, J., HECKER, M., FLEMING, I. & BUSSE, R. (1996). A transferable, beta-naphthoflavone-inducible, hyperpolarizing factor is synthesized by native and cultured porcine coronary endothelial cells. *J Physiol*, **497 (Pt 3),** 699-709.

POPP, R., BRANDES, R.P., OTT, G., BUSSE, R. & FLEMING, I. (2002). Dynamic modulation of interendothelial gap junctional communication by 11,12-epoxyeicosatrienoic acid. *Circ Res*, **90,** 800-6.

PRAKRIYA, M., FESKE, S., GWACK, Y., SRIKANTH, S., RAO, A. & HOGAN, P.G. (2006). Orai1 is an essential pore subunit of the CRAC channel. *Nature*, **443,** 230-3.

PRAKRIYA, M. & LEWIS, R.S. (2001). Potentiation and inhibition of Ca(2+) release-activated Ca(2+) channels by 2-aminoethyldiphenyl borate (2-APB) occurs independently of IP(3) receptors. *J Physiol*, **536,** 3-19.

PREDESCU, D., VOGEL, S.M. & MALIK, A.B. (2004). Functional and morphological studies of protein transcytosis in continuous endothelia. *Am J Physiol Lung Cell Mol Physiol*, **287,** L895-901.

PRENTICE, D.J., PAYNE, S.L. & HOURANI, S.M. (1997). Activation of two sites by adenosine receptor agonists to cause relaxation in rat isolated mesenteric artery. *Br J Pharmacol*, **122,** 1509-15.

PUTNEY, J.W., JR. (1986). A model for receptor-regulated calcium entry. *Cell Calcium*, **7,** 1-12.

QUAST, U. & BAUMLIN, Y. (1991). Cromakalim inhibits contractions of the rat isolated mesenteric bed induced by noradrenaline but not caffeine in Ca(2+)-free medium: evidence for interference with receptor-mediated Ca2+ mobilization. *Eur J Pharmacol*, **200,** 239-49.

QUAST, U. & VILLHAUER, E.B. (1993). The individual enantiomers of cis-cromakalim possess K+ channel opening activity. *Eur J Pharmacol*, **245,** 165-71.

RALEVIC, V. & BURNSTOCK, G. (1998). Receptors for purines and pyrimidines. *Pharmacol Rev*, **50,** 413-92.

RANDALL, M.D., ALEXANDER, S.P., BENNETT, T., BOYD, E.A., FRY, J.R., GARDINER, S.M., KEMP, P.A., MCCULLOCH, A.I. & KENDALL, D.A. (1996). An endogenous cannabinoid as an endothelium-derived vasorelaxant. *Biochem Biophys Res Commun*, **229,** 114-20.

RAPOPORT, R.M. & MURAD, F. (1983). Agonist-induced endothelium-dependent relaxation in rat thoracic aorta may be mediated through cGMP. *Circ Res*, **52,** 352-7.

RASHATWAR, S.S., CORNWELL, T.L. & LINCOLN, T.M. (1987). Effects of 8-bromo-cGMP on Ca2+ levels in vascular smooth muscle cells: possible regulation of Ca2+-ATPase by cGMP-dependent protein kinase. *Proc Natl Acad Sci U S A*, **84,** 5685-9.

RATZ, P.H., BERG, K.M., URBAN, N.H. & MINER, A.S. (2005). Regulation of smooth muscle calcium sensitivity: KCl as a calcium-sensitizing stimulus. *Am J Physiol Cell Physiol*, **288,** C769-83.

RAY, C.J., ABBAS, M.R., CONEY, A.M. & MARSHALL, J.M. (2002). Interactions of adenosine, prostaglandins and nitric oxide in hypoxia-induced vasodilatation: in vivo and in vitro studies. *J Physiol*, **544,** 195-209.

RAY, C.J. & MARSHALL, J.M. (2005). Measurement of nitric oxide release evoked by systemic hypoxia and adenosine from rat skeletal muscle in vivo. *J Physiol*, **568,** 967-78.

RAY, C.J. & MARSHALL, J.M. (2006). The cellular mechanisms by which adenosine evokes release of nitric oxide from rat aortic endothelium. *J Physiol*, **570,** 85-96.

REIDY, M.A., CHOPEK, M., CHAO, S., MCDONALD, T. & SCHWARTZ, S.M. (1989). Injury induces increase of von Willebrand factor in rat endothelial cells. *Am J Pathol*, **134,** 857-64.

REMBOLD, C.M. & MURPHY, R.A. (1988). Myoplasmic [Ca2+] determines myosin phosphorylation in agonist-stimulated swine arterial smooth muscle. *Circ Res*, **63,** 593-603.

RICHARDS, G.R., WESTON, A.H., BURNHAM, M.P., FELETOU, M., VANHOUTTE, P.M. & EDWARDS, G. (2001). Suppression of K(+)-induced hyperpolarization by phenylephrine in rat mesenteric artery: relevance to studies of endothelium-derived hyperpolarizing factor. *Br J Pharmacol*, **134,** 1-5.

RIVERS, R. (1997a). Conducted arteriolar dilations persist in the presence of nitroarginine. *J Cardiovasc Pharmacol*, **30,** 309-12.

RIVERS, R.J. (1997b). Components of methacholine-initiated conducted vasodilation are unaffected by arteriolar pressure. *Am J Physiol Heart Circ Physiol*, **272,** H2895-2901.

RIVERS, R.J. & FRAME, M.D. (1999). Network vascular communication initiated by increases in tissue adenosine. *J Vasc Res*, **36,** 193-200.

RIVERS, R.J., HEIN, T.W., ZHANG, C. & KUO, L. (2001). Activation of barium-sensitive inward rectifier potassium channels mediates remote dilation of coronary arterioles. *Circulation*, **104,** 1749-53.

RIZZO, V., SUNG, A., OH, P. & SCHNITZER, J.E. (1998). Rapid Mechanotransduction in Situ at the Luminal Cell Surface of Vascular Endothelium and Its Caveolae. *J. Biol. Chem.*, **273,** 26323-26329.

ROBERTSON, B.E., SCHUBERT, R., HESCHELER, J. & NELSON, M.T. (1993). cGMP-dependent protein kinase activates Ca-activated K channels in cerebral artery smooth muscle cells. *Am J Physiol*, **265,** C299-303.

RODENWALDT, B., POHL, U. & DE WIT, C. (2007). Endogenous and exogenous NO attenuates the conduction of vasoconstrictions along arterioles in the microcirculation. *Am J Physiol Heart Circ Physiol.*

ROMANELLO, M., CODOGNOTTO, A., BICEGO, M., PINES, A., TELL, G. & D'ANDREA, P. (2005). Autocrine/paracrine stimulation of purinergic receptors in osteoblasts: contribution of vesicular ATP release. *Biochem Biophys Res Commun*, **331,** 1429-38.

ROOS, J., DIGREGORIO, P.J., YEROMIN, A.V., OHLSEN, K., LIOUDYNO, M., ZHANG, S., SAFRINA, O., KOZAK, J.A., WAGNER, S.L., CAHALAN, M.D., VELICELEBI, G. & STAUDERMAN, K.A. (2005). STIM1, an essential and conserved component of store-operated Ca2+ channel function. *J Cell Biol*, **169,** 435-45.

ROSENMEIER, J.B., HANSEN, J. & GONZALEZ-ALONSO, J. (2004). Circulating ATP-induced vasodilatation overrides sympathetic vasoconstrictor activity in human skeletal muscle. *J Physiol*, **558,** 351-65.

ROSS, G.R. & YALLAMPALLI, C. (2006). Endothelium-independent relaxation by adrenomedullin in pregnant rat mesenteric artery: role of cAMP-dependent protein kinase A and calcium-activated potassium channels. *J Pharmacol Exp Ther*, **317,** 1269-75.

RUBANYI, G.M. & VANHOUTTE, P.M. (1986). Oxygen-derived free radicals, endothelium, and responsiveness of vascular smooth muscle. *Am J Physiol*, **250,** H815-21.

RUBINO, A., RALEVIC, V. & BURNSTOCK, G. (1995). Contribution of P1-(A2b subtype) and P2-purinoceptors to the control of vascular tone in the rat isolated mesenteric arterial bed. *Br J Pharmacol*, **115,** 648-52.

RYCHLIK, B., BALCERCZYK, A., KLIMCZAK, A. & BARTOSZ, G. (2003). The role of multidrug resistance protein 1 (MRP1) in transport of fluorescent anions across the human erythrocyte membrane. *J Membr Biol*, **193,** 79-90.

SAEZ, J.C., BERTHOUD, V.M., BRANES, M.C., MARTINEZ, A.D. & BEYER, E.C. (2003). Plasma membrane channels formed by connexins: their regulation and functions. *Physiol Rev*, **83,** 1359-400.

SAIAG, B., BODIN, P., SHACOORI, V/. CATHELINE, M., RAULT, B. & BURNSTOCK, G. (1995). Uptake and flow-induced release of uridine nucleotides from isolated vascular endothlial cells. *Endothelium*, **2,** 279-285.

SAKURADA, S., TAKUWA, N., SUGIMOTO, N., WANG, Y., SETO, M., SASAKI, Y. & TAKUWA, Y. (2003). Ca2+-dependent activation of Rho and Rho kinase in membrane depolarization-induced and receptor stimulation-induced vascular smooth muscle contraction. *Circ Res*, **93,** 548-56.

SANDOW, S.L., BRAMICH, N.J., BANDI, H.P., RUMMERY, N.M. & HILL, C.E. (2003a). Structure, function, and endothelium-derived hyperpolarizing factor in the caudal artery of the SHR and WKY rat. *Arterioscler Thromb Vasc Biol*, **23,** 822-8.

SANDOW, S.L., GOTO, K., RUMMERY, N.M. & HILL, C.E. (2004). Developmental changes in myoendothelial gap junction mediated vasodilator activity in the rat saphenous artery. *J Physiol*, **556,** 875-86.

SANDOW, S.L. & HILL, C.E. (2000). Incidence of myoendothelial gap junctions in the proximal and distal mesenteric arteries of the rat is suggestive of a role in endothelium-derived hyperpolarizing factor-mediated responses. *Circ Res*, **86,** 341-6.

SANDOW, S.L., LOOFT-WILSON, R., DORAN, B., GRAYSON, T.H., SEGAL, S.S. & HILL, C.E. (2003b). Expression of homocellular and heterocellular gap junctions in hamster arterioles and feed arteries. *Cardiovasc Res*, **60,** 643-53.

SANDOW, S.L., NEYLON, C.B., CHEN, M.X. & GARLAND, C.J. (2006). Spatial separation of endothelial small- and intermediate-conductance calcium-activated potassium channels (K(Ca)) and connexins: possible relationship to vasodilator function? *J Anat*, **209,** 689-98.

SANDOW, S.L. & TARE, M. (2007). C-type natriuretic peptide: a new endothelium-derived hyperpolarizing factor? *Trends Pharmacol Sci*, **28,** 61-7.

SANDOW, S.L., TARE, M., COLEMAN, H.A., HILL, C.E. & PARKINGTON, H.C. (2002). Involvement of myoendothelial gap junctions in the actions of endothelium-derived hyperpolarizing factor. *Circ Res*, **90,** 1108-13.

SASAKI, D.T., DUMAS, S.E. & ENGLEMAN, E.G. (1987). Discrimination of viable and non-viable cells using propidium iodide in two color immunofluorescence. *Cytometry*, **8,** 413-20.

SCHUSTER, A., OISHI, H., BENY, J.L., STERGIOPULOS, N. & MEISTER, J.J. (2001). Simultaneous arterial calcium dynamics and diameter measurements: application to myoendothelial communication. *Am J Physiol Heart Circ Physiol*, **280,** H1088-96.

SEDOVA, M. & BLATTER, L.A. (1999). Dynamic regulation of [Ca2+]i by plasma membrane Ca(2+)-ATPase and Na+/Ca2+ exchange during capacitative Ca2+ entry in bovine vascular endothelial cells. *Cell Calcium*, **25,** 333-43.

SEGAL, S.S. (1994). Cell-to-cell communication coordinates blood flow control. *Hypertension*, **23,** 1113-20.

SEGAL, S.S. (1991). Microvascular recruitment in hamster striated muscle: role for conducted vasodilation. *Am J Physiol*, **261,** H181-9.

SEGAL, S.S. (2005). Regulation of blood flow in the microcirculation. *Microcirculation*, **12,** 33-45.

SEGAL, S.S., DAMON, D.N. & DULING, B.R. (1989). Propagation of vasomotor responses coordinates arteriolar resistances. *Am J Physiol*, **256,** H832-7.

SEGAL, S.S. & DULING, B.R. (1986a). Communication between feed arteries and microvessels in hamster striated muscle: segmental vascular responses are functionally coordinated. *Circ Res*, **59,** 283-90.

SEGAL, S.S. & DULING, B.R. (1989). Conduction of vasomotor responses in arterioles: a role for cell-to-cell coupling? *Am J Physiol*, **256,** H838-45.

SEGAL, S.S. & DULING, B.R. (1986b). Flow control among microvessels coordinated by intercellular conduction. *Science*, **234,** 868-70.

SEGAL, S.S. & DULING, B.R. (1987). Propagation of vasodilation in resistance vessels of the hamster: development and review of a working hypothesis. *Circ Res*, **61,** II20-5.

SEGAL, S.S. & JACOBS, T.L. (2001). Role for endothelial cell conduction in ascending vasodilatation and exercise hyperaemia in hamster skeletal muscle. *J Physiol*, **536,** 937-46.

SEGAL, S.S. & NEILD, T.O. (1996). Conducted depolarization in arteriole networks of the guinea-pig small intestine: effect of branching of signal dissipation. *J Physiol*, **496 (Pt 1),** 229-44.

SEGAL, S.S., WELSH, D.G. & KURJIAKA, D.T. (1999). Spread of vasodilatation and vasoconstriction along feed arteries and arterioles of hamster skeletal muscle. *J Physiol*, **516 (Pt 1),** 283-91.

SHAW, L., O'NEILL, S., JONES, C.J., AUSTIN, C. & TAGGART, M.J. (2004). Comparison of U46619-, endothelin-1- or phenylephrine-induced changes in cellular Ca2+ profiles and Ca2+ sensitisation of constriction of pressurised rat resistance arteries. *Br J Pharmacol*, **141,** 678-88.

SHAW, L., SWEENEY, M.A., O'NEILL, S.C., JONES, C.J.P., AUSTIN, C. & TAGGART, M.J. (2006). Caveolae and sarcoplasmic reticular coupling in smooth muscle cells of pressurised arteries: The relevance for Ca2+ oscillations and tone. *Cardiovascular Research*, **69,** 825-835.

SHIMOKAWA, H. & MATOBA, T. (2004). Hydrogen peroxide as an endothelium-derived hyperpolarizing factor. *Pharmacol Res*, **49,** 543-9.

SHIMOKAWA, H., YASUTAKE, H., FUJII, K., OWADA, M.K., NAKAIKE, R., FUKUMOTO, Y., TAKAYANAGI, T., NAGAO, T., EGASHIRA, K., FUJISHIMA, M. & TAKESHITA, A. (1996). The importance of the hyperpolarizing mechanism increases as the

vessel size decreases in endothelium-dependent relaxations in rat mesenteric circulation. *J Cardiovasc Pharmacol*, **28,** 703-11.

SI, H., HEYKEN, W.T., WOLFLE, S.E., TYSIAC, M., SCHUBERT, R., GRGIC, I., VILIANOVICH, L., GIEBING, G., MAIER, T., GROSS, V., BADER, M., DE WIT, C., HOYER, J. & KOHLER, R. (2006). Impaired endothelium-derived hyperpolarizing factor-mediated dilations and increased blood pressure in mice deficient of the intermediate-conductance Ca2+-activated K+ channel. *Circ Res*, **99,** 537-44.

SIMARD, J.M., CHEN, M., TARASOV, K.V., BHATTA, S., IVANOVA, S., MELNITCHENKO, L., TSYMBALYUK, N., WEST, G.A. & GERZANICH, V. (2006). Newly expressed SUR1-regulated NC(Ca-ATP) channel mediates cerebral edema after ischemic stroke. *Nat Med*, **12,** 433-40.

SIMIONESCU, M. & SIMIONESCU, N. (1984). Ultrastructure of the microvascular wall: functional correlations. In *Handbook of Physiology: A critical, comprehensive presentation of physiological knowledge and concepts*. eds Geiger, S., Renkin, E. & Michel, C.: American Physiological Society.

SINGER, H.A. & PEACH, M.J. (1982). Calcium- and endothelial-mediated vascular smooth muscle relaxation in rabbit aorta. *Hypertension*, **4,** 19-25.

SKINNER, M.R. & MARSHALL, J.M. (1996). Studies on the roles of ATP, adenosine and nitric oxide in mediating muscle vasodilatation induced in the rat by acute systemic hypoxia. *J Physiol*, **495 (Pt 2),** 553-60.

SLANINOVA, I., KUCSERA, J. & SVOBODA, A. (1999). Topology of microtubules and actin in the life cycle of Xanthophyllomyces dendrorhous (Phaffia rhodozyma). *Antonie Van Leeuwenhoek*, **75,** 361-8.

SMYTH, J.T., DEHAVEN, W.I., JONES, B.F., MERCER, J.C., TREBAK, M., VAZQUEZ, G. & PUTNEY, J.W., JR. (2006). Emerging perspectives in store-operated Ca(2+) entry: Roles of Orai, Stim and TRP. *Biochim Biophys Acta*, **1763,** 1147-60.

SOBOLOFF, J., SPASSOVA, M.A., TANG, X.D., HEWAVITHARANA, T., XU, W. & GILL, D.L. (2006). Orai1 and STIM reconstitute store-operated calcium channel function. *J Biol Chem*, **281,** 20661-5.

SODERSTROM, K.O. (1987). Lectin binding to collagen strands in histologic tissue sections. *Histochemistry*, **87,** 557-60.

SOMLYO, A.P. & HIMPENS, B. (1989). Cell calcium and its regulation in smooth muscle. *Faseb J*, **3,** 2266-76.

SOMLYO, A.P. & SOMLYO, A.V. (1998). From pharmacomechanical coupling to G-proteins and myosin phosphatase. *Acta Physiol Scand*, **164,** 437-48.

SOMLYO, A.P. & SOMLYO, A.V. (1994). Signal transduction and regulation in smooth muscle. *Nature*, **372,** 231-6.

SOMLYO, A.P. & SOMLYO, A.V. (2000). Signal transduction by G-proteins, rho-kinase and protein phosphatase to smooth muscle and non-muscle myosin II. *J Physiol*, **522 Pt 2,** 177-85.

SOMLYO, A.V. & SOMLYO, A.P. (1968). Electromechanical and pharmacomechanical coupling in vascular smooth muscle. *J Pharmacol Exp Ther*, **159,** 129-45.

STAM, W.B., VAN DER GRAAF, P.H. & SAXENA, P.R. (1999). Analysis of alpha 1L-adrenoceptor pharmacology in rat small mesenteric artery. *Br J Pharmacol*, **127,** 661-70.

STANDEN, N.B., QUAYLE, J.M., DAVIES, N.W., BRAYDEN, J.E., HUANG, Y. & NELSON, M.T. (1989). Hyperpolarizing vasodilators activate ATP-sensitive K+ channels in arterial smooth muscle. *Science*, **245,** 177-80.

STANKEVICIUS, E., LOPEZ-VALVERDE, V., RIVERA, L., HUGHES, A.D., MULVANY, M.J. & SIMONSEN, U. (2006). Combination of Ca2+ -activated K+ channel blockers

inhibits acetylcholine-evoked nitric oxide release in rat superior mesenteric artery. *Br J Pharmacol*, **149,** 560-72.

STEPHENS, D.J. & ALLAN, V.J. (2003). Light microscopy techniques for live cell imaging. *Science*, **300,** 82-6.

STERGIOPOULOS, K., ALVARADO, J.L., MASTROIANNI, M., EK-VITORIN, J.F., TAFFET, S.M. & DELMAR, M. (1999). Hetero-domain interactions as a mechanism for the regulation of connexin channels. *Circ Res*, **84,** 1144-55.

STINGO, A.J., CLAVELL, A.L., HEUBLEIN, D.M., WEI, C.M., PITTELKOW, M.R. & BURNETT, J.C., JR. (1992). Presence of C-type natriuretic peptide in cultured human endothelial cells and plasma. *Am J Physiol*, **263,** H1318-21.

STROMER, M.H., MAYES, M.S. & BELLIN, R.M. (2002). Use of actin isoform-specific antibodies to probe the domain structure in three smooth muscles. *Histochem Cell Biol*, **118,** 291-9.

STUHLMEIER, K.M. (2000). Effects of quinacrine on endothelial cell morphology and transcription factor-DNA interactions. *Biochimica et Biophysica Acta (BBA) - General Subjects*, **1524,** 57-65.

SU, C. (1983). Purinergic neurotransmission and neuromodulation. *Annu Rev Pharmacol Toxicol*, **23,** 397-411.

SWEENEY, H.L., YANG, Z., ZHI, G., STULL, J.T. & TRYBUS, K.M. (1994). Charge replacement near the phosphorylatable serine of the myosin regulatory light chain mimics aspects of phosphorylation. *Proc Natl Acad Sci U S A*, **91,** 1490-4.

TAGUCHI, K., UEDA, M. & KUBO, T. (1997). Effects of cAMP and cGMP on L-type calcium channel currents in rat mesenteric artery cells. *Jpn J Pharmacol*, **74,** 179-86.

TAKANO, H., DORA, K.A. & GARLAND, C.J. (2005). Spreading vasodilatation in resistance arteries. *J Smooth Muscle Res*, **41,** 303-11.

TAKANO, H., DORA, K.A., SPITALER, M.M. & GARLAND, C.J. (2004). Spreading dilatation in rat mesenteric arteries associated with calcium-independent endothelial cell hyperpolarization. *J Physiol*, **556,** 887-903.

TANAKA, Y., MOCHIZUKI, Y., HIRANO, H., AIDA, M., TANAKA, H., TORO, L. & SHIGENOBU, K. (1999). Role of MaxiK channels in vasoactive intestinal peptide-induced relaxation of rat mesenteric artery. *Eur J Pharmacol*, **383,** 291-6.

TANG, G., WU, L., LIANG, W. & WANG, R. (2005). Direct stimulation of K(ATP) channels by exogenous and endogenous hydrogen sulfide in vascular smooth muscle cells. *Mol Pharmacol*, **68,** 1757-64.

TARBELL, J.M. & PAHAKIS, M.Y. (2006). Mechanotransduction and the glycocalyx. *J Intern Med*, **259,** 339-50.

TARE, M., COLEMAN, H.A. & PARKINGTON, H.C. (2002). Glycyrrhetinic derivatives inhibit hyperpolarization in endothelial cells of guinea pig and rat arteries. *Am J Physiol Heart Circ Physiol*, **282,** H335-41.

TAYLOR, H.J., CHAYTOR, A.T., EVANS, W.H. & GRIFFITH, T.M. (1998). Inhibition of the gap junctional component of endothelium-dependent relaxations in rabbit iliac artery by 18-alpha glycyrrhetinic acid. *Br J Pharmacol*, **125,** 1-3.

TAYLOR, M.S., BONEV, A.D., GROSS, T.P., ECKMAN, D.M., BRAYDEN, J.E., BOND, C.T., ADELMAN, J.P. & NELSON, M.T. (2003). Altered expression of small-conductance Ca2+-activated K+ (SK3) channels modulates arterial tone and blood pressure. *Circ Res*, **93,** 124-31.

TAYLOR, M.S., GAO, H., GARDNER, J.D. & BENOIT, J.N. (1999). Effects of IBMX on norepinephrine-induced vasoconstriction in small mesenteric arteries. *Am J Physiol Gastrointest Liver Physiol*, **276,** G909-914.

TAYLOR, S.G., SOUTHERTON, J.S., WESTON, A.H. & BAKER, J.R. (1988). Endothelium-dependent effects of acetylcholine in rat aorta: a comparison with sodium nitroprusside and cromakalim. *Br J Pharmacol*, **94,** 853-63.

TAYLOR, S.G. & WESTON, A.H. (1988). Endothelium-derived hyperpolarizing factor: a new endogenous inhibitor from the vascular endothelium. *Trends Pharmacol Sci*, **9,** 272-4.

TEUBL, M., GROSCHNER, K., KOHLWEIN, S.D., MAYER, B. & SCHMIDT, K. (1999). Na(+)/Ca(2+) exchange facilitates Ca(2+)-dependent activation of endothelial nitric-oxide synthase. *J Biol Chem*, **274,** 29529-35.

THENGCHAISRI, N. & RIVERS, R.J. (2005). Remote arteriolar dilations caused by methacholine: a role for CGRP sensory nerves? *Am J Physiol Heart Circ Physiol*, **289,** H608-13.

THORNELOE, K.S. & NELSON, M.T. (2005). Ion channels in smooth muscle: regulators of intracellular calcium and contractility. *Can J Physiol Pharmacol*, **83,** 215-42.

THORSGAARD, M., LOPEZ, V., BUUS, N.H. & SIMONSEN, U. (2003). Different modulation by Ca2+-activated K+ channel blockers and herbimycin of acetylcholine- and flow-evoked vasodilatation in rat mesenteric small arteries. *Br J Pharmacol*, **138,** 1562-70.

TRIGGLE, C.R. & DING, H. (2002). Endothelium-derived hyperpolarizing factor: is there a novel chemical mediator? *Clin Exp Pharmacol Physiol*, **29,** 153-60.

TUTTLE, J.L. & FALCONE, J.C. (2001). Nitric oxide release during alpha1-adrenoceptor-mediated constriction of arterioles. *Am J Physiol Heart Circ Physiol*, **281,** H873-81.

TWORT, C.H. & VAN BREEMEN, C. (1988). Cyclic guanosine monophosphate-enhanced sequestration of Ca2+ by sarcoplasmic reticulum in vascular smooth muscle. *Circ Res*, **62,** 961-4.

UCHIDA, E., BOHR, D.F. & HOOBLER, S.W. (1967). A method for studying isolated resistance vessels from rabbit mesentery and brain and their responses to drugs. *Circ Res*, **21,** 525-36.

UHRENHOLT, T.R., DOMEIER, T.L. & SEGAL, S.S. (2007). Propagation of calcium waves along endothelium of hamster feed arteries. *Am J Physiol Heart Circ Physiol*, **292,** H1634-40.

UNGER, V.M., KUMAR, N.M., GILULA, N.B. & YEAGER, M. (1999). Three-Dimensional Structure of a Recombinant Gap Junction Membrane Channel. *Science*, **283,** 1176-1180.

UNGVARI, Z., CSISZAR, A. & KOLLER, A. (2002). Increases in endothelial Ca(2+) activate K(Ca) channels and elicit EDHF-type arteriolar dilation via gap junctions. *Am J Physiol Heart Circ Physiol*, **282,** H1760-7.

URAKAMI-HARASAWA, L., SHIMOKAWA, H., NAKASHIMA, M., EGASHIRA, K. & TAKESHITA, A. (1997). Importance of endothelium-derived hyperpolarizing factor in human arteries. *J Clin Invest*, **100,** 2793-9.

VAN DER GRAAF, P.H., SHANKLEY, N.P. & BLACK, J.W. (1996). Analysis of the effects of alpha 1-adrenoceptor antagonists on noradrenaline-mediated contraction of rat small mesenteric artery. *Br J Pharmacol*, **118,** 1308-16.

VANBAVEL, E., VAN DER MEULEN, E.T. & SPAAN, J.A. (2001). Role of Rho-associated protein kinase in tone and calcium sensitivity of cannulated rat mesenteric small arteries. *Exp Physiol*, **86,** 585-92.

VANE, J.R. (1994). The Croonian Lecture, 1993. The endothelium: maestro of the blood circulation. *Philos Trans R Soc Lond B Biol Sci*, **343,** 225-46.

VANHEEL, B. & VAN DE VOORDE, J. (1997). Evidence against the involvement of cytochrome P450 metabolites in endothelium-dependent hyperpolarization of the rat main mesenteric artery. *J Physiol*, **501 (Pt 2),** 331-41.

VANTEEFFELEN, J.W.G.E. & SEGAL, S.S. (2006). Rapid dilation of arterioles with single contraction of hamster skeletal muscle. *Am J Physiol Heart Circ Physiol*, **290,** H119-127.

VEQUAUD, P. & THORIN, E. (2001). Endothelial G Protein {beta}-Subunits Trigger Nitric Oxide- but not Endothelium-Derived Hyperpolarizing Factor-Dependent Dilation in Rabbit Resistance Arteries. *Circ Res*, **89,** 716-722.

VIG, M., PEINELT, C., BECK, A., KOOMOA, D.L., RABAH, D., KOBLAN-HUBERSON, M., KRAFT, S., TURNER, H., FLEIG, A., PENNER, R. & KINET, J.P. (2006). CRACM1 is a plasma membrane protein essential for store-operated Ca2+ entry. *Science*, **312,** 1220-3.

VIRGINTINO, D., ROBERTSON, D., ERREDE, M., BENAGIANO, V., GIROLAMO, F., MAIORANO, E., RONCALI, L. & BERTOSSI, M. (2002). Expression of P-glycoprotein in human cerebral cortex microvessels. *J Histochem Cytochem*, **50,** 1671-6.

VOETS, T., DROOGMANS, G. & NILIUS, B. (1996). Membrane currents and the resting membrane potential in cultured bovine pulmonary artery endothelial cells. *J Physiol*, **497 (Pt 1),** 95-107.

VRIENS, J., OWSIANIK, G., FISSLTHALER, B., SUZUKI, M., JANSSENS, A., VOETS, T., MORISSEAU, C., HAMMOCK, B.D., FLEMING, I., BUSSE, R. & NILIUS, B. (2005). Modulation of the Ca2 permeable cation channel TRPV4 by cytochrome P450 epoxygenases in vascular endothelium. *Circ Res*, **97,** 908-15.

WALDRON, G.J. & GARLAND, C.J. (1994). Contribution of both nitric oxide and a change in membrane potential to acetylcholine-induced relaxation in the rat small mesenteric artery. *Br J Pharmacol*, **112,** 831-6.

WALKER, B.D. & SEGAL, S.S. (1998). Role of smooth muscle activation in conduction of vasodilation along isolated hamster feed arteries. *J Vasc Res*, **35,** 405-12.

WALKER, S.D., DORA, K.A., INGS, N.T., CRANE, G.J. & GARLAND, C.J. (2001). Activation of endothelial cell IK(Ca) with 1-ethyl-2-benzimidazolinone evokes smooth muscle hyperpolarization in rat isolated mesenteric artery. *Br J Pharmacol*, **134,** 1548-54.

WANG, M.H., ZHANG, F., MARJI, J., ZAND, B.A., NASJLETTI, A. & LANIADO-SCHWARTZMAN, M. (2001). CYP4A1 antisense oligonucleotide reduces mesenteric vascular reactivity and blood pressure in SHR. *Am J Physiol Regul Integr Comp Physiol*, **280,** R255-61.

WANG, X., LAU, F., LI, L., YOSHIKAWA, A. & VAN BREEMEN, C. (1995). Acetylcholine-sensitive intracellular Ca2+ store in fresh endothelial cells and evidence for ryanodine receptors. *Circ Res*, **77,** 37-42.

WANG, X., WU, J., LI, L., CHEN, F., WANG, R. & JIANG, C. (2003). Hypercapnic acidosis activates KATP channels in vascular smooth muscles. *Circ Res*, **92,** 1225-32.

WANG, Y., YOSHIOKA, K., AZAM, M.A., TAKUWA, N., SAKURADA, S., KAYABA, Y., SUGIMOTO, N., INOKI, I., KIMURA, T., KUWAKI, T. & TAKUWA, Y. (2006). Class II phosphoinositide 3-kinase alpha-isoform regulates Rho, myosin phosphatase and contraction in vascular smooth muscle. *Biochem J*, **394,** 581-92.

WARD, D.T., ALDER, A.C., OHANIAN, J. & OHANIAN, V. (2002). Noradrenaline-induced paxillin phosphorylation, ERK activation and MEK-regulated contraction in intact rat mesenteric arteries. *J Vasc Res*, **39,** 1-11.

WARNER, A., CLEMENTS, D.K., PARIKH, S., EVANS, W.H. & DEHAAN, R.L. (1995). Specific motifs in the external loops of connexin proteins can determine gap junction formation between chick heart myocytes. *J Physiol*, **488 (Pt 3),** 721-8.

WATANABE, H., VRIENS, J., PRENEN, J., DROOGMANS, G., VOETS, T. & NILIUS, B. (2003). Anandamide and arachidonic acid use epoxyeicosatrienoic acids to activate TRPV4 channels. *Nature*, **424,** 434-8.

WEERTH, S.H., HOLTZCLAW, L.A. & RUSSELL, J.T. (2007). Signaling proteins in raft-like microdomains are essential for Ca(2+) wave propagation in glial cells. *Cell Calcium*, **41,** 155-67.

WEIDELT, T., BOLDT, W. & MARKWARDT, F. (1997). Acetylcholine-induced K+ currents in smooth muscle cells of intact rat small arteries. *J Physiol*, **500 (Pt 3),** 617-30.

WELLMAN, G.C. & NELSON, M.T. (2003). Signaling between SR and plasmalemma in smooth muscle: sparks and the activation of Ca2+-sensitive ion channels. *Cell Calcium*, **34,** 211-29.

WELLMAN, G.C., QUAYLE, J.M. & STANDEN, N.B. (1998). ATP-sensitive K+ channel activation by calcitonin gene-related peptide and protein kinase A in pig coronary arterial smooth muscle. *J Physiol*, **507 (Pt 1),** 117-29.

WELSH, D.G. & SEGAL, S.S. (1998). Endothelial and smooth muscle cell conduction in arterioles controlling blood flow. *Am J Physiol Heart Circ Physiol*, **274,** H178-186.

WESSELMAN, J.P., SCHUBERT, R., VANBAVEL, E.D., NILSSON, H. & MULVANY, M.J. (1997). KCa-channel blockade prevents sustained pressure-induced depolarization in rat mesenteric small arteries. *Am J Physiol*, **272,** H2241-9.

WESTON, A.H. & ABBOTT, A. (1987). New class of antihypertensive acts by opening K+ channels. *Trends in Pharmacological Sciences*, **8,** 283-284.

WESTON, A.H., ABSI, M., WARD, D.T., OHANIAN, J., DODD, R.H., DAUBAN, P., PETREL, C., RUAT, M. & EDWARDS, G. (2005). Evidence in Favor of a Calcium-Sensing Receptor in Arterial Endothelial Cells. Studies With Calindol and Calhex 231. *Circ Res.*

WESTON, A.H., RICHARDS, G.R., BURNHAM, M.P., FELETOU, M., VANHOUTTE, P.M. & EDWARDS, G. (2002). K+-induced hyperpolarization in rat mesenteric artery: identification, localization and role of Na+/K+-ATPases. *Br J Pharmacol*, **136,** 918-26.

WHITE, R. & HILEY, C.R. (1997a). A comparison of EDHF-mediated and anandamide-induced relaxations in the rat isolated mesenteric artery. *Br J Pharmacol*, **122,** 1573-84.

WHITE, R. & HILEY, C.R. (1998a). Effects of K+ channel openers on relaxations to nitric oxide and endothelium-derived hyperpolarizing factor in rat mesenteric artery. *Eur J Pharmacol*, **357,** 41-51.

WHITE, R. & HILEY, C.R. (1997b). Endothelium and cannabinoid receptor involvement in levcromakalim vasorelaxation. *Eur J Pharmacol*, **339,** 157-60.

WHITE, R. & HILEY, C.R. (2000). Hyperpolarisation of rat mesenteric endothelial cells by ATP-sensitive K(+) channel openers. *Eur J Pharmacol*, **397,** 279-90.

WHITE, R. & HILEY, C.R. (1998b). Modulation of relaxation to levcromakalim by S-nitroso-N-acetylpenicillamine (SNAP) and 8-bromo cyclic GMP in the rat isolated mesenteric artery. *Br J Pharmacol*, **124,** 1219-26.

WHITE, R. & HILEY, C.R. (1998c). The actions of some cannabinoid receptor ligands in the rat isolated mesenteric artery. *Br J Pharmacol*, **125,** 533-41.

WHITE, R., HO, W.S., BOTTRILL, F.E., FORD, W.R. & HILEY, C.R. (2001). Mechanisms of anandamide-induced vasorelaxation in rat isolated coronary arteries. *Br J Pharmacol*, **134,** 921-9.

WIER, W.G. & MORGAN, K.G. (2003). Alpha1-adrenergic signaling mechanisms in contraction of resistance arteries. *Rev Physiol Biochem Pharmacol*, **150,** 91-139.

WIHLBORG, A.K., BALOGH, J., WANG, L., BORNA, C., DOU, Y., JOSHI, B.V., LAZAROWSKI, E., JACOBSON, K.A., ARNER, A. & ERLINGE, D. (2006). Positive inotropic effects by uridine triphosphate (UTP) and uridine diphosphate (UDP) via P2Y2 and P2Y6 receptors on cardiomyocytes and release of UTP in man during myocardial infarction. *Circ Res*, **98,** 970-6.

WILSON, A.J., JABR, R.I. & CLAPP, L.H. (2000). Calcium modulation of vascular smooth muscle ATP-sensitive K(+) channels: role of protein phosphatase-2B. *Circ Res*, **87,** 1019-25.

WINQUIST, R.J., BUNTING, P.B. & SCHOFIELD, T.L. (1985). Blockade of endothelium-dependent relaxation by the amiloride analog dichlorobenzamil: possible role of Na+/Ca++ exchange in the release of endothelium-derived relaxant factor. *J Pharmacol Exp Ther*, **235,** 644-50.

WINTER, P. & DORA, K.A. (2006a). ATP and UTP stimulate spreading dilatation responses in rat isolated small mesenteric arteries. In *British Pharmacological Society 75th Anniversary Meeting*. Oxford.

WINTER, P. & DORA, K.A. (2006b). Contribution of PKC to the desensitisation of relaxation to luminally-perfused purinoceptor agonists in rat small mesenteric arteries. In *8th International Symposium on Adenosine and Adenine Nucleotides*. ed. Burnstock, G. pp. 157. Ferrara, Italy: Springer.

WINTER, P. & DORA, K.A. (2005). Differential role of KCa in dilatation evoked by luminally-perfused purinoceptor agonists in rat small mesenteric arteries In *British Pharmacological Society, Winter Meeting*. pp. 039P. School for Education, London: pa2online.

WINTER, P., SANDOW, S.L., DORA, K.A., MATHER, S. & GARLAND, C.J. (2004). Specificity and viability of a pinocytotic method for loading endothelial cells in intact arteries. *Journal of Vascular Research*, **41,** 1-68, PEF 5.

WOODRUM, D.A. & BROPHY, C.M. (2001). The paradox of smooth muscle physiology. *Mol Cell Endocrinol*, **177,** 135-43.

WU, C.C., CHEN, S.J. & YEN, M.H. (1997). Loss of acetylcholine-induced relaxation by M3-receptor activation in mesenteric arteries of spontaneously hypertensive rats. *J Cardiovasc Pharmacol*, **30,** 245-52.

WU, D.Q., LEE, C.H., RHEE, S.G. & SIMON, M.I. (1992). Activation of phospholipase C by the alpha subunits of the Gq and G11 proteins in transfected Cos-7 cells. *J Biol Chem*, **267,** 1811-7.

WU, X.C., JOHNS, E., MICHAEL, J. & RICHARDS, N.T. (1994). Interdependence of contractile responses of rat small mesenteric arteries on nitric oxide and cyclo-oxygenase and lipoxygenase products of arachidonic acid. *Br J Pharmacol*, **112,** 360-8.

XIA, J. & DULING, B.R. (1995). Electromechanical coupling and the conducted vasomotor response. *Am J Physiol*, **269,** H2022-30.

XIA, J., LITTLE, T.L. & DULING, B.R. (1995). Cellular pathways of the conducted electrical response in arterioles of hamster cheek pouch in vitro. *Am J Physiol*, **269,** H2031-8.

XU, C., LU, Y., TANG, G. & WANG, R. (1999). Expression of voltage-dependent K(+) channel genes in mesenteric artery smooth muscle cells. *Am J Physiol*, **277,** G1055-63.

YAMADA, M., ISOMOTO, S., MATSUMOTO, S., KONDO, C., SHINDO, T., HORIO, Y. & KURACHI, Y. (1997). Sulphonylurea receptor 2B and Kir6.1 form a sulphonylurea-sensitive but ATP-insensitive K+ channel. *J Physiol*, **499 (Pt 3),** 715-20.

YAMAMOTO, K., SOKABE, T., OHURA, N., NAKATSUKA, H., KAMIYA, A. & ANDO, J. (2003). Endogenously released ATP mediates shear stress-induced Ca2+ influx into pulmonary artery endothelial cells. *Am J Physiol Heart Circ Physiol*, **285,** H793-803.

YAMAMOTO, Y., FUKUTA, H., NAKAHIRA, Y. & SUZUKI, H. (1998). Blockade by 18beta-glycyrrhetinic acid of intercellular electrical coupling in guinea-pig arterioles. *J Physiol*, **511 (Pt 2),** 501-8.

YAMAMOTO, Y., KLEMM, M.F., EDWARDS, F.R. & SUZUKI, H. (2001). Intercellular electrical communication among smooth muscle and endothelial cells in guinea-pig mesenteric arterioles. *J Physiol*, **535,** 181-95.

YAMAZAKI, J. & KITAMURA, K. (2003). Intercellular electrical coupling in vascular cells present in rat intact cerebral arterioles. *J Vasc Res*, **40,** 11-27.

YANG, Y. & LOSCALZO, J. (2005). S-nitrosoprotein formation and localization in endothelial cells. *Proc Natl Acad Sci U S A*, **102,** 117-22.

YAO, X. & GARLAND, C.J. (2005). Recent developments in vascular endothelial cell transient receptor potential channels. *Circ Res*, **97,** 853-63.

YASHIRO, Y. & DULING, B.R. (2000). Integrated Ca2+ Signaling Between Smooth Muscle and Endothelium of Resistance Vessels. *Circ Res*, **87,** 1048-1054.

YASHIRO, Y. & DULING, B.R. (2003). Participation of intracellular Ca2+ stores in arteriolar conducted responses. *Am J Physiol Heart Circ Physiol*, **285,** H65-73.

YEGUTKIN, G.G., MIKHAILOV, A., SAMBURSKI, S.S. & JALKANEN, S. (2006). The detection of micromolar pericellular ATP pool on lymphocyte surface by using lymphoid ecto-adenylate kinase as intrinsic ATP sensor. *Mol Biol Cell*, **17,** 3378-85.

YEROMIN, A.V., ZHANG, S.L., JIANG, W., YU, Y., SAFRINA, O. & CAHALAN, M.D. (2006). Molecular identification of the CRAC channel by altered ion selectivity in a mutant of Orai. *Nature*, **443,** 226-9.

YUSTE, R. (2005). Fluorescence microscopy today. *Nat Methods*, **2,** 902-4.

ZANG, W.J., BALKE, C.W. & WIER, W.G. (2001). Graded alpha1-adrenoceptor activation of arteries involves recruitment of smooth muscle cells to produce 'all or none' Ca(2+) signals. *Cell Calcium*, **29,** 327-34.

ZHANG, H. & BOLTON, T.B. (1995). Activation by intracellular GDP, metabolic inhibition and pinacidil of a glibenclamide-sensitive K-channel in smooth muscle cells of rat mesenteric artery. *Br J Pharmacol*, **114,** 662-72.

ZHANG, H., BOLTON, T.B., PIEKARSKA, A.E. & MCPHERSON, G.A. (1998). The electrophysiological effects of tetraphenylphosphonium on vascular smooth muscle. *Eur J Pharmacol*, **347,** 119-23.

ZHANG, J., WIER, W.G. & BLAUSTEIN, M.P. (2002). Mg2+ blocks myogenic tone but not K+-induced constriction: role for SOCs in small arteries. *Am J Physiol Heart Circ Physiol*, **283,** H2692-705.

ZHANG, S.L., YU, Y., ROOS, J., KOZAK, J.A., DEERINCK, T.J., ELLISMAN, M.H., STAUDERMAN, K.A. & CAHALAN, M.D. (2005). STIM1 is a Ca2+ sensor that

activates CRAC channels and migrates from the Ca2+ store to the plasma membrane. *Nature*, **437,** 902-905.

ZYGMUNT, P.M. & HOGESTATT, E.D. (1996). Role of potassium channels in endothelium-dependent relaxation resistant to nitroarginine in the rat hepatic artery. *Br J Pharmacol*, **117,** 1600-6.

ZYGMUNT, P.M., PETERSSON, J., ANDERSSON, D.A., CHUANG, H., SORGARD, M., DI MARZO, V., JULIUS, D. & HOGESTATT, E.D. (1999). Vanilloid receptors on sensory nerves mediate the vasodilator action of anandamide. *Nature*, **400,** 452-7.

ZYGMUNT, P.M., RYMAN, T. & HOGESTATT, E.D. (1995). Regional differences in endothelium-dependent relaxation in the rat: contribution of nitric oxide and nitric oxide-independent mechanisms. *Acta Physiol Scand*, **155,** 257-66.